

INTERNATIONAL CONFERENCE

Condensed Matter Research at the IBR-2

FL'nP₆₅

ABSTRACT

BOOK

Soft Condensed Matter

Application of Complementary Techniques

Functional and Nanostructured Materials

Development of Neutron Scattering Techniques and Instruments

Stress and Texture Investigations of Materials

Neutron Imaging and Cultural Heritage

Magnetic Nanomaterials



April 25 – 29, 2022, Dubna, Russian Federation

CMR@IBR-2

Joint Institute for Nuclear Research

**CONDENSED MATTER RESEARCH
AT THE IBR-2**

International Conference

Dubna, April 25–29, 2022

Programme and Abstracts

УДК 538.9
ББК 22.386
С74

Organized by

the Frank Laboratory of Neutron Physics of the Joint Institute for Nuclear Research

**LOCAL ORGANIZING
COMMITTEE**

Prof. D. P. Kozlenko — Chairman
Mrs. V. V. Alfer'eva
Dr. M. V. Avdeev
Dr. M. Balasoiv
Dr. N. M. Belozeroва
Dr. V. I. Bodnarchuk
Dr. G. D. Bokuchava
Dr. D. M. Chudoba
Dr. Yu. E. Gorshkova
Dr. T. I. Ivankina
Mr. S. V. Kozenkov
Dr. B. N. Savenko
Ms. V. S. Smirnova — Scientific Secretary
Dr. T. V. Tropin

**INTERNATIONAL
PROGRAMME COMMITTEE**

Prof. V. L. Aksenov (Russia)
Prof. P. A. Alekseev (Russia)
Prof. A. M. Balagurov (Russia)
Prof. A. V. Belushkin (Russia)
Prof. L. A. Bulavin (Ukraine)
Prof. E. Burzo (Romania)
Prof. V. T. Em (Russia)
Prof. A. Ivanov (France)
Prof. P. Kopčanský (Slovak Republic)
Prof. D. Nagy (Hungary)
Prof. W. Nawrocik (Poland)
Prof. P. Mikula (Czech Republic)
Prof. D. Sangaa (Mongolia)
Prof. A. Senyshyn (Germany)
Prof. J. Wąsicki (Poland)
Prof. D. Uhríková (Slovak Republic)

Editor V. S. Smirnova

The contributions are reproduced directly from the originals
presented by the Organizing Committee.

Condensed Matter Research at the IBR-2: Programme and Abstracts of the
C74 International Conference (Dubna, Apr. 25–29, 2022). — Dubna: JINR, 2022. — 192 p.
ISBN 978-5-9530-0568-5

Исследования конденсированных сред на реакторе ИБР-2: Программа и анно-
тации международной конференции (Дубна, 25–29 апр. 2022 г.). — Дубна: ОИЯИ,
2022. — 192 с.

ISBN 978-5-9530-0568-5

ISBN 978-5-9530-0568-5

© Joint Institute for Nuclear
Research, 2022

Preface

The International Conference “Condensed Matter Research at the IBR-2” (CMR@IBR2 -2022) takes place in Dubna, Moscow Region, Russian Federation on April 25 – 29, 2022. The Conference is organized by the Frank Laboratory of Neutron Physics of the Joint Institute for Nuclear Research.

After modernization completed in 2011, the IBR high flux pulsed reactor renewed a regular operation and realization of the User Programme. Neutron scattering research at IBR-2 reactor covers different fields of condensed matter physics, materials science, chemistry, biophysical, geophysical and engineering sciences. During last years, over 200 experiments were performed annually by scientists from more than 20 countries at the IBR-2 instruments in the framework of the User Programme.

The aim of the Conference on Condensed Matter Research at IBR-2 reactor, playing the role of the User Meeting, is to bring together the users of the neutron facility for discussion of recent experimental results, prospects of future research and development of IBR-2 instruments.

The previous Conferences held in 2014, 2015, 2017 and 2020 attracted participants from Azerbaijan, Belarus, Bulgaria, Czech Republic, Estonia, Germany, Italy, Kazakhstan, Latvia, Moldova, Mongolia, Poland, Romania, Russia, Serbia, Slovak Republic, Ukraine and Vietnam.

The present conference is dedicated to the 65th Anniversary of the Frank Laboratory of Neutron Physics, JINR.

The topics of the Conference will highlight results of interdisciplinary research and development of neutron instruments and techniques, including:

- Functional and nanostructured materials;
- Magnetic colloid systems;
- Layered magnetic nanostructures;
- Carbon nanostructures;
- Materials under extreme conditions;
- Soft condensed matter (biological nanosystems, lipid membranes, polymers);
- Lattice and molecular dynamics of materials;
- Texture and properties of rocks, minerals and industrial materials;
- Residual stresses in materials and products;
- Neutron imaging
- Cultural heritage and applied research;
- Development of IBR-2 instruments;
- Development of neutron scattering techniques and detectors;
- Application of complementary techniques in condensed matter research.

Due to Coronavirus outbreak, the conference will be held online via Video conference.

We wish the CMR@IBR2-2022 Conference participants successful work and significant results!

Dubna, April 2022

Organizing Committee

Oral Programme

CMR@IBR2 2022 Scientific Programme

The conference will be held online via Video conference.

Monday, April 25, 2022

INTRODUCTORY SESSION

Chair: Kozlenko D.

- 10.00 – 10.20 Opening and Welcome (Shvetsov V.)
- 10.20 – 10.50 **Invited: Shvetsov V.** (FLNP JINR, Russian Federation).
Current Status and Upgrade Plans of the IBR-2 Pulsed Reactor.
- 10.50 – 11.20 Kozlenko D. (FLNP JINR, Russian Federation).
Neutron scattering instrumentation for condensed matter research at the IBR-2 pulsed reactor: current state and further developments.
- 11.20 – 11.50 **Invited: Korsunsky A.** (University of Oxford, United Kingdom/Skolkovo Institute of Science and Technology, Russian Federation)
Deep insights into hierarchical material structures with penetrating beams: neutrons, X-rays, and electron microscopies.
- 11.50 – 14.30 Lunch

PLENARY SESSION 1: FUNCTIONAL AND NANOSTRUCTURED MATERIALS

Chair: Balagurov A.

- 14.30 – 15.00 **Invited: Streltsov S.** (IMP UB RAS, Russian Federation)
The spin-orbit coupling and magnetic and structural properties of transition metal compounds: novel effects.
- 15.00 – 15.20 Turchenko V. (FLNP JINR, Russian Federation)
Temperature dependence of spontaneous polarization in barium hexaferrite.
- 15.20 – 15.40 Lushnikov S. (MSU, Russian Federation)
Structure of RNi₃ (R-Ce, Ho)-based intermetallic hydrides with different anisotropy of the lattice at 5 K and 293 K temperatures.
- 15.40 – 16.00 Titova S. (IMET UB RAS, Russian Federation)
Pressure dependence of phase transitions in double manganite PrBaMn₂O₆.
- 16.00 – 16.20 Lis O. (FLNP JINR, Russian Federation)
The pressure effect on the crystal and magnetic structure properties of van der waals material CrBr₃.
- 16.20 – 16.40 Bobrikov I. (FLNP JINR, Russian Federation)
Application of neutron diffraction to study the structural features of materials for Na-ion batteries.

Tuesday, April 26, 2022

PLENARY SESSION 1: FUNCTIONAL AND NANOSTRUCTURED MATERIALS

Chair: Avdeev M.

- 10.00 – 10.30 **Invited: Rogozhkin S.** (NRNU “MEPhI”, Russia)
Complementary analysis of nanostructure in structural materials.

- 10.30 – 11.00 **Invited: Lebedev V.** (PNPI NRC “Kurchatov Institute”, Russian Federation)
Effect of lanthanide atoms squeezing in Ln-endofullerenols and their ordering in solutions.
- 11.00 – 11.20 Kulvelis Yu. (PNPI NRC “Kurchatov Institute”, Russian Federation)
Small-angle scattering on proton-conducting membranes with nanodiamonds.
- 11.20 – 11.40 Yerdauletov M. (INP, Kazakhstan)
Nanoscale structure of positive electrodes for Li-ion batteries with carbon-based additives by SANS.
- 11.40 – 12.00 Zelenyak T. (FLNP JINR, Russian Federation)
The influence of ion implantation with Cs⁺ ion to the multilayer structure of perovskite CH₃NH₃PbI₃ materials.
- 12.00 – 12.20 Break

PLENARY SESSION 2: DEVELOPMENT OF NEUTRON SCATTERING TECHNIQUES AND INSTRUMENTS

Chair: Lychagin E.

- 12.20 – 12.50 **Invited: Grigoriev S.V.** (PNPI NRC “Kurchatov Institute”, Russian Federation)
Project of compact neutron source dedicated for academic research and industrial applications DARIA.
- 12.50 – 13.10 Nikitenko Yu. (FLNP JINR, Russian Federation)
Cold neutrons storage for pulsed source.
- 13.10 – 13.30 Hassan A. (FLNP JINR, Russian Federation, NRNU “MEPhI”, Russian Federation)
Cold moderator optimization for IBR-3.

13.30 – 15.00 Lunch

Chair: Altynbaev E.

- 15.00 – 15.20 Churakov A. (FLNP JINR, Russian Federation)
Recent developments of linear position-sensitive neutron detectors in DSC FLNP.
- 15.20 – 15.40 Buchny D. (INR RAS, NRNU “MEPhI”, Russian Federation)
Monte Carlo simulation of a scintillator neutron counter for ring detector array.
- 15.40 – 16.00 Chernikov A.N. (FLNP JINR, Russian Federation)
Refrigerator ³He based on closed cycle cryocooler cooling.
- 16.00 – 16.20 Podlesnyy M.M. (FLNP JINR, Russian Federation)
Prototype of two-dimensional scintillator detector based on ZnS(Ag)/⁶LiF with wavelength-shifting fibers.
- 16.20 – 16.40 Petrova M. (FLNP JINR, Russian Federation)
Status report of developing plate chamber detector with B-10 for thermal neutrons.
- 16.40 – 17.00 Golubev M.A. (PNPI NRC “Kurchatov Institute”, Russian Federation)
4-channel data acquisition device with user web interface for 2D multi-wire proportional chambers with a delay line readout.

- 17.00 – 17.10 Break
 17.10 – 19.00 *Poster Session I*

Wednesday, April 27, 2022

PLENARY SESSION 3: SOFT CONDENSED MATTER (BIOLOGICAL NANOSYSTEMS, LIPID MEMBRANES, POLYMERS)

Chair: Kucerka N.

- 10.00 – 10.30 **Invited: Angelova A.** (UPS, France)
Lipid nanocarriers for delivery of natural neuroprotective compounds.
- 10.30 – 10.50 Gorshkova Yu. (FLNP JINR, Russian Federation)
Biohybrid nanocomplexes and their potential application in biomedicine.
- 10.50 – 11.10 Lebedev D. (PNPI NRC “Kurchatov Institute”, Russian Federation)
Supromolecular protein structure formation in animal and human skin investigated by SANS.
- 11.10 – 11.30 Ryzhykau Yu. (MIPT, Russian Federation)
Study of oligomerization polydispersity of methionine gamma-lyase.
- 11.30 – 11.50 Anghel L. (IC, Moldova)
Small-angle scattering structural study of pH effect in beta-lactoglobulin - alginate complexes.
- 11.50 – 12.10 Break

Chair: Gorshkova Yu.

- 12.10 – 12.30 Almasy L. (CER, Hungary)
Structure of aqueous solutions of heterocyclic amines.
- 12.30 – 12.50 Shibaev A. (MSU, Russian Federation)
Responsiveness to hydrocarbons of mixed anionic/cationic wormlike surfactant micelles.
- 12.50 – 13.10 Molchanov V. (MSU, Russian Federation)
Gel-like structures of long mixed wormlike micelles.
- 13.10 – 13.30 Krakovsky I. (Charles University, Czech Republic)
Surfactant-polymer interactions in polymer hydrogels investigated by SANS.
- 13.30 – 15.00 Lunch

Chair: Kuklin A.

- 15.00 – 15.20 Kwiatkowski A. (MSU, Russian Federation)
Structure of beads-on-string complexes formed by ionic surfactant and hydrophobic polymer at low salt content.
- 15.20 – 15.40 Ivanova L. (PNPI NRC “Kurchatov Institute”, Russian Federation)
Evolution of the structure of calcium carbonate precipitates formed in the process of biomineralization.
- 15.40 – 16.00 Skoi V. (FLNP JINR, Russian Federation)
DMPC multi- and unilamellar vesicles under pressure.

16.00 – 16.20	Kruglyak A. (FLNP JINR, Russian Federation) <i>Application of the accelerator mass spectrometry method to study the mechanisms of radiation mutagenesis of rice crops: the current state of the issue.</i>
16.20 – 16.40	Pakhnevich A. (PIN RAS, Russian Federation) <i>Crystallographic texture of the gryphaea dilatata bivalve shells.</i>
16.40 – 17.00	Break
17.00 – 19.00	Poster Session II

Thursday, April 28, 2022

PLENARY SESSION 4: MAGNETIC NANOMATERIALS

Chair: Lebedev V.

10.00 – 10.30	Invited: Kantorovich S. (Vienna University, Austria) <i>Soft magnetic materials: current state and new trends.</i>
10.30 – 10.50	Balasoiu M. (FLNP JINR, Russian Federation) <i>Small-angle neutron scattering investigation of a ferrofluid with anisometric CuFe₂O₄ nanoparticles.</i>
10.50 – 11.10	Chilom C. (University of Bucharest, Romania) <i>Biogenic ferrihydrite nanoparticles - serum proteins complexes as biocompatible systems for medical applications.</i>
11.10 – 11.30	Mistonov A. (SPbU, Russian Federation) <i>Magnetic properties of ordered arrays of iron nanowires: the impact of the length.</i>
11.30 – 11.50	Azarova L. (PNPI NRC “Kurchatov Institute”, Russian Federation) <i>Measurement of the spin-wave stiffness and the energy gap in the magnon spectrum of amorphous ferromagnets by small-angle scattering of polarized neutrons.</i>
11.50 – 12.10	M.V.Avdeev (FLNP JINR, Russian Federation) <i>Structural and magnetic properties of magnetoferritin in various conditions.</i>
12.10 – 12.30	Break

Chair: Bodnarchuk V.

12.30 – 12.50	Zhaketov V. (FLNP JINR, Russian Federation) <i>Reflectometry with nuclear reactions and neutron spin flip in neutron wave.</i>
12.50 – 13.10	Devyaterikov D. (IMET UB RAS, Russian Federation) <i>Observation of helimagnetism in Dy/Ho superlattice via neutron reflectivity measurements.</i>
13.10 – 14.30	Lunch

PLENARY SESSION 5: STRESS AND TEXTURE INVESTIGATIONS OF MATERIALS

Chair: Bokuchava G.

- 14.30 – 15.00 **Invited: Em V.** (NRC “Kurchatov Institute”, Russian Federation)
Stress diffractometry and development prospects.
- 15.00 – 15.20 Vasin R. (FLNP JINR, Russian Federation)
Intrinsic elastic anisotropy of Westerly granite and its evolution due to thermal treatment.
- 15.20 – 15.40 Valkov S. (IE BAS, Bulgaria)
Synthesis, structure and tensile properties of AlMg₅Cr and Al₅Si components produced by wire-arc additive manufacturing.
- 15.40 -16.00 Break

Chair: Ivankina T.

- 16.00 – 16.20 Markova G. (TSU, Russian Federation)
Effect of thermomechanical treatment on the texture and functional properties of powder TiNi.
- 16.20 – 16.40 Zel I. (FLNP JINR, Russian Federation)
Approximation of elastic velocity-pressure relation in rocks.

Friday, April 29, 2022

PLENARY SESSIONS 6: NEUTRON IMAGING AND CULTURAL HERITAGE

Chair: Belushkin A.

- 10.00 – 10.30 **Invited: Sitdikov A.** (A. Kh. Khalikov Institute of Archeology, Tatarstan Academy of Sciences, Russian Federation)
Actual problems of the archaeology of Volga region.
- 10.30 – 10.50 Kichanov S. (FLNP JINR, Russian Federation)
Neutron radiography and tomography at the IBR-2 reactor: the main scientific directions.
- 10.50 – 11.10 Saprykina I. (IA RAS, Russian Federation)
Neutron diffraction as a method of analysis of Samanid silver dirchams from the ancient muroma burial ground Podbolot'ie.
- 11.10 – 11.30 Bakirov B. (KFU, Russian Federation / FLNP JINR, Russian Federation)
A study of antique and medieval coins by non-destructive methods of neutron tomography and diffraction.
- 11.30 – 11.50 Break

PLENARY SESSION 7: APPLICATION OF COMPLEMENTARY TECHNIQUES

Chair: Kichanov S.

- | | |
|---------------|--|
| 11.50 – 12.10 | Doroshkevich A. (FLNP JINR, Russian Federation)
<i>Condensed matter research at the EG-5 accelerator.</i> |
| 12.10 – 12.30 | Savin A. (NIRDTP, Iasi, Romania)
<i>Evaluation of flaw severity in cylindrical products by an electromagnetic method.</i> |
| 12.30 – 12.50 | Steigmann R. (NIRDTP, Iasi, Romania)
<i>Microwave measurements for biological tissues.</i> |
| 12.50 – 13.10 | Workshop closing |

Poster Programme

1. Aleksiyaynak Yu. (FLNP JINR, Russian Federation)
Influence of neutron irradiation on the elemental content and optical properties of the CaF_2 and BaF_2 crystals.
2. Khongorzul B. (Institute of Physics and Technology, Mongolian Academy of Science, Mongolia)
Theoretical investigation of structure and magnetic property of Ni substituted MgFe_2O_4 .
3. Belozeroва N. (FLNP JINR, Russian Federation)
High pressure effect on internal structure and atomic dynamics of pharmaceutical compounds.
4. Chebyshev K. (Donetsk National University, Ukraine)
Neutron diffraction investigation of pressure dependence of $\text{Nd}_5\text{Mo}_3\text{O}_{16+\delta}$ crystal structure.
5. Craus M. (FLNP JINR, Russian Federation)
Magnetic and crystalline structure of some doped with Cr manganites.
6. Craus M. (FLNP JINR, Russian Federation)
Correlation between the Cr concentration and magnetic nanostructure parameters for $\text{La}_{0.54}\text{Ho}_{0.11}\text{Sr}_{0.35}\text{Mn}_{1-x}\text{Cr}_x\text{O}_3$ manganites.
7. Fedoseev M. (NRC «Kurchatov Institute» – CRISM «Prometey», Russian Federation)
Study of sigma phase emergence in stainless steel welds.
8. Genov I. (Institute of Electrochemistry and Energy System-Bulgarian Academy of Sciences, Bulgaria / FLNP JINR, Russian Federation)
Structural properties of bifunctional catalysts for zinc-air batteries.
9. Hashimov R. (Institute of Physics, ANAS, Azerbaijan)
Structural analysis of $\text{La}_{0.78}\text{Ba}_{0.22}\text{MnO}_3$ by X-ray diffraction.
10. Hristea G. (INCDIE ICPE CA, Romania)
Inherent impurities in graphene-like materials.
11. Kalanda N. (Scientific-Practical Materials Research Centre of NAS of Belarus, Belarus)
Effect of oxygen nonstoichiometry on the magnetic properties of $\text{La}_{0.7}\text{Sr}_{0.3}\text{Mn}_{0.95}\text{Fe}_{0.05}\text{O}_{3-\delta}$ manganites.

12. Kirillov A. (FLNP JINR, Russian Federation)
Permeability of a coal seam with respect to fractal features of pore space of fossil coals.
13. Kosiachkin Y. (FLNP JINR, Russian Federation)
Neutron and x-ray reflectometry studies of planar interfaces for lithium power sources.
14. Thao T.P. Le (The University of Danang, University of Science and Education, Vietnam)
High pressure-enhanced magnetic ordering and magnetostructural coupling in geometrically frustrated spinel Mn_3O_4 .
15. Lis O. (FLNP JINR, Russian Federation)
The pressure effect on the crystal and magnetic structure of $ScMnO_3$.
16. Nagorna T. (FLNP JINR, Russian Federation)
Preliminary studies on magnetic and non-magnetic core silica gels by SAXS, SANS, ESR, and VSM methods.
17. Pernikov M. (University of Chemical Technology and Metallurgy, Bulgaria)
Spectroscopic and neutron diffraction investigations on glasses and glass-ceramics in the $Na_2O/BaO/TiO_2/B_2O_3/SiO_2/Al_2O_3$ system.
18. Petrov A. (Scientific-Practical Materials Research Centre of NAS of Belarus, Belarus)
Crystal and magnetic structures of $Sr_2FeMoO_{6-\delta}$ at high pressure.
19. Popov E. (FLNP JINR, Russian Federation)
Investigation of phase transitions in sintered $W-6wt.\%B_4C-2wt.\%TiC-1wt.\%C$ alloy irradiated by He ions.
20. Rutkauskas A. (FLNP JINR, Russian Federation)
Crystal and magnetic structure of half-Heusler compounds $MnNi_{0.9}M_{0.1}Sb$ ($M = Ti, V, Cr, Fe, Co$) at low temperatures.
21. Rzayev R. (Azerbaijan State Pedagogical University, Azerbaijan)
Thermophysical properties of Y_2O_3 nanoparticles under the influence of high-intensity fast neutrons.
22. Skanchenko D. (PNPI, Russian Federation)
Neutron diffraction studies of compounds based on $MnGe$ under high pressure at low temperatures in high magnetic fields.
23. Tomchuk O. (Institute of Environmental Geochemistry, National Academy of Sciences of Ukraine, Ukraine)

Structural organization of nanodispersed aluminic material synthesized in a plasma reactor.

24. Tomchuk O. (Institute of Environmental Geochemistry, National Academy of Sciences of Ukraine, Ukraine)

Structural features of liquid crystalline suspensions of diamond nanoparticles by neutron scattering.

25. Zakharova A. (FLNP JINR, Russian Federation)

Electrical properties of a hydrated contact of different-sized YSZ –particles.

26. Yarmolich M. (Scientific-Practical Materials Research Centre of NAS of Belarus, Belarus)

Obtaining of nanosized powders of the Sr-Ba-Fe-Mo-O system by sol-gel technique.

DEVELOPMENT OF NEUTRON SCATTERING TECHNIQUES AND INSTRUMENTS

27. Altynbaev E. (PNPI, Russian Federation)

Development of linear position-sensitive neutron detector for modern neutron sources.

28. Glushkova T. (PNPI, Russian Federation)

Prototypes of neutron scintillation detectors based on ZnS(Ag)/LiF and SiPM.

29. Kirilov A. (FLNP JINR, Russian Federation)

Instruments control software at the IBR-2 reactor: experience and prospects.

30. Kolesnikov A. (FLNP JINR, Russian Federation)

The preparation of thin film coating converter $^{10}\text{B}_4\text{C}$ for slow neutron detectors.

31. Kruglov A. (FLNP JINR, Russian Federation)

Results of modernization of the FSS neutron Fourier diffractometer at the IBR-2 reactor.

32. Kurilkin A. (FLNP JINR, Russian Federation)

GEANT4 simulation of a thermal neutron detector with a boron converter.

33. Litvin V. (INR RAS, Russian Federation)

SANS research of heat-resistant nonmagnetic alloys at neutron reflectometr - SANS instrument «GORIZONT» in INR RAS.

34. Paveleva A. (PNPI, Russian Federation)

Variations of piston-cylinder cells for neutron scattering under high pressure.

35. Remizov M. (PNPI, Russian Federation)

Physical model of the in-beam spectrometer on PIK reactor.

36. Sikolenko V. (FLNP JINR, Russian Federation)

Upgrade plans for Epsilon diffractometer.

POSTER SESSION II (Wednesday, April 27, 2022)

SOFT CONDENSED MATTER (BIOLOGICAL NANOSYSTEMS, LIPID MEMBRANES, POLYMERS)

1. Artykulnyi O. (FLNP JINR, Russian Federation)

Structural studies of surfactant-polymer associations in bulk and at interfaces.

2. Avdeev M. (MSU, Russian Federation)

Synthesis of polyacrylamide gel nanolayers on oxidized silicon surface for use as smart coatings with controlled release of antiseptics.

3. Balasoiu M. (FLNP JINR, Russian Federation)

Investigation of several mollusk shells from Danube Delta and Constanta Black sea shore by means of small-angle neutron scattering.

4. Balasoiu M. (FLNP JINR, Russian Federation)

Small-angle neutron scattering investigation of ferrofluids with magnetite nanoparticles coated with aspartic-acid, starch and hyaluronic acid.

5. Balasoiu M. (FLNP JINR, Russian Federation)

Structural investigation of magnetite and cobalt ferrite mesoporous nanoparticles coated with amino acids as stabilizing accents.

6. Baranova I. (Institute of Physics, ELI Beamlines, Academy of Sciences of the Czech Republic, Czechia)

Crystallographic and small angle scattering studies of hemoglobin crystal nucleation and cluster formation.

7. Burgakov V. (PNPI, Russian Federation)

Chromatin structure in the tumor cells with radioresistant phenotype.

8. Kurakin S. (FLNP JINR, Russian Federation)

Characterization of cation-zwitterionic lipid interactions: small angle neutron/X-ray scattering and densitometry study.

9. Makhaldiani N. (LIT JINR, Russian Federation)

Methods of fundamental physics and applied mathematics, there is no silver lining or how to treat chronic diseases with Covid.

10. Kosiachkin Y. (FLNP JINR, Russian Federation)

Development and operation tests of the temperature/humidity sample cell for neutron reflectometry.

11. Kuzmenko M. (FLNP JINR, Russian Federation)

Structuring of trisiloxanes-based superspreaders at interface and in bulk by neutron scattering.

12. Iashina E. (SPSU, PNPI NRC KI, Russian Federation)

Model of large scale chromatin organisation in biological cell nuclei based on SANS data.

13. Kuklina D. (MIPT, Russian Federation)

Stability of trimers of dimers of NpSR_{II}/NpHtr_{II} complex at low salt concentration.

14. Makarova A. (MSU, Russian Federation)

Viscoelastic properties and structure of dual networks of polymer and micellar chains.

15. Ospennikov A. (MSU, Russian Federation)

Study of the effect of a water-soluble monomer on micelles of surfactants for micellar polymerization problems.

16. Ospennikov A. (MSU, Russian Federation)

Structure, synergistic enhancement of viscoelastic properties and responsiveness to hydrocarbons of a new mixed viscoelastic surfactant system.

17. Pavlova A. (PNPI NRC “Kurchatov Institute”, Russian Federation)

Novel resorcinol-formaldehyde aerogels: synthesis, structure and fractal properties.

18. Slavkova Z. (G. Nadjakov Institute of Solid State Physics Bulgarian Academy of Sciences, Bulgaria)

Interaction of N,N'-disubstituted benzimidazole-2-thione derivatives containing vanilloid-like fragments with model phospholipid membranes.

19. Tropin T. (FLNP JINR, Russian Federation)

On the temperature dependence of the thickness and structure of C₇₀/polystyrene thin films.

20. Verlov N. (PNPI NRC “Kurchatov Institute”, Russian Federation)

Chromatin structure in the tumor cells with radioresistant phenotype.

21. Shnyrkov O. (PNPI, Russian Federation)

Fractal characteristics of coniferous and deciduous trees.

MAGNETIC NANOMATERIALS

22. Antropov N. (Institute of Metal Physics, Russian Federation)
Tunable spin-flop transition in artificial ferrimagnets.
23. Darziyeva T. (Baku State University, Azerbaijan)
Effect of high temperatures on the magnetic properties of Fe_3O_4 nanoparticles.
24. Karpets M. (The Institute of Experimental Physics of the Slovak Academy of Sciences (IEP SAS) in Košice (Department of Magnetism)/The Faculty of Electrical Engineering and Informatics of the Technical University of Košice (Department of Physics), Slovakia)
Self-assembled particle layering induced by electric field in transformer oil-based ferrofluid by neutron reflectometry.
25. Kolupaev E. (MSU / FLNP JINR, Russian Federation)
Absorption and scattering of neutrons in a resonator structure.
26. Kozhevnikov S. (FLNP JINR, Russian Federation)
Angular divergence of neutron microbeams from planar waveguides.
27. Makarova M. (Institute of Metal Physics, Russian Federation)
Magnetic structure of Dy-Co near the compensation temperature.
28. Nagornyi A. (Institute for Environment Geochemistry of the National Academy of Sciences of Ukraine, Ukraine / FLNP JINR, Russian Federation)
Interaction of aggregates in ferrofluids according to small-angle scattering data.
29. Nikova E. (IMP UB RAS, Russian Federation)
Investigation of the Fe-Cr superlattice with non-collinear magnetic ordering.
30. Yakunina E. (IMP UB RAS, Russian Federation)
Structural and magnetic characterization of Fe/MgO/Gd nanosystems.

NEUTRON IMAGING AND CULTURAL HERITAGE

31. Zel I. (FLNP JINR, Russian Federation)
Simple method for correction of center of rotation in neutron tomography.
32. Zhomartova A. (FLNP JINR, Russian Federation)
Study of cultural heritage objects from the ancient Turkic cult-memorial complex of East Kazakhstan with non - destructive neutron methods.

33. Dashdemirov A. (Azerbaijan State Pedagogical University, Azerbaijan)
Photoconductivity of $Ge_{1-x}Nd_xS$ at high temperatures.
34. Didenko E. (JINR, Russian Federation)
Research of electric properties of hydratable crystal $MnSe-CuInSe_2$ promising for using in renewable energy.
35. Harutyunyan V. (A. Alikhanyan National Laboratory, Armenia)
Radiation resistance of thermoregulating coatings irradiated using IBR-2.
36. Ivanshina O. (FLNP JINR, Russian Federation)
Thermal analysis and synthesis of new materials in FLNP JINR.
37. Nabiyeva A. (Institute of Physics ANAS, Azerbaijan)
Thermal properties of the $La_{0.73}Ba_{0.27}MnO_3$ at high temperature.
38. Kazantsev A. (MIPT, Russian Federation)
New program in Wolfram Mathematica: calculate peaks easily.
39. Soran M.L. (National Institute for Research and Development of Isotopic and Molecular Technologies, Romania)
*Evaluation of copper salts consequence on *Triticum aestivum*.*

**Abstracts:
Introductory
Session**

NEUTRON SCATTERING INSTRUMENTATION FOR CONDENSED MATTER RESEARCH AT THE IBR-2 PULSED REACTOR: CURRENT STATE AND FURTHER DEVELOPMENTS

D.P. Kozlenko

*Frank Laboratory of Neutron Physics, Joint Institute for Nuclear Research, 141980 Dubna
Moscow Reg., Russia*

E-mail: denk@nf.jinr.ru

The complex of neutron scattering instruments of the IBR-2 high flux pulsed reactor presently consists of 14 instruments, including diffractometers, small angle scattering spectrometer, reflectometers, inelastic neutron scattering spectrometer.

The recent developments of the instruments focused on improvement of the technical parameters of the spectrometers and extension of research capabilities are reviewed. They include installation of the intermediate part of the supermirror neutron guide at the DN-6 diffractometer, installation of new Fourier chopper at the FSD diffractometer, replacement of the Fourier chopper of the FSS diffractometer, fabrication of new changeable collimation unit for YuMO SANS spectrometer.

The progress in development of the new small angle neutron scattering and imaging spectrometer to be installed at the 10A beamline is discussed. The realization of the first state of the project of the new inelastic neutron scattering spectrometer in inverted geometry BJN is started.

**Abstracts:
Oral
Presentations**

TEMPERATURE DEPENDENCE OF SPONTANEOUS POLARIZATION IN BARIUM HEXAFERRITE

V. Turchenko¹, D.B. Migas², S.V. Trukhanov³, A.V. Rutkauskas¹, B. Bozzo⁴, I. Fina⁴, A.V.Trukhanov³

¹ Joint Institute for Nuclear Research, 6 Joliot-Curie Str., Dubna, 141980, Russia;

² Belarusian State University of Informatics and Radioelectronics, P. Browka 6, 220013 Minsk, Belarus;

³ SSPA “Scientific and Practical Materials Research Centre of NAS of Belarus”, 19 P. Brovki str., 220072 Minsk, Belarus;

⁴ Institut de Ciència de Materials de Barcelona-CSIC, Campus de la UAB, Bellaterra, Barcelona, 08193, Spain

E-mail: turchenko@jinr.ru

Among the large number of types of hexaferrites with different crystal structures, the M-type is the simplest. Hexaferrites have a rather complex crystal structure, which is represented as a sequence of spinel and hexagonal blocks alternating along the c axis and containing a rather large number of iron cations [1].

Nowadays these materials are considered as a perspective multiferroics or materials that demonstrate coexistence and correlation between dielectric and magnetic ordering at room temperature [2]. The milestone in multiferroics would be the realization of

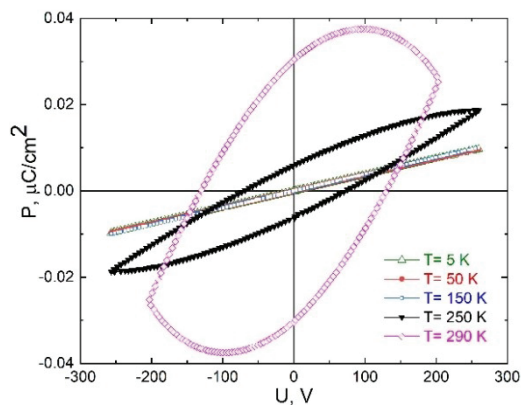


Fig.1. Electrical field dependence of the electrical polarization for BaFe₁₂O₁₉

simultaneous coexistence of large ferroelectricity and strong ferromagnetism, together with giant ME coupling effects in one single phase at room temperature. Observation of the non-zero dipole electrical moment with remnant magnetization and relationship between magnetic and electrical sub-systems open broad perspectives for development of the room-temperature functional devices based on hybrid materials with enhanced properties such as composites based on M-type hexaferrites.

In Fig.1 shows the polarization electric hysteresis loops for BaFe₁₂O₁₉ at different temperatures. This is an interesting fact that P(U) dependences measured at 5, 50 and 150K were characterized by the linear behavior. Our NEB calculations for the fully relaxed unit cell allows to explain such behavior due to energy barrier, which associated with two Fe²⁺ ions shifting along the c axis in one direction.

[1] D.A. Vinnik, A.S. Chernukha, S.A. Gudkov et al. / Morphology and magnetic properties of pressed barium hexaferrite BaFe₁₂O₁₉ materials // JMMM 459, (2018) 131-135.

[2] G. Tan, X. Chen / Structure and multiferroic properties of barium hexaferrite ceramics // JMMM 327, (2013) 87-90.

STRUCTURE OF RNi₃ (R-Ce, Ho)-BASED INTERMETALLIC HYDRIDES WITH DIFFERENT ANISOTROPY OF THE LATTICE AT 5K AND 293K TEMPERATURE

S.A. Lushnikov¹, T.V. Filippova¹ and I.A. Bobrikov²

¹*Chemistry Department of Lomonosov Moscow University, Moscow, Russia*

²*Joint Institute for Nuclear Research, Dubna, Moscow oblast, Russia*

E-mail: steplushnikov@yandex.ru

Intermetallic compounds (IMC) are materials for compact and safety storage of the hydrogen. These materials can be using for the development of hydrogen energy. The group of RNi₃ (R-Ce, Ho)-based compounds is also interesting for application as reversible hydrogen accumulator under soft pressure and temperature [1]. These compounds crystallized in PuNi₃ (space group *R-3m*, No 166) and CeNi₃ (space group *P6₃/mmc*, No 194) structure types. Both these structures are hybrid and consists of structural slabs with RT₂ (MgZn₂ structure type) and RT₅ (CaCu₅ structure type) composition, arranging in the direction perpendicular of the *z* crystallographic axis. Through the process of interaction of the hydrogen with intermetallic compounds and hydride phase formation, atoms of the hydrogen occupy interstitial sites in the crystal lattice. The crystallographic positions, occupied with hydrogen atoms, form several hydrogen sublattices in the structure of hydride [2]. The reaction of hydrogenation, when hydrogen atoms occupy sites in hydrogen sublattice, can lead to formation of the different hydride phases. In some cases, on cooling down of hydride sample, there may be decomposition this hydride into several new hydride phases. These transformations during lowering of temperature occur due to the redistribution of the hydrogen atoms in the sites of hydrogen sublattices. In early literature works, this redistribution of the interstitial atoms at low temperature was detect in the hydrides of *d*-metals [3]. In this work showed, that such behavior of hydrogen in the crystal lattice described with good agreement using of the lattice gas model. The RNi₃(R- Ce, Ho)-based hydride samples with medium hydrogen content (3.0-4.0 H/IMC) during lowering of the temperature also can decompose into several hydride phases. These new hydrides after heating back up to the room temperature transformed into phases with low stability. In literature is describe, that stability of hydrides might be different: the high stable hydrides not desorb of hydrogen at increased temperature, while the hydrides with low stability desorbs easy all hydrogen yet at the room temperature [4]. As was reveal RNi₃ (R- Ce, Ho)-based hydrides have different anisotropy of their crystal lattice [5]. More pronounced anisotropy was observe for hydrides containing R-metal of the cerium subgroup. Hydrides with R-metal of the yttrium subgroup have lattice with the small anisotropy. At the same time RNi₃(R- Ce, Ho)-based hydrides with low hydrogen amount (about of 1.0 H/IMC) have crystal lattice with small expansion and anisotropy. When these hydride samples were cooling down and heating back up to the room temperature, they rapidly desorbed all hydrogen. It was observe for both types of hydride samples, containing both cerium and holmium metals. The study of the RNi₃ (R- Ce, Ho)-based hydride structure with medium concentration was describe well in work [6]. In this work was reveal, that atoms of the hydrogen mostly occupy interstitial sites in the slabs with RNi₂ composition, containing more amount of the R-metal. We can suggest that in these hydrides with low hydrogen content, distribution of the hydrogen atoms in the lattice would be analogical. In this case, the different anisotropy of the hydride lattice first will be depend from the hydrogen amount in these hydrides. In structure of the RNi₃ (R- Ce, Ho)-based hydride with medium concentration, hydrogen atoms are ordered and have long-rang interaction each with other. In the structure of

hydride phases with low hydrogen amount, hydrogen atoms are as a disordered interstitial solution, without any interaction. At the same time, cooling down of the hydride samples with low concentration accompany with the hydrogen atoms redistribution in the hydrogen sublattices. This process may leads to possibility of appearing of the long-range interaction between atoms of hydrogen. For better understanding this behavior of hydrogen in the crystal lattice, it is necessary to perform the study of their structure. The most reliable method of the hydride structure study is neutron diffraction. At present work using neutron diffraction method were study samples of the RNi_3 (R- Ce, Ho)-based hydrides containing about of 1.0 H/IMC and having small lattice anisotropy at 5K and 293K temperature. For this study, samples with deuterium were prepared. Using of deuterium allows decreasing of the incoherent neutron scattering and obtain spectra that are more appropriate for refining. Obtained neutron data allows to determinate site positions of the hydrogen atoms and monitoring hydrogen redistribution in the sites of the structure.

- [1] M. Latroche, A. Percheron-Guegan (2003). Structural and thermodynamic studies of some RM_3 -compounds (R=lanthanide, M=transition metal). *J. Alloys Compd.* 356-357, 461-468.
- [2] V.A. Yartys (1992). New aspects of the structural chemistry of intermetallic hydrides: «isotropic» and «anisotropic» structures. *Koord. Khim.* 18, № 4, 401-408.
- [3] V.A. Somenkov (1972). Structure of hydrides. *Ber. Bunsen-Ges. Phys. Chem.* 76, 724–728.
- [4] S.A. Lushnikov, T.V. Filippova, I.A. Bobrikov (2017). On the structure stable $CeNi_3$ -based hydrides. *J. Surf. Investig.* 11, №1, 190-193.
- [5] R.H. Van Essen, K.H.J. Bushow (1980). Hydrogen sorption characteristics of Ce-3d and Y-3d intermetallic compounds. *J. Less-Common.* 70, 189-198.
- [6] V.A. Yartys, O.Isnard, A.B. Riabov, L.G. Akselrud (2003). Unusual effect on hydrogenation: anomalous expansion and volume contraction. *J. Alloys Compd.* 356–357. 109–113.

PRESSURE DEPENDENCE OF PHASE TRANSITIONS IN DOUBLE MANGANITE $\text{PrBaMn}_2\text{O}_6$

S.G. Titova¹, E.V. Sterkhov¹, S.V. Kichanov² and V.A. Sidorov³

¹*Institute of Metallurgy Urals Branch of RAS, Ekaterinburg, Russia*

²*JINR, Dubna, Russia*

³*Institute of High pressure Physics, Moscow, Russia*

E-mail: sgtitova@mail.ru

Double manganites RBaMn_2O_6 (R – rare earth) are built as a sequence of RMnO_3 and BaMnO_3 cubic perovskite cells in c -direction forming resulting tetragonal cell. In spite of ordinary manganites the temperatures of magnetic phase transition are much higher; that makes these materials perspective magnetoresistors, sensors, magnetocalorics *etc.* [1]. As for ordinary manganites the properties of double manganites are formed as a result of competition between the AFM superexchange and the FM double interaction in Mn-O subsystem. The temperatures of magnetic and electric phase transitions changes when type of R -element varies, so some size effect is present. The size effect may be tuned by applying of the external pressure, the pressure influence on magnetic and electric states of double manganites was not studied yet. We performed neutron diffraction in temperature range 50 – 320 K and pressure range 0 – 5.2 GPa for $\text{PrBaMn}_2\text{O}_6$ as magnetic and electric phase transitions for this compound were studied previously [2].

Neutron diffraction study was performed at DN-12 spectrometer (IBR-2 reactor) using the high pressure cell with sapphire anvils. The pressure was controlled using ruby fluorescence within 0.05 GPa accuracy. The external standard Al-LaB₆ was used for refinement of instrumental and profile parameters. Crystal and magnetic structure was refined by full-profile analysis with FullProf program.

Experimental diffraction patterns at external pressure 0, 3.1 and 5.2 GPa are shown in Fig. 1. Only without external pressure single phase ferromagnetic state was observed as an enhancement of diffraction line (200) at absence of AFM (111) line. External pressure leads to AFM state already at 320 K as an appearance of AFM (111) line (Fig. 1).

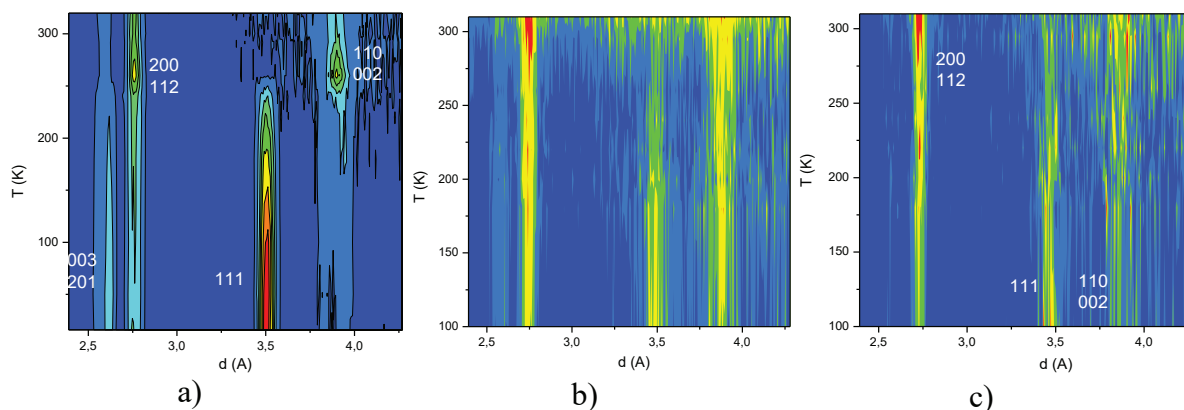


Fig. 1. Neutron diffraction patterns for $\text{PrBaMn}_2\text{O}_6$ at external pressure 0 (a), 3.1 GPa (b), 5.2 GPa (c).

Calculated unit cell dimensions are shown in Fig. 2. At ambient pressure the structural phase transition with a jump of $(a-c/2)$ ratio occurs at ~ 250 K attributing the metal-insulator transition [2]. At 3.1 GPa already at 320 K we observe high value of $(a-c/2)$ ratio noted the insulating state.

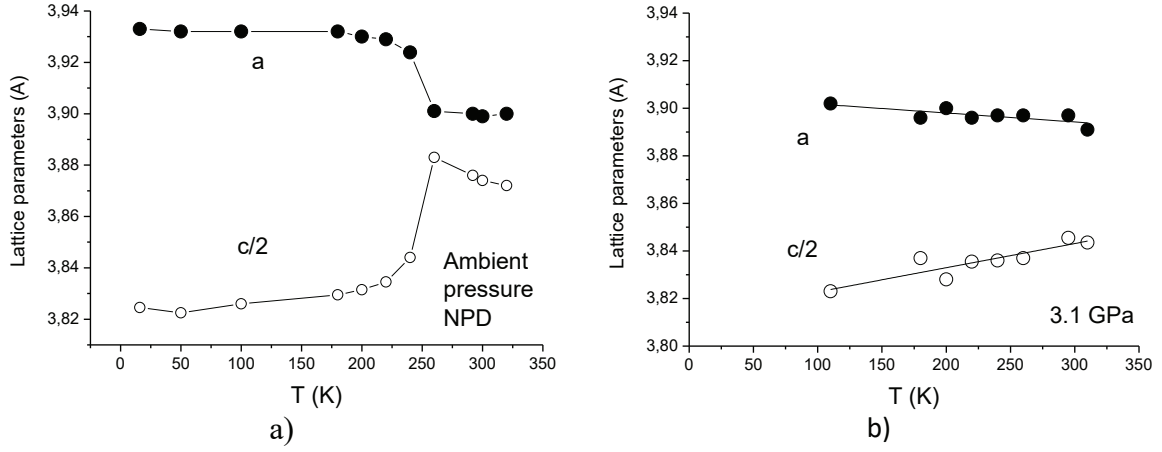


Fig. 2. Unit cell parameters ($I4/mmm$ tetragonal structure) a and $c/2$ at ambient pressure (a) and 3.1 GPa (b).

For the same sample we measured ac-specific heat, magnetic susceptibility and electric conductivity in the pressure range 0 – 5 GPa (Fig. 3). The results show the presence of ferromagnetic conducting state at high temperature for all pressure values.

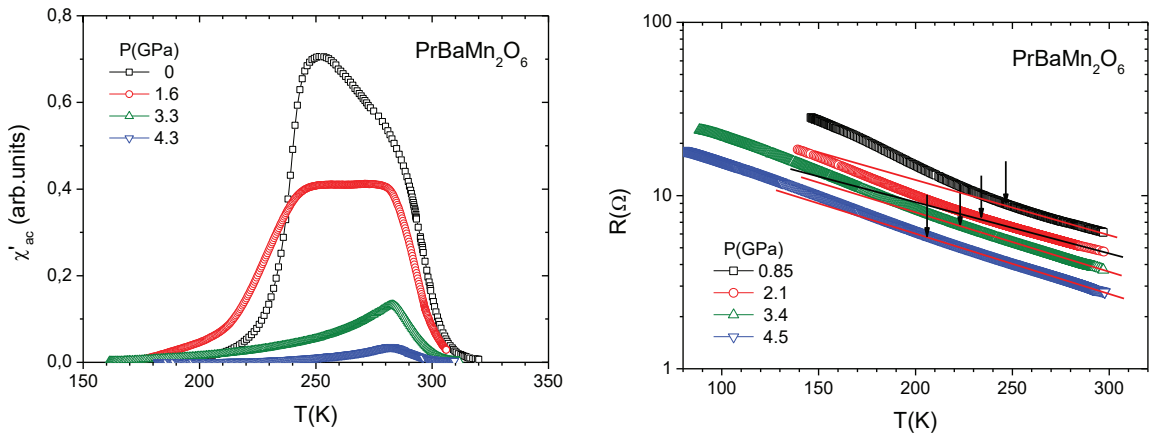


Fig. 3. Temperature dependences of magnetic susceptibility (left) and electric resistance (right) for $\text{PrBaMn}_2\text{O}_6$ at different external pressure.

We explain the results as a presence of ferromagnetic conducting clusters in antiferromagnetic insulator matrix at external pressure.

The work is supported by RFBR, grant No 19-29-12013.

[1] S.W. Nakajima T., Kageyama H., Yoshizawa H., Ohoyama K., Ueda Y (2003). Ground state properties of the a-site ordered manganites, $\text{R}\text{BaMn}_2\text{O}_6$ ($R = \text{La}, \text{Pr}$ and Nd). *J. Phys. Soc. Jpn.* 72, 3237–3242.

[2] E.V. Sterkhov, N.M. Chtchelkatchev, E.V. Mostovshchikova, R.E. Ryltsev, S.A. Uporov, G.L. Pascut, A.V. Fetisov, S.G. Titova (2021). The origin of the structural transition in double-perovskite manganite $\text{PrBaMn}_2\text{O}_6$ ” *Journal of Alloys and Compounds.* 892, 162034.

THE PRESSURE EFFECT ON THE CRYSTAL AND MAGNETIC STRUCTURE PROPERTIES OF VAN DER WAALS MATERIAL CrBr₃

O.N. Lis^{1,2}, D.P. Kozlenko¹, S.E. Kichanov¹ and E.V. Lukin¹

¹*Frank Laboratory of Neutron Physics, Joint Institute for Nuclear Research, Dubna, Russia*

²*Kazan Federal University, Kazan, Russia*

E-mail: olis@jinr.ru

Two-dimensional (2D) magnetic materials have attracted immense attention for their possible use in a variety of spin-based applications, ranging from spin-tronics, magnetic memories to topologically protected magnons. In layered magnetic materials, the strength of interlayer and

the intralayer magnetic interaction remains significantly different, opening the possibility to control their interlayer interaction electrically. Chromium tribromide, which crystal structure is comprising two-dimensional sheets of composition CrBr₃ van der Waals bonded to one another, is of particular interest due to its extraordinary electronic and magnetic properties. The Curie temperature for CrBr₃ is reported to be about 37 K, crystallizing in the rhombohedral BiI₃ structure of R $\bar{3}$ symmetry and retains this structure at low temperatures [1]. The recent discoveries of magnetism in the monolayer limit have also opened up new possibilities for the study of two-dimensional materials [2]. Although the knowledge of CrX₃ in general is still limited, these compounds, especially CrBr₃, are perfect model systems to search for possible spin-lattice coupling phenomena in CrX₃ family due to absence of structural phase transitions at low temperatures and similarity of magnetic order in bulk and few-layer forms.

The present work focuses on the investigations of crystal and magnetic structures of chromium tribromide in wide temperature and pressure ranges. The detailed studies of the crystal structure of CrBr₃ were carried out using neutron diffraction on a DN-6 diffractometer of a pulsed high-flux IBR-2 reactor (FLNP, JINR, Dubna, Russia) in temperature range of 6-300 K and at pressure up to 5 GPa. Neutron diffraction investigations of CrBr₃ revealed to observe the formation of the long-range ferromagnetic order which leads to the negative thermal volume expansion and anomalous thermal variation of interatomic distances and angles, caused by the spin-lattice coupling. Related effects were found in vibrational spectra of this compound. Noticeable anomalies near the Curie point are observed on the temperature dependences of Raman peak frequencies as well as on their full-width at half-maximum which indicates the strong spin-phonon coupling in CrBr₃. The high pressure effect made it possible to identify unusual changes in the diffraction spectra and changes of Raman modes, which may be associated with some crystal changes in CrBr₃. However, X-ray diffraction shows that the structure with initial symmetry remains up to high pressures. It was also obtained the evolution of the unit cell parameters, bond lengths under high pressure.

[1] E. J. Samuelsen, R. Silberglitt, G. Shirane, and J. P. Remeika (1971). Spin Waves in Ferromagnetic CrBr₃ Studied by Inelastic Neutron Scattering. *Phys. Rev. B.* 3. 157

[2] H.H. Kim, Bowen Yang, Siwen Li, et al. (2019). Evolution of interlayer and intralayer magnetism in three atomically thin chromium trihalides. *Proc. Natl Acad. Sci. USA* 116, 11131–11136

EFFECT OF LANTHANIDE ATOMS SQUEEZING IN LN-ENDOFULLERENOLS AND THEIR ORDERING IN SOLUTIONS

V.T.Lebedev¹, M.V.Remizov¹, A.D.Belyaev², V.S.Kozlov¹, V.G.Zinoviev¹, E.V.Fomin¹

¹ *B.P.Konstantinov Petersburg Nuclear Physics Institute, NRC Kurchatov Institute, 188300 Gatchina, Leningrad distr., Russia*

² *National Research Center “Kurchatov Institute”, 123182 Moscow, Russia*

E-mail: Lebedev_vt@pnpi.nrcki.ru

Series of water-soluble endofullerenols $\text{Ln}@C_{82}(\text{OH})_x$ ($X \sim 30$) ($\text{Ln} = \text{Pr, Sm, Eu, Gd, Tb, Dy, Ho, Tm}$) in aqueous solutions has been studied by small angle neutron scattering at ambient and physiological temperature in the conditions of neutrality and weak acidity of surrounding medium to establish crucial features of molecular self-assembly as dependent on the atomic number ($Z = 59-69$) of encapsulated atoms with a progressive decrease in size and electronegativity lowering. Fine effects of molecular clustering were found at a primary level of a molecule assembly with neighboring molecules within the first coordination sphere and the features of molecular ordering were interpreted in terms of structural characteristics of fullerenols studied previously by EXAFS, X-ray fluorescent and gamma-resonance spectroscopy delivered a set of intermolecular parameters (mode of metal atom localization, spacings between metal and carbon atoms interior fullerene cage, degree of charge transfer and valence of encapsulated atom) [1]. Structural modeling based on the neutron scattering data enabled us to visualize different globular and chain-like fractal forms of molecular assembly at the scales from molecular diameter to the scales two orders in magnitude higher. The fundamental results obtained are also of practical importance assuming possible relevant applications of magnetic and luminescent endofullerenols in theranostics as contrasting agents and photosensitizers in Magnetic Resonance Imaging and Photodynamic Therapy [1,2]. The latter is considered especially profitable by using X-rays which are strongly absorbed and scattered by heavy atoms inside fullerenols producing secondary light emission for excitation fullerene cages or photosensitizers linked to them to prepare effective photodynamic preparations [3].

[1] V. M.Cherepanov, V. T.Lebedev, A. A.Borisenkova, E. V.Fomin, A. N.Artemiev, A. D. Belyaev, G.A.Knyazev, A.Y.Yurenya, M.A.Chuev (2020). Valence and Coordination of Iron with Carbon in Structures Based on Fullerene C_{60} According to NGR Spectroscopy and EXAFS. Crystallography Reports. 65, 3, 404–408. © Pleiades Publishing, Inc.

[2] V.T.Lebedev, Gy.Török, Yu.V.Kulvelis, O.I.Bolshakova, N.P.Yevlampieva, M.A.Soroka, E.V.Fomin, A.Ya.Vul, S.Garg (2021). Diamond-based nanostructures with metal-organic molecules. Soft Materials. DOI: 10.1080/1539445X.2021.1992425.

[3] V.T.Lebedev, Gy.Török, Yu.V.Kulvelis, M.A.Soroka, V.A.Ganzha, V.A.Orlova, E.V. Fomin, L.V.Sharonova, A.V.Shvidchenko (2022). New Photocatalytic Materials Based on Complexes of Nanodiamonds with Diphthalocyanines of Rare Earth Elements. In: Garg S., Chandra A. (eds.) Green Photocatalytic Semiconductors. Green Chemistry and Sustainable Technology. Springer, Cham. Ch.7. pp.179-208. https://doi.org/10.1007/978-3-030-77371-7_7

SMALL-ANGLE SCATTERING ON PROTON-CONDUCTING MEMBRANES WITH NANODIAMONDS

Yu.V. Kulvelis¹, V.T. Lebedev¹, O.N. Primachenko² and A.I. Kuklin³

¹Petersburg Nuclear Physics Institute named by B.P. Konstantinov of NRC “Kurchatov Institute”, Gatchina, Russia

²Institute of Macromolecular Compounds of Russian Academy of Sciences, St Petersburg, Russia

³Joint Institute for Nuclear Research, Dubna, Russia

E-mail: kulvelis_yv@pnpi.nrcki.ru

In order to create more efficient and economical hydrogen fuel cells, new proton-conducting membranes based on Nafion® and Aquivion® matrices (perfluorinated copolymers with different side chain lengths) modified with detonation nanodiamonds have been developed [1, 2]. The method of preparing membranes with enhanced conducting properties has been improved by introducing into the polymer solution small amounts (≤ 1 wt. %) of detonation nanodiamond particles 4–5 nm in size with groups (H, OH, COOH, SO₃H) grafted to the surface, removing the solvent, and precipitating the mixture on a solid substrate.

The combined mechanism of conduction is most successfully implemented in the presence of protonated diamonds (positively charged, Z⁺ type) [3] or diamond particles with sulfonic acid groups. According to small-angle neutron scattering (SANS) data, the structure of membranes in the presence of diamonds demonstrates the ionomer peak is retained at a scattering vector value of $q \sim 2 \text{ nm}^{-1}$, which means that the main structural elements in the polymer matrix - hydrophilic conducting channels and their mutual arrangement - are preserved (Fig. 1). Similar structural data were obtained for a series of Nafion® type membranes with Z⁺ nanodiamonds. However, the proton conductivity of these membranes is significantly reduced in the presence of 2-3 wt. % of diamonds.

For a deeper integration of diamond particles into the polymer matrix, an experiment was carried out on the preparation of a copolymer (emulsion copolymerization, [4]) of the Nafion® type in a mixture with Z⁺ nanodiamonds. The obtained composite membrane demonstrates a narrowed ionomer peak on the X-ray scattering curves, shifted to higher q (Fig. 2). Such changes reflect an increase in channel ordering with a decrease in the distance between neighboring channels under conditions of high diamond content (4.1 wt. %) due to a more uniform distribution in the membrane material, which showed good conducting properties.

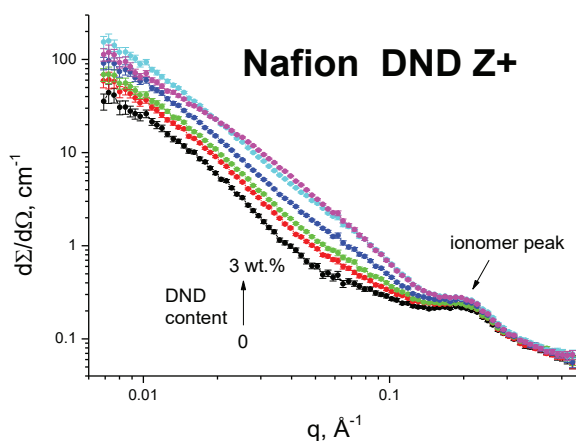


Fig. 1. SANS on Nafion®-type compositional membranes with DND Z⁺ in air-dry condition.

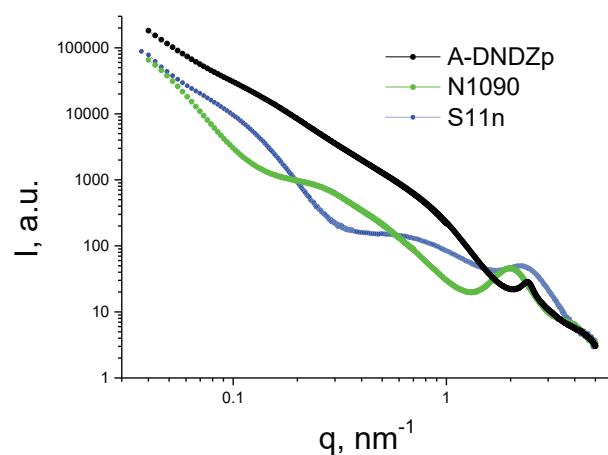


Fig. 2. SAXS on an A-DNDZp composite membrane obtained by copolymerization in the presence of diamonds and comparison with other membranes of Nafion®-type (N1090) and Aquivion®-type (S11n) without diamonds.

- [1] O.N.Primachenko (2021). State of the art and prospects in the development of proton-conducting perfluorinated membranes with short side chains: A review. *Polym. Adv. Technol.* 32,1386-1408.
- [2] V.T. Lebedev (2021). Structure of Diffusion Polymer Membranes for Molecular and Ionic Transport. *J. Surf. Inv.* 15,939-946.
- [3] Yu.V.Kulvelis (2021). Modification of the mechanism of proton conductivity of the perfluorinated membrane copolymer by nanodiamonds. *Russ. Chem. Bull.* 70,1713-1717.
- [4] O.N.Primachenko (2021). Influence of sulfonyl fluoride monomers on the mechanism of emulsion copolymerization with the preparation of proton-conducting membrane precursors. *J. Fluor. Chem.* 244,109736.

THE INFLUENCE OF ION IMPLANTATION WITH Cs⁺ ION TO THE MULTILAYER STRUCTURE OF PEROVSKITE CH₃NH₃PbI₃ MATERIALS

T.Yu. Zelenyak¹, V.A. Kinev², M. Kulik³, A. Pyshniak³, A.S. Doroshkevich^{1,4}, P.L. Tuan^{1,5}, P.P. Gladyshev², A. I. Madadzada^{1,6}, A. Stanculescu⁷, B. Jasinska³, R.G. Nazmitdinov^{1,2}, J. Žuk³

¹ Joint Institute for Nuclear Research, Dubna, Moscow region, Russia

² State University "Dubna", Dubna, Moscow region, Russia

³ Institute of Physics, Maria Curie-Skłodowska University, Pl. Marii Curie-Skłodowskiej 1, Lublin, Poland

⁴ Donetsk Institute for Physics and Engineering named after O.O. Galkin NAS of Ukraine, Kyiv, Ukraine

⁵ Hanoi Irradiation Center, Vietnam Atomic Energy Institute, Hanoi, Vietnam

⁶ Department of Neutron Physics, National Nuclear Research Centre JSC, Baku, Azerbaijan

⁷ National Institute of Materials Physics, Magurele, Romania

E-mail: Tatyana.Zelenyak@nf.jinr.ru

The influence of ion implantation on the atomic composition and the changing of the phase composition in the perovskite CH₃NH₃PbI₃ films on the (glass/ITO/TiO₂) substrates have been investigated. The analysis is done by means of the Fourier transform infrared (FTIR) reflectance spectroscopy and Energy-dispersive X-ray spectroscopy method (EDS). The multilayer structures are implanted by Cs⁺ ion beam with the energy of 100 keV and 200 keV at room temperature. The ion dose is varied from 1x10¹³ ion/cm² to 3x10¹⁴ ion/cm².

The FTIR method has shown the change of the organic cation CH₃NH₃⁺ in the CH₃NH₃PbI₃ structure after ion implantation, and the partial destruction of the structure occurs during ion implantation. The FTIR spectra of samples (glass/ITO/TiO₂/CH₃NH₃PbI₃) are shown before and after ion implantation with the energy of 100 keV (Fig. 1a) and 200 keV (Fig. 1b).

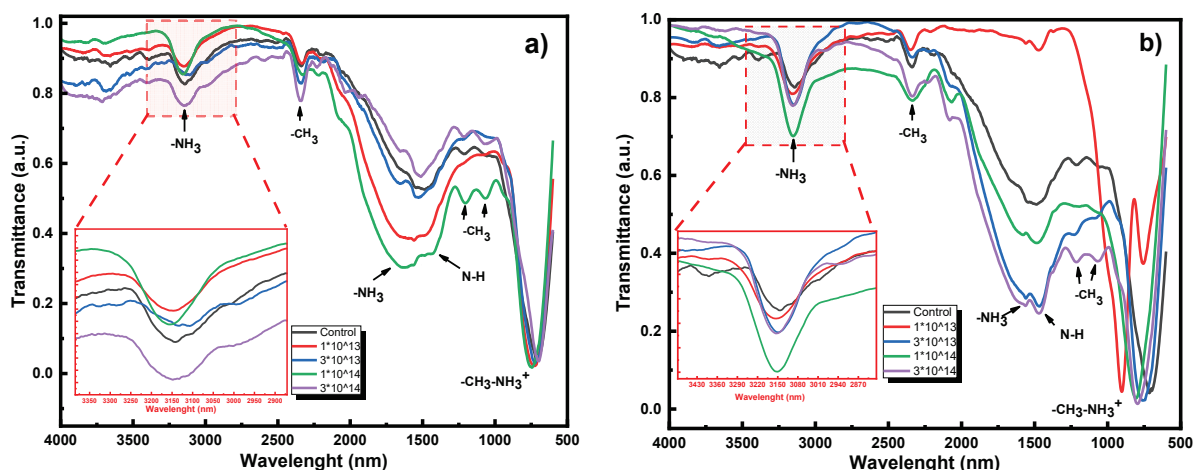


Fig.1 FTIR spectra for the perovskite CH₃NH₃PbI₃ thin films before and after ion implantation Cs⁺: a) 200 keV; b) 100 keV

There are bands of internal vibrations of the organic perovskite molecule. The first one is the rocking mode of methyl ammonium (CH₃-NH₃⁺) at the wavelength at 740 to 1220 nm [1]. It corresponds to the vibration which is observed at the CH₃, CN, and NH₃ bands, between the wavelengths 1300 - 2000 nm. The same effect was described in [2, 3]. The asymmetrical CH₃ stretch vibration produces the dominant and broad absorption band

with two peaks at 2341 (Fig. 1a) and 2336 (Fig. 1b) nm. This may be due to a significant increase in hydrogen bonding between the methylammonium and the iodide [4]. At the wavelength 3101 and 3175 nm, two bands appear, corresponding to vibrational modes from the NH₃ stretching band [2, 3]. We speculate that the partial destruction of the structure occurs during ion implantation. At low energies, the destruction occurs in the near-surface layer of the sample. It can be confirmed by the appearance of a band in the FTIR spectrum (Fig. 2b), associated with vibrations of the NH₃ bond at the wavelength 1463 nm [4].

The EDS method demonstrates the presence of the following elements in the multilayer structure of the glass/ITO/TiO₂/CH₃NH₃PbI₃ samples: Pb - 32.16%; I - 56.04%; Ti - 4.00%; O - 2.94%; Sn - 4.86%.

The study was funded by the Plenipotentiary Representative of the Government of the Poland Republic in JINR within the framework of the Poland – JINR Cooperation Project PPPB/120-25/1128/2022 and within the framework of the JINR – Romania cooperation program in 2022 (topic 03-4-1128-2017/2022).

[1] C Del Angel-Olarte, et.al. (2021). One-step method for the fabrication of high-quality perovskite thin-films under ambient conditions: Stability, morphological, optical, and electrical evaluation. *Thin Solid Films*. 717, 138438-11.

[2] Panneerselvam V., et al. (2019). Vibrational modes, chemical states and thermal stability of mechanochemically synthesized methylammonium lead iodide (CH₃NH₃PbI₃) perovskites. *Materials Letters*. 241,140-143.

[3] Abdelmageed G. et al. (2016). Mechanisms for light induced degradation in MAPbI₃ perovskite thin films and solar cells. *Applied Physics Letters*. 23, 233905.

[4] Pitchaiya, S., et al. (2018). The Performance of CH₃NH₃PbI₃-Nanoparticles based–Perovskite Solar Cells Fabricated by Facile Powder press Technique. *Materials Research Bulletin* 108, 61-72.

NANOSCALE STRUCTURE OF POSITIVE ELECTRODES FOR LI-ION BATTERIES WITH CARBON-BASED ADDITIVES BY SANS

M. Yerdauletov^{1,2,3}, M.V. Avdeev^{1,4}, O.V. Tomchuk¹, O.I. Ivankov¹, Ph.S. Napolsky⁴, V.A. Krivchenko⁴

¹*Frank Laboratory of Neutron Physics, Joint Institute for Nuclear Research, Dubna, Moscow Region, Russia*

²*Institute of Nuclear Physics, Ministry of Energy of the Republic of Kazakhstan, Almaty, Kazakhstan*

³*L.N.Gumilev Eurasian National University, Astana, Kazakhstan*

⁴*Dubna State University, Dubna, Moscow Region, Russia*

E-mail: meyr2008@mail.ru

Energy storage technology based on lithium-ion electrochemical systems makes it possible to manufacture batteries with high specific energy and power densities. Over the past decades, such batteries have been the most widely used ones in applications related to electric vehicles, portable electronics, and robotics. Lithium-ion battery specific parameters can be significantly improved by reducing the mass contribution of inactive components, as well as by controlling the microstructure of the electrode layers. The present work is related to the development of scientific and technical tools for studying microstructure of a wide range of active cathode materials with carbon-based additives and improving their characteristics in respect with the specific energy of batteries.

Using the small-angle neutron scattering (SANS) method, the effect of conducting carbon additives (carbon black, carbon nanotubes, graphene and electrochemical graphen oxide) on the porous structure of positive electrodes based on lithium iron phosphate (LFP), lithium titanate (LTO), and lithium nickel manganese cobalt oxide (NMC) is studied. To separate the scattering by closed and open pores, the electrodes are wetted with deuterated electrolytes, which makes it possible to match the scattering by open pores. Conducting carbon additives are found to change the electrode porosity to different extent and affect the wettability of the materials, both due to the different effects on the degree of incorporation into the pores of the cathode matrix, and to the impact on the cathode matrix itself. The effect of the polymer binder (PVDF) is also revealed.

The structure analysis allowed us to improve and optimize the technology of the fabrication of high-capacity cathodes for lithium-ion batteries.

[1] M.V. Avdeev, M.S. Yerdauletov, O. I. Ivankov, et al., *J. Surf. Investigation* 13(4), 614 (2019).

[2] F.Napolskiy, M. Avdeev, M. Yerdauletov, et al., *Energy Technology* 8, 2000146 (2020).

**PLENARY SESSION 2 : DEVELOPMENT OF NEUTRON SCATTERING
TECHNIQUES AND INSTRUMENTS**

COLD NEUTRONS STORAGE AT PULSED SOURCE

Yu.V. Nikitenko¹, V.L. Aksenov¹

¹*JINR, 141980 Dubna, Russian Federation*

E-mail: nikiten@nf.jinr.ru

Proposed a cold neutrons circular storage for projected at JINR a pulsed periodic reactor NEPTUNE. The relations for calculation of storage parameters, neutron current and holding time are received. It is shown the holding time can be increased significantly in compare a neutron flight time for distance which is compared with storage sizes. Possibilities are considered for conducting an experiment on measurement of probability of mirror neutrons formation. It is shown the measured minimal probability value for reactor NEPTUNE with radius 50 m is less on order than the probability for 300 m flight distance beam experiment at ESS.

WATER AND COLD MODERATOR FOR NEW RESEARCH REACTOR NEPTUN

A.A. Hassan^{1,2}, E. P. Shabalin², V. I. Savander¹

¹ *National Research Nuclear University MEPhI (Moscow Engineering Physics Institute), Moscow, Russia.*

² *Joint Institute for Nuclear Research (JINR), Dubna, Russia.*

E-mail: AKhassan@mephi.ru

At present, neutrons are widely used in different experiments to investigate interactions, structure and properties of nuclei, condensed matter including solid states, liquids, polymers, biological systems and chemical reactions. Neutrons are produced in high intensity mainly by reactors (steady state or pulsed) and spallation sources. Thermal and cold neutron spectrum can be controlled by interest through optimizing the thermal and cold moderator. Pulsed mode of neutron source and high-intensity sources are prospects for increasing the accuracy of experiments that use cold neutrons as neutron diffraction, reflection and small angle neutron scattering.

Ultra-cooled neutrons were discovered by F.L.Shapiro's group in 1968 at FLNP in Dubna, Russia. Cooled neutrons are these neutrons which have energy within the range (10-7 to 10-3 eV) or wavelengths between (930 to 10 Å) Which has great advantages in most modern experiments at the present time. Neutrons having wavelengths greater than 4 Å are useful for scattering experiments. The ratio of these neutrons in extracted neutron beams from research reactors are very small according to Maxwellian distribution. To increase the cooled neutrons ratio, a complex of thermal and cooled moderators must be used. Cooled moderators are moderators having a very cooled temperature (≈ 20 K) like mesitylene, methane, beryllium ortho and para hydrogen and deuterium and ice water [1, 2]. At these low temperatures only hydrogen or deuterium can be in liquid phase, other possible moderators like ice or mesitylene will be solids. In high neutron flux these solid materials will suffer from many problems like heat removal, radiation damage and decomposition only liquid materials at low temperatures can be more reliable. For these reasons hydrogen can be the best moderator because of good heat removal properties, most economical in size, but of its relatively large absorption cross section, an increase in volume above optimum will not give any increasing in cooled neutron flux. On the other hand, deuterium has a low absorption cross sections and also low scattering cross sections so in the case of using deuterium a huge volume must be used to get the optimum neutron flux [3].

FLNP at Dubna, Russia has overcome problems of solid moderators and used solid methane to enhance the cold neutron flux ($\lambda > 6$ Å) by a factor of 20. And concluded that solid methane cold moderator can increase the flux 2 to 3 times that of liquid hydrogen [4]. This was confirmed the results from America and Japan [4-6]. In 2012 in Dubna cold neutrons were generated for the first time with the unique cold moderator on the basis of pelletized mesitylene carried by helium gas at 25 K [7-9].

This work is aims to optimize the thermal and cold moderators for the fourth-generation neutron source in Dubna (reactor NEPTUN) to get the higher possible thermal and cold neutron fluxes in extracted neutron beams.

[1] Carter, P. and D.J.J.o.N.E. Jones, A study of cold neutron spectra emerging from sources of liquid hydrogen and deuterium and a Monte Carlo method for optimisation. 1972. 26(5): p. 237-249.

[2] Carpenter, J.M., Cold moderators for pulsed neutron sources. 1990.

[3] Ageron, P., et al., Experimental and theoretical study of cold neutron sources of liquid hydrogen and liquid deuterium. 1969. 9(1): p. 42-50.

[4] Beljakov, A., et al., Solid methane cold moderator for the IBR-2 reactor. 1996. 3(3): p. 209-221.

- [5] Carpenter, J.M.J.N., Thermally activated release of stored chemical energy in cryogenic media. 1987. 330(6146): p. 358-360.
- [6] Beliakov, A., E. Shabalin, and I. Tretyakov, First experience with the new solid methane moderator at the IBR-2 reactor. 2001.
- [7] Kuklin, A., et al., Analysis of neutron spectra and fluxes obtained with cold and thermal moderators at IBR-2 reactor: Experimental and computer-modeling studies. 2011. 8(2): p. 119-128.
- [8] Anan'ev, V., et al., Cold neutron moderator on an upgraded IBR-2 reactor: the first set of results. 2014. 59(2): p. 283-286.
- [9] Ananiev, V., et al., The world's first pelletized cold neutron moderator at a neutron scattering facility. 2014. 320: p. 70-74.

RECENT DEVELOPMENTS OF LINEAR POSITION-SENSITIVE NEUTRON DETECTORS IN DSC FLNP

A.V. Churakov^{1,2}, A.A. Bogdzal¹ and E.I. Litvinenko¹

¹*Joint Institute for Nuclear Research, Dubna, Russia*

²*Dubna State University, Dubna, Russia*

E-mail: churakov@nf.jinr.ru

Linear position-sensitive neutron detectors (LPSD) are used to measure the spatial distribution of neutron beams in various types of experiments. However, along with the advantages, the currently used counters have certain disadvantages, the main of which are the limitation on load and service life in high-power neutron beams. The new high-flux neutron sources raises the requirements for detecting part of scientific installations. The Department of the Spectrometers Complex of the Frank Laboratory of Neutron Physics (DSC FLNP) is conducting research aimed at evaluating the perspectives of using LPSDs, based on helium proportional position-sensitive counters (PSC) with a resistive anode. Theoretical calculations and simulations have shown the possibility of distortion of the amplitude spectrum with a decrease in the diameter of the counter less than 6 mm. This is due to the fact that the ranges of primary ionization particles do not fit into the counters volume. This effect decrease the signal-to-noise ratio and leads to a deterioration in the characteristics of the counters.

To test the capabilities of industrial detectors with a resistive anode, a test module of 2 position-sensitive counters made by Toshiba was designed. Measurements were carried out on the channel number 9 of the IBR-2 research reactor. Experimental results have shown the possibility of using counters on modern pulse reactors in the time-of-flight mode. The measured spatial resolution was about 0.5% of the counter length.

As a result of cooperation between JINR and the St. Petersburg Nuclear Physics Institute (PNPI, Gatchina, Russia), the development of linear position-sensitive neutron detectors has started. The counters were developed at the production base of LLC “SPF Consensus” (Zaprudnya, Russia). Thermal neutron LPSDs of various lengths, 8 mm in diameter, have been developed and are ready for industrial production. Test modules assembled from these counters were tested at the IR-8 research reactor of the Kurchatov Institute (KI), Moscow, Russia.

On the basis of SPF Consensus counters, a typical module was developed for use in detector systems of neutron scattering experimental facilities used in nuclear and condensed matter physics. The detector system can consist of one or more modules, the modules can be connected to each other without gaps along the axis perpendicular to the anode.

The authors express their gratitude to E.V. Altyntbaev (PNPI) for the experimental equipment provided and to A. I. Kalyukanov (KI) for the help in measurements.

Results were carried out with the financial support of the Russian Federation represented by the Ministry of Science and Higher Education, agreement No. 075-10-2021-115 of 13 October 2021 (internal number 15.СИИ.21.0021).

MONTE CARLO SIMULATION OF A SCINTILLATOR NEUTRON COUNTER FOR RING DETECTOR ARRAY

D.A. Buchnyy^{1,2}, V.S. Litvin¹, D.N. Trunov¹, V.N. Marin¹, S.N. Axenov¹ and R.A. Sadykov¹

¹ Institute for Nuclear Research RAS, Moscow, Russia

² National Research Nuclear University MEPhI, Moscow, Russia

E-mail: dbuchnyy@yandex.ru

Ring neutron detectors composed of linear scintillation counters based on ZnS(Ag)/LiF and solid-state photomultipliers were developed in INR RAS [1, 2]. Relatively high detection efficiency along with compact size of these instruments enable their usage as units composing detection arrays that simultaneously record a variety of diffraction patterns in a wide range of transmitted momenta for time-of-flight powder neutron diffraction.

In current research the numerical efficiency and resolution analysis of various linear neutron counter configurations was performed in order to optimize its design while maintaining technical simplicity. Two stages of Monte Carlo simulation were carried out using VITESS software package [3] and Python programming language. Models include passing of a scintillation counter by an arbitrary neutron flux as well as full-fledged neutron scattering experiment on a polycrystalline sample. Figure 1 shows the efficiency of the neutron counter obtained during the simulation varying the orientation of the scintillator layers relative to the neutron beam at different scattering angles.

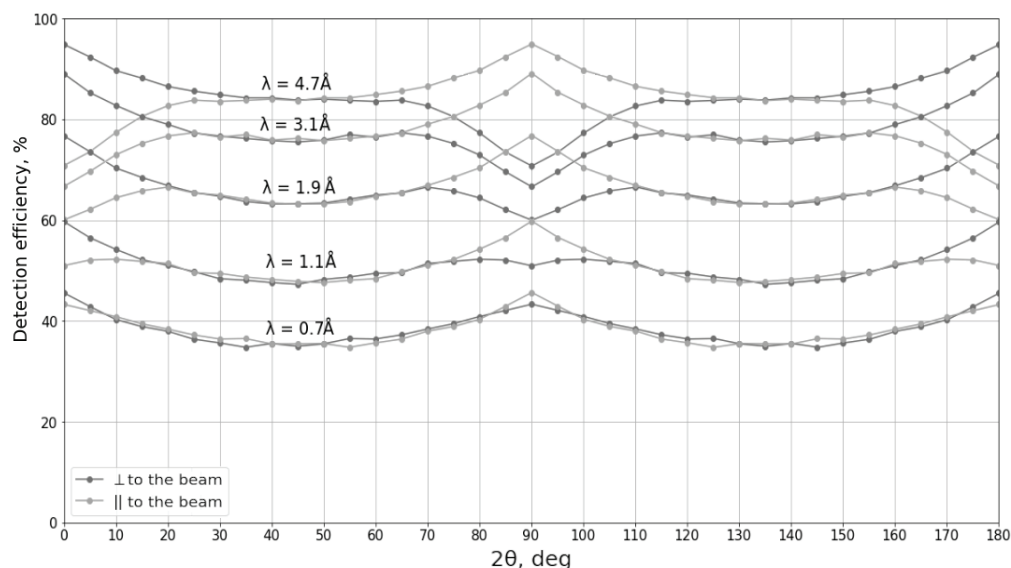


Fig. 1. Neutron detection efficiency at scattering angles 0-180° for various scintillator plane orientations relative to the incident neutron beam (R is the sample-detector distance, λ is the neutron wavelength).

This data indicates that if certain conditions are met, the detector units of different orientation can be interchangeable efficiency-wise which encourages the usage of movable segments in possible detector arrays. Powder diffraction experiment resolution using INR RAS pulsed neutron source is estimated at 2-7.6% for neutron scattering angles 150-30 degrees respectively.

The work has been supported by the Russian Ministry of Education and Science (Agreement No. 075-10-2021-115 dated October 13, 2021 [internal number 15.SIN.21.0021], project identification number 000000S507521RGN002) within the research collaboration program "Development of modern experimental stations for pulsed or constant type sources" with Joint Institute for Nuclear research (JINR).

- [1] V.S. Litvin, V.N. Marin, S.K. Karaevsky et al (2016). Scintillation neutron detectors based on solid-state photomultipliers and lightguides. *Crystallography Reports*. 61, 106–110.
- [2] V.N. Marin, R.A. Sadykov, D.N. Trunov et al (2018). A Ring Neutron Detector for a Time-of-flight Diffractometer Based on Linear Scintillation Detectors with Silicon Photomultipliers. *Instruments and Experimental Techniques*. 61, 1-8.
- [3] C. Zendler, K. Lieutenant, D. Nekrassov et al (2014). VITESS 3 – Virtual Instrumentation Tool for the European Spallation Source. *J. Phys.: Conf. Ser.* 528, 012036.

REFRIGERATOR ^3He BASED ON CLOSED CYCLE CRYOCOOLER COOLING

A.N. Chernikov¹

¹Joint Institute for Nuclear Research, Dubna, Russia

E-mail: chern@nf.jinr.ru

FLNP JINR is developing gas-filled thermal neutron detectors [1]. One of the components of the mixture of gases filling such detectors is ^3He . The detector assembly technology involves the addition of pure ^3He to a pre-prepared mixture of other gases. At the end of the service life, the detectors require refilling with a mixture of gases. The use of factory-made ^3He for these purposes is an expensive solution due to the high price of ^3He . It seems more rational to extract ^3He from the previously used gas mixture in the detector by a cryogenic means. To do this, it is necessary to have temperatures below 3.3 K, corresponding to the liquid state of ^3He . These temperatures can be obtained in helium cryostats or using closed-cycle cryocoolers, for example, Gifford-McMahon (GM), and combining with them a ^3He refrigerator - a device in which ^3He is liquefied and its vapors are pumped out.

This paper describes the design of a ^3He refrigerator specialized for the task of purifying ^3He from impurities based on a GM cryocooler (Fig. 1).

Refrigerator ^3He is a column of heat exchangers located on the regenerative part of the cold head. Here 1 is the main flange, on which container 2 is mounted from below, a pipe with a diameter of 150 mm made of thin-walled stainless steel and a length of 390 mm. 3 - cryostat manifold, on which a cold head 4 is installed coaxially with the container. The length of the container was determined by the requirement to accommodate the entire cold head and heat exchangers in it.

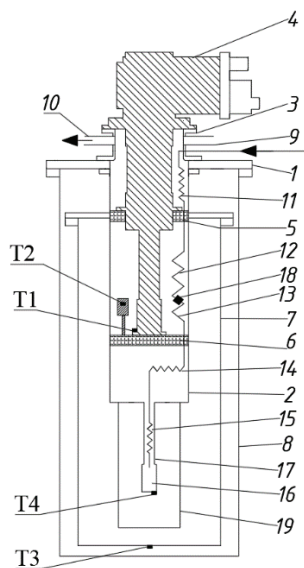


Fig.1. Scheme of the ^3He refrigerator and cryostat

The first and second stages are equipped with heat exchangers 5 and 6, respectively, which provide thermal connection of helium with the cryocooler stages. The thermal connection of these heat exchangers with the container wall is carried out due to the thermal conductivity of helium. 7 – thermal screen mechanically connected to the container wall at the level of the first stage of the cryocooler; 8 – vacuum housing of the cryostat.

^3He is fed into the container through tube 9, and is pumped out through pipe 10. Tube 9 passes into a tubular heat exchanger consisting of several sections connected in series (11, 12, 13 and 14) wound around the regenerator part of the cold head.

The heat exchanger ends with a throttle 15, which provides the necessary condensation pressure ^3He . Liquid ^3He accumulates in the evaporator 16, which is connected to the container by means of a thin-walled stainless steel tube 17 12 mm in diameter and 60 mm long.

To separate ^3He from impurities, a pump with activated carbon 18 is installed between the sections of the heat exchangers.

Helium vapor ^3He from the evaporator enters the container and then is pumped out through pipe 10.

An important element of the refrigerator is the heat shield 19, which takes a temperature close to the temperature of the second stage of the cold head, about 2.5 K.

The temperature was measured by temperature sensors - silicon diodes - T1, T2, T3 and thermistor T4. Figure 2 shows a photograph of the refrigerator heat exchangers, the numbering corresponds to Figure 1.

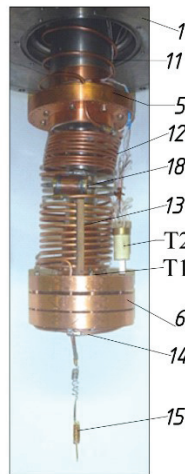


Fig.2. Refrigerator heat exchanger system

In the mode of evacuation of ^3He vapors through pipe 10 with a pump with a capacity of 35 m^3/h and replenishment of liquid ^3He in the evaporator by continuous condensation through throttle 15, a temperature of 0.78 K was obtained (thermistor T4).

In the mode of pumping out vapors of pre-condensed ^3He without replenishing it, a temperature of 0.52 K is reached in the evaporator (thermistor T4).

[1] A. V. Belushkin et al. (2010). Development of gas-filled position-sensitive detectors of thermal neutrons at the Frank Laboratory of Neutron Physics of the Joint Institute for Nuclear Research. Phys. of the S. St., 52, 1025–1028

PROTOTYPE OF TWO-DIMENSIONAL SCINTILLATOR DETECTOR BASED ON ZnS(Ag)/⁶LiF WITH WAVELENGTH-SHIFTING FIBERS

M. M. Podlesnyy^{1,2}, V. Milkov¹, A. A. Bogdzel¹, V. I. Bodnarchuk¹, O. Daulbaev^{1,3,4},
A. K. Kurilkin¹, M. O. Petrova¹

¹ Joint Institute for Nuclear Research (JINR), Dubna, Russian Federation

² Moscow Institute of Physics and Technology (National Research University), Dolgoprudny, Russian Federation

³ The Institute of Nuclear Physics, Ministry of Energy of the Republic of Kazakhstan, Almaty, Kazakhstan

⁴ Al-Farabi Kazakh National University, 050038 Almaty, Kazakhstan

E-mail: maxim.podlesnyy@nf.jinr.ru

Prototype of two-dimensional scintillator detector based on ZnS(Ag)/⁶LiF with wavelength-shifting fibers has been developed in the Frank Laboratory of Neutron Physics of the Joint Institute for Nuclear Research (Dubna).

The detector consists of 4-layers of scintillator plates (ND screen) 9.6 x 9.6 cm² and 5-layers of wavelength shifting optical fibers with a thickness of 1 mm (square cross section), located between plates (fig. 01). The detector is divided into 16 channels along the X coordinate and the Y coordinate. One channel equals 6 mm and includes three fibers. The channels are separated using 14 μm aluminum foil.

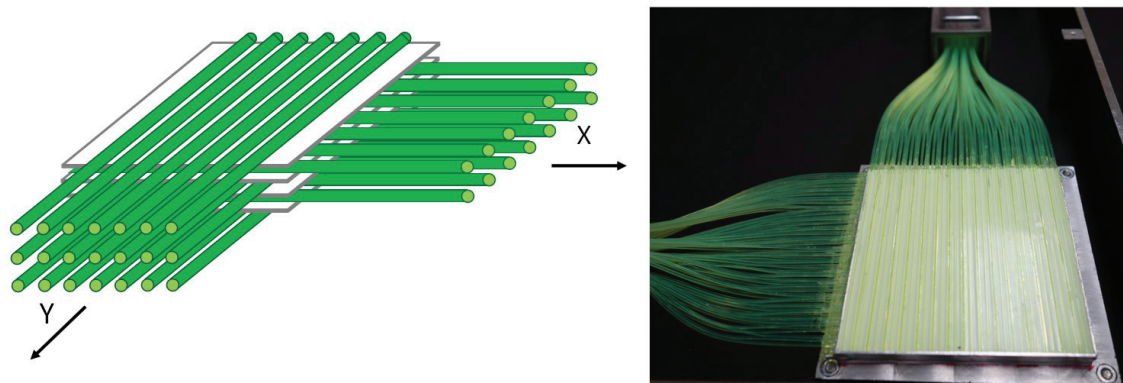


Fig. 1. Simplified layout of the scintillator and optical fibers (left), photo of the detector assembly(right).

There were used two 16-channel photomultipliers Hamamatsu - H8711-100 (photocathode 30x30 mm) for the formation of an electronic signal and its amplification. Further signals were recorded and processed using multichannel digitizers from CAEN and a personal computer. Data were obtained on an experimental bench using a ²⁵²Cf neutron source. The report will present the first results obtained, as well as methods for selecting and processing these results and their efficiencies.

STATUS REPORT OF DEVELOPING PLATE CHAMBER DETECTOR WITH B-10 FOR THERMAL NEUTRONS

Petrova M.O.^{*1}, Bogdzel, A.A.¹, Milkov V.M.¹, Bodnarchuk V.I.¹, Daulbaev O.¹, Bulatov K. V.¹

¹*Frank Laboratory of Neutron Physics, Joint Institute for Nuclear Research, Dubna, Russia*

E-mail: mbelova@jinr.ru

Currently studies of condense matters give preference to neutron graphic methods. These methods are non-destructive and allow us to study both the surface and internal structure of the sample. The main part of all neutron scattering facility is a detector system. Resistive plate chamber detector's type has wide application in high energy physics because their time resolution and the availability of materials for their producing. The electrical signal is induced on the reading cuprum strips. The spatial resolution of the detector can reach hundreds of micrometers. These reasons prompted us to create a new type of thermal and cold neutron detector – a single-band resistive plate chamber with a ¹⁰B converter. A conceptual design of detector will be presented in the report.

4-CHANNEL DATA ACQUISITION DEVICE WITH USER WEB INTERFACE FOR 2D MULTI-WIRE PROPORTIONAL CHAMBERS WITH A DELAY LINE READOUT

M.A. Golubev, V.A. Solovei, T.V. Saveleva, A.O. Polyushkin

NRC KI PNPI, Gatchina, Russian Federation

E-mail: golubev_ma@pnpi.nrcki.ru

The device is PCB with 4-channel TDC coupled with INTEL ALTERA DE0-NANO development board which runs the firmware and the software that are essential for data acquisition and watching online data graphical representation in the client as an experiment goes. As a part of neutron detector this device needs to be connected with other electronic devices that converting signals to appropriate form for TDC chip, so the key value of the project is three parts of the software. The FPGA firmware, the ARM-Linux web server and the JavaScript client for modern web browsers.

The work was supported by the Ministry of Science of the Russian Federation, grant No. 075-10-2021-115 dated October 13, 2021.

LIPID NANOCARRIERS FOR DELIVERY OF NATURAL NEUROPROTECTIVE
COMPOUNDS

A. Angelova

Université Paris-Saclay, CNRS, Institut Galien Paris-Saclay, F-92296 Châtenay-Malabry,
France

E-mail: angelina.angelova@universite-paris-saclay.fr

An overview on current research and future prospects for the development of soft lipid-based nanocarriers of neuroprotective drugs will be presented. The small-angle scattering techniques are indispensable for the development of lipid-based nanoformulations for drug delivery. They can determine the structure of smart nanomaterials and nanoscale objects obtained by self-assembly of lipids and other biomolecules (peptides, proteins, nucleic acids, *etc.*). Lipid bilayer membranes control the effective adsorption and anchoring of peptide or nucleic sequences, which allow fabrication of nanocarriers for biomolecular targeting. The formation of supramolecular complexes between lipid membranes and protein-derived sequences may yield different structural organizations as a function of the biomolecule affinity for insertion into the lipid bilayers. Examples will be presented to demonstrate the tuning of the structural organization of lipid nanoparticles (vesicles, cubosomes, spongosomes, or multilamellar liposomes) upon biomolecular loading influenced by the hydrophobic/hydrophilic balance of the investigated self-assembled mixtures [1-3]. We conclude that SAXS and SANS are required for understanding the mechanism of loading and release of drugs in self-assembled amphiphilic nanocarriers that are suitable for development of neuroprotective nanomedicines.

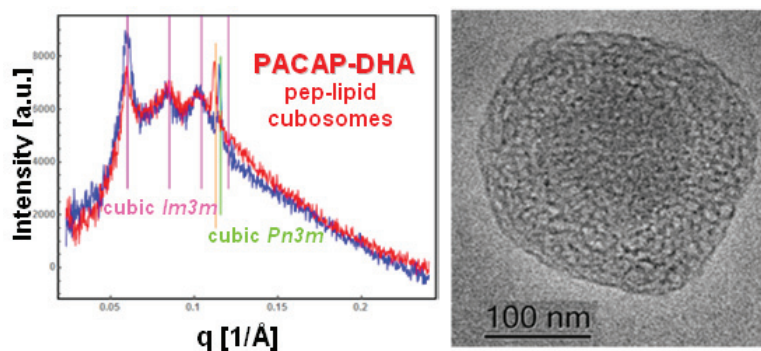


Fig.1 SAXS patterns and cryo-TEM image of peptide drug-loaded cubosome nanoparticles.

- [1] Angelova, A.; Drechsler, M.; Garamus, V.M.; Angelov, B. (2019) Pep-lipid cubosomes and vesicles compartmentalized by micelles from self-assembly of multiple neuroprotective building blocks including a large peptide hormone PACAP. *ChemNanoMat* 5, 1381-1389.
- [2] Angelov, B.; Angelova, A.; Filippov, S. K.; Drechsler, et al. (2014) Multicompartment lipid cubic nanoparticles with high protein upload: Millisecond dynamics of formation. *ACS Nano* 8, 5216-5226.
- [3] Angelov, B.; Angelova, A.; Filippov, S. K.; Narayanan, et al. (2013) DNA/fusogenic lipid nanocarrier assembly: Millisecond structural dynamics. *The Journal of Physical Chemistry Letters* 4, 1959-1964.

SUPROMOLECULAR PROTEIN STRUCTURE FORMATION IN ANIMAL AND HUMAN SKIN INVESTIGATED BY SANS

Lyubov Ivanova¹, Nikolay Verlov¹, Julia Gorshkova², Gennady Kopitsa¹, Andrey Pantelev¹, Dmitry Lebedev¹

¹*Petersburg Nuclear Physics Institute NRC KI, Orlova Roscha, Gatchina, Russia*

²*Frank Laboratory of Neutron Physics Joint Institute for Nuclear Research, Dubna, Russia*

E-mail: ivanova_la@pnpi.nrcki.ru

The etiology of many diseases of the skin, the respiratory system and the digestive tract is associated with functional disorders of ordered systems in their surface layers. Psoriasis [1], ichthyosis [2], asthma, bronchitis, chronic obstructive pulmonary disease, cystic fibrosis [3], many dysfunctions of the digestive tract and reproductive system - all these pathologies are associated with disturbances in the structural organization of the ordered systems of integumentary tissues. Although the first structural information from skin was obtained by electron microscopy and X-ray diffraction more than half a century ago, at this time the structural organization can be considered well described only for the lipid component of the stratum corneum [4], whereas the structural and functional properties of the protein component of the surface layer of skin formed by keratins and proteins of the epidermal differentiation complex, its formation and interaction with the components of the lipid matrix and cell membrane as well as the role in the barrier function of the epidermis are much less understood. Existing models suggest self-organization of intermediate protein filaments in interaction with lipid membranes [5] into a dense highly ordered package. We used contrast variation SANS that revealed a series of diffraction maxima in the skin preparations of adult mice that can be attributed to the presence of a hierarchy of ordered protein structures with the characteristic sizes of 10 – 60 nm. The diffraction pattern was significantly less pronounced in the skin and the epidermis samples from newborn mice, and was completely absent in undifferentiated keratinocyte cultures. Treatment of preparations with collagenases led to a significant decrease in the amplitude of the observed diffraction pattern with the protein structures with the characteristic size of ca. 10 nm being the least affected. In the human skin bioprobes the intensity of the maxima varied depending on the age of the donor and the site of the biopsy but were always observed in the region 0.01 - 0.03 Å⁻¹ while in isolated human epidermis these maxima were completely absent with a pronounced maximum observed near 0.07 Å⁻¹. These data have implications in understanding of the process of wound healing as well as the protein structural organization involved in dynamics of formation of skin corneal envelope.

The work was supported by NRC "Kurchatov Institute" (№2757)

[1] R. Chovatiya, J.I. Silverberg (2019). Pathophysiology of atopic dermatitis and psoriasis: implications for management in children. *Children*. 6(10), 108.

[2] J.J. DiGiovanna, L. Robinson-Bostom (2003). Ichthyosis. *American journal of clinical dermatology*. 4(2), 81-95.

[3] D.A. Stoltz, D.K. Meyerholz, M.J. Welsh (2015). Origins of cystic fibrosis lung disease. *New England Journal of Medicine*. 372(4), 351-362.

[4] P.M. Elias (2012). Structure and function of the stratum corneum extracellular matrix. *Journal of investigative dermatology*. 132(9), 2131-2133.

[5] L. Norlén, A. Al-Amoudi (2004). Stratum corneum keratin structure, function, and formation: the cubic rod-packing and membrane templating model. *Journal of Investigative Dermatology*. 123(4), 715-732.

STUDY OF OLIGOMERIZATION POLYDISPERSITY OF METHIONINE GAMMA-LYASE

Yu.L. Ryzhikau^{1,2}, N.A. Bondarev¹, I.V. Manukhov^{1,3} and A.I. Kuklin²

¹Research Center for Mechanisms of Aging and Age-Related Diseases, Moscow Institute of Physics and Technology, 141700 Dolgoprudny, Russia

²Frank Laboratory of Neutron Physics, Joint Institute for Nuclear Research, 141980 Dubna, Russia

³State Research Institute of Genetics and Selection of Industrial Microorganisms, Moscow, Russia

E-mail: rizhikov@phystech.edu

Testing the functional activity of proteins may require characterizing their oligomeric state, for which the small-angle scattering method is well suited. This work presents the results of a study of the oligomerization of methionine gamma-lyase (MGL), the main functional state of which assumed to be a tetramer [1]. Samples of methionine gamma-lyase were studied with small-angle neutron scattering (SANS) on a YuMO spectrometer at IBR-2 [2], [3].

Methionine gamma-lyase is an enzyme that degrades sulfur-containing amino acids to α -keto acids, ammonia, and thiols. Regulation of these amino acids is important because sulfur-containing amino acids play a role in many biological processes.

Comparison of the SANS data obtained for MGL from *Clostridium tetani* with the theoretical curve calculated for the crystal structure of their homolog, MGL from *Clostridium sporogenes* (PDB ID: 5DX5), shows that experimentally obtained structural parameters (R_g , D_{MAX}) exceed those of the tetramer model.

The availability of information about the crystal packing of proteins and/or their homologs makes it possible to build models of oligomers, which can then be verified using small-angle scattering data. For example, the literature describes how the early stages of lysozyme crystallization were studied using small-angle scattering [4], [5]; the interaction interface between monomers in oligomers corresponded to crystalline contacts. Following this idea, we construct a model of an octamer (dimer of tetramers) of MGL based on crystalline contacts (PDB ID: 5DX5) [1]. Along with the tetramer and octamer models, the MGL monomer and dimer models were also used in the calculations.

Processing of the experimental SANS data with OLIGOMER program [6] shows that the fractions of monomers, tetramers and octamers are approximately 15%, 65%, and 20%, respectively, while the fraction of dimers is zero.

This result confirms that the tetramer is the main oligomeric state of MGL in solution. However, there is also a certain proportion of octamers, which can be characterized as a dimer of tetramers formed at crystalline contacts.

[1] S. Revtovich, N. Anufrieva, E. Morozova, V. Kulikova, A. Nikulin, and T. Demidkina, "Structure of methionine γ -lyase from *Clostridium sporogenes*," Acta Crystallogr. Sect. F Struct. Biol. Commun., vol. 72, no. 1, pp. 65–71, Jan. 2016, doi: 10.1107/S2053230X15023869.

[2] A. I. Kuklin et al., "New opportunities provided by modernized small-angle neutron scattering two-detector system instrument (YuMO)," J. Phys. Conf. Ser., vol. 291, no. 1, p. 012013, 2011, doi: 10.1088/1742-6596/291/1/012013.

[3] A. I. Kuklin et al., "Neutronographic investigations of supramolecular structures on upgraded small-angle spectrometer YuMO," J. Phys. Conf. Ser., vol. 848, p. 012010, 2017, doi: 10.1088/1742-6596/848/1/012010.

- [4] M. V. Kovalchuk et al., “Investigation of the Initial Crystallization Stage in Lysozyme Solutions by Small-Angle X-ray Scattering,” *Cryst. Growth Des.*, vol. 16, no. 4, pp. 1792–1797, Apr. 2016, doi: 10.1021/acs.cgd.5b01662.
- [5] M. A. Marchenkova et al., “In situ study of the state of lysozyme molecules at the very early stage of the crystallization process by small-angle X-ray scattering,” *Crystallogr. Reports*, vol. 61, no. 1, pp. 5–10, Jan. 2016, doi: 10.1134/S1063774516010144.
- [6] P. V. Konarev, V. V. Volkov, A. V. Sokolova, M. H. J. Koch, and D. I. Svergun, “PRIMUS: A Windows PC-based system for small-angle scattering data analysis,” *J. Appl. Crystallogr.*, vol. 36, no. 5, pp. 1277–1282, Oct. 2003, doi: 10.1107/S0021889803012779.

SMALL-ANGLE SCATTERING STRUCTURAL STUDY OF pH-EFFECT IN BETA-LACTOGLOBULIN – ALGINATES COMPLEXES

L. Anghel¹, A.I. Kuklin², O. Ivankov², V.I. Bodnarchuk², and R.V. Erhan^{2,3}

¹*Institute of Chemistry, Chisinau, Republic of Moldova*

²*Frank Laboratory of Neutron Physics, Joint Institute for Nuclear Research, Dubna, Russia*

³*Horia Hulubei National Institute for R&D in Physics and Nuclear Engineering, Bucharest - Magurele, Romania*

E-mail: anghel.lilia@gmail.com

β -Lactoglobulin is the major whey protein abundant in cow's milk. β -Lactoglobulin is a lipocalin whose structure contains β -barrel with eight antiparallel β -strands and one major α -helix at the end of the molecule. This protein has been widely used in the food and pharmaceutical industries due to its rheological and structural characteristics (e.g. unfolding, aggregation and gelation properties) [1].

β -Lactoglobulin is capable of binding various hydrophobic ligands, such as fatty acids and vitamins, carbohydrates, proteins and even inorganic elements [2]. At the present there is a gap with regard to the knowledge of β -lactoglobulin and polysaccharides interactions.

Our previous results from SANS data reduction and ab initio modeling for the systems containing only β -lactoglobulin showed that at pH 5.8 this protein possibly undergoes two processes: (I) the N-to-Q transition, i.e. the transition from the more compact conformation of the native form (N), $R_g=19.43 \text{ \AA}$, to the acidic form (Q), $R_g=25.59 \text{ \AA}$, and (II) aggregation or chain-like homo-multimeric protein complexes [3]. SANS data reduction and ab initio modeling of systems containing β -lactoglobulin and sodium alginate show that at pH 5.8 in the presence of sodium alginate, β -lactoglobulin predominates in a compact chain-like arrangement of corresponding to the size of the β -lactoglobulin homo-dimer.

We found that at pH 5.8, β -lactoglobulin undergoes homo-oligomerization –concentration dependent process, whilst the presence of sodium alginate in the system stabilizes β -lactoglobulin homo-dimeric forms.

Thus, a complex SANS study was carried out at the YuMO small-angle neutron spectrometer, IBR-2 pulsed reactor within $0.01 \text{ \AA}^{-1} \leq q \leq 0.30 \text{ \AA}^{-1}$ q-range for the β -lactoglobulin / sodium alginate system. The general goal of this study is to examine the influence of pH on the β -lactoglobulin alginate interactions and formation of the complexes.

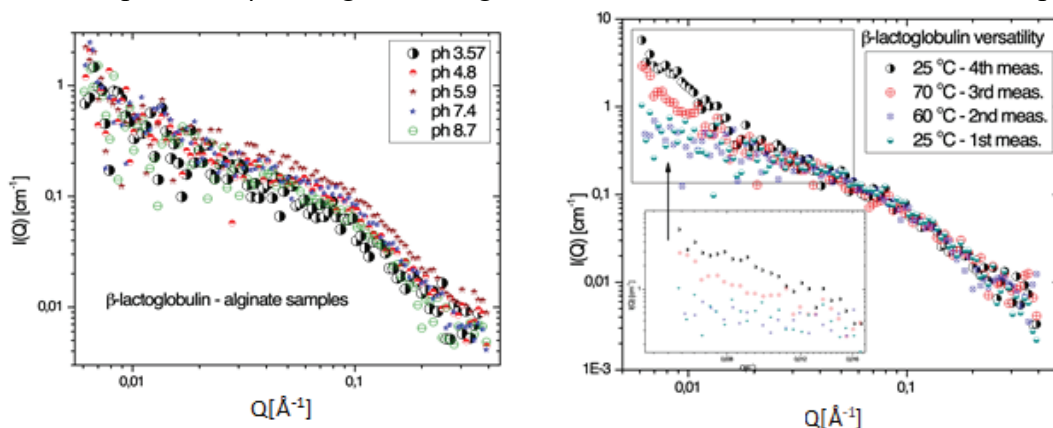


Figure 1. pH and temperature influence studied by small angle neutron scattering (preliminary data).

[1] C. Schmitt, S.L. Turgeon (2011), *Advances in Colloid and Interface Science*. 167, 1–2 pp. 63-70.

[2] S. Le Maux, et al. (2014), *Dairy Science & Technology*. 94, 5 pp 409-426.

[3] L.Anghel, A.Rogachev, A.Kuklin, R.V.Erhan (2019). β -Lactoglobulin associative interactions: a small-angle scattering study. *European Biophysics Journal*. 48, 285-295.

SURFACTANT-POLYMER INTERACTIONS IN POLYMER HYDROGELS INVESTIGATED BY SANS

Ivan Krakovsky¹ and Timur V. Tropin²

¹*Department of Macromolecular Physics, Faculty of Mathematics and Physics, Charles University, V Holešovičkách 2, 180 00 Praha 8, Czech Republic*

²*Frank Laboratory of Neutron Physics, Joint Institute of Nuclear Research, 141980 Dubna, Russia*

E-mail: ivank@kmf.troja.mff.cuni.cz

Nanophase separated structure of epoxy hydrogels containing polyoxyethylene (POE) and polyoxypropylene (POP) has been revealed and investigated by SANS in recent years [1]. The hydrogels respond sensitively to external stimuli such as change of temperature or presence of a surfactant in swelling solution [2]. The main focus of this project is investigation of the effect of interaction of ionic surfactants with POE and POP on swelling behavior and structure of the hydrogels.

Stoichiometric amphiphilic epoxy network containing POE and POP was prepared by reaction of α , ω -diamino terminated POP and POE bis(glycidyl ether) of molar masses ca 4000 and 526 g.mol⁻¹. A series of hydrogels was obtained by swelling of the network in D₂O and excess volume of solutions of two ionic surfactants: myristyltrimethylammonium bromide (C₁₄TAB) and sodium dodecylsulfate (SDS) in D₂O. SANS measurements were carried out at the YuMO small-angle instrument at the IBR-2 pulsed reactor (JINR, Dubna, Russia) in the time-of-flight regime.

A nanophase separated structure consisting of water-rich and water-poor domains with Bragg's distance ca 110 Å is revealed by SANS from the hydrogels obtained by swelling in D₂O, C₁₄TAB solutions and subcritical SDS solutions (see Figures 1 and 2). A significant increase of swelling degree was observed for all hydrogels obtained from supercritical SDS solutions. This is accompanied by change of hydrogel structure from a two-phase morphology of water-rich and water-poor domains to a morphology composed of micelles dispersed in highly swollen polymer network. Details of hydrogels structure were obtained by fitting experimental SANS profiles to models with morphology of polydisperse spheres with interaction described by hard-sphere (HS) potential and rescaled mean spherical approximation (RMSA). Average radius of water-poor domains of ca 40 Å was determined for hydrogels in case of two-phase morphology. In hydrogels containing micelles, average micelle radius of 25 Å (C₁₄TAB) and 17 Å (SDS) was found. Differences in hydrogel behavior and structure are attributed to different degrees of ionization of SDS and C₁₄TAB micelles in the hydrogels.

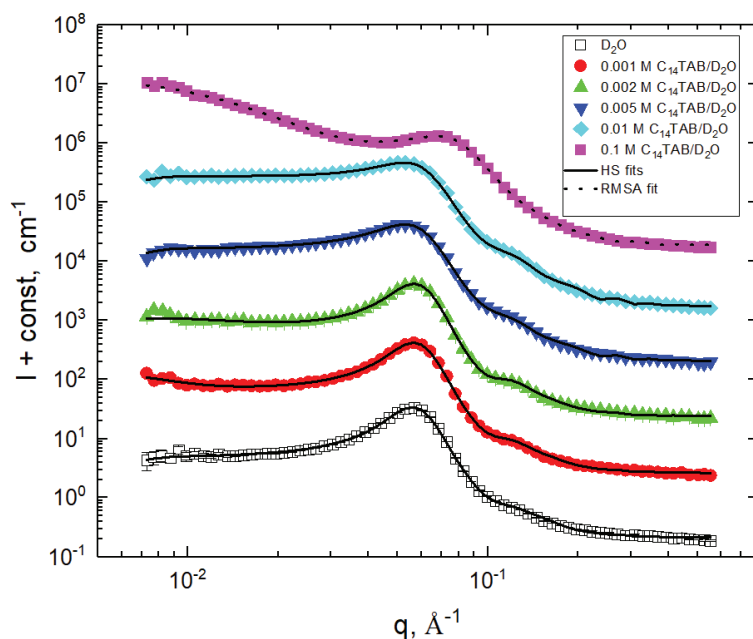


Figure 1. SANS profiles and best fitting curves for $C_{14}TAB$ hydrogels. Data are shifted for clarity.

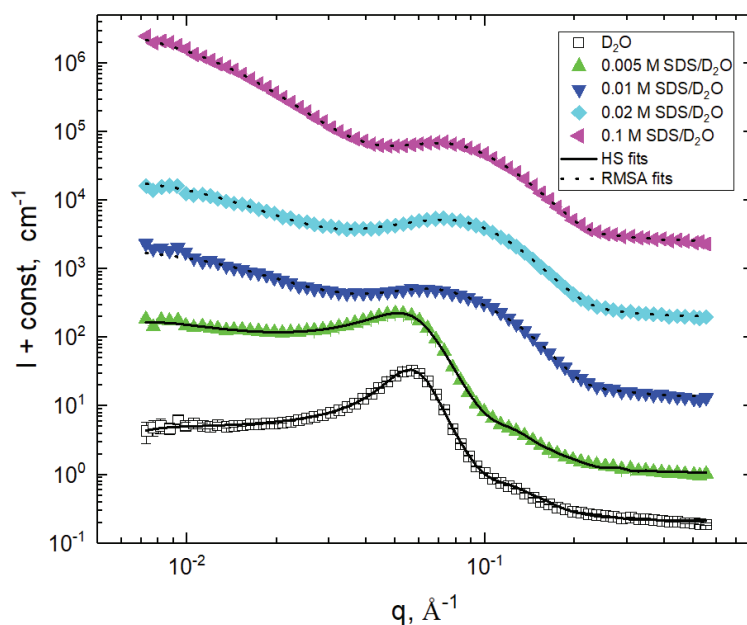


Figure 2. SANS profiles and best fitting curves for SDS hydrogels. Data are shifted for clarity.

- [1] I. Krakovský, N.K. Székely (2011). SANS and DSC study of water distribution in epoxy-based hydrogels, *Eur. Polym. J.*, 47, 2177.
- [2] I. Krakovský I., N.K. Székely (2016). SANS study on the surfactant effect on nanophase separation in epoxy-based hydrogels prepared from α , ω -diamino terminated polyoxypropylene and polyoxyethylene bis(glycidyl ether), *Eur. Polym. J.* 85, 452.

STRUCTURE OF AQUEOUS SOLUTIONS OF HETEROCYCLIC AMINES

L. Almásy¹, B. Fehér¹, W. Marczak¹

¹*Centre for Energy Research, Budapest, Hungary*

²*Jan Długosz University in Czestochowa, Czestochowa, Poland*

E-mail: almasy.laszlo@energia.mta.hu

Heterocyclic amines, such as piperidine and N-methylpiperidine, and their hydrates aggregate in aqueous solutions due to hydrogen bonds between hydration water molecules. No such aggregation occurs in the mixtures of these amines with other hydrogen-bonded solvents, such as methanol or ethanol. This difference highlights the active role of water solvent in promoting the self-aggregation.

However, the role of various contributions in thermodynamic functions due to specific interactions, van der Waals forces, and the size and shape of the molecules remains open. In the present communication we explore and discuss the family of solutions of pyrrolidine, N-methylpyrrolidine, piperidine, and N-methylpiperidine in water and methanol, as revealed by thermodynamic measurements as well as by direct structural visualisation of the mesoscopic structure employing small-angle neutron scattering.

While the limiting partial molar enthalpies of solution of pyrrolidine, N-methylpyrrolidine, piperidine, and N-methylpiperidine in methanol follow closely the trend assessed from theoretically calculated molecular interaction energies, their behavior is markedly different in water solutions, which require an empirical hydrophobic hydration term to be considered.

SANS evidenced that the aqueous amine solutions are microheterogeneous on the nanometer-order length scale. Various models are considered for describing the structural arrangement of the hydrated amine molecules. The tendency of approaching phase separation increases in the order: N-methylpiperidine < N-methylpyrrolidine < piperidine < pyrrolidine.

RESPONSIVENESS TO HYDROCARBONS OF MIXED ANIONIC/CATIONIC WORMLIKE SURFACTANT MICELLES

A.V. Shibaev¹, A.I. Kuklin^{2,3}, O.E. Philippova¹

¹ *Physics Department, Lomonosov Moscow State University, Moscow, Russia*

² *Frank Laboratory of Neutron Physics, Joint Institute for Nuclear Research, Dubna, Russia*

³ *Moscow Institute of Physics and Technology, Dolgoprudny, Russia*

E-mail: shibaev@polly.phys.msu.ru

Surfactant molecules can self-assemble into long cylindrical or wormlike micelles (WLMs) which behave like reversibly breakable polymers. WLMs can entangle and form a network which imparts viscoelastic properties to solutions. WLMs are highly responsive to the addition of hydrocarbons, which destroy the structure of WLMs. Mixed anionic/cationic WLMs are currently attracting much attention, but the influence of hydrocarbons on their structure is not well understood. The aim of this work is to study the structural and rheological transformations produced by n-decane for mixed wormlike micelles of cationic (n-octyltrimethylammonium bromide, C8TAB) and anionic (potassium oleate) surfactants.

Viscoelastic solutions of long WLMs are formed at various ratios of C8TAB to oleate. Addition of small amounts of oil results in the transformation of highly viscoelastic fluids to water-like liquids. As shown by SANS, this is due to the solubilization of hydrocarbon in the micellar hydrophobic cores leading to the change of surfactant packing and breaking of WLMs. Higher amounts of hydrocarbon are needed to disrupt the network of micelles at higher C8TAB content than for those at lower C8TAB content, even though the initial viscosity is lower at high C8TAB concentration. This is explained by preferential solubilization of hydrocarbon inside the branching points. SANS shows that hydrocarbon-induced transition of long WLMs with elliptical cross-section to ellipsoidal microemulsion droplets occurs. The internal structure of the droplets is revealed by contrast variation SANS. Ellipsoidal shape of the droplets is attributed to partial segregation of longer- and shorter-tailed surfactants inside the surfactant monolayer, providing an optimum curvature for both of them.

Responsiveness to hydrocarbons of mixed anionic/cationic WLMs studied in this work is a key property for the application of such viscoelastic surfactant solutions as hydraulic fracturing fluids in oil recovery.

Acknowledgment: the work was financially supported by the Russian Science Foundation (project 21-73-30013).

[1] Shibaev A.V., Aleshina A.L., Arkharova N.A., Orekhov A.S., Kuklin A.I., Philippova O.E. (2020) Disruption of Cationic/Anionic Viscoelastic Surfactant Micellar Networks by Hydrocarbon as a Basis of Enhanced Fracturing Fluids Clean-Up. 10, 2353.

[2] Shibaev A.V., Kuklin A.I., Philippova O.E. (2019) Different responsiveness to hydrocarbons of linear and branched anionic/cationic-mixed wormlike surfactant micelles. 297, 351-362.

GEL-LIKE STRUCTURES OF LONG MIXED WORMLIKE MICELLES

Vyacheslav Molchanov¹, Alexander Kuklin², Olga Philippova¹

¹*Lomonosov Moscow State University, Moscow, Russia*

²*Joint Institute for Nuclear Research, Dubna, Russia*

E-mail: molchan@polly.phys.msu.ru

Over the past few decades, there has been a great deal of interest in the aqueous self-assembly of surfactant molecules into giant wormlike micelles (WLMs). These cylindrical aggregates undergo reversible breakdown processes and in favorable cases can grow up to few tens of micrometers that is comparable with the length of high molecular weight polymer.

Rheometry, small-angle neutron scattering, and cryo-transmission electron microscopy were combined to investigate the structure and properties of mixed WLMs of zwitterionic and anionic surfactants. This system demonstrates the formation of giant linear long-lived WLMs, which even at extremely low surfactant concentration reach a sufficient length to entangle with each other and form a three-dimensional temporally persistent network. Stability of these micelles can be due to electrostatic attraction between the headgroups of the anionic and zwitterionic surfactants and favorable volume/length hydrophobic ratio in the surfactant mixture. Heating of these systems leads to the transition of temporally persistent network with predominantly elastic properties into transient network exhibiting viscoelasticity, which is due to the shortening of long-lived WLMs. At increasing surfactant concentration, the long-lived linear micelles transform into fast-breaking branched micelles, which is due to the screening of electrostatic interactions by salt released from the dissociated surfactant molecules. The transition results in the drop of viscosity and approaches the system to the behavior of Maxwell fluid with a single relaxation time.

This work was supported by the Russian Science Foundation (project № 21-73-30013).

STRUCTURE OF BEADS-ON-STRING COMPLEXES FORMED BY IONIC SURFACTANT AND HYDROPHOBIC POLYMER AT LOW SALT CONTENT

A.L. Kwiatkowski¹, V.S. Molchanov¹ and O.E. Philippova¹

¹ *Lomonosov Moscow State University, Moscow, Russian Federation*

E-mail: kvyatkovskij@physics.msu.ru

During the last years, one can observe an increased interest for using surfactants together with polymers in many industrial applications. Polymer/surfactant systems in aqueous medium yield a variety of objects with morphology and properties governed by its' chemical structure. The present paper represents one the study of beads-on-string polymer/surfactant complexes comprising anionic surfactant potassium oleate and hydrophobic polymer poly(4-vinylpyridine) (P4VP).

The structural transformations of charged spherical surfactant micelles of potassium oleate upon solubilization of water-insoluble P4VP were studied in salt-free aqueous solutions by several complementary techniques including small-angle neutron scattering (SANS) with contrast variation, NMR (1H and 2D 1H NOESY) spectroscopy, dynamic light scattering (DLS), cryo-TEM, and fluorescence spectroscopy. The SANS experiments were performed at the Frank Laboratory of Neutron Physics (Joint Institute for Nuclear Research, Dubna, Russia) with the YuMO instrument at the high-flux pulsed reactor IBR-2

By SANS it was shown that solubilization of polymer in the micelles results in the formation of complexes with necklace structure, where the mean distance between the micelles bound to polymer (beads) is governed by electrostatic repulsion between them. Direct imaging of complexes was carried out by cryo-TEM. Fluorescence spectroscopy, together with SANS evidence, that the polymer penetrates deep into the hydrophobic core of the beads and occupies ca. 60% of their volume. As a result, the average number of surfactant ions in the micelles decreases. The bound charged micelles impart water solubility to the polymer-surfactant system, and, according to DLS, it behaves like a polymer coil in a thermodynamically good solvent.

This work is financially supported by the Russian Science Foundation (project № 21-73-30013).

EVOLUTION OF THE STRUCTURE OF CALCIUM CARBONATE PRECIPITATES FORMED IN THE PROCESS OF BIOMINERALIZATION

Lyubov Ivanova¹, Elena Zhurishkina¹, Darya Golovkina¹, Alexander Baranchikov², Alexey Yaprntsev², Yulia Gorshkova³, Gennady Kopitsa¹, Natalia Tsvigun⁴, Vladimir Egorov⁵, Dmytry Lebedev¹, Anna Kulminskaya¹

¹*Petersburg Nuclear Physics Institute named by B.P. Konstantinov of National Research Center "Kurchatov Institute", Russia*

²*Kurnakov Institute of General and Inorganic Chemistry of the RAS, Russia*

³*Joint Institute for Nuclear Research, Dubna, Russia.*

⁴*FSRC "Crystallography and Photonics" RAS, Russia*

⁵*DMRB Petersburg Nuclear Physics Institute NRC KI, Russia*

E-mail: ivanova_la@pnpi.nrcki.ru

Biom mineralization, a phenomenon of the mineral formation by living organisms, is widespread in nature. During the metabolic reactions the various bacteria often induce calcium carbonate precipitation in soil and rocks or form an encrusted biofilms that clog urinary catheters, causing significant problem in clinical practice [1]. The ongoing research of the biom mineralization mechanisms is important for solving the clinical problems by inhibition of calcite crystallization, as well as for application of new technologies to restore concrete structures securing integrity of porous media, hydraulic control and restoration of the environment [2, 3, 4]. Abiogenic calcium carbonate crystallization is known to pass through several stages, during which the amorphous phase is successively transforming into vaterite and then calcite/argonite, as shown by the FTIR method in in situ experiments [5]. However, this process can be significantly altered by bacterial cells and their extracellular matrix (ECM). In our work, SANS, FTIR, XRD, SEM and confocal microscopy methods were used to study the evolution of the precipitated calcium carbonate structure formed during biom mineralization by the bacterium *Bacillus licheniformis* DSMZ 878 in a planktonic culture. The precipitates containing amorphous CaCO₃ in the form of fractal aggregates were detected at 24 hours of bacteria's growth in the Ca²⁺ and urea-rich medium. Fractal clusters hundreds of Angstroms in size and the fractal dimension near 2.7 (volume fractal) were detected in the precipitate. Observed over 14 days transformation of CaCO₃ polymorphs along the ACC-vaterite-calcite/argonite pathway was accompanied by a significant increase in the characteristic size of the fractal clusters and compaction of their structure yielded in an increase in the dimension of the volume fractal. The co-localization of CaCO₃ precipitates with components of ECM that included charged macromolecules (extracellular DNA, amyloid proteins and polysaccharides), was confirmed by confocal fluorescent microscopy using specific fluorescent dyes, indicating that ECM could serve as a template for the mineral formation.

[1] F. Yuan, Z. Huang, T. Yang (2021). Pathogenesis of *Proteus mirabilis* in Catheter-Associated Urinary Tract Infections. *Urol Int* 105, 354-361.

[2] N.K. Dhami, M.S. Reddy, A. Mukherjee (2014). Application of calcifying bacteria for remediation of stones and cultural heritages. *Front Microbiol* 5.

[3] G. Le Métayer-Levrel, S. Castanier, G. Oriol (1999). Applications of bacterial carbonatogenesis to the protection and regeneration of limestones in buildings and historic patrimony. *Sediment Geol* 126, 25–34.

[4] W. De Muynck, N. De Belie, W. Verstraete (2010). Microbial carbonate precipitation in construction materials: A review. *Ecol Eng* 36, 118–136.

[5] M. Cheng, S. Sun, P. Wu (2019). Microdynamic changes of moisture-induced crystallization of amorphous calcium carbonate revealed via in situ FTIR spectroscopy. *Phys. Chem. Chem. Phys.* 21, 21882-21889.

DMPC MULTI- AND UNILAMELLAR VESICLES UNDER PRESSURE

V.V. Skoj^{1,2}, A.K. Islamov, P.K. Utrobina, D.I. Soloviov^{1,2,3}, N. Kučerka¹,
V.I. Gordeliy^{2,4,5}, A.I. Kuklin^{1,2}

¹ Joint Institute for Nuclear Research, Dubna, Russia

² Moscow Institute of Physics and Technology, Dolgoprudny, Russia

³ Institute for Safety Problems of Nuclear Power Plants NAS of Ukraine, Kyiv, Ukraine

⁴ Institute of Complex Systems: Structural Biochemistry (ICS-6), Research Centre Julich, Germany

⁵ Institut de Biologie Structurale Jean-Pierre Ebel, Universite Grenoble Alpes, Grenoble, France

E-mail: vskoj@yandex.ru

The present work is devoted to the study of the effect of high hydrostatic pressure on the structure of phospholipid vesicle membranes in the vicinity of phase transitions induced by a combination of temperature and pressure.

The influence of high hydrostatic pressure on structure and phase behavior of lipid membranes has been a subject of interest over the past decades. The importance of studying these effects can be explained both by the possibility of expanding the understanding of the cellular processes of deep-sea extremophilic organisms and by applied goals, in particular, by the ability to control the phase state of the membrane without changing the temperature in order to study the effect of membranotropic agents. The results of studies of multilamellar phospholipid vesicles by neutron and X-ray small-angle scattering show a significant shift of the main phase transition (from «rigid» gel-phase L_{β} to «fluid» L_{α} phase) to higher temperatures regions [1,2].

Structural parameters of 1,2-dimyristoyl-sn-glycero-3-phosphocholine (DMPC) multilamellar (MLV) and unilamellar (ULV) vesicles in D₂O solution were investigated by SANS method on YuMO spectrometer equipped with specially designed high-pressure chamber [3]. High-pressure setup could produce pressure up to 4000 bar with an accuracy of 2.5 - 10% (depending on the pressure value). The temperature of the pressure cell containing the sample was controlled using the Lauda thermostat.

For each isothermal or isobaric scan, repeat distances (membrane thickness plus water interlayer thickness) of MLV were determined and membrane thicknesses and radii for ULV were estimated. Based on the dependences obtained, the shifts of the temperatures of phase transitions were determined. For DMPC ULV a presence of previously unobserved phase pretransition is assumed.

[1] R. Winter, C. Jeworrek (2009). Effect of pressure on membranes. *Soft Matter*. 5(17). 3157–3173.

[2] D.V. Solov'ev, et al. X-ray scattering and volumetric PVT studies of the dimyristoylphosphatidylcholine-water system. (2011). *Journal of Surface Investigation. X-ray, Synchrotron and Neutron Techniques*. 5.1. 7-10.

[3] A.I. Kuklin, D.V. Soloviov, A.V. Rogachev, *et al.* (2011). New opportunities provided by modernized small-angle neutron scattering two-detector system instrument (YuMO). *Journal of Physics: Conference Series*. 291(1).

APPLICATION OF THE ACCELERATOR MASS SPECTROMETRY METHOD TO STUDY THE MECHANISMS OF RADIATION MUTAGENESIS OF RICE CROPS: THE CURRENT STATE OF THE ISSUE

A.I. Kruglyak¹, A.S. Doroshkevich^{1,2}, Yu. Aleksiyenak¹, N.O. Appazov^{3,4}, K.B. Bakiruly⁴, M. Balasoui^{1,5}, M.N. Mirzayev^{1,6}, A.A. Nabiyeu^{1,6}, E. Popov^{1,7,8}

¹*Joint Institute for Nuclear Research, Dubna, Russia*

²*Donetsk Institute for Physics and Engineering named after O.O. Galkin, Kiev, Ukraine*

³*Korkyt Ata Kyzylorda University, Kyzylorda, Kazakhstan*

⁴*Kazakh Research Institute of Rice named after I. Zhakhaev, Kyzylorda, Kazakhstan*

⁵*Horia Hulubei National Institute for R&D in Physics and Nuclear Engineering (IFIN-HH), Bucharest – Magurele, Romania*

⁶*Institute of Radiation Problems, Azerbaijan National Academy of Sciences, Baku, Azerbaijan*

⁷*Institute of Solid-State Physics, Bulgarian Academy of Sciences, Sofia, Bulgaria*

⁸*Institute for Nuclear Research and Nuclear Energy, Bulgarian Academy of Sciences, Sofia, Bulgaria*

E-mail: Anastasiya.Kruglyak@nf.jinr.ru

Breeding rice crops resistant to drought and new diseases is a vital strategic task of modern rice growing due to the increasing shortage of water resources and the natural evolution of pathogens and viruses. The use of ionizing radiation for induced mutagenesis in plants allows creating crop varieties with desired properties. Ionizing radiation makes it possible to obtain a high percentage of chromosomal disorders with a high probability, which compares favourably with chemical mutagens, which usually lead to changes in individual genes. However, at the moment the mechanism of radiation mutagenesis is not fully understood, which does not allow to use this method to the full extent for breeding new crops with desired properties. The purpose of this study is to formulate a scientific research problem of investigating the effects of neutron radiation on the rice crop's mutagenesis and developing a new drought-resistant rice variety using the obtained knowledge.

According to study [1], rice has a relatively simple genome, which makes it a convenient model object for biotechnological research using ionizing effects.

Neutron radiation is actively used as a mutagenic ionizing effect for several crops. In particular, the authors [2], using the example of cotton seeds, empirically established a proportional dependence in the degree of biological potential disclosure with the absorbed dose when irradiated with neutrons for 24, 48, 72 and 96 hours (neutron flux was $8,64 \times 10^8$ n·s, $17,28 \times 10^8$ n·s, $25,92 \times 10^8$ n·s and $34,68 \times 10^8$ n·s, respectively). Increasing the exposure time up to 120 and 144 hours, on the contrary, led to a decrease of the germination energy in comparison with the control seeds. It means that under the influence of neutron irradiation the indicators of germination energy and seed viability increase, but with a further increase of seed irradiation time, these indicators decrease.

It has been shown that one of the possible mechanisms of the neutron irradiation effects on the change in the energy of seed germination is the formation of stable isotopes ^{15}N and ^{14}C as a result of nuclear reactions [3, 4].

According to research [5], accelerator mass spectrometry is one of the most efficient and versatile methods for elemental composition determination and can be used to determine the isotopic composition of studied objects. The method allows determining isotopes which content is less than 10^{-12} in the examined sample. Conventionally, such installation is divided into three parts: a low-energy mass spectrometer, an ion accelerator, and a high-energy mass spectrometer and can potentially be implemented on the basis of the EG-5 electrostatic accelerator at JINR (Dubna, Russia).

In addition to the isotopes ${}^7\text{N}^{15}$ and ${}^6\text{C}^{14}$, accelerator mass spectrometry makes it possible to analyze the content of cosmogenic nuclides in the Earth's crust, such as ${}^{14}\text{C}$, ${}^{10}\text{Be}$, ${}^{26}\text{Al}$, ${}^{36}\text{Cl}$, ${}^{129}\text{I}$, which are formed in the atmosphere [6] as a result of cosmic rays exposure. That opens up prospects for studying the fundamental mechanisms of living organisms adaptation to the environmental changes.

Thus, the analysis of the available literary sources indicates the possibility of solving the problem of breeding a drought-resistant rice variety by using the neutron generator options and the developing accelerator mass spectrometry option based on the EG-5 electrostatic accelerator (JINR, Dubna, RF).

The study was performed in the scope of the Ministry of Agriculture of the Republic of Kazakhstan project number BR10765056 and within the framework of the JINR-Romania cooperation program in 2022 (topic 03-4-1128-2017/2022).

[1] V.E. Viana, C. Pegoraro, C. Busanello and A. Costa de Oliveira (2019). Mutagenesis in Rice: The Basis for Breeding a New Super Plant. *Front. Plant Sci.* 10:1326. doi: 10.3389/fpls.2019.01326

[2] T.A. Khodzhaev (2014). Influence of neutron radiation on seeds of cotton. *Mir sovremennoj nauki.* 3 (25), 57-62.

[3] K.N. Mukhin (1974). *Experimental nuclear physics.* Atomizdat. 584

[4] T. A. Khodzhaev (2015). IR spectroscopic study of the mechanism of the effect of pre-sowing irradiation of cotton seeds with thermal neutrons in the process of germination and productivity in the field conditions. *Izvestiya VUZov Kyrgyzstana.* 9, 3-6.

[5] A.R. Striganov (1955). Isotopic effect in atomic spectra. *Uspekhi Fizicheskikh Nauk.* V.55, 3, 365-414.

[6] A. V. Blinov (1999). Accelerator mass-spectrometry of cosmogenic nuclides. *Soros educational journal.* 8, 71-75.

CRYSTALLOGRAPHIC TEXTURE OF THE GRYPHAEA DILATATA BIVALVE SHELLS

A.V. Pakhnevich^{1,2}, D.I. Nikolaev², T.A. Lychagina²

¹*Borissiak Paleontological Institute of RAS, Moscow, Russia*

²*Joint Institute for Nuclear Research, Dubna, Russia*

E-mail: alvpb@mail.ru

In the seas of the Middle and Late Jurassic of the East European Platform, bivalve mollusks of the family Gryphaeidae were a frequently occurring fauna element. The most common were the species of the genus *Gryphaea* (Lamarck, 1801). The shells of these mollusks were large and thick-walled. At the same time, the left valve is strongly convex with a curved umbo, while the right valve is flattened. The thick-walled shell protected well from predators, withstood abrasion in shallow water due to wave activity; thickened walls coalesced better when beds were formed. Such a shell organization turned out to be very evolutionarily successful; therefore, the genus existed from the Late Triassic to the Paleogene [1]. A similar adaptation was also characteristic of the Cenozoic Gryphaeidae, and it also manifested itself within the closely related bivalve family Ostreidae.

It can be assumed that the thickened shell of fossil mollusks may have a more ordered crystallographic texture, which is necessary to preserve its integrity. The aim of this work is to compare the crystallographic textures of the bivalve mollusks *Gryphaea dilatata* Sowerby, 1816 from three remote localities formed under different diagenetic conditions.

Valves were taken from the Mikhailovsky quarry near the city of Zheleznogorsk (Kursk region) from the deposits of the Callovian stage of the Middle Jurassic. Valves collected in a quarry near the village of Sukhochevo (Oryol region) also originate from the Callovian deposits. Only the left valves of this species were found in the urban quarry in the town of Roshal (Moscow region). The complex of accompanying fauna was analyzed to determine the geological age. For comparison with *G. dilatata*, the left valve of *Pycnodonte mirabilis* (Rousseau, 1842) (family Gryphaeidae) was selected from the Cretaceous deposits of the Crimea, as well as recent (Maly Utrish coast, Black Sea; Portugal, port of Lagos) and Pleistocene (Arabat Bay of the Sea of Azov; Chushka Spit, coast of the Taman Peninsula) *Ostrea edulis* Linnaeus, 1758.

The crystallographic texture was studied by means of time-of-flight neutron diffraction at the SKAT facility at the Frank Laboratory of Neutron Physics (JINR, Dubna, Russia) [2]. It was analyzed according to the pattern of isolines on the pole figures and the numerical values of the greatest sharpness.

It has been established that the shells of *G. dilatata* from the Mikhailovsky quarry can be Middle or Upper Callovian. The gryphaea shells found near the village of Sukhochevo are Middle Callovian age, and those found in the vicinity of the Roshal town are among Callovian or Early Oxfordian age.

Only calcite was found in all valves. In terms of the maximum sharpness of the crystallographic texture, the shells of *G. dilatata* from the three localities almost do not differ, that is the habitat conditions and fossilization did not affect the texture, and it can be considered a very stable feature.

For the first time, using neutron diffraction and pole figures, the features of *G. dilatata* shells recrystallization that affect the crystallographic texture were revealed.

It has been established that in one mollusk the crystallographic texture of the left and right valves of various shapes differs: to a greater extent by the pattern of isolines, to a lesser extent by the values of maximum sharpness.

The calcite pole figures and the maximum sharpness of the *G. dilatata* left valves and those of *O. edulis* are similar. The pole figures and values of the maximum sharpness of the *G. dilatata* right valves are similar to the same parameters of the left valve of *P. mirabilis*. All

listed species are characterized by either an axial pole figure with a sharpness maximum in the center, or a figure with an arcuately curved sharpness maximum (Fig. 1). Possibly, it is the pole figures with such isoline patterns that are characteristic of thick-walled shells.

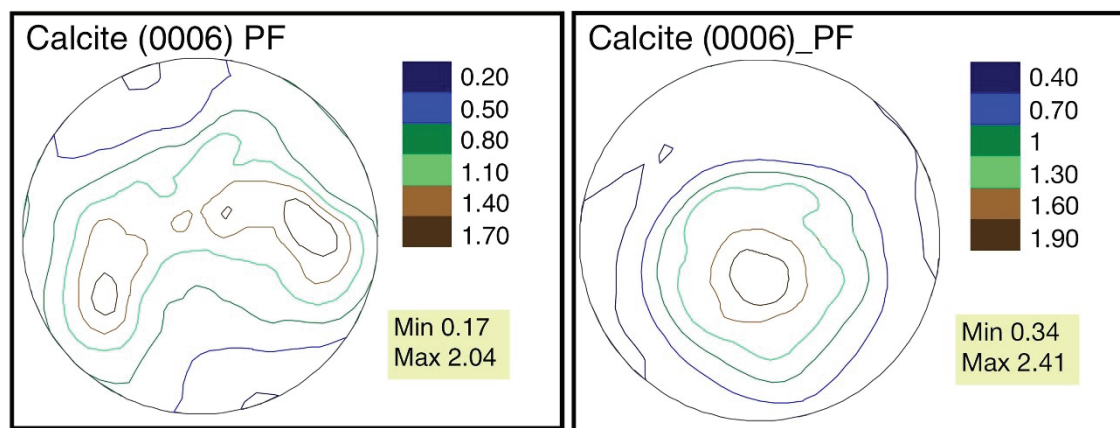


Fig.1 Pole figures of calcite in the left valves of *Gryphaea dilatata* (left) (Mikhailovsky quarry) and *Pycnodonte mirabilis* (right). The colour scale in the right top corner marks the intensity of isolines presented in units of random distribution (mrd).

The thick-walled valves of *G. dilatata*, *O. edulis*, and *P. mirabilis* have low values of the crystallographic texture maximum sharpness. These values are very close for these mollusks. Perhaps this is a characteristic feature of all thick-walled valves and reflects adaptation to shell construction, because more energy is required to build more ordered texture of a thick-walled shell.

[1] Neveskaya L.A., Popov S.V., Goncharova I.A., Guzhov A.V., Yanin B.T., Polubotko I.V., Byakov A.S., Gavrilova V.A. (2013). Bivalves of Russia and neighboring countries in the Phanerozoic. M.: Scientific world.

[2] D. Nikolaev, T. Lychagina, A. Pakhnevich (2019). Experimental neutron pole figures of minerals composing the bivalve mollusk shells. Springer Nature Appl. Sci. 1. 344

SMALL-ANGLE NEUTRON SCATTERING INVESTIGATION OF A FERROFLUID WITH ANISOMETRIC CuFe_2O_4 NANOPARTICLES

M. Balasoïu^{1,2}, S. Astaf'eva³, S. Lysenko³, D. Yakusheva³, E. Kornilitsina³, O. Ivankov^{2,4}, A.I. Kuklin^{2,5}, A. Lebedev⁶, V. Turchenko^{1,7,8}, and A-M. Balasoïu-Gaina^{1,9}

¹*Joint Institute of Nuclear Research, Dubna, Moscow Region, 141980, Russia*

²*Horia Hulubei National Institute for R&D in Physics and Nuclear Engineering, Bucharest - Magurele, Romania*

³*Institute of Technical Chemistry, Perm Federal Research Center, Ural Branch, Russian Academy of Sciences, Perm, Russia*

⁴*Institute for Safety Problems of Nuclear Power Plants of the Ukrainian NAS, Kyiv, Ukraine*

⁵*Moscow Institute of Physics and Technology, Dolgoprudny, Moscow Region, Russia*

⁶*Institute of Continuous Media Mechanics, Perm Federal Research Center, Ural Branch, Russian Academy of Sciences, Perm, Russia*

⁷*South Ural State University, 76, Lenin Aven., Chelyabinsk, 454080, Russia*

⁸*Donetsk Institute for Physics and Engineering named after O.O. Galkin, Kiev, Ukraine*

⁹*West University of Timisoara, Timisoara, Romania*

E-mail: masha.balasoïu@gmail.com

Ferrofluids are colloidal liquids having strong magnetic features whose physical properties can be altered or controlled when exposed to a magnetic field [1,2].

Research in ferrofluid synthesis has considerably increased in the past 50 years. While a large number of research articles published in the early years might not be available online, there has been a large increase in publications in the last 20 years. There is a record in Google Scholar of the publication of 1500% more articles in the synthesis of ferrofluids during the years 2001–2021 compared to those during 1981–2000 [1], which reflects the growing interest in the synthesis and applications of these magnetic fluids.

Ferrofluids are being widely investigated for technical and biomedical applications including water treatment, energy harvesting and transfer, vibration control, magnetic electromagnetic wave absorption, energy storage applications, hyperthermia, magnetic drug delivery, biocatalysis, enzyme immobilization, DNA separation and purification, and magnetic resonance imaging non-invasive magnetic resonance imaging, etc [1,2,3,4,5,6,7]. Many of the chemical and physical properties associated to nanoparticles are strongly dependent on the nanoparticle shapes and dimensions. Recently, the manufacture of controlled form ferrite nanoparticles has become another requirement of interest for researchers [8,9,10,11].

In the present paper, a new ferrofluid with copper ferrite nanoparticles and aqueous media is investigated in terms of structural behavior. The nanoparticles obtained by coprecipitation are usually characterized by a homogeneous composition, predetermined stoichiometry and narrow size distribution. The novelty of the present variant of coprecipitation method lies in the type of the oxidant used for transformation of Fe (II) to Fe (III), relatively low temperature and a short reaction time [10].

Different approaches of the small-angle neutron scattering of ferrofluid with anisotropic nanoparticles are used for the microstructural characterization of the investigated system.

The results obtained are analyzed in comparison with the SANS results for isometric particle ferrofluids.

The work was financially supported by the Government of Perm Krai, the research project No. S-26/791 and RO-JINR Project No.366/2021 item 44 (JINR Theme 04-4-1142-21/25).

- [1] O. Oehlsen, S. I. Cervantes-Ramírez, P. Cervantes-Avilés, I. A. Medina-Velo (2022). Approaches on Ferrofluid Synthesis and Applications: Current Status and Future Perspectives, *ACS Omega*. 7, 3134–3150.
- [2] V.M. Socoliuc, M. Avdeev, V. Kuncser, R. Turcu, E. Tombácz, L. Vekas (2022). *Nanoscale* (online). doi:10.1039/D1NR05841J
- [3] M. Kole, S. Khandekar (2021) Engineering applications of ferrofluids: A review *Journal of Magnetism and Magnetic Materials* 537, 168222. doi:10.1016/j.jmmm.2021.168222
- [4] V. Shukla (2019). Review of electromagnetic interference shielding materials fabricated by iron ingredients, *Nanoscale Adv.* 1, 1640–1671. doi: 10.1039/c9na00108e
- [5] Y. Liu, N. Wu, Z. Wang, H. Cao and J. Liu (2017). Fe₃O₄ nanoparticles encapsulated in multi-walled carbon nanotubes possess superior lithium storage capability, *New J. Chem.* 41, 6241. doi:10.1039/C7NJ00230K.
- [6] M. Imran, A. M. Affandi, M. M. Alam, Afzal Khan, A. I. Khan (2021). Advanced biomedical applications of iron oxide nanostructures based ferrofluids, *Nanotechnology*, 32, 422001.
- [7] Stanciu L, Won YH, Ganesana M, Andreescu S (2009) Magnetic particle-based hybrid platforms for bioanalytical sensors. *Sensors (Basel)* 9 (4):2976-2999. doi:10.3390/s90402976
- [8] Y. Y. Zheng, X. B. Wang, L. Shang, C. R. Li, C. Cui, W. J. Dong, W. H. Tang, B. Y. Chen (2010). Fabrication of shape controlled Fe₃O₄ nanostructure, *Materials Characterization* 61, 489. doi: 10.1016/j.matchar.2010.01.008
- [9] D. Ficai, A. Ficai, B. S. Vasile, M. Ficai, O. Oprea, C. Guran, E. Andronescu (2011). Synthesis of rod-like magnetite by using low magnetic field, *Digest Journal of Nanomaterials and Biostructures*. 6(3), 943 – 951.
- [10] S.N. Lysenko, A.V. Lebedev, S.A. Astafeva, D.E. Yakusheva, M. Balasoiu, A.I. Kuklin, Yu.S. Kovalev and V.A. Turchenko (2020). Preparation and magneto-optical behavior of ferrofluids with anisometric particles, *Phys. Scr.* 95(4), 044007.
- [11] Andrey V. Shibaev, Petr V. Shvets, Darya E. Kessel, Roman A. Kamyshinsky, Anton S. Orekhov, Sergey S. Abramchuk, Alexei R. Khokhlov and Olga E. Philippova (2020). Magnetic-field-assisted synthesis of anisotropic iron oxide particles: Effect of pH, *Beilstein J. Nanotechnol.* 11, 1230–1241. doi:10.3762/bjnano.11.107

BIOGENIC FERRIHYDRITE NANOPARTICLES – SERUM PROTEINS COMPLEXES AS BIOCOMPATIBLE SYSTEMS FOR MEDICAL APPLICATIONS

C.G. Chilom¹, N. Cazacu, A. Bălan¹, S. Iftimi¹, M. Bălăsoiu^{2,3,4}, A. Rogachev^{2,4}, O. Orelovich², V. Turchenko^{2,5}, V. Ladygina⁶, S. Stolyar⁶, and A. Kuklin^{2,4}

¹*University of Bucharest, Faculty of Physics, Măgurele, Ilfov, Romania*

²*Joint Institute for Nuclear Research, Dubna, Russian Federation*

³*“Horia Hulubei” National Institute of Physics and Nuclear Engineering, Romania*

⁴*Moscow Institute of Physics and Technology, Dolgoprudny, Russian Federation*

⁵*South Ural State University, Chelyabinsk, Russian Federation*

⁶*Federal Research Center KSC, Siberian Branch, Russian Academy of Sciences, Krasnoyarsk, Russian Federation*

E-mail: claudia.chilom@fizica.unibuc.ro

Iron oxide nanoparticles, including ferrhydrite nanoparticles, are used in various biomedical applications as magnetic resonance imaging, magnetic hyperthermia and targeted drug delivery [1]. These nanoparticles interact with biological structures as cell membrane and proteins, modifying their structure and, consequently, modulating their activity [2]. Thus, it is necessary to understand better the mechanisms governing the interaction between magnetic nanoparticles and cellular proteins and help to reduce the potential risks, especially immunogenicity (i.e. the ability to induce an immune response).

One of the limitations of using biogenic ferrhydrite nanoparticles in medical applications is their interaction with proteins (for example, with serum proteins). Protein adsorption may affect the functionality and biocompatibility of nanoparticles [3]. In this context, structural and spectroscopic investigation of nanoparticles interactions with serum proteins may open new perspectives on the use of NPs as a nanopatform for future applications.

The *in vivo* efficacy of biogenic nanoparticles is closely related to their physicochemical characteristics. Iron nanoparticles synthesis and design is a very current topic, given their size and magnetic properties, which allow them to be biocompatible and bind to biomolecules very easily, due to coating with organic and inorganic polymers or selective ligands. Such complex structures can simultaneously have several functions, such as local delivery of drugs, with real-time monitoring and imaging of the target area. Microorganisms have the ability to mineralize large specific amounts of iron under anaerobic conditions, in particular, accumulating in ferrihydrite. Due to the high specific surface, biogenic ferrihydrite in the ultrafine state is a chemically active substance and interacts with a number of chemicals and organic molecules by the mechanism of surface adsorption/or coprecipitation. Biogenic ferrihydrite nanoparticles are synthesized by bacteria, such as *Klebsiella oxytoca*, under very strict and controlled conditions regarding size, shape, dimension and structure of produced nanoparticles [4]. These nanoparticles usually coated with polysaccharides and protein traces, exhibit very low toxicity, and good biocompatibility.

Serum proteins (such as albumin and transferrin) attach to the surface of nanoparticles, following an adsorption process [5]. This adsorption onto nanoparticles surface is the first line of defense against foreign agents, aiming to neutralize and eliminate these invading agents. Therefore, it is important to know how serum protein structures and properties are modified after the adsorption, as well as those of nanoparticles after serum protein coating. We propose the biophysical characterization of biogenic ferrihydrite nanoparticles in interaction with proteins. We focused on the binding of the nanoparticles to human serum albumin (HSA) for two reasons: 1) Serum proteins play an important role in the transport of nanoparticles and 2) protein corona arranged around nanoparticles can significantly influence the behavior of the nanoparticles in biological environments.

One first step is the investigation of the HSA structural stability in the presence of the nanoparticles. Consequently, this study aims to provide valuable details about structural changes induced in the protein conformation by nanoparticles binding. This study could be a starting point for generating bio-compatible nanomaterials with controlled surface characteristics for medical applications. Employing HSA as model, could allow understanding and improving the knowledge on how a particular type of iron nanoparticles binds its protein corona. This study can provide significant insight into future clinical research.

Investigation of particle structure and morphology was assessed by surface and volume measurements such as scanning electron microscopy (SEM), energy dispersive X-ray analysis (EDX), transmission electron microscopy (TEM), X-ray diffraction (XRD) and small-angle X-ray scattering (SAXS). Atomic Force Microscopy (AFM) revealed the topography and contrast phase images and the profiles of the nanoparticles obtained for the simple and coated NPs with HSA. Spectrophotometric methods - UV-Vis absorption spectroscopy, steady state and time resolved fluorescence, Fourier transform infrared spectroscopy (FTIR) monitored the mechanism of the binding and the effect of the binding of the ferrihydrite nanoparticles to HSA and related biophysical properties. The results obtained by spectroscopic methods were confirmed by molecular docking (PyRx and UCSF Chimera virtual screening software).

Therefore, the biophysical characterization of HSA – biogenic ferrihydrite nanoparticles interactions is of real use in understanding the behavior of the magnetic nanoparticles *in vitro* and also *in vivo*. These studies require a detailed experiment, focused on understanding the influence of magnetic nanoparticles on protein structure and its biological activity.

This work was supported by the JINR-RO project Ferrihydrite nanoparticles - serum proteins complexes as biocompatible systems for medical applications, Theme codes: 04-5-1131-2017/2023, 02-1-1107-2011/2023 and 04-4-1133-2018/2023.

- [1] M.G. Montiel Schneider, M.J Martín, J. Otarola, E. Vakarelska, V. Simeonov, V. Lassalle, and M. Nedyalkova (2022). Biomedical Applications of Iron Oxide Nanoparticles: Current Insights Progress and Perspectives, *Pharmaceutics*, 14(1), 204.
- [2] S.R.Saptarshi, A. Duschl and A.L. Lopata (2013). Interaction of nanoparticles with proteins: relation to bio-reactivity of the nanoparticle, *J Nanobiotechnol* 11, 26.
- [3] Park S.J. (2020). Protein–Nanoparticle Interaction: Corona Formation and Conformational Changes in Proteins on Nanoparticles., *Int J Nanomedicine.*, 15:5783-5802
- [4]. N. Cazacu., C.G. Chilom, S. Iftimie., M. Balasoiu., V.P. Ladygina, S.V. Stolyar, O.L. Orelovich, Yu.S. Kovalev, A.V. Rogachev (2022). Biogenic ferrihydrite nanoparticles produced by *Klebsiella oxytoca*: characterization, physicochemical properties and bovine serum albumin interactions, *Nanomaterials*, 12(2), 1-18
- [5] C.G. Chilom, D.M. Găzdaru, M. Bălăsoiu, M. Bacalum, S.V. Stolyar, A.I. Popescu (2017). Biomedical application of biogenic ferrihydrite nanoparticles, *Romanian Journal of Physics*, 62, 701(13).

MAGNETIC PROPERTIES OF ORDERED ARRAYS OF IRON NANOWIRES: THE IMPACT OF THE LENGTH

A. Mistonov¹, A.H.A. Elmekawy², E. Iashina^{1,3}, I. Dubitskiy³, S. Sotnichuk⁴, I. Bozhev⁴,
D. Kozlov^{4,5}, K. Napolskii⁴, D. Menzel⁶,

¹*St. Petersburg State University, St. Petersburg, Russia*

²*Cyclotron Project, Nuclear Research Center, Cairo, Egypt*

³*Petersburg Nuclear Physics Institute named by B. P. Konstantinov of National Research Centre Kurchatov Institute, Gatchina, Leningrad Region, Russia*

⁴*M. V. Lomonosov Moscow State University, Moscow, Russia*

⁵*Kurnakov Institute of General and Inorganic Chemistry of the Russian Academy of Sciences, Moscow, Russia*

⁶*Institute of Condensed Matter Physics, 308108 Braunschweig, Germany*

E-mail: a.mistonov@spbu.ru

Arrays of magnetic nanowires are of great interest due to a wide range of possible applications, as well as a good model system for considering the fundamental problems of nanomagnetism [1-3]. Modern synthesis methods make it possible to obtain high-quality structures with well-controlled geometric and structural parameters [4]. However, the lack of a complete understanding of the correlation between these parameters and the magnetic properties of the arrays requires a large amount of new research.

The use of pure iron as a material for nanowires offers many advantages. First, there are no problems with the control of the composition characteristic of the alloys. Secondly, iron has a high magnetization, which is important for magnetic storage devices. And, finally, the lattice of pure iron is cubic, with a small magnetocrystalline anisotropy, which makes the magnetic behavior more predictable. Thus, only shape anisotropy and magnetostatic interactions mainly determine the magnetic behavior of the studied arrays of nanowires. A notable disadvantage of iron is its tendency to oxidize, which has probably made it less studied in recent years than nickel, cobalt, and multicomponent alloys. However, at the moment, synthesis methods have already overcome this problem.

This work is devoted to the study of the magnetic properties of hexagonally ordered arrays of iron nanowires electrodeposited into porous matrices of anodic alumina. A series of 9 nanowire arrays with a diameter of 52 nm, an array periodicity of 101 nm, and a length of 3.6 to 21.2 μm was analyzed. Scanning electron microscopy and X-ray diffraction were used to characterize the structure. SQUID magnetometry and first order remagnetization curve (FORC) analysis were used to study the magnetic characteristics.

It was demonstrated that the length dependence of the coercive force is well described by the model of long interacting nanowires, with the interaction decreasing with increasing length. An estimate of the coercive force of an isolated nanowire showed that the remagnetization process highly likely occurs due to the motion of the vortex domain wall. An analysis of the first-order remagnetization curves showed that the nanowires exhibit single-domain behavior with a narrow distribution of the remagnetization field. Local interactions presented in short nanowires are replaced by average field interactions with increasing length. The decrease in the width of the distribution of fields on FORC-diagrams additionally confirms the decrease in interactions.

The work was supported by Russian Science Foundation (project No. 18-72-00011). The authors are grateful to the Research Park of St. Petersburg State University and the staff of the resource centers “Nanotechnologies” (<http://nano.spbu.ru>), “X-ray diffraction methods of research” (<http://xrd.spbu.ru>), and “Innovative technologies of composite nanomaterials” (<https://nanocomposites.spbu.ru/>) V. Kalganov, I. Kasatkin and D. Nazarov, respectively, for their invaluable contribution in obtaining experimental data. “Educational and Methodical Center of Lithography and

Microscopy” (Lomonosov Moscow State University Research Facilities Sharing Centre) was used for the preparation of current collectors. SS and KN are grateful for the support of the Interdisciplinary Scientific and Educational School of Moscow University “Future Planet: Global Environmental Change”.

- [1] J. Um et al. (2020) Fabrication of long-range ordered aluminum oxide and Fe/Au multilayered nanowires for 3-d magnetic memory, *IEEE Trans. Magn.* 56 (2), 1 – 6
- [2] S. Parkin et al. (2015), Memory on the racetrack, *Nat. Nanotechnol.* 10 (3) 195 – 198
- [3] M.R.Z. Kouhpanji et al. (2020), A guideline for effectively synthesizing and characterizing magnetic nanoparticles for advancing nanobiotechnology: A review, *Sens.* 20(9), 2554.
- [4] K.S. Napolskii et al. (2011), Tuning the microstructure and functional properties of metal nanowire arrays via deposition potential, *Electrochim. Acta* 56 (5) 2378 – 2384.

MEASUREMENT OF THE SPIN-WAVE STIFFNESS AND THE ENERGY GAP IN THE MAGNON SPECTRUM OF AMORPHOUS FERROMAGNETS BY SMALL-ANGLE SCATTERING OF POLARIZED NEUTRONS

L.A. Azarova^{1,2*}, K.A. Pschenichniy², S.V. Grigoriev^{1,2}

¹ Saint Petersburg State University, 199034 Saint Petersburg, Russia

² Petersburg Nuclear Physics Institute named by B.P. Konstantinov of NRC “Kurchatov Institute”, 188300 Gatchina, Russia

E-mail: loveazarova@gmail.com

Amorphous magnetic materials are of considerable interest, both from a fundamental and applied point of view. The low coercive field in an amorphous magnet is an important property for its application as a core material in electrical transformers. The structural and magnetic properties of amorphous magnetic systems can be quite complex. The presence of structural as well as magnetic disorders plays an important role in amorphous systems. However, understanding the formation and growth of spin clusters in amorphous systems is a difficult task. The properties of spin clusters in an amorphous system under the influence of an external magnetic field depend on their morphology. Therefore, from the magnetism point of view, interesting aspects are: (1) correlation between structural and magnetic properties; (2) understanding the behaviour of spin clusters and (3) investigation of magnetic excitations in such systems.

This work presents studies of magnetic excitations of amorphous ferromagnetic FeNi alloys by small-angle scattering of polarized neutrons. It is widely known that the most direct methods of studying magnetic excitations are the methods of three-axis and time-of-flight spectroscopy. However, both of these methods have a limitation – it is impossible to carry out measurements near a direct beam, i.e. for small momentum transfer. Hence, the technique of small-angle scattering of polarized neutrons in inclined geometry was proposed and implemented at the St. Petersburg Institute of Nuclear Physics in the mid-eighties [1]. By measuring the difference in the dependence of scattering intensities at different initial polarization of the neutron beam on the momentum transfer, it is possible to register scattering by spin waves. In this case, a chiral scattering channel of polarized neutrons is used, which makes it possible to measure the asymmetry of the scattering intensity, which manifests itself best when an external magnetic field is applied at an angle of 45° [2]. In this case, it turns out that the scattering by spin waves is concentrated in a cone bounded by the cut-off angle θ_c . Thus, by obtaining the dependence of the cut-off angle on the applied magnetic field or on the wavelength of neutrons, it is possible to determine the stiffness of spin waves.

In this work, the dependences of the scattering intensity of polarized neutrons on spin waves on the applied external magnetic field H and on the wavelength of neutrons λ on samples of amorphous FeNi alloys were obtained at the SANS-1 instrument (MLZ, Germany). According to the results of the studies carried out, it is shown that the spectrum of spin waves is not just quadratic in terms of the transmitted pulse, but it contains an additional term in the form of a gap E_g of a non-field nature $\varepsilon = Aq^2 + g\mu_B H + E_g$. The presence of a gap independent of the field in the spectrum of amorphous ferromagnets has already been previously detected in amorphous microconducts of the compound Fe_{77.5}Si_{15.5}B₁₅ [3]. We discuss aspects of measurements and extraction of the energy gap. In particular, we show that only by measuring simultaneously two dependencies of the cut-off angle θ_c – on the applied magnetic field and the neutron wavelength – it is possible to obtain reliable information about the spin-wave stiffness and the spin-wave gap in the amorphous ferromagnetic system.

- [1] A.I. Okorokov, V.V. Runov, B.P. Toperverg, A.D. Tretyakov, E.I.Maltsev, I.M.Puzeii, V.E.Mikhailova, JETP Lett., 43, 503(1986).
- [2] S.V. Grigoriev, E. V. Altynbaev, H. Eckerlebe, A. I. Okorokov, Surface. X-ray, synchrotron and Neutron Investigations, 10, 71-78 (2014).
- [3] S. V. Grigoriev, K.A. Pschenichny, I.A.Baraban, V.V. Rodionova, K.A.Chichai, A. Heinemann, JETP Letters, 110, 800 – 806 (2019).

REFLECTOMETRY WITH NUCLEAR REACTIONS AND NEUTRON SPIN FLIP IN NEUTRON WAVE

V.D. Zhaketov¹, Yu.N. Khaydukov^{2,3}, A.V. Petrenko¹, Yu.M. Gledenov¹, Yu.N. Kopatch¹, N.A. Gundorin¹, Yu.V. Nikitenko¹, V.L. Aksenov¹

¹*Joint Institute for Nuclear Research, Dubna, Russia*

²*Research Institute of Nuclear Physics, Moscow State University, Moscow, Russia*

³*Max-Planck Institute for Solid State Research, Stuttgart, Germany*

E-mail: zhaketov@nf.jinr.ru

Nowadays investigation of proximity effects at the interface between two media are in focus of view [1-5]. In particular it relates to the interface between superconductor and ferromagnet. Due to the mutual influence of ferromagnetism and superconductivity, because of the finite values of the coherence lengths, a significant modification of the magnetic and superconducting properties occurs. It appears, in particular, as changing of magnetization's spatial distribution. It is important to establish the correspondence of the magnetic spatial profile (spatial dependence of magnetization) to the nuclear spatial profiles of the elements of the contacting media. To determine the spatial magnetic profile, the standard method of reflectometry of polarized neutrons is used, which makes it possible to determine the energy of the potential interaction of a neutron with a medium. At the interface between two media, the interaction potential is the sum of the interaction potentials of elements penetrating each other. Standard neutron reflectometry does not make it possible to establish which elements are associated with changes in the interaction potential and, in particular, in the magnetic profile. To determine the profile of the interaction potential of a neutron with individual elements, it is necessary to register the secondary radiation of the elements.

At the moment, channels for recording charged particles [6], gamma quanta and spin-flip neutrons [7] have been realized at the REMUR spectrometer of IBR-2 reactor in Dubna. Several tens of isotopes and magnetic elements are available for measurements. For the layer with thickness 5 nm: a) for the charged particles registration channel, the minimum value of the cross section is $\sigma_{min}=0.025$ barn, the cross section $\sigma>\sigma_{min}$ has 22 isotopes; b) for the gamma-quanta registration channel, $\sigma_{min}=0.3$ barn, more than 100 isotopes have a cross section $\sigma>0.3$ barn; c) for the polarized neutrons registration channel, the minimum, perpendicular to the neutron polarization, component is 1 G.

[1] V.D. Zhaketov et al. // JETP, Vol. 156, № 2, pp. 310 (2019)

[2] V.D. Zhaketov et al. // JETP, Vol. 152, № 3, pp. 565 (2017)

[3] Yu.N. Khaydukov et al. // Phys. Rev. B, 99(14), 140503 (2019)

[4] Yu.N. Khaydukov et al. // Phys. Rev. B, 97(14), 144511 (2018)

[5] D.I. Devyaterikov et al. // PMM, Vol. 122, № 5, pp. 465-471 (2021)

[6] V.D. Zhaketov et al. // Journal of Surface Investigation, Vol. 6, pp. 20–30 (2019)

[7] V.D. Zhaketov et al. // Journal of Surface Investigation, Vol. 6, pp. 1-15 (2021)

STRESS DIFFRACTOMETRY AND DEVELOPMENT PROSPECTS

Viacheslav Em¹

¹*National Research Center «Kurchatov Institute», Russia*

E-mail: vtem9@mail.ru

Residual stresses can be harmful and significantly degrade the strength characteristics of the component. On the other hand, they can be useful and purposefully introduced into the material, for example, by surface treatment, to improve the performance properties of the component. Therefore, reliable quantitative information about the strain-stress state of the material of the component is extremely important for choosing the optimal manufacturing technology and design of the component. Such information is also important for the verification of various calculation models of residual stresses, which are necessary for a better understanding of the residual stresses.

Thanks to the high penetrating ability of neutrons in most industrial metals, the neutron method makes it possible to measure stresses in bulk materials. Currently, this is the only non-destructive method that allows you to measure the distribution of all three components of the strain/stress tensor in bulk materials (at depth from 0.1 to 50 mm in steel).

Due to the importance of stress diffractometry for solving applied and fundamental problems, specialized stress diffractometers have been created in almost at all centers with neutron sources. Currently, 13 stress diffractometers are actively operating in the world at stationary and 5 at pulsed neutron sources. Devices on stationary and pulsed sources differ greatly methodically. The analysis of the main components affecting the characteristics of both types of devices is carried out.

TOF stress diffractometers based on pulsed neutron sources have advantages in the studies of properties of materials under load. Stress diffractometers with a fixed neutron wavelength, based on stationary reactors, have an advantage when studying the residual-strain/stress distribution in samples of large thickness or in surface layers of materials.

There are both types of stress diffractometers in Russia. Three stress diffractometers FSD, FSS and EPSILON are installed at the IBR-2 pulsed reactor at JINR (Dubna). The FSD stress diffractometer, which is equipped with a loading machine and furnaces, has the best technical characteristics. High intensity stress diffractometer STRESS is installed at the stationary research reactor IR-8 at NRC “Kurchatov Institute” (Moscow). The examples of researches carried out at FSD and STRESS are presented.

It is proposed to create a stress diffractometer with record characteristics at the new high flux PIK reactor with a power of 100 MW. This will be achieved not only due to the high neutron flux of the reactor ($1.5 \times 10^{15} \text{ n} \cdot \text{cm}^{-2} \cdot \text{s}^{-1}$), but mainly due to the use of the latest achievements in neutron instrumentation.

INTRINSIC ELASTIC ANISOTROPY OF WESTERLY GRANITE AND ITS EVOLUTION DUE TO THERMAL TREATMENT

R.N. Vasin¹, T. Lokajíček², T. Svitek³, M. Petružálek², M. Kotrlý³, I. Turková³,
R. Onysko^{3,4}, and H.-R. Wenk⁵

¹Joint Institute for Nuclear Research, Dubna, Russian Federation

²Institute of Geology of the Czech Academy of Sciences, Prague, Czech Republic

³Institute of Criminalistics Praha, Prague, Czech Republic

⁴SG Geotechnika, a.s., Praha, Prague, Czech Republic

⁵University of California, Berkeley CA, USA

E-mail: vasin@nf.jinr.ru

Granitic rocks are intensively studied because of their physical properties relevant to development of nuclear waste storage [1], geothermal energy technologies [2], rock mechanics experiments, and studies of crustal seismic anisotropy. One of the classical granitic rocks is Westerly granite from Rhode Island, USA, which is mostly composed by quartz and feldspars with small amount of mica and accessories. It is thoroughly investigated with respect to its composition, microstructure, elastic, thermal, and mechanical properties, etc. (e.g., [3-6]). Westerly granite is often described as an intrinsically elastically isotropic, or very weakly anisotropic rock. It was shown that deviatoric stresses, increased pressure and temperature, as well as temperature and pressure cycling, may lead to development of different crack systems in the granite, which are mostly related to elongated grain boundaries, or cleavage planes of feldspars and mica. The latter may have certain preferred orientation, and therefore induce shape texture for the microcracks, which may significantly enhance the granite elastic anisotropy.

To study this effect, a combination of optical and electron microscopy, neutron diffraction at the SKAT texture diffractometer in FLNP JINR (Dubna) [7], and multidirectional ultrasonic sounding at increased confining pressures using a special apparatus in Institute of Geology AS CR (Prague) [8] was applied to a set of Westerly granite samples preheated to different temperatures up to 600°C. Elastic wave velocities measured at different pressures were compared with the results of microstructure-based modelling of the granite properties using the Geo-Mix-Self algorithm [9].

Our results indicate that Westerly granite consists of 4 main minerals: plagioclase, orthoclase, quartz and biotite. Surprisingly, plagioclase has the sharpest preferred orientation, which strongly influences the intrinsic elastic anisotropy. Heating of the granite leads to formation of different systems of microcracks, depending on the maximum preheating temperature. The shape preferred orientation of cracks is linked to the structure and texture of feldspars and biotite. Experimental data and numerical modeling show that formed oriented cracks may completely invert the elastic anisotropy of Westerly granite, practically exchanging minimum and maximum elastic wave velocity directions. As a result, Westerly granite exhibits two characteristic types of elastic anisotropy, expressed by microcracks at low pressure and by crystal preferred orientations at high pressure where microcracks are closed. At intermediate pressures, the granite anisotropy should be lowest. Some implications of these results for rocks at crustal conditions are discussed.

[1] P.M.Bell (1980). A first in nuclear waste storage: Back to granite. EOS. 61(30), 546.

[2] J.I.Farquharson, A.R.L.Kushnir, B.Wild, P.Baud (2020). Physical property evolution of granite during experimental chemical stimulation. Geotherm Energy. 8, 14.

[3] F.Chayes (1950). Composition of the granites of Westerly and Bradford, Rhode Island. Am J Sci. 248, 378-407.

[4] F.J.Flanagan (1967). U.S. Geological Survey silicate rock standards. Geochimica et Cosmochimica Acta. 31(3), 289-308.

- [5] J.V. Spencer Jr., A.M.Nur (1976). The effects of pressure, temperature, and pore water on velocities in Westerly granite. *J Geophys Res.* 81(5), 899-904.
- [6] R.D.Dwivedi, R.K.Goel, V.V.R.Prasad, A.Sinha (2008). Thermo-mechanical properties of Indian and other granites. *Int J Rock Mech Min Sci.* 45(3), 303-315.
- [7] R.Keppler, K.Ullemeyer, J.H.Behrmann, M.Stipp (2014). Potential of full pattern fit methods for the texture analysis of geological materials: Implications from texture measurements at the recently upgraded neutron time-of-flight diffractometer SKAT. *J App Crystallogr.* 47(5), 1520-1534.
- [8] T.Lokajíček, T.Svitek (2015). Laboratory measurement of elastic anisotropy on spherical rock samples by longitudinal and transverse sounding under confining pressure. *Ultrasonics.* 56, 294-302.
- [9] S.Matthies (2012). GEO-MIX-SELF calculations of the elastic properties of a textured graphite sample at different hydrostatic pressures. *J Appl Crystallogr.* 45(1), 1-16.

SYNTHESIS, STRUCTURE AND TENSILE PROPERTIES OF AlMg₅Cr AND Al₅Si COMPONENTS PRODUCED BY WIRE-ARC ADDITIVE MANUFACTURING

Stefan Valkov^{1,2}, Georgi Kotlarski¹, Maria Ormnaova¹, Nikolay Doynov³, Ralf Ossenbring³, Vesselin Michailov³ and Gizo Bokuchava⁴

¹*Institute of Electronics, Bulgarian Academy of Sciences, 1784 Sofia, Bulgaria*

²*Technical University of Gabrovo, 5300 Gabrovo, Bulgaria*

³*Department Joining and Welding Technology Brandenburg University of Technology, 03046 Cottbus, Germany*

⁴*Frank Laboratory of Neutron Physics, Joint Institute for Nuclear Research, 141980 Dubna, Russia*

E-mail: stsvalkov@gmail.com

In recent years, the growing demand for efficient and high-precision manufacturing methods has led to the increased popularity of additive manufacturing processes. These methods are known as layer-by-layer techniques for the modification and manufacturing of components.

In this study, we present results of the evolution of the crystallographic structure, as well as the corresponding mechanical properties of wire arc additively manufactured (WAAM) AlMg₅Cr and Al₅Si specimens, studied by X-ray diffraction (XRD) and tensile testing, respectively.

The results show that the phase composition is in the form of a face-centred cubic (fcc) crystal structure in both cases, corresponding to the base material, as well as some traces of oxide phase Al₂O₃ for AlMg₅Cr and pure Si for Al₅Si components, respectively. The WAAM specimens growing are accompanied by a slight change in the preferred crystallographic orientation and a decrease in the imperfections concentration. Also, it was found that the ultimate tensile strength (UTS), yield strength (YS), and elongation slightly decrease from the initial to the more advanced stages of growth. Further investigations of the residual stresses and strains of wire-arc additively manufactured Al-based specimens are considered.

Acknowledgments: The financial support from the Bulgarian Nuclear Regulatory Agency (BNRA) and JINR–Bulgaria Project No. 13/2021 is highly appreciated.

EFFECT OF THERMOMECHANICAL TREATMENT ON THE TEXTURE AND FUNCTIONAL PROPERTIES OF POWDER TiNi

G.V. Markova¹, T.I.Ivankina², D.M.Levin¹, S. S. Volodko¹

¹ *Tula State University, 300012 Tula Russia*

² *Frank Laboratory of Neutron Physics, Joint Institute for Nuclear Research, 141980 Dubna, Russia*

E-mail: Galv.mark@rambler.ru

The degree of development of functional properties in polycrystalline shape memory alloys is concerned with the orientation of grains in respect to the direction of the given deformation. In practice, functional alloys should have crystallographic preferred orientations of grains (texture), acquired by prior plastic deformation of various types.

The aim of this work is to establish the influence of the crystallographic texture developed during diverse thermomechanical processing (TMP) on the shape memory and superelasticity characteristics of titanium nickelide obtained by sintering calcium hydride powder.

Structurally homogeneous billets of titanium nickelide were received by pressing and vacuum sintering of calcium hydride powders. Thermomechanical processing of sintered billets was carried out by rotational forging (RF), radial shear rolling (RSR) or extrusion (Ex). The maximum true deformation e was: after rotational forging $e = 0.63$, after extrusion $e = 0.8$ and radial shear rolling - $e = 1.4$.

Neutron diffraction texture analysis of samples that experienced deformation up to the maximum was performed at the time-of-flight (TOF) texture diffractometer SKAT at Dubna, Russia. Плоскость проекции экспериментальных полюсных фигур перпендикулярна оси образца и оси деформации. It has been established that after all TMT technologies, an axial-type texture is formed. The sharpness of the texture and the fraction of textured grains after each type of TMT were estimated. The most complete texture development is demonstrated by samples after RF at 600 °C and extrusion: the fraction of textured grains reaches 85-88%, and the maximum value of pole intensities on pole figures is observed in the interval of 2.76-3.19 m.r.d. Similar TMT technologies provide the highest functional properties.

The shape memory characteristics were determined during torsion deformation on wire samples cut from rods along the TMT direction. The maximum value of the restored deformation (excluding elastic) is demonstrated by the sample after RF at 600°C, the maximum elastic deformation is shown by the sample after extrusion. The extruded sample also shows the highest value of induced strain (15%), which provide complete recovery of the shape, which is comparable to the values typical for single crystals.

This study were carried with the financial support of the Russian Science Foundation, project number 22-23-20124, <https://rscf.ru/project/22-23-20124/> and the region (Tula Region Committee on Science and Innovation).

APPROXIMATION OF ELASTIC VELOCITY-PRESSURE RELATION IN ROCKS

I.Yu. Zel¹, M. Petruzalek²

¹*Joint Institute for Nuclear Research, FLNP, Dubna, Russia*

²*Institute of Geology of the Czech Academy of Sciences, Prague, Czech Republic*

E-mail: zel@jinr.ru

The nonlinear dependency of elastic velocities in rocks on high confining pressures is routinely observed in high pressure ultrasonic experiments on rock samples with different mineral composition or occurrence. This well-known relationship mostly reflects the deformation of cracks and pores either by the lithostatic pressure or during the confining load in laboratory experiments. In this work we have considered the velocity-pressure relationship, aiming to obtain the widely used approximation formula $v(p) = V_0 + Bp - De^{-kp}$ with four parameters, that are usually found as a result of the approximation. It has been shown that under condition of low concentrations of non-interacting pores and cracks and isotropic elasticity of mineral matrix, whose elastic constants weakly depend on pressure and with an assumption of constant effective aspect ratio, all four parameters can be expressed through the elastic constants of rock matrix, porosity, crack densities and crack orientations. The obtained results were tested on published data on elastic velocities and on the P -wave velocity data from measurements on two anisotropic rock spheres. Key assumptions of our derivation approach as well as the application of the obtained formulas have been discussed.

**NEUTRON RADIOGRAPHY AND TOMOGRAPHY AT THE IBR-2 REACTOR:
THE MAIN SCIENTIFIC DIRECTIONS**

S.E. Kichanov¹, I. Yu. Zel¹, D. P. Kozlenko¹, B. A. Bakirov¹, B.A. Abdurakhimov¹ and I.A.Saprykina^{1,2}

¹*Frank Laboratory of Neutron Physics, Joint Institute for Nuclear Research, Dubna, Russia*

²*Institute of Archaeology RAS, Moscow, Russia*

E-mail: ekich@nf.jinr.ru

Information about the internal structure of materials with a spatial resolution at the micron level can be obtained using neutron radiography due to the difference in the degree of attenuation of neutron beam intensity in materials with different chemical composition, density, and thickness of the components entering the material composition. Neutron radiography provides a two-dimensional projection of an object under study, while tomography is used to obtain a three-dimensional image, where a volumetric reconstruction of the internal structure of object studied is performed based on a set of radiographic projections obtained at different angular positions of the sample relative to the beam direction. The fundamental difference in nature of neutron interaction with matter compared to X-rays provides additional benefits to neutron methods, including sensitivity to light elements, a notable difference in contrast between isotopes, high penetration effect through metals or heavy elements. Nowadays, the detailed neutron structural studies of different types of objects in order to obtain the necessary data for the growth of knowledge on those objects for the purpose of improving existing models and scientific ideas about the nature, formation, and evolution is request. The three-dimension (3D) arrangement of the inner components, as well as the morphological parameters of structural elements of different objects, were studied using neutron tomography. It should be noted that the neutron tomography method provides the detailed spatial distribution of different elements inside a given volume with a relatively high spatial resolution. In the report, the neutron tomography experiments at the neutron radiography and tomography facility placed on beamline 14 of the IBR-2 high-flux pulsed reactor were provided. The main scientific directions and results obtained on this experimental station are reviewed.

Meteorites are quite rare representatives of extraterrestrial matter. And as expected, the scientific community is fully focused on the study of elemental and isotopic content, chemical and mineral composition, the search for metallic inclusions of the recently discovered meteorites. The determination of major and minor phases, their textural associations, dimensions, shapes, and spatial arrangement is important for understanding the petrography of meteorites. And only recently, it became possible to study the rather large fragment of the Kunya-Urgench meteorite using modern methods of neutron non-destructive testing. As a result, the internal structural organization, phase analysis, three-dimension (3D) volume data, as well as the results of the corresponding morphological calculations, of the large fragment of the Kunya-Urgench meteorite are reported.

Currently, coins are being intensely investigated by means of non-destructive physical methods, such as traditional techniques like metallography or X-ray diffraction. In this context, we should also mention the neutron radiography and neutron diffraction methods as the relative modern structural non-destructive experimental approach. We present neutron tomography and diffraction data supported X-ray fluorescence analysis, for the non-destructive identification of the copper alloy composition, and reconstruction of the initial view of original coins and their remain parts under from the patina layer.

NEUTRON DIFFRACTION AS A METHOD OF ANALYSIS OF SAMANID SILVER DIRCHAMS FROM THE ANCIENT MUROMA BURIAL GROUND PODBOLOT'IE

Saprykina I.A.^{1,2}, Kichanov S.E.², Bakirov B.A.², Chugaev A.V.³, Zelentsova O.V.¹

¹*Institute of Archaeology, Russian Academy of Sciences, 19, Dm.Ulyanova st., Moscow, 117292, Russia*

²*International Intergovernmental Organization Joint Institute for Nuclear Research, 6, Joliot-Curie St., Dubna, Moscow Region, 141980, Russia*

³*Institute of Geology of Ore Deposits, Petrography, Mineralogy and Geochemistry, Russian Academy of Sciences, 35, Staromonetny Lane, 35, Moscow, 119017, Russia*

E-mail: dolmen200@mail.ru

Series of silver Samanid dirhams from excavated in 2012 burial ground Podbolot'ie (dated by 8 – middle of 11 cc.), left by the ancient Muroma tribe, were studied by several methods: XRF, neutron diffraction and isotope analyses by Pb-Pb method.

The silver fineness of Arab coins was very high up only to the middle of 10th century. Most of the coins we studied dated by the end of 9th c. – the middle of 10th century. Studied sample of coins from the Podbolot'ie burial ground were manufactured from fine silver, or from silver-copper alloys; the lead was detected in coins as impurity with content up to 1% (XRF; M1 Mistral, Bruker). It is very interesting that all studied coins had a peculiar surface with 'craquelure', which characterizes the presence of a larger amount of lead, which causes 'brittleness' of the alloy.

The neutron diffraction method performed at the DN-12 neutron diffractometer at the IBR-2 high-flux pulsed reactor (Frank Laboratory for Neutron Physics, JINR, Dubna, Russia) turned out to be more informative in this case for obtaining the necessary data on the content of both copper and lead. Almost of coins were manufactured from the fine silver and some coins – from the "yellow multicomponent" silver (content of silver ranged from 900 to 985⁰). But the content of lead in coins, according to the neutron diffraction, was reached up to 4%, in contrast to the data recorded by the XRF-method. Such a high lead content correlates with the marked presence of "craquelures" on the surface of coins. This behavior of lead (lack of liquation on the surface, higher content in the thickness of the coin) may indirectly indicate a special methods of processing the coins during minting.

In most cases the content of the lead in silver ranging from 0,5 to 2,5% indicates its hit from the ore sources (the natural impurity). The neutron diffraction data about content of the lead allowed to study the isotope composition of Pb in silver of coins for determination of the most probable ore source of metal.

STUDY OF ANTIQUE AND MEDIEVAL COINS BY NON-DESTRUCTIVE METHODS OF NEUTRON TOMOGRAPHY AND DIFFRACTION

B.A. Bakirov^{1,2}, S.E. Kichanov¹, D.P. Kozlenko¹, I.A. Saprykina^{1,3} and B.A. Abdurakhimov¹

¹*Frank Laboratory of Neutron Physics, Joint Institute for Nuclear Research, 141980 Dubna, Russia*

²*Kazan (Volga Region) Federal University, 420008 Kazan, Republic of Tatarstan, Russia*

³*Institute of Archaeology RAS, 117036 Moscow, Russia*

E-mail: bulatbakirov@jinr.ru

Detailed studies of the physicochemical properties of ancient and medieval coins by modern non-destructive methods are an important task for archeology and sciences related to history. Numismatic material contains valuable information about the trade, economic, technological and social development of ancient states. It is known [1] that the study of the phase and chemical composition, the internal structure of coins can provide important information about the deposits of the ore from which the coins are made, the correspondence to a certain historical period or features of coinage, and the identification of fakes. It should be noted that the experimental data obtained are of great importance for the development of the methodology for the restoration and preservation of not only numismatic, but also other metal archaeological finds [2].

In this work, coins from different territories and historical periods were studied. A set of nine bronze coins from the excavations of the 6th - 3rd BC necropolis on the Taman Peninsula (Krasnodar Territory, Russia) belongs to the Bosporan Kingdom and characterizes the period of active interaction between the Greek and barbarian population of this region. Two silver coins from the territory of Volga Bulgaria (Republic of Tatarstan, Russia), dated to the 10th and 14th centuries AD, correspond to two periods of the maximum distribution of metal coins in the trading operations of this medieval state. Another silver coin dated approximately to the 10th - 13th century AD, minted by the Karakhanid dynasty and found on the territory of modern Uzbekistan, is a clear marker of the so-called "silver crisis". Thus, data studies are of great importance in clarifying some aspects of the development of these ancient states.

To determine the spatial distribution of chemical elements over the volume of coins, neutron radiography and tomography experiments were carried out at a specialized experimental station on the 14th channel of the IBR-2 pulsed high-flux reactor. The studies of the crystal structure and phase composition of the coins were carried out using the neutron diffraction method on a specialized DN-6 diffractometer on the 6th channel of the IBR-2 pulsed high-flux reactor, the analysis of diffraction data was carried out by the Rietveld method.

As a result, for bronze coins, the degree of degradation (the ratio of the volumes of the metal part and patina), the phase composition of the patina, and the tin content in the copper-tin alloy were determined. Additionally, three-dimensional surface models of three coins were successfully restored, which made it possible to correctly identify them. For silver coins, the content of the copper phase and the spatial distribution of the silver and copper phases by the volume of the coins were determined. An increased silver content was found on the surface of two coins, indicating a silvering of the surface.

[1] K.M. Podurets (2021). Modern Methods of Neutron Radiography and Tomography in Studies of the Internal Structure of Objects. *Crystallogr. Rep.* 66, 254–266.

[2] Th. Rehren (2008). Coins, artefacts and isotopes-archaeometallurgy and Archaeometry. *Archaeometry.* 50, 232–248.

CONDENSED MATTER RESEARCH AT THE EG-5 ACCELERATOR

A.S. Doroshkevich^{1,2}, T.Yu Zelenyak¹, A.I. Madadzada^{1,4}, A.N. Lihachev¹, M.A. Balasoui⁵, E.V.Lychagin¹, P. Badica⁶, M. Stef⁷, B. Jasinska³, I.M. Chepurchenko¹, K.Ye. Studnev¹, T.V.Phuc^{1,8,9}, L.H.Khiem^{8,9}, P.L.Tuan^{1,10}, Vesna Teofilović¹¹, Ivan Ristić¹¹, Roman Balvanović^{12,13,14}, Zoran Jovanović^{12,13,14}, A. Stanculescu¹⁵, C. Mita¹⁶, D Mardare¹⁶, J. Žuk³, D. Luca¹⁷

¹ *Joint Institute for Nuclear Research, Dubna, Russia;*

² *Donetsk Institute for Physics and Engineering named after O.O. Galkin, Kiev, Ukraine;*

³ *Institute of Physics, Maria Curie-Skłodowska University, Lublin, Poland;*

⁴ *National Center for Nuclear Research, Baku, Azerbaijan;*

⁵ *Horia Hulubei National Institute for R&D in Physics and Nuclear Engineering (IFIN-HH), Bucharest Romania;*

⁶ *National institute of materials physics, Măgurele, Romania;*

⁷ *West University of Timisoara, Timisoara, Romania;*

⁸ *Graduate University of Science and Technology, Vietnam Academy of Science and Technology, 18 Hoang Quoc Viet, CauGiay, Ha Noi10000, Vietnam;*

⁹ *Institute of Physics, Vietnam Academy of Science and Technology, 10 Dao Tan, Ba Dinh, Ha Noi10000, Vietnam;*

¹⁰ *Vietnam Atomic Energy Institute, 59 Ly ThuongKiet, HoanKiem, Hanoi, Vietnam;*

¹¹ *University of Belgrade, INN Vinča, Laboratory of Physics;*

¹² *National Museum Belgrade, Serbia;*

¹³ *University of Belgrade- Archaeology Department, Serbia;*

¹⁴ *National Museum Požarevac, Serbia;*

¹⁵ *National Institute of Materials Physics, Magurele, Romania;*

¹⁶ *”Alexandru Ioan Cuza” University of Iasi, Faculty of Physics, Iasi, Romania;*

¹⁷ *”Gheorghe Asachi” Technical University of Iasi (TUIASI), Iasi Romania*

E-mail: doroh@jinr.ru

The purpose of the electrostatic accelerator (ESA) EG-5. Along with the experimental nuclear reactor and the IREN electron accelerator, the EG-5 ESA occupies its unique niche as part of the complex of nuclear physics facilities of the FLNP. The beams of high-energy particles produced using EG-5 have extremely high energy stability (± 15 keV per 2 MeV), which makes it possible to conduct unique studies of the elemental composition of solids, including deep profiling, conducting studies of nuclear reactions on fast neutrons, etc. ESA EG-5 is a universal research device that allows to conduct both elemental composition studies and physical, chemical and biological modification of objects of inanimate and living nature, respectively. In particular, there is a unique possibility of irradiating materials with hydrogen ions, helium and fast neutrons, the ability to create structures with layer-by-layer variation of phase and chemical composition through ion implantation in the surface layers of materials, and to cause mutagenesis in biological objects.

The range of ESA energies allows simulating the radiation conditions of near space and nuclear reactors. The absence of slow neutrons in the spectrum produced by the neutron installation allows to conduct irradiation without induced radioactivity, which is extremely important when studying unique samples, in particular, objects of cultural heritage.

Condensed matter physics At the moment, using the EG-5 accelerator, studies are being conducted on the resistance to neutron and proton radiation of Al_2O_3 - ZrO_2 - Y_2O_3 - ceramics, NiTi - alloys promising for the radiation-resistant superconducting solenoids; high-entropy alloys promising for the manufacture of thermonuclear reactor shell; unique

studies of degradation of semiconductor heterojunctions of solar cells ($\text{SiO}_2/\text{TiO}_2$) under the action of cosmogenic radiation [1]. ESA is used to perform physical modification of materials by a beam of high-energy ions to interface materials with significantly different temperature expansion coefficients by creating helium or hydrogen porosity (Poland - JINR Cooperation Project PPPB/120-26/1128/2022). Using the EG-5 installation on helium ion beams, unique non-destructive experimental studies of elemental depth profiles (RBS method) [2] of metal oxide ceramics based on ZrO_2 , Al_2O_3 , CuO , ZnO , SnO_2 [3-4], high-entropy metal alloys, borides, nitrides, semiconductors based on Si, SiO_2 , ZnO_2 , GaAs [5-7], are carried out. The sensitivity limit of the method is 10^{15} at. cm cm^{-2} [8], which allows, for example, to determine the impurity content of heavy elements in the amount of 0.001 at.% [9] or to recognize the substance as a layer up to 1 nm thick. There is a unique opportunity to study layered structures. Within the framework of the JINR – Participating countries cooperation program, a study of multilayer semiconductor architectures such as $\text{TiO}_2/\text{SiO}_2/\text{Si}$, $\text{SiO}_2/\text{TiO}_2/\text{Si}$, GaAs; metallic (Fe, Cu) and (ZrO_2) solid solutions, nanopowder and micropowder systems of the composition $\text{Al}_2\text{O}_3 + x\% \text{Y}_2\text{O}_3$, where $x = 0, 0.5$ and 1 , nanoscale diamonds, sphalerites, perovskites, ferrites, etc. [10] was carried out.

Radiation biology. On the example of the sorts "Sur sului", "AiKerim" and "Leader" in cooperation with the Kazakh Rice Research Institute named after Jakhaev the possibility of obtaining a drought-resistant rice sort through radiation mutagenesis using neutron irradiation is in investigating.

The study was funded by the Plenipotentiary Representative of the Government of the Poland Republic in JINR within the framework of the Poland – JINR Cooperation Projects PPPB/120-25/1128/2022, PPPB/120-26/1128/2022 and within the framework of the JINR-Romania cooperation program in 2022 (topic 03-4-1128-2017/2022 and 04-4-1143-2021/2025)..

[1] T.V. Phuc, and all. (2022). Variation of $\text{TiO}_2/\text{SiO}_2$ mixed layers induced by Xe^+ ion irradiation with energies from 100 to 250 keV. *Materials Science and Engineering: B*, Volume 277, 115566. <https://doi.org/10.1016/j.mseb.2021.115566>.

[2] Oura K. et al . *Introduction to Surface Physics / M.: Nauka, 2006— - 490 p.*

[3] Maletsky A.V. and all. (2021). Structure formation and properties of ceramics based on θ -Aluminium oxide doped with stabilized Zirconium dioxide. *Ceramics International* <https://doi.org/10.1016/j.ceramint.2021.03.286>.

[4] D.R.Belichko, and all. (2020) Influence of hafnium oxide on the structure and properties of powders and ceramics of the YSZ– HfO_2 composition. *Ceramics International* 10.1016/j.ceramint.2020.09.151.

[5] P.L. Tuan, and all. Investigations of chemical and atomic composition of native oxide layers covering SI GaAs implanted with Xe ions, *Surface and Coatings Technology*, Volume 394, 25 July (2020), 12587. <http://dx.doi.org/10.1016/j.surfcoat.2020.125871>

[6] P. Horodek, and all. (2015) Positron beam and RBS studies of thermally grown oxide films on stainless steel grade 304, *Applied Surface Science*, 333 96–103

[7] M. Kulik, and all. (2015) Effect of N^+ ion implantation and thermal annealing on near-surface layers of implanted GaAs”, *Acta Physica Polonica A* 128 (5), 918-922.

[8] Komarov and all. *Non-destructive analysis of the surface of solids by ion beams. Mn.:- University.1986, - 256p.*

[9] Tashlykova-Bushkevich I.I. *The Rutherford backscattering method in the analysis of solids. Educational and methodical manual. Mn.: BSUIR, 2003. – 52p.*

[10] Tatarinova Alisa and all. (2021) Application of the Rutherford Backscattering Method in Powder Nanotechnology / Spring Meeting of the European Materials Research Society (E-MRS) VIRTUAL Conference from May 31st to June 3rd, 2021. ALTECH 2021 - Analytical techniques for precise characterization of nano materials.

EVALUATION OF FLAW SEVERITY IN CYLINDRICAL PRODUCTS BY AN ELECTROMAGNETIC METHOD

A.Savin¹, R.Steigmann¹, M.L.Craus^{1,2}

¹National Institute of R&D for Technical Physics, Nondestructive Testing Department, Iasi, Romania

²Joint Institute for Nuclear Research, Frank Laboratory for Neutron Physics, Dubna, Russia

E-mail: asavin@phys-iasi.ro

Non-destructive material evaluations (NDEs) have undergone a continuous transformation in the last decade, from the detection of discontinuities and the characterization of the condition of materials to their automatic classification using robotics for inspection and maintenance. This requirement goes once with the apparition of new materials, which require certification and improvement of future maintenance systems forecasting methods [1]. The use of eddy current (EC) technology to detect damage in complex structures with hard-to-reach areas is a key part of NDE that requires connecting technology to industrial / sectoral requirements. These structures require an accurate and precise assessment of any detected discontinuities to properly guide repairs and support the tasks of maintenance programs. The efficient use of information technology to improve human knowledge, although it seemed a futuristic theory, is proving necessary to increase the quality of life. NDE automated operating systems are designed to improve human reaction in decision making. These systems used in NDE, automated systems, can be applied for a variety of purposes from image processing to database development in decision making [2]. An effective NDE flowchart requires a robust schema for diagnosing damage and causes, including establishing the nature of the damage, the location, and the volume of the defect. The problem of damage diagnosis is one of model recognition, each state of damage has a collection of measurement data from sensors. Knowing that none non-destructive testing method can be qualified as maximum detection capability and maximum sensitivity, more reliable information and a correct characterization of defects is obtained by data fusion. Figure 1 shows the block diagram of the processing algorithms.

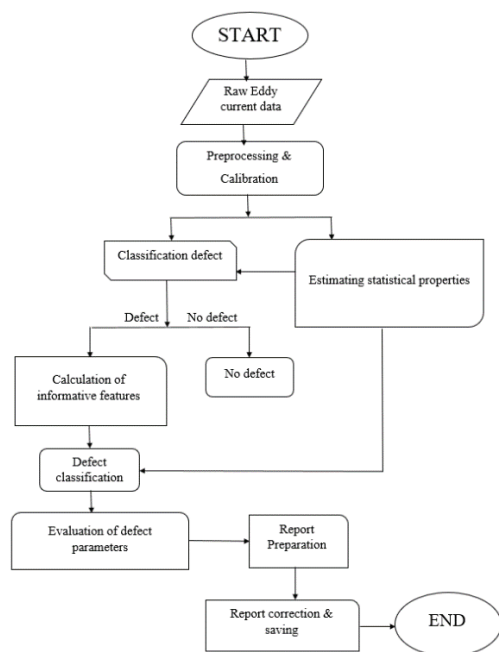


Figure 1.

The detection and classification of the information obtained from the EC technique offers the premise of several approaches for extracting information on the integrity of the examined structures [3]. Discontinuity image reconstruction technology overcomes the shortcomings of traditional EC testing that cannot provide detailed information on discontinuities. In recent years, in the field of image processing, the neural network has been widely applied, offering a new idea for the recognition and classification of EC images of existing discontinuities in complex structures.

To increase the probability of detection (POD), an automatic system that pre-filters the signal can be used, a Neyman Pearson detector with the probability of false alarm imposed allows to determine those areas from the fault signal provided by the EC equipment.

Figure 2 presents the filtered signal and the effect of Neyman-Pearson on this signal. The emphasized points appertain with POD 95%.

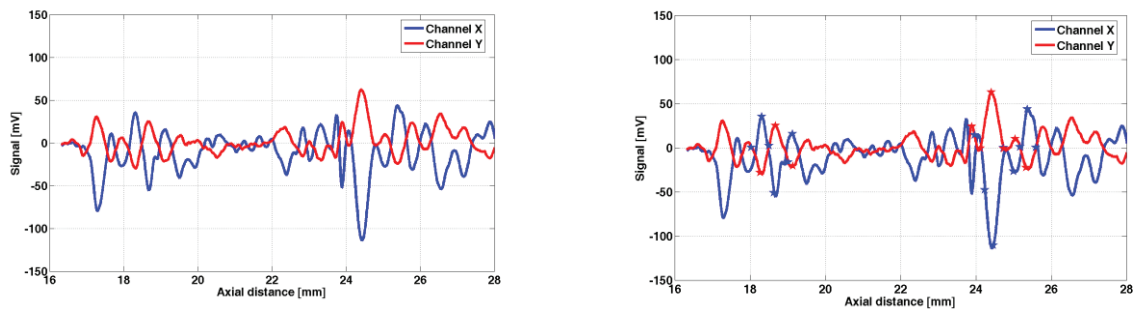


Figure 2.

The EC method as a fast and reliable method is gaining terrain in inspections of cylindrical products, for emphasizing surface and subsurface discontinuities, being able to digitally test complex shapes and storing a large volume of information without operator dependence. In order to reach a decision, the information must be processed by going through a product history (manufacturing data, previously performed tests, conditions of use, etc.), the whole system requires learning, images recognition, planning, problem solving, knowledge. Step by step, as these machine learning (ML) become able to make decisions on tests, their tasks are no longer in the domain of artificial intelligence (AI). The EC technique can use both a single coil transducer and a transducer based on a sensors array, able of covering a large inspection area. Each sensor from array generates a signal that can be detected in amplitude and phase and provides information about the inspected area. Thus, low sensitivity to lift off allows a less difficult inspection of complex geometries that can then be automated. It is also useful to characterize the location and shape of the defects provided that adequate maps of the impedance variations induced by the defects are available. This can be done with Mahalanobis distance, membership being ensured by minimizing distance. This variation data can be collected by the transducer operating at a single frequency / multifrequency and displacing at a constant velocity close to the inner / outer surface of the cylindrical product, sweeping the surface.

The real flaws have various causes and shapes, the method of analysis can allow a classification in quality classes of the severity of possible discontinuities. Thus, there is the possibility of managing the results much faster by establishing the quality and classification of the product. This paper proposes to present a short overview of automated data analysis algorithms for processing and automated evaluation of data, being based on Bayesian and fuzzy logic methods. These methods help both at the evaluation of flaws nature using feature extraction and clustering as well as well their severity using a data mining procedure. The data referring to noises and data of emphasized flaws are considered “apriori” knowledge [4].

[1] Trampus, P., Krstelj, V. and Nardoni, G., 2019. NDT integrity engineering—A new discipline. *Procedia Structural Integrity*, 17, pp.262-267.

[2] Yusa, N. and Knopp, J.S., 2016. Evaluation of probability of detection (POD) studies with multiple explanatory variables. *Journal of Nuclear Science and Technology*, 53(4), pp.574-579.

[3] Deng, W., Bao, J. and Ye, B., 2020. Defect Image Recognition and Classification for Eddy Current Testing of Titanium Plate Based on Convolutional Neural Network. *Complexity*, 2020.

[4] Cosarinsky, G., Ruch, M., Rugirello, G., Domizzi, G., Grimberg, R., Steigmann, R. and Savin, A., 2012. Automatic eddy current classification of signals delivered by flaws—application to nuclear fuel cladding. *Insight-Non-Destructive Testing and Condition Monitoring*, 54(6), pp.316-321.

MICROWAVE MEASUREMENTS FOR BIOLOGICAL TISSUES

R.Steigmann¹, D.Faktorova², N.Iftimie¹ and A.Savin¹

¹National Institute of R&D for Technical Physics, Nondestructive Testing Department, Iasi, Romania

²University of Trencin, Slovak Republic

E-mail: steigmann@phys-iasi.ro

Monitoring the dielectric properties of biological tissues, especially in the microwave frequency domain, and investigation of the possibilities of applying new metamaterial elements and additional treatment using high-loss dielectrics are required in optimizing the procedures of microwave hyperthermia of cancer. Biological tissues are considered dipolar materials [1]. In addition to electron and atomic polarization, these materials exhibit polarization resulting from a change in the orientation of the dipolar groups of atoms that are part of their structure. A typical representative of such a structure is water, which shows strong dipolar polarization. Biological tissues contain a high proportion of water and behave like dipolar materials. With a water relaxation time of 53 ps, microwaves are a suitable tool for examining biological tissues. And since the main indicator of dielectric materials is complex permittivity, the greatest attention is paid to measuring changes in complex permittivity in different tissues and under different conditions [2]. This work is focused on monitoring the interaction of electromagnetic EM radiation with biological tissues in the microwave frequency domain.

Biological tissues are dielectric materials with losses and are defined by relative permittivity ϵ_r and loss tangent $\tan \delta$. Under interaction with electric field, the layout of atoms and molecules in the dielectrics is changed and dielectric reaction depend on frequency, given a complex entity to relative permittivity

$$\hat{\epsilon}_r = \epsilon_r' - j\epsilon_r'' \quad (1)$$

where ϵ_r' quantify the energy received and stored by material from electric field and ϵ_r'' measure the losses due to frequency dependency. The loss tangent $\tan \delta$ is defined as the ratio of the imaginary part to the real part of the relative permittivity.

For experimental measurements, waveguide methods in particular have been used, which prove to be very accurate (Figure 1).

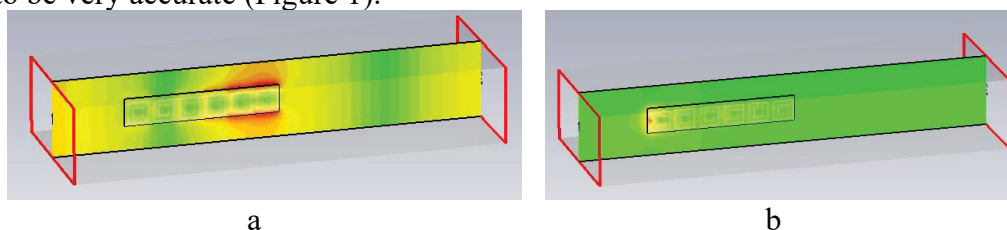


Figure 1. The electromagnetic field distribution in waveguide sensor with metamaterial structure at (a) nonzero and (b) zero transmission.

The CST Microwave Studio software environment was used to model EM phenomena in biological tissues - a simulation environment designed to simulate EM phenomena and high-frequency components. This simulation environment enables fast and accurate analysis of antennas, filters, waveguides, planar and layered structures and EM field effects in interaction with other objects.

The optimal number of substrates with metamaterials structures inserted to the volume of waveguide is three, Figure 2.

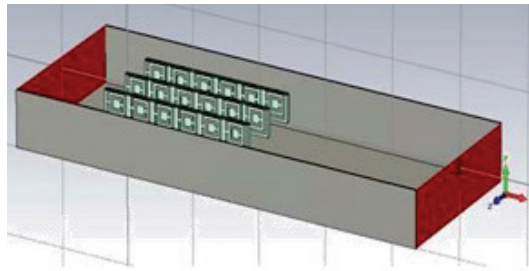


Figure 2. The optimized tuning of waveguide sensor

In order to achieve the simulation result as close as possible to the result of the real simulated problem, the accuracy of the calculation is of paramount importance. However, the increasing accuracy of the calculation is directly proportional to the demands on the computational technique, and thus to the total computational time, especially for more complex and layered structures. Therefore, in the implemented numerical simulations, it was necessary to define and approximate the simulated model with regard to accuracy and computer performance.

The dielectric properties of tumor tissues are of interest for several reasons. They are needed in microwave hyperthermia [3] as a modality in cancer treatment, as well as in the development of inhomogeneous models simulating the dielectric properties of organs with pathological features. Other potential applications include microwave imaging (Figure 3). In addition, investigation of the biophysical mechanisms of microwave interactions with tumor tissue can provide information regarding functional and structural relationships during tumor development. At microwave frequencies, the dielectric properties of biological tissues are determined by the change in cell membrane charge and the chemical composition of the tissue [4].

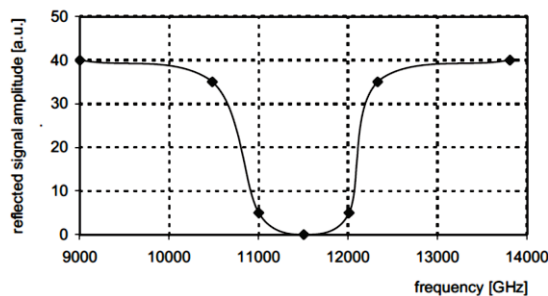


Figure 3. The frequency dependence of reflected signal from the dielectric sample.

- [1] Gabriel, S., Lau, R.W. and Gabriel, C., 1996. The dielectric properties of biological tissues: III. Parametric models for the dielectric spectrum of tissues. *Physics in medicine & biology*, 41(11), p.2271.
- [2] Popovic, D., McCartney, L., Beasley, C., Lazebnik, M., Okoniewski, M., Hagness, S.C. and Booske, J.H., 2005. Precision open-ended coaxial probes for in vivo and ex vivo dielectric spectroscopy of biological tissues at microwave frequencies. *IEEE Transactions on Microwave Theory and Techniques*, 53(5), pp.1713-1722..
- [3] Altintas, G., Akduman, I., Janjic, A. and Yilmaz, T., 2021. A Novel Approach on Microwave Hyperthermia. *Diagnostics*, 11(3), p.493.
- [4] Faktorova, D. Isteníková, K. 2010 Influence of Biological Materials Dielectric Parameters on Electromagnetic Wave Propagation. *Proceedings of the 8th International Conference ELEKTRO 2010*.

**Abstracts:
Poster
Presentations**

POSTER SESSION I:
FUNCTIONAL AND NANOSTRUCTURED MATERIALS

INFLUENCE OF NEUTRON IRRADIATION ON THE ELEMENTAL CONTENT AND OPTICAL PROPERTIES OF THE CaF_2 AND BaF_2 CRYSTALS

Yu.V. Aleksiyayenak¹, A.S. Doroshkevich^{1,2}, M. Stef³, M. Balasoui^{1,4}, A.S. Zakharova^{1,5},
E. A. Gridina^{1,5}, A.I. Kruglyak¹, T.Yu. Zelenyak¹, T. Phan Luong^{1,6}, L. H. Khiem^{7,8}

¹ *Joint Institute for Nuclear Research, Dubna, Russia*

² *Donetsk Institute for Physics and Engineering named after O.O. Galkin, Kiev, Ukraine*

³ *Faculty of Physics, West University of Timisoara, Timisoara, Romania*

⁴ *Horia Hulubei National Institute for R&D in Physics and Nuclear Engineering (IFIN-HH), Bucharest, Romania*

⁵ *Dubna State University, Dubna, Russia*

⁶ *Hanoi Irradiation Center, Vietnam Atomic Energy Institute, Hanoi, Vietnam*

⁷ *Graduate University of Science and Technology, Vietnam Academy of Science and Technology, Ha Noi, Vietnam*

⁸ *Institute of Physics, Vietnam Academy of Science and Technology, Ha Noi, Vietnam*

E-mail: beataa@gmail.com

The alkaline-earth fluorides represent an important class of relatively simple ionic crystals that are crystallised in the cubic structure and due to their optical and lattice-dynamical properties have theoretical and experimental interest. These alkaline-earth fluorides crystals can be doped with rare earth elements (RE, RE=La, Er, Yb, etc.) and exhibit good optical properties [1-4] that have been studied for various applications [5]. Pure and Er^{3+} barium fluoride crystals are the fastest known scintillator. Also, the optical and luminescence behaviour of $\text{Er}^{3+}:\text{BaF}_2$ crystals is very promising [6-8]. Crystals of pure and Er^{3+} high-doped BaF_2 were grown at the West University of Timisoara, Romania. Neutron irradiation of samples and further elemental composition studies were conducted at the Joint Institute for Nuclear Research. Elemental content was studied by Particle-induced X-ray emission (PIXE) and Rutherford backscattering spectrometry (RBS) was applied to study elemental depth profile before and after irradiation with fast neutrons (2.5 MeV, dose $D = 10^{12}$ particles / cm^2).

It found out that neutron irradiation changed elements distribution in depth of the samples. Thus, light atoms of Ba are transferred inside samples while heavier atoms of Er are coming close to the surface. Moreover, at the depth of 100 nm surface deformation was observed. Studies of the optical characteristics of different crystals showed slight difference between non-irradiated and irradiated samples.

The study was performed in the framework of the JINR-Romania cooperation program in 2022 (topic 03-4-1128-2017/2022).

[1] I. Nicoara, M. Stef, A. Pruna (2008). Growth of YbF_3 -doped CaF_2 crystals and characterization of $\text{Yb}^{3+}/\text{Yb}^{2+}$ conversion. *Journal of Crystal Growth*. 310, 1470-1475.

[2] M. Stef, A. Pruna, N. Pecingina-Garjoaba, I. Nicoara (2007). Influence of various impurities on the optical properties of YbF_3 doped CaF_2 crystals. *Acta Physica Polonica A*. 112, 1013-1018

[3] E. Preda, M. Stef, G. Buse, A. Pruna, I. Nicoara (2009). Concentration dependence of Judd-Ofelt parameters of Er^{3+} ions in CaF_2 crystals. *Physica Scripta*. 79, 035304

[4] G. Buse, E. Preda, M. Stef, I. Nicoara (2011). Influence of Yb^{3+} ions on the optical properties of double-doped Er, Yb: CaF_2 crystals. *Physica Scripta*. 83, 025604

- [5] D. Hahn (2014) Calcium fluoride and barium fluoride crystals in optics. *Optik & Photonik*. 9(4), 45–48
- [6] A. Racu, M. Stef, G. Buse, I. Nicoara, D. Vizman (2021). Luminescence Properties and Judd–Ofelt Analysis of Various ErF_3 Concentration-Doped BaF_2 Crystals. *Materials*. 14, 4221
- [7] M. Stef, I Nicoara, A. Racu, G. Buse, D. Vizman (2020). Spectroscopic properties of the gamma irradiated ErF_3 -DOPED BaF_2 crystals. *Radiation Physics and Chemistry*. 176, 109024
- [8] I. Nicoara, M. Stef, G. Buse, A. Racu (2020). Growth and characterization of ErF_3 doped BaF_2 crystals. *Journal of Crystal Growth*. 547, 125817

THEORETICAL INVESTIGATION OF STRUCTURE AND MAGNETIC PROPERTY OF Ni SUBSTITUTED $MgFe_2O_4$

B.Khongozul^{1,2}, N.Tsogbadrakh², N.Jargalan¹, D.Odkhuu³ and D.Sangaa¹

¹*Institute of Physics and Technology, Mongolian Academy of Sciences, Ulaanbaatar, Mongolia*

²*National University of Mongolia, Ulaanbaatar, Mongolia*

³*Incheon National University, Incheon, South Korea*

E-mail: khongorzulb@mas.ac.mn

The ferrite magnetic nanoparticles have been studied in many fields such as microwave devices, semiconductors, low magnetic materials, gas sensing, and hyperthermia therapy [1]. The hyperthermia therapy can be realized by the application of an AC magnetic field from external coils to cancer tumors using magnetic ferrite materials. Magnetite has been mainly investigated as the candidate material for this type of therapy [2-3].

In this study, we considered Nickel (Ni) substituted Magnesium ferrite ($Mg_{1-x}Ni_xFe_2O_4$ [$x = 0.0, 0.2, 0.4, 0.6, 0.8, 1$]) using the first-principles method within framework of density functional theory (DFT) as implemented in the VASP (Vienna Ab-initio Simulation package). The calculations were performed by the pseudopotential plane-wave self-consistent field (PWscf) method with the Generalized Gradient Approximation (GGA). The Brillouin zone was integrated to different k-point sets generated with the Monkhorst-Pack method centered at the 5x5x5 point with optimized 500eV energy cutoff. The stability of the structure is calculated for the normal, the fully inverse, and partially inverse structure of pure $MgFe_2O_4$. Figure 1 shows, our created structure of Ni substituted $MgFe_2O_4$ in the partially inverse type. From the optimization, partially inverse was found most stable structure from all of the types.

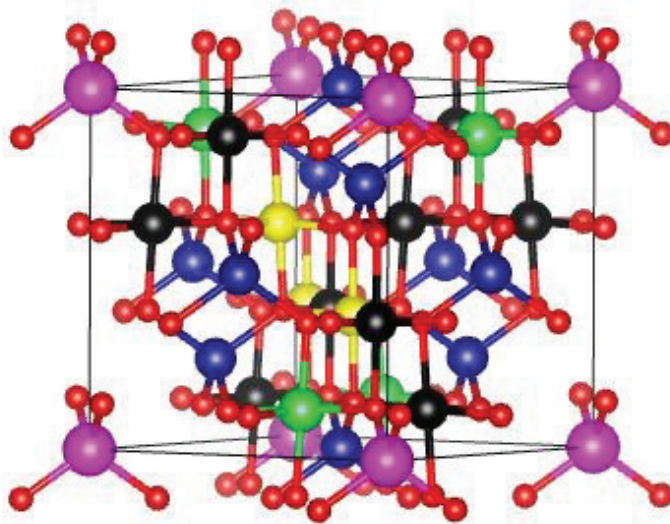


Figure 1: The crystal structure of $Mg_{1-x}Ni_xFe_2O_4$ ($x = 0.4$) spinel. Yellow - Ni, green and pink - Mg, dark and blue - Fe atoms at octahedral and tetrahedral sites, respectively.

We have predicted the lattice parameter and magnetic moments from the spin-polarized calculation for $Mg_{1-x}Ni_xFe_2O_4$ [$x = 0.0, 0.2, 0.4, 0.6, 0.8, 1$] compounds and compared them with neutron diffraction results. Neutron diffraction measurements were performed at HRFD JINR, Dubna [4].

The obtained magnetic moment values agree with the neutron diffraction study for $MgFe_2O_4$ (see Table 1).

Table 1. Stability energy gains δE (units of $meV/f.u$) for the AFM states between the full inverted (FI) and the normal (N) spinels ($\delta E = E_{tot} [AFM](FI) - E_{tot}[AFM](N)$), magnetic energy gains δE (units of $eV/f.u$) for each spinel ($\delta E = E_{tot} [FM] - E_{tot} [AFM/FIM]$), optimized lattice parameters (units of \AA), magnetic moments (units of μ_B) of each atomic sites for cubic $Mg_{1-x}Ni_xFe_2O_4$ [$x = 0.0, 0.2, 0.4, 0.6, 0.8, 1$] phases using the GGA + U method.

$Ni(x)$	alat(A^0)	MM(Mg)	MM(Ni)	MM(Fe _{tet})	MM(Fe _{oct})	δE
exp*	-	-	-	3.5	4.8	-
0.0	8.37	0.004	-	-4.2	4.2	-125.0
0.2	8.35	0.006	1.22	-3.5	3.6	-225.9
0.4	8.43	0.007	1.35	-4.1	4.2	-352.0
0.6	8.42	0.007	1.34	-4.2	4.2	-417.3
0.8	8.41	0.008	1.36	-4.1	4.5	-216.5
1	8.32	-	1.20	-3.6	3.7	-334.2

We have performed band gap, band structure and density of states calculations for all samples. The bandgap values of $MgFe_2O_4$ were obtained from 0.00 to 0.72eV depend on Ni concentrations.

[1] W.B.K.Putri, E.A.Setiadi, V.Herika, A.P.Tetuko and P.Sebyang (2019). Natural iron sand-based $Mg_{1-x}Ni_xFe_2O_4$ nanoparticles as potential adsorbents for heavy metal removal synthesized by co-precipitation method. IOP Conf. Series: Earth and Environmental Science 277, 012031, 1755-1315.

[2] B.Khongorzul, N.Tsogbadrakh and D.Sangaa (2017). Theoretical investigation of structure and magnetic property of cubic $MgFe_2O_4$. Mongolian Journal of Physics 25, ISSN 2311-1097, 50-54.

[3] E.Uyanga, D.Sangaa, H.Hirazawa, N.Tsogbadrakh, N.Jargalan, I.A.Bobrikov, A.M.Balagurov (2018). Structural investigation of chemically synthesized Ferrite magnetic nanomaterials. Journal of Molecular Structure, 1160, 1 447-454.

[4] D.Sangaa, B.Khongorzul, E.Uyanga, N.Jargalan, N.Tsogbadrakh, H.Hirazawa (2017). An overview of Investigation for Ferrite Magnetic Nanomaterials, Solid State Phenomena.

HIGH - PRESSURE EFFECT ON INTERNAL STRUCTURE AND ATOMIC DYNAMICS OF PHARMACEUTICAL COMPOUNDS

N.M.Belozerova¹, D.P. Kozlenko¹, J. Wąsicki², P. Bilski², E.V. Lukin¹, B.N. Savenko¹

¹*Frank Laboratory of Neutron Physics, Joint Institute for Nuclear Research, 141980, Dubna, Russia*

²*Faculty of Physics, A. Mickiewicz University, ul. Umultowska 85, 61-614 Poznań, Poland*

E-mail: nmbelozerova@mail.ru

Due to the wide variety of phenomena realized in organic crystals at high pressure: polymorphic phase transitions, amorphization, etc., studies of pressure-induced changes in the crystal structure and atomic dynamics of complex molecular crystals is an urgent task in condensed matter physics [1,2]. In addition, structural studies of molecular crystals are important for optimization of the pharmaceutical production process, where, under additional mechanical influences (grinding or tableting), irreversible polymorphic phase transitions or its amorphization can develop in the initial material, which entails significant changes in the physicochemical and pharmaceutical properties material. [3].

The use of high-pressure diffraction and Raman spectroscopy to study pharmacological components makes possible investigation of their structure and physical properties in the most complete way, which is necessary to understanding the nature and mechanisms of physical phenomena observed in them [4].

Therefore, the main objective of this study was detail investigation of physical properties and dynamics of the group of pharmaceutical compounds by means of different methods: X-ray diffractometry and Raman spectroscopy.

Investigation of internal structure and atomic dynamics of pharmacological components hypolipidemic agent lovastatin $C_{24}H_{36}O_5$ and antibacterial agent ofloxacin $C_{18}H_{20}FN_3O_4$ were carried out.

The pressure dependence of vibrational modes of lovastatin measured at high pressures up to 9.8 GPa and room temperature were shown. The changes in a pressure behavior of the Raman lines were observed at pressures 3 and 5.2 GPa. Those changes can indicate the polymorphic phase transitions lovastatin under pressure. At pressures above 9 GPa a gradual broadening of Raman lines is followed by their disappearance up on further compression. Such a behavior corresponds to a gradual phase transition to the amorphous phase of lovastatin.

At pressure $P > 4.8$ GPa, several changes in the X-ray diffraction data and Raman spectra of ofloxacin were observed, which indicate a pressure-induced phase transformation from initial form to HP-form of ofloxacin. Around this phase transformation, the noticeable anomalies in the pressure behaviour of different vibration frequencies of ofloxacin were found.

At $P > 7.3$ GPa a gradual broadening of Raman modes, followed by disappearance of the most of them at about 10 GPa, were observed. Such a behavior corresponds to a gradual phase transition to the amorphous phase of the ofloxacin.

The structural mechanisms of the phase transitions in presented pharmaceutical compounds were discussed.

[1] H.G. Brittain, S.R. Byrn // *Drugs and the Pharmaceutical Sciences Series*, 95, 73-124 (1999).

[2] V.V. Boldyrev // *Journal of Materials Science* 39, 5117-5120 (2004).

[3] M. Otsuka, T. Matsumoto, N. Kaneniwa // *J Pharm Pharmacol* 41, 665–669 (1989).

[4] S.E. Kichanov, D.P. Kozlenko, P. Bilski // *Journal of Molecular Structure* 1006, 337-343 (2013).

NEUTRON DIFFRACTION INVESTIGATION OF PRESSURE DEPENDENCE OF $\text{Nd}_5\text{Mo}_3\text{O}_{16+\delta}$ CRYSTAL STRUCTURE

K.A. Chebyshev¹, S.E. Kichanov²

¹Donetsk national university, Donetsk, Ukraine

²Frank Laboratory of Neutron Physics, Joint Institute for Nuclear Research, Dubna, Russia

E-mail: Chebyshev.konst@mail.ru

We have previously studied isomorphic substitutions of neodymium for other rare-earth elements in the $\text{Nd}_{5-x}\text{Ln}_x\text{Mo}_3\text{O}_{16+\delta}$ series [1, 2]. It was found that the introduction of rare-earth elements with a smaller ionic radius in comparison with neodymium into $\text{Nd}_5\text{Mo}_3\text{O}_{16+\delta}$ molybdate leads to decreasing in the unit cell parameter. When the substitution limit is reached, a morphotropic transition occurs from the cubic phase to the monoclinic one (gp. gr. C2/c). $\text{Ln}_5\text{Mo}_3\text{O}_{16+\delta}$ molybdates have a monoclinic structure for lanthanides with a smaller ionic radius than neodymium and are included in the homogeneity region of Ln_2MoO_6 molybdates. It is possible that this transition of neodymium molybdate will also occur with a decrease in the unit cell parameter caused by high pressure. To establish the effect of pressure on the crystal structure of $\text{Nd}_5\text{Mo}_3\text{O}_{16+\delta}$ molybdate, neutron diffraction experiments were carried out on the DN-6 instrument on IBR-2 pulsed reactor in the pressure range of 0 - 5.9 GPa [3].

Single phase $\text{Nd}_5\text{Mo}_3\text{O}_{16+\delta}$ molybdate with cubic fluorite-related structure (sp.gr. Pn-3n) was prepared by solid state method. Analysis of neutron spectra showed the $\text{Nd}_5\text{Mo}_3\text{O}_{16+\delta}$ neodymium molybdate retains a cubic fluorite-like structure over the entire studied pressure range at room temperature.

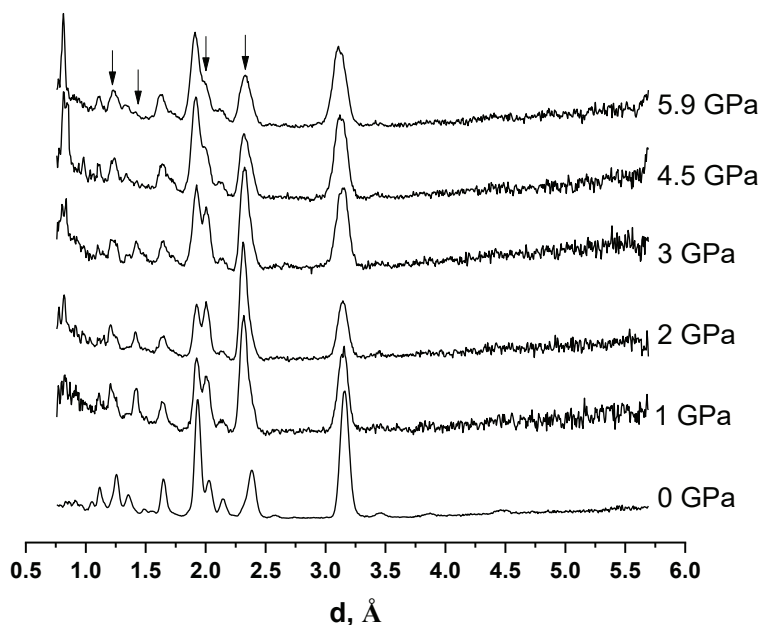


Fig. 1. Neutron diffraction patterns of neodymium molybdate at different pressure (Arrows indicate materials of high pressure equipment)

The unit cell parameters calculated by full profile analysis of neutron diffraction patterns using Rietveld method are shown in fig. 2.

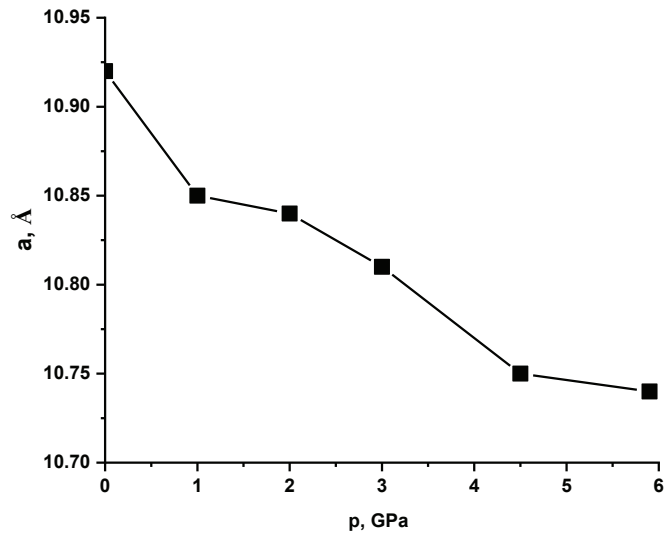


Fig. 2. Dependence of unit cell parameter on pressure value.

An increasing of pressure leads to decreasing in the unit cell parameter of neodymium molybdate without any phase transitions. This can be explained by the fact that, monoclinic phase of $\text{Ln}_5\text{Mo}_3\text{O}_{16+\delta}$ are subtraction solid solutions ($\text{Ln}_{5/3}\text{MoO}_{16/3+\delta}$) with respect to the compositions of Ln_2MoO_6 . Therefore, the transition from the cubic to the monoclinic phase should be accompanied by the formation of vacancies in the sublattice of the rare earth element and oxygen, which is energetically disadvantageous at elevated pressure.

- [1] K.A. Chebyshev (2015). Crystal structure and electrical conductivity of $\text{Nd}_{5-x}\text{Sm}_x\text{Mo}_3\text{O}_{16}$ solid solutions. *Inorganic Materials*. 51, 1033–1038.
- [2] E.I. Get'man (2016). Isomorphous substitutions and conductivity in molybdates $\text{Nd}_{5-x}\text{Ln}_x\text{Mo}_3\text{O}_{16+y}$ ($y \sim 0.5$), where $\text{Ln} = \text{La}, \text{Ce}, \text{Pr}$. *Journal of Alloys and Compounds*. 686, 90-94.
- [3] D. Kozlenko (2018). The DN-6 Neutron Diffractometer for High-Pressure Research at Half a Megabar Scale. *Crystals*. 8, 331.

MAGNETIC AND CRYSTALLINE STRUCTURE OF SOME DOPPED WITH Cr MANGANITES

M.L. Craus^{1,2}, V.A. Turchenko¹, A. Islamov¹, E. Anitsas¹, R.Erhan¹, A.Savin² and N. Cornei³

¹Joint Institute for Nuclear Research, 141980, Dubna, 6 Joliot-Curie Street, Russia;

²National Institute for Research and Development for Technical Physics, 700050 -Iasi, 47 Mangeron, Romania;

³"Al.I. Cuza" University of Iasi, Faculty of Chemistry, Bld. Carol I, No. 11, Iasi 700506, Romania.

E-mail: craus@phys-iasi.ro

The $\text{La}_{0.54}\text{Ho}_{0.11}\text{Sr}_{0.35}\text{Mn}_{1-x}\text{Cr}_x\text{O}_3$ ($x=0.05, 0.10, 0.15, 0.20$) manganites were synthesized by starting from La_2O_3 and Ho_2O_3 (purity: 99.99%), SrCO_3 and the Mn and Cr acetates (purity: 99.00%). The presintered samples were again ground and finally sintered at 1200°C for 10 hours in air atmosphere. The phase composition, structure, lattice constants, positions of cations and anions in unit cell, BO distances, BOB bond angles, average size of mosaic blocks and microstrains were determinate by using Fullprof or PowderCell code. The variation of the specific magnetization with temperature, implicitly Curie temperature and molar magnetization, were determined by using a VSM type magnetometer, working at $H_{\text{max}}=1\text{T}$, between 77 and 400 K. The variation of resistance with temperature and magnetic field was performed with a close cycle refrigerator, working between 7 and 350 K, at $H_{\text{max}}=1\text{T}$, by means of four probe method, by using a magnetic field $H_{\text{max}}=1\text{T}$.

Table 1. Variation of the lattice constants (a, b, c), unit cell volume (V), average size of mosaic blocks (D) and microstrains (ϵ) for $\text{La}_{0.54}\text{Ho}_{0.11}\text{Sr}_{0.35}\text{Mn}_{1-x}\text{Cr}_x\text{O}_3$ manganites (one phase model)

x	a (Å)	b (Å)	c (Å)	V (Å ³)	D (Å)	ϵ
0.05	5.464 ₂	7.709 ₇	5.495 ₀	231.49	621	0.000298
0.10	5.466 ₇	7.711 ₉	5.497 ₅	231.77	664	0.000359
0.15	5.470 ₄	7.714 ₆	5.498 ₄	232.04	703	0.000149
0.20	5.467 ₃	7.708 ₅	5.495 ₈	231.62	698	0.000157

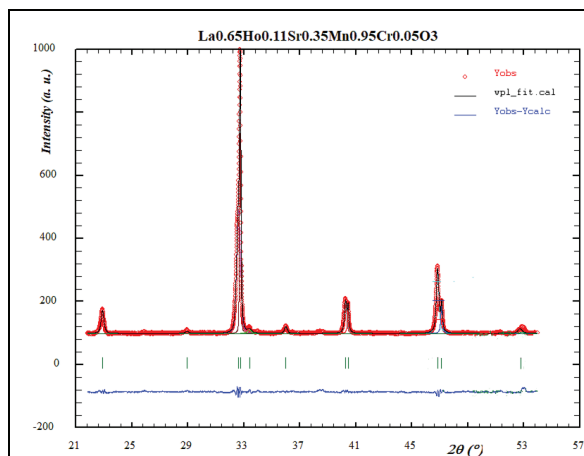


Figure 1. X ray diffractogram of $\text{La}_{0.54}\text{Ho}_{0.11}\text{Sr}_{0.35}\text{Mn}_{0.95}\text{Cr}_{0.05}\text{O}_3$

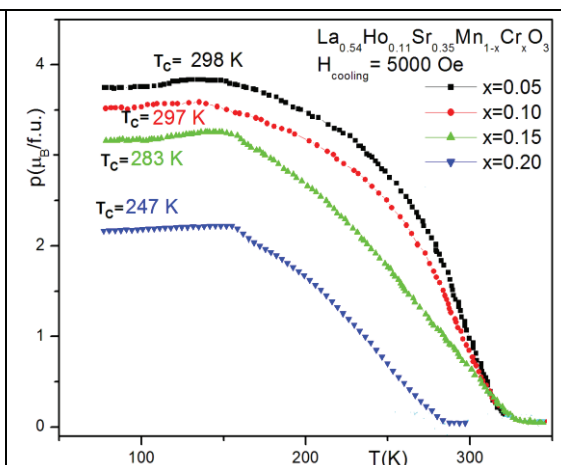


Figure 2. The variation of molar magnetization with temperature and Cr concentration

A large difference exists between the Mn^{3+} or Mn^{4+} and Cr^{3+} or Cr^{2+} behavior, concerning the contribution at the magnetic structure: only Mn^{3+} and Mn^{4+} contribute to the magnetic moment of the samples, apparently no exchange takes place between the Mn and Cr cations. Magnetic measurement, performed between 77 and 400 K indicate a decrease of the molar magnetization vs increase of Cr concentration in the samples for an intensity of 5000 Oe

(see Figure 2). At low intensity field the molar magnetization shows an unusual dependence of the temperature, especially with the increase of Cr concentration over $x=0.10$ (see Figure 2). For low Cr concentration the dependence of molar magnetization on temperature have a form close to those of ferromagnetic materials. However, at low temperature a maximum of the molar magnetization was observed (see Figure B). We attributed the observed maximum to a transition from the ferromagnetic to spin glass state, with the increase of the temperature.

Ferromagnetic to spin-glass transition.

The specific magnetization presents a strong dependence in the intensity of magnetic field and on thermal treatment of the samples.

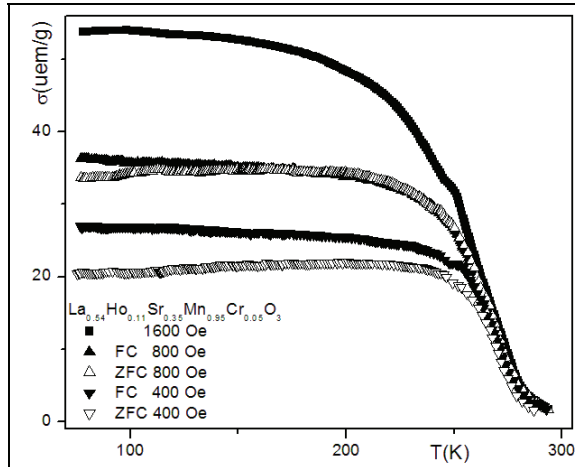


Figure 3. Variation of specific magnetization with intensity of magnetic field and temperature for $La_{0.54}Ho_{0.11}Sr_{0.35}Mn_{0.95}Cr_{0.05}O_3$

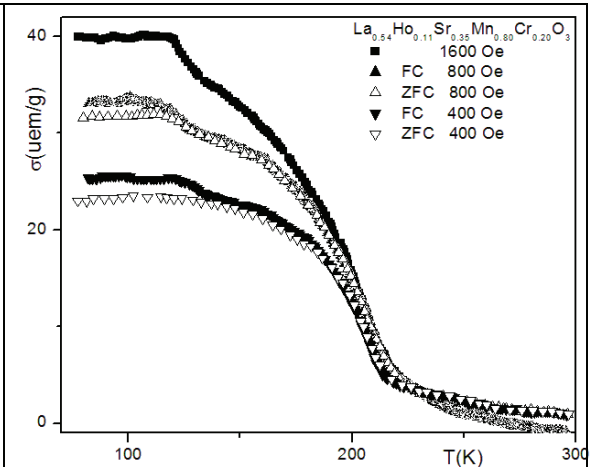


Figure 4. Variation of specific magnetization with intensity of magnetic field and temperature for $La_{0.54}Ho_{0.11}Sr_{0.35}Mn_{0.8}Cr_{0.2}O_3$

For the samples cooled in low magnetic field the magnetization ($H \leq 800$ Oe) remains practically constant for a large range of temperatures (see Figures 3 and 4). On other hand, we observed an increase of magnetization from low to higher temperature, close to transition temperature between spin-glass and ferromagnetic state. The behavior of specific magnetization is characteristic for the presence of the spin state. We concluded that at low temperatures the samples are formed by a mixture of spin glass and ferromagnetic state.

If the samples are cooled without magnetic field a partial transition from a ferromagnetic state (parallel magnetic moments) to a spin glass state (disordered magnetic moments) takes place, it means a decrease of the magnetic moment of the samples with temperature. If the samples are cooled in magnetic field at temperature lower as transition temperature some magnetic moments remain parallel with the direction of the applied magnetic field direction. The transition temperature strongly depends on the Cr concentration in the samples (see Figures 3 and 4). Such behavior can be attributed 1) to the presence of the B sites of an increase Cr concentration, which did not contribute directly to the magnetic moment of the samples and 2) to a decrease of the direct exchange interaction due the presence of Cr cations in B lattice.

CORRELATION BETWEEN THE Cr CONCENTRATION AND MAGNETIC NANOSTRUCTURE PARAMETERS FOR $\text{La}_{0.54}\text{Ho}_{0.11}\text{Sr}_{0.35}\text{Mn}_{1-x}\text{Cr}_x\text{O}_3$ MANGANITES

M.L. Craus^{1,2}, V.A. Turchenko¹, A. Islamov¹, E. Anitsas¹, R.Erhan¹, A.Savin² and N. Cornei³

¹Joint Institute for Nuclear Research, 141980, Dubna, 6 Joliot-Curie Street, Russia;

²National Institute for Research and Development for Technical Physics, 700050 -Iasi, 47 Mangeron, Romania;

³"Al.I. Cuza" University of Iasi, Faculty of Chemistry, Bld. Carol I, No. 11, Iasi 700506, Romania.

E-mail: craus@phys-iasi.ro

We investigated the magnetic, crystalline structure of $\text{La}_{0.54}\text{Ho}_{0.11}\text{Sr}_{0.35}\text{Mn}_{1-x}\text{Cr}_x\text{O}_3$ ($x=0.05, 0.20$) manganites. The synthesis of investigated manganites was performed by starting from La_2O_3 and Ho_2O_3 (purity: 99.99%), SrCO_3 and the Mn and Cr acetates (purity: 99.00%) [1]. The phase composition, structure, lattice constants, positions of cations and anions in unit cell, BO distances, BOB bond angles, average size of mosaic blocks and microstrains were determinate by using Fullprof or PowderCell code. Neutron diffractometry was used to obtain corresponding data (s. Fig. 1).

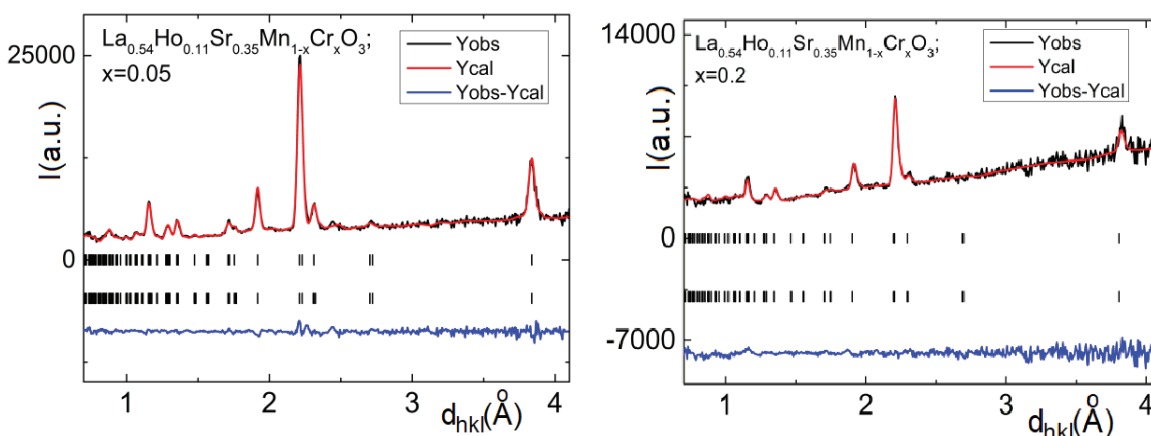


Figure 1. Refined powder neutron diffraction pattern at 300 K. Continuous lines represent observed (black line), calculated (red) and difference (blue) patterns. Tick markers correspond to the position of the allowed Bragg reflections: first rows (above) are the crystal reflections and second rows (below) are the magnetic reflections of $\text{La}_{0.54}\text{Ho}_{0.11}\text{Sr}_{0.35}\text{Mn}_{1-x}\text{Cr}_x\text{O}_3$ with the space group $R-3c$

Table 1. Variation of the lattice constants (a, b, c), unit cell volume (V), average size of mosaic blocs (D) and microstrains (ϵ) for $\text{La}_{0.54}\text{Ho}_{0.11}\text{Sr}_{0.35}\text{Mn}_{1-x}\text{Cr}_x\text{O}_3$ manganites (two phases model, $R-3c$ phase and Pnma parameters)

x	a (Å)	b (Å)	c (Å)	V (Å ³)	D (Å)	ϵ	SG
0.05	5.469 ₈	5.469 ₈	13.449 ₃	348.48	457	0.00215	R-3c
0.20	5.473 ₃	5.473 ₃	13.434 ₄	348.54	641	0.00249	R-3c
0.05	5.500 ₆	7.705 ₀	5.459 ₅	231.39	989	0.000175	Pnma
0.20	5.502 ₀	7.705 ₅	5.461 ₄	231.54	1004	0.000204	Pnma

Lattice constants change due the modification of cations distribution, with the increase of the Cr concentration in the samples. We supposed that cations distribution is characterized by the presence of the Mn^{3+} (HS - 0.645 Å), Mn^{4+} (0.53 Å), Cr^{3+} (0.615 Å), Cr^{2+} (0.80 Å) in various concentrations.

A large difference exists between the Mn^{3+} or Mn^{4+} and Cr^{3+} or Cr^{2+} behavior, because only Mn^{3+} and Mn^{4+} contribute to the magnetic moment of the samples, apparently no exchange takes place between the Mn and Cr cations. The presence of large amount of Mn^{3+} cations leads to a structural transition from a cubic to a lower symmetry. Implicitly, the presence of a large amount of non-JT cations decreases the concentration of crystalline distortions.

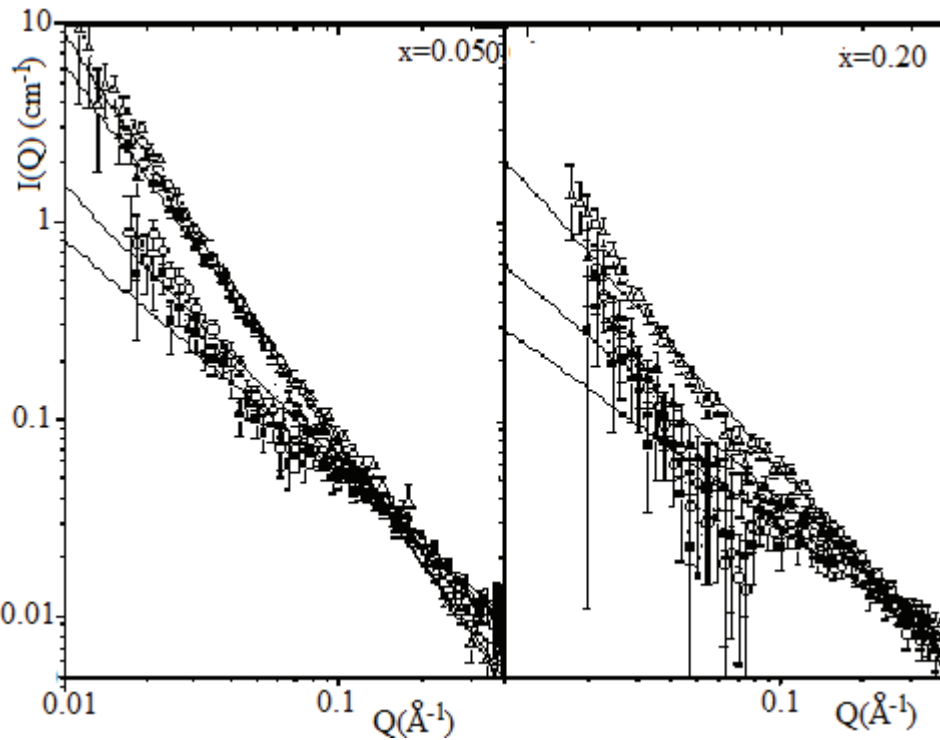


Figure 2. Magnetic scattering curves at temperatures 258K – 353K (Δ - 258 K; \blacktriangle - 293 K; \diamond - 333 K; \blacksquare - 353 K)

A combination of both SAXS and SANS techniques was useful to determine the contribution of the magnetic scattering without the additional use of the external magnetic field and polarized neutrons due to X-ray scattering is not sensitive to magnetic moments.

By subtracting the contribution of nuclear scattering from total scattering we obtain

$x \rightarrow$	0.05			0.20		
	α	φ_{exp}	$V(nm^3)$	α	φ_{exp}	V, nm^3
258	2.06	0.26	203	1.57	0.08	75
293	1.94	0.16	47	1.19	0.05	23
333	1.40	0.14	47	1.01	0.03	12
353	1.19	0.12	16	1	0.03	10

scattering from magnetic domains (see Figure 2). We are interested here in SANS at high Q, since in this regime the scattering intensity is associated with magnetic scattering.

Table 2. Variation of parameters of magnetic clusters with temperature and Cr concentration. V – is the volume of cluster, φ – is the volume fraction of magnetic clusters in the sample, α – scattering exponent.

The microscopic magnetic domains have a radius bigger than $0.5 \mu m$, as indicated by the Porod law $I(Q) \propto Q^{-4}$ at low Q values (see Fig.2). Formation of disk-like and 3D mass fractal structures for other Sr concentrations ($x = 0.00$, 0.05 and $x = 0.20$) may be possible, but at much lower temperatures.

STUDY OF SIGMA PHASE EMERGENCE IN STAINLESS STEEL WELDS

O.Yu. Prokoshev¹, S.N. Petrov¹, M.L. Fedoseev¹, A.Kh. Islamov²

¹NRC “Kurchatov institute” – CRISM “Prometey”, St. Petersburg, Russia

²Joint Institute for Nuclear Research, Dubna, Russia

E-mail: npk3@crism.ru

Long-term aging of austenitic stainless steels (steel: 0.1% C, 18% Cr, 9% Ni, welding wire: 0.04% C, 17% Cr, 10% Ni, 2% Mo) at a temperature of 500-550° C leads to a decrease in ductility, impact toughness and crack resistance of the metal. This is due to the formation of secondary phases at intergranular, special and interphase boundaries, leading to a decrease in their adhesive strength.

To predict the degradation of the material for the entire service life of the equipment (up to 50 years), experimental data are not enough and the method of laboratory accelerated (simulation) aging at temperatures above operational temperatures were used. The temperature of laboratory aging was 700° C. The aging time was determined according to the Holomon parameter $P = T \cdot (5,15 + \lg\tau)$, where T – temperature, τ – time [1]. Welds were austenized (heat treatment for 30 min at 1050° C) to increase resistance to local fractures. Additional austenization after aging was done to reestablish the initial state of the welds.

Changes in the phase composition of the weld metal after laboratory aging and aging at the basic temperature were studied. X-ray and neutron diffraction, small-angle neutron scattering data on fine precipitates, impact bending test data (at a temperature of +20°C, which is most revealing) were used, see Fig. 1. A sharp drop in impact strength for a non-austenized weld occurs during the first 2000 hours, Fig. 1. This is in good agreement with the decay of the initial δ -ferrite, which was detected approximately in this range. The strongest decrease in impact toughness for an austenized weld occurs within 4000-6500 hours (Fig. 1), while this is not related to the decay of δ -ferrite, since it almost dissolved even before aging in the process of austenization. The state of the material after ~ 20,000 hours was also studied, using diffraction: a mixture of FCC-Fe with σ -phase is observed, no difference between the austenized and the non-austenized state was found.

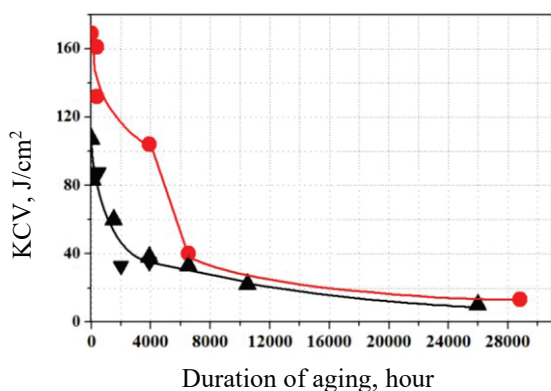


Fig. 1 Dependence of the impact toughness on the duration of aging for the weld metal:

- – austenized weld;
- ▲, ▼ – non-austenized weld;
- , ▲ – $T_{ag} = 700^\circ C$; ▼ – $T_{ag} = 750^\circ C$

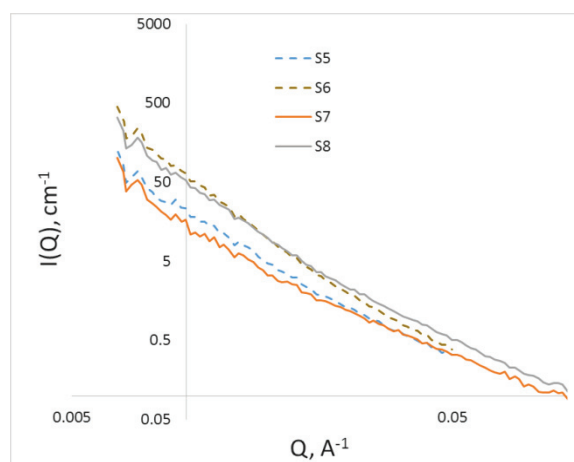


Fig. 2 Curves of small-angle neutron scattering of the initial state (s5, s7) and after aging (s6, s8), samples s5, s6, after laboratory aging, and s7, s8 after aging under basic conditions.

Fig. 2 shows the curves of small-angle neutron scattering of welds after laboratory aging and aging at operating temperature. The curves of the initial and the sample after aging

coincide for the two types of aging. The curves of the initial samples are below the curves after aging both for the given case and for other states.

Thus, the laboratory aging of the metal of austenized and non-austenized welds showed that thermal embrittlement occurs due to the formation and growth of brittle intermetallic σ - and χ -phases. Impact toughness at the initial stage of aging depends on the content of the δ -ferrite, the positive effect of austenization is explained by a decrease in its content. After a long time of aging, austenization does not affect the impact elasticity of these welds. The use of neutron instruments along with traditional methods of analysis provides additional data and allows for independent verification of the results obtained.

The work has been performed with the financial support of a grant from the Russian Scientific Foundation "New Physical and Chemical Principles of the Technology of Metal, Ceramic and Ceramic Materials with Controlled Macro, Micro and Nanostructure and Unique Service Characteristics" (No. 21-73-30019).

Experimental studies were carried out on the equipment of the Core shared research facilities "Composition, structure and properties of structural and functional materials" of the NRC «Kurchatov Institute» – CRISM "Prometey" with the financial support of the state represented by the Ministry of Education and Science of the Russian Federation under agreement No. 13.CKP.21.0014. The unique identifier is RF----2296.61321X0014.

[1] J.H. Hollomon (1945). Time - temperatures relations in tempering steel. Transactions of the American Institute of Mining and Metallurgical Engineers. 162, 223-249

STRUCTURAL PROPERTIES OF BIFUNCTIONAL CATALYSTS FOR ZINC-AIR BATTERIES

I.G. Genov^{1,3}, T. Malakova², G.S. Raikova¹, K.A. Krezhov², D.P. Kozlenko³, E.V. Lukin³, A.V. Rutkauskas³, I.Y. Zel³, S. Vasilev¹, M.V. Gabrovska⁴, D.A. Nikolova⁴

¹*Institute of Electrochemistry and Energy Systems, Bulgarian Academy of Sciences, Sofia, Bulgaria*

²*Institute of Electronics, Bulgarian Academy of Sciences, Sofia, Bulgaria*

³*Frank Laboratory of Neutron Physics, Joint Institute for Nuclear Research, Dubna, Moscow Region, Russia*

⁴*Institute of Catalysis, Bulgarian Academy of Sciences, Sofia, Bulgaria*

E-mail: dedfin45@abv.bg

The zinc-air batteries are a type of the group of metal-air systems that use the oxidation of a metal with oxygen from atmospheric air to generate electricity [1]. It is furnished with an anode prepared from an appropriate metal and a gas diffusion electrode (GDE), which is connected to a source of air. The catalysts in the air cathode support the electrochemical reaction with the oxygen gas. Lately, metal-air batteries have attracted considerable research attention as a new generation of high-performance batteries as they feature simple design structure, very high energy density, and a relatively inexpensive production. The use of a zinc anode is particularly attractive due to its low cost, non-toxicity, and potential for high energy density (1.3 kWh kg⁻¹ theoretically). Most commonly, the GDE consists of two layers: (i) a porous gas diffusion layer (GDL), which serves to transport oxygen and is composed of both a carbon-based material and a hydrophobic binder, and (ii) a catalytic layer (CL) composed of carbon material, which provides the electrochemical reaction in combination with a metal conductor [2]. It has been identified that the main reason for the limitation in the battery system performance and lifetime is the use of carbon in GDE. The problem of replacing the carbon-containing GDE with a novel design of a carbon-free electrode is currently very relevant. A possible approach is to use some catalysts with electronic conductivity [2-5]. The latest advances in developing non-precious metal catalysts are achieved by utilizing of bifunctional catalysts based on transition metal oxides. We report the performance of test electrodes employing catalyst powder materials both commercially available and nanostructured powders prepared by a specific innovative procedure as well as the structural characterization of such catalysts as Co₃O₄, Ni+ Co₃O₄, (70:30), NiCO₂O₄, Ni+ NiCO₂O₄ (70:30) by several techniques including X-ray diffraction (XRD) and neutron diffraction (ND). The ND studies were conducted by the time of the flight method (TOF) on the spectrometer DN-12 of JINR, Dubna at the pulsed reactor IBR-2M. The ND data were analysed using the FULLPROF suite by applying profile matching mode followed by full profile Rietveld refinement of the structural model.

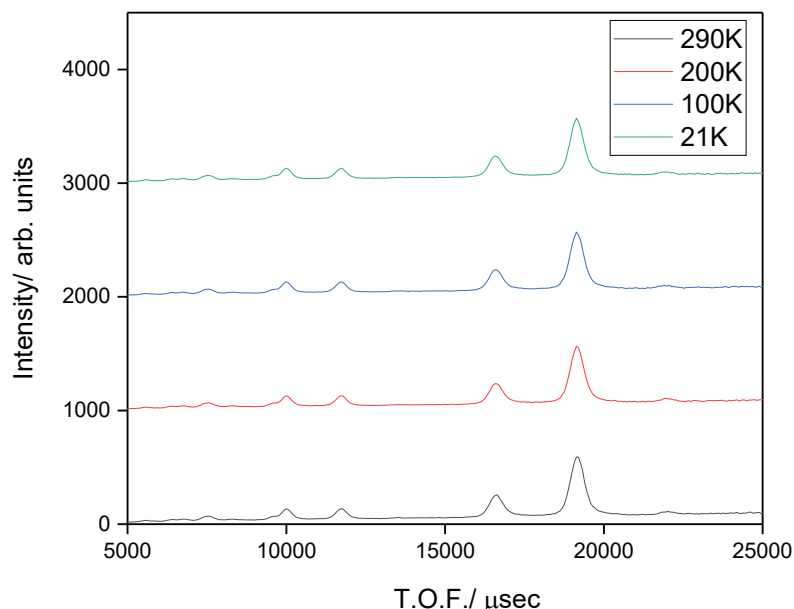


Fig.1 Successive TOF patterns taken at stabilized temperatures in decreasing order (in K): 290, 200, 100, 21. The patterns are vertically shifted to improve visibility.

- [1] B. Dunn, H. Kamath, J.-M. Tarascon (2011). Electrical energy storage for the grid: a battery of choices, *Science*.
- [2] A.R. Mainara, E.Iruina, L.C. Colmenares, A.Kvashaa, I. de Meazza, M. Bengoecheaa, O.Leoneta, I.Boyanoa, Zhengcheng Zhangc, J. Alberto Blazqueza (2018). An overview of progress in electrolytes for secondary zinc-air batteries and other storage systems based on zinc, *Journal of Energy Storage*. 15, 304-328.
- [3] D. Wittmaier, S. Aisenbrey, N.Wagner, K. Andreas Friedrich (2014). Bifunctional, Carbon-Free Nickel/Cobalt-Oxide Cathodes for Lithium-Air Batteries with an Aqueous Alkaline Electrolyte, *Electrochimica Acta*. 149, 355-363.
- [4] H. M.A. Amin, H. Baltruschat, D. Wittmaier, K. Friedrich, A Highly (2015). Efficient Bifunctional Catalyst for Alkaline Air-Electrodes Based on a Ag and Co₃O₄ Hybrid: RRDE and Online DEMS Insights, *Electrochimica Acta*. 151, 332-339.
- [5] Zhong-Li Wang, Dan Xu, Ji-Jing Xu and Xin-Bo Zhang (2014). Oxygen electrocatalysts in metal-air batteries: from aqueous to nonaqueous electrolytes, *Chem. Soc. Rev.* 43, 7746-7786.

STRUCTURAL ANALYSIS OF $\text{La}_{0.78}\text{Ba}_{0.22}\text{MnO}_3$ BY X-RAY DIFFRACTION

R.F. Hashimov

Institute of Physics ANAS, Baku, Azerbaijan

E-mail: fizik-3@mail.ru

Manganites AMnO_3 and $\text{AA}'\text{MnO}_3$ are the most widely used compounds among compounds with antiferromagnetic properties. New structural phases and physical properties are observed in compounds synthesized depending on A and A' atoms with a variety of ion radii [1,2]. One of the compounds recently investigated in this direction is the $\text{Ba}_{0.5}\text{La}_{0.5}\text{MnO}_3$ crystals. Structural studies conducted by X-ray diffraction method have shown that, the crystal structure of this compound is the ideal perovskite structure. Under normal circumstances, space group is Pm-3m by cubic symmetry. The value of the lattice parameters equal to $a = b = c = 3.9073 \text{ \AA}$ that, this is also very close to the ideal state ($a = b = c \approx 4 \text{ \AA}$). More complicated character was observed in DTA spectrum obtained at high temperatures. The DTA and TG results obtained confirmed each other. It was known that, $30 \leq T \leq 130 \text{ }^\circ\text{C}$, $130 \leq T \leq 315 \text{ }^\circ\text{C}$, $315 \leq T \leq 370 \text{ }^\circ\text{C}$, $370 \leq T \leq 527 \text{ }^\circ\text{C}$, $527 \leq T \leq 667 \text{ }^\circ\text{C}$ and $677 \leq T \leq 890 \text{ }^\circ\text{C}$ parts at a temperature range of $30 \leq T \leq 890 \text{ }^\circ\text{C}$ were observed that, these have also been explained by transitions corresponding to oxidation processes, evaporation of water molecules, and structural transformations [3]. The crystal structure of $\text{La}_{1-x}\text{Ba}_x\text{MnO}_3$ solid solutions should differ at different values of x concentration due to the difference occurred in ionic radii of the La and Ba atoms. Therefore, it is significant to synthesize new crystals included in the $\text{La}_{1-x}\text{Ba}_x\text{MnO}_3$ system and to study various physical properties. The polycrystals of the $\text{La}_{0.78}\text{Ba}_{0.22}\text{MnO}_3$ compound were synthesized and the structure phase analysis was performed by X-ray diffraction method in the presented research.

Structural phase analysis of $\text{La}_{0.78}\text{Ba}_{0.22}\text{MnO}_3$ powder research samples were investigated at room temperature and in D8 Advance (Bruker) diffractometer by X-ray diffraction method. The obtained X-ray diffraction spectrum were analyzed by the Rietveld method in Fullprof program.

Analysis of the X-ray diffraction spectrum by the Rietveld method revealed that, maximums obtained in the spectrum do not correspond to one phase. Therefore, second structure phase was added. This corresponds to a maximum of two different phases. One of the phases corresponds to cubic symmetry with Pm-3m space group and $a = 3.90478 \text{ \AA}$ lattice parameters, other one corresponds to the rhombohedral symmetry with R-3c space group with $a = 5.54711 \text{ \AA}$ and $c = 13.47908 \text{ \AA}$ lattice parameters.

[1] N.T.Dang, V.S.Zakhvalinskii, D.P.Kozlenko, T.-L.Phan, S.E.Kichanov, S.V.Trukhanov, A.V.Trukhanov, Yu.S.Nekrasova, S.V.Taran, S.V.Ovsiyannikov, S.H.Jabarov, E.L.Trukhanova (2018). Effect of Fe doping on structure, magnetic and electrical properties $\text{La}_{0.7}\text{Ca}_{0.3}\text{Mn}_{0.5}\text{Fe}_{0.5}\text{O}_3$ manganite, *Ceramics International*, 44, 13, 14974-14979.

[2] S.G. Jabarov, N.T. Dang, V.S. Zakhvalinskii, D.P. Kozlenko, Yu.S. Nekrasova, The-Long Phan, Ta Thu Thang, S.E. Kichanov, T. D. Thanh, B.N. Savenko, L.H. Khiem, S.V. Taran (2016). Crystal structure, magnetic properties and conductivity mechanisms of $\text{La}_{0.7}\text{Ca}_{0.3}\text{Mn}_{0.5}\text{Fe}_{0.5}\text{O}_3$, *Ferroelectrics*, 501, 1, 129-144.

[3] R.F.Hashimov, F.A.Mikailzade, S.V.Trukhanov, N.M.Lyadov, I.R.Vakhitov, A.V.Trukhanov, M.N.Mirzayev (2019). Structure and thermal analysis of $\text{Ba}_{0.5}\text{La}_{0.5}\text{MnO}_3$ polycrystalline powder, *International Journal of Modern Physics B*, 33, P.1950244.

INHERENT IMPURITIES IN GRAPHENE-LIKE MATERIALS

G. Hristea¹, O. Culicov^{1,2}, V. Marinescu¹, M. Lungulescu¹, C. Obreja¹, I. Zinicovscaia^{2,3}

¹National Institute for R&D in Electrical Engineering, INCDIE ICPE CA, Splaiul Unirii 313, Bucharest 030138, Romania

²Joint Institute for Nuclear Research, Dubna, Joliot Curie 6, Moscow Region, Russian Federation

³Horia Hulubei National Institute for R&D in Physics and Nuclear Engineering, 30 Reactorului Str., MG-6, Bucharest-Magurele, Romani

E-mail: gabriela.hristea@icpe-ca.ro

The capabilities of graphene are well recognized (from flexible displays or ultra-lightweight devices to memory chips and high-capacity batteries). But even so, several issues must be addressed. The greatest difficulty is in producing large quantities of graphene in various formats and at a reasonable cost, while maintaining effective yields and purity levels that do not hinder graphene's requested chemistry. Since metallic impurities can directly affect many features of graphene materials, their implications are far-reaching, potentially affecting many suggested graphene applications. Because impurity-free materials are practically difficult to handle, understanding how defects and impurities influence the physical-chemical properties of these systems is crucial [1]. Some evidence suggests that different synthesis routes for graphene-like materials involving different oxidation and reduction processes may imply different types and amounts of metallic components [2]. Alternative synthesis routes for graphene-like materials that include different oxidation and reduction processes may indicate various kinds of metallic components, according to some data.

These elements may originate from impurities in the synthesis of raw materials/precursors. Metallic impurities, in particular, can significantly alter the chemical properties of graphene materials. Extensive measurements of the metallic impurities inherent in chemically reduced graphene oxides are important to ensure that the level of contamination does not affect the intended purpose of the graphene-like material.

In this work, few synthetic routes for graphene-like materials synthesis are developed, by applying different oxidation and reduction strategies and tracking the concentrations of metallic impurities at each stage of synthesis. Morphological and structural characterizations of synthesized graphene-like materials implying Energy-dispersive X-ray spectroscopy analysis (EDX), scanning electronic microscopy (SEM), and neutron activation analysis (NAA) have been done.

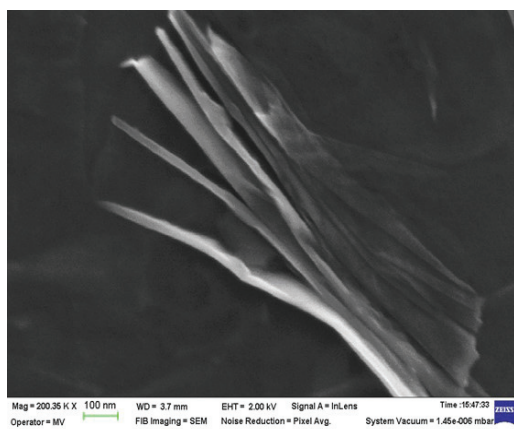


Fig. 1. Scanning electron microscopy of a stack of few graphene sheets

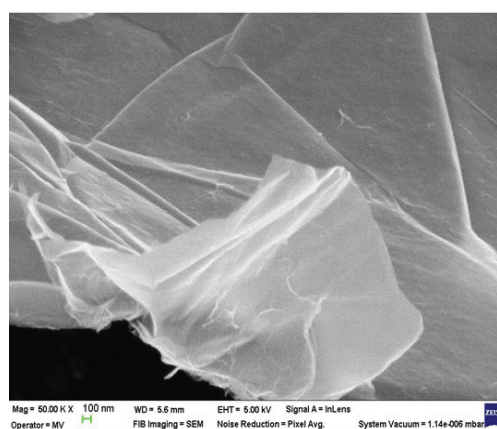


Fig. 2. Scanning electron microscopy of a plain sheet of graphene

Neutron activation analysis (NAA) was used as the primary method to determine the levels of impurities present in processed materials because of its accuracy and robustness. Additionally, because the materials being studied can be irradiated directly, true bulk analysis of the material can be performed as well as the elimination of the possibility of contamination during sample preparation for analysis.

[1] P.T. Araujo, M. Terrones, M. S. Dresselhaus (2012), Defects and impurities in graphene-like materials, *Materials Today*, 15 (3), 98-109.

[2]. HJ Shin, et al. (2009), Efficient reduction of graphite oxide by sodium borohydride and its effect on electrical conductance, *Adv Funct Mater*, 19(12):1987–1992.

EFFECT OF OXYGEN NONSTOICHIOMETRY ON THE MAGNETIC PROPERTIES OF $\text{La}_{0.7}\text{Sr}_{0.3}\text{Mn}_{0.95}\text{Fe}_{0.05}\text{O}_{3-\delta}$ MANGANITES

N.Kalanda¹, M.Yarmolich¹, A.Gurskii², A.Petrov¹, A.Zhaludkevich¹, O.Ignatenko¹ and M.Serdechnova³

¹ *Scientific-Practical Materials Research Centre of NAS of Belarus, Minsk, Belarus*

² *Belarusian State University of Informatics and Radioelectronics, Minsk, Belarus*

³ *Helmholtz-Zentrum Hereon, Geesthacht, Germany*

E-mail: kalanda@physics.by

Particular interest in doped $\text{La}_x\text{R}_{1-x}\text{MnO}_{3-\delta}$ manganites (where R is a rare earth element) is due to the presence of competing electron-electron and electron-phonon interactions which contribute to the formation of spatially separated ferromagnetic and antiferromagnetic regions [1, 2]. The most promising is the partially substituted lanthanum-strontium manganite of the composition $\text{La}_{0.7}\text{Sr}_{0.3}\text{Mn}_{0.95}\text{Fe}_{0.05}\text{O}_{3-\delta}$, which is characterized by the maximum values of the magnetoresistive effect near the “ferro-paramagnetic” phase transition. In order to purposefully optimize the production of a $\text{La}_{0.7}\text{Sr}_{0.3}\text{Mn}_{0.95}\text{Fe}_{0.05}\text{O}_{3-\delta}$ magnet with specified magnetic properties, it is important to establish the relationship between the macroscopic and microscopic parameters of the material, at which the saturation magnetization and the general course of the temperature dependence are determined by microscopic parameters.

With oxygen desorption, an increase in the molar volume of manganite is observed, as a result, in $\text{La}_{0.7}\text{Sr}_{0.3}\text{Mn}_{0.95}\text{Fe}_{0.05}\text{O}_{3-\delta}$, a stress state is formed in the grains during annealing, which leads to a decrease in the mobility of oxygen vacancies in the process of reduction of cations according to the $\text{Mn}^{4+} + e^- \rightarrow \text{Mn}^{3+}$. In this case, the oxygen desorption rate is determined by its diffusion in the strained regions of the grains. It has been established that in the low-temperature region of the temperature dependence of magnetization measured in the “zero-field-cooling” mode at $T < T_B$ (where T_B is the blocking temperature), the particles are in a frozen ferromagnetic state. The presence of ferromagnetism at $T > T_B$ leads to a magnetically ordered state, in which the resulting magnetic moment of a magnetic particle is subject to the influence of thermal fluctuations. It has been established that with an increase in oxygen deficiency, the values of T_B decrease, which indicates an increase in the influence of magnetocrystalline anisotropy. The observed temperature dependence of the magnetization, measured in the “field-cooling” mode, was approximated taking into account the quadratic and non-quadratic dispersion law of the magnon spectrum. The calculated values of the Bloch coefficients and the exchange interaction constant indicate their dependence on the composition of the magnet. It has been established that the exchange interaction constant in the compound $\text{La}_{0.7}\text{Sr}_{0.3}\text{Mn}_{0.95}\text{Fe}_{0.05}\text{O}_{3-\delta}$ decreases with increasing oxygen nonstoichiometry.

This work was supported by the European project H2020-MSCA-RISE-2018-823942 – FUNCOAT and the project of the Belarusian Republican Foundation for Fundamental Research No.F21ISR-004.

[1] D. Serrate, et al. (2007). Double perovskites with ferromagnetism above room temperature. *Journal of Physics: Condensed Matter* 18, 1 – 86.

[2] D. Topwal, et al. (2006). Structural and magnetic properties of $\text{Sr}_2\text{Fe}_{1+x}\text{Mo}_{1-x}\text{O}_6$ ($-1 \leq x \leq 0.25$). *Physical Review B*. 73, 094419 – 1 – 6.

PERMEABILITY OF A COAL SEAM WITH RESPECT TO FRACTAL FEATURES OF PORE SPACE OF FOSSIL COALS

A.K. Kirillov¹, T.A. Vasilenko², A. Kh. Islamov¹, A.S. Doroshkevich¹

¹Frank Laboratory of Neutron Physics - Joint Institute for Nuclear Research (FLNP/JINR), Dubna, Russian Federation

²Saint Petersburg Mining University, Saint Petersburg, Russian Federation

E-mail: kirillov1953@inbox.ru

The present study is aimed at demonstration of possible calculation of permeability of coal beds with respect to their depth that is based on the measurement of coal porosity taking into account their hierarchical structure. The characteristics of pore space obtained by small-angle neutron scattering (SANS) with the use of fractal theory allow explanation of the regularities of coal permeability evolution within the frameworks of a model differing from the traditional concepts of the theory of deformation of an elastic and plastic solid. Now we shall analyze the data available for coals of Donets basin [1]. Coals of Lean baking rank have been selected (volatile content is $V^{\text{daf}} = 15\text{-}20\%$). All the samples are related to the same geological conditions of mine named after A.I. Gayevoy, Ukraine, but of different beds. The total porosity was found by uniaxial deformation of cylindrical samples in a high-pressure chamber [2]. Surface fractal dimension, specific pore surface with respect to fractality were calculated on the basis of neutron scattering curves registered by a spectrometer of small-angle scattering of YuMO pulse reactor IBR-2, Frank laboratory of nuclear physics, JINR, Dubna, Russia. For this uniform series of coal samples, the dependences of surface fractal dimension on the occurrence depth, and specific surface S/V have been calculated (Table 1).

Table 1. Basic data about coals

Number of the sample	Occurrence depth, m	Fractal dimension (SANS)	A, m ² /g	S/V, 10 ⁶ m ² /m ³	Total porosity	Open porosity
1	680	2.98	3.38	4.48	0.220	0.034
2	820	2.92	2.51	3.57	0.240	0.061
3	975	2.93	3.62	5.02	0.194	0.027
4	975	2.84	0.95	1.44	0.187	0.143
5	1080	2.75	0.192	0.60	0.189	-
6	1090	2.66	0.033	0.26	0.188	-

Note: A, S/V are specific surfaces of pores related as $A = (S/V)/\rho_c$, where ρ_c is coal mass density (kg/m³).

The last column contains the data about the open porosity obtained by the standard analysis of adsorption curves of nitrogen at 77 K. Note that contrary to open porosity, other parameters are of conventional occurrence depth dependence. Here we use the data about the samples of mine named after A.I. Gayevoy in order to provide calculation of permeability at the same conditions of rock massif. The modified Kozeny-Carman equation [3] is applied to calculate the permeability.

Results. The result is that the total porosity is slightly decreased at the depth increase, but the specific pore surface is reduced substantially (Table 1). It means that micropores are “healed” at a depth. Thus, the average pore size increases when the fractal dimension is reduced with the depth rising. So, a consequence is a sharp increase in permeability that cannot be explained by conventional formula for reduced relative permeability k/k_0 that employs the change in stress (rock pressure) and the pressure of adsorbed gas [4]. At real values of elastic and plastic characteristics of rock massif at the depth of 500 - 1000 m, permeability is not modified significantly as follows from estimates of real parameters of the tested samples taken under almost the same geological conditions of mine named after A.I. Gayevoy .

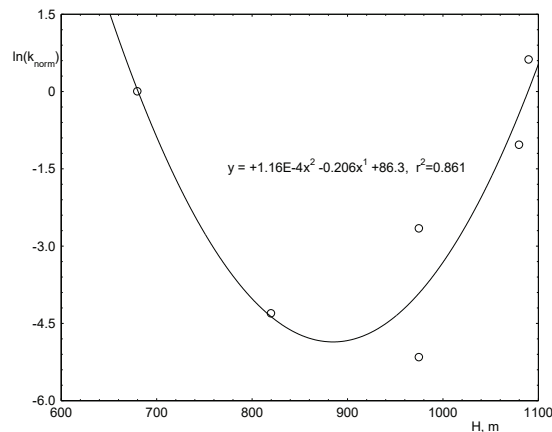


Fig. 1. Depth dependence of reduced relative permeability (to $H = 680$ m), coal mine named after A.I. Gayevoy.

Non-linear behavior of permeability (Fig. 1) can be explained by changes in the specific surface of pore space calculated with account of fractality on the basis of SANS curves. Actually, value of $(S/V)^{-2}$ in eq. for permeability [3] is changed substantially at depths close to $H = 1000$ m. So, the depth dependence of permeability is parabolic due to changes in pore parameters.

Reduction of permeability down to a certain level is a result of deformation of pores and cracks under rock pressure. At the next stage, under a higher loading, larger agglomerates of the matrix of coal substance are formed and the related increase in the permeability of the beds formed at large depth. This conclusion is also confirmed by depth dependence of the specific surface of pores found by SANS. Reduction of $S/V \sim r^{-1}$ is associated with an increase in size of pores formed by consolidation due to plastic deformation of large aggregates that are characterized by a lower surface fractal dimension. Similar regularities have been observed when calculating fractal dimension of the coal samples exposed to uniaxial loading in a chamber of high pressure up to 2 GPa [5].

Conclusions. Permeability of coal beds determines the processes of gas transfer with in their porous structure. When methane is extracted in the vicinity of the holes or coal excavation proceeds at large depth, fractured porous structure of a coal bed and surrounding rocks be substantially changed. The present study demonstrates that the hierarchical size distribution of fractured porous structure of coals provides explanation of a change in permeability when the occurrence depth of a coal bed is increased. A substantial advantage of this study is the use of SANS that accounts for both open and closed porosity of coal when analyzing the reservoir properties of coal beds.

An important fact is that the depth dependence is derived without invoking the data about the gas pressure in coal beds. Only laboratory data about the structural characteristics of coal samples have been used.

- [1] T.Vasilenko, A. Kirillov, A. Islamov, A. Doroshkevich (2021). Study of hierarchical structure of fossil coals by small-angle scattering of thermal neutrons. *Fuel*, 292, 120304
- [2] T.A. Vasilenko, A.K. Kirillov, V.V. Slyusarev. (2015) Study of the hierarchical structure of coals by pressing. Measuring of the total porosity. *Fiz. Tekh. Vys. Davlenii.* 25(3-4), 122-132.
- [3] Carman P.C. (1937). Fluid flow through granular beds. *Trans. Inst. Chem. Eng. London* 15, 150-166.
- [4] Zheng G., et.al. (2012). Laboratory study of gas permeability and cleat compressibility for CBM/ECBM in Chinese coals. *Energy Exploration&Exploitation.* 30(3), 451–476.
- [5] Vasilenko T.A., Polyakov P.I., Slyusarev V.V. (2000). Investigation of physical and mechanical properties of coals under hydrostatic reduction and quasi-hydrostatic compression fracture. *Fiz. Tekh. Vys. Davlenii.* 10(3), 72-85.

NEUTRON AND X-RAY REFLECTOMETRY STUDIES OF PLANAR INTERFACES FOR LITHIUM POWER SOURCES

Ye.N. Kosiachkin^{1,2,3}, M.V. Avdeev^{1,4}, I.V. Gapon^{1,5}, D.I. Boronin^{4,1} and L.A. Bulavin²

¹*Frank Laboratory of Neutron Physics, Joint Institute for Nuclear Research, Dubna, Russia*

²*Physics Department, Taras Shevchenko National University of Kyiv, Kyiv, Ukraine*

³*Institute for Scintillation Materials of NAS of Ukraine, Kharkiv, Ukraine*

⁴*Faculty of Physics, Moscow State University, Moscow, Russia*

⁵*Institute for Safety Problems of Nuclear Power Plants, NAS of Ukraine, Chornobyl, Ukraine*

E-mail: kosiachkin@jinr.ru

Nowadays, rapid development of technologies leads to abundance of the most diverse electronic devices. As well, green energy and low-carbon economy development is not less important, while we have drastically high level of Earth pollution. Both of these trends lead to the need of reliable and safe accumulators with high capacities and low pollution risks. Today, the highest specific capacity in industrial batteries is achieved for lithium-ion accumulators of the ‘intercalating type’. The prospects are foreseen for the batteries with metal electrodes, especially lithium anodes. However, the processes on electrochemical interfaces with liquid electrolytes are not fully understood, which slows the progress in this area. In particular, this concerns the controllable formation of a passivating layer – solid electrolyte interphase (SEI), as well as the inhomogeneous lithium deposition on metal electrodes, which both affect performances and safety operation of such kind of batteries.

The given work reports about the applications of neutron (NR) and X-ray (XRR) reflectometry to study planar interfaces related to the lithium power sources. Firstly, XRR is applied for controlling and optimizing substrates for neutron experiments. It is well suited for determining the initial comparatively simple structures with thin (thickness ~50 nm) metal electrodes deposited (magnetron sputtering) on crystalline silicon. More complicated heterostructures including multilayers with regulated mean scattering length density in quasihomogeneous approximation are also tested in the frame of the general task of optimizing NR experiment [1,2]. This problem appears, since the changes of the working electrochemical interfaces are small, and certain steps are to be done to enhance relative reflectivity changes during interface evolution. The application of NR makes it possible to in situ investigate the influence on the interface evolution of the environmental parameters, anode initial characteristics, electrolyte composition, current density, overvoltage and so on. For this purpose, electrochemical cells for simultaneous monitoring of voltage/current at the interface under study is designed [3]. The results of the adaptation of the NR experiment to study the structure of electrochemical interfaces are summarized.

[1] M.V. Avdeev, A.A. Rulev, E.E. Ushakova, Ye.N. Kosiachkin, et al. (2019). On nanoscale structure of planar electrochemical interfaces metal/liquid lithium ion electrolyte by neutron reflectometry. *Applied Surface Science*. 486, 287–291.

[2] V.I. Petrenko, Ye.N. Kosiachkin, L.A. Bulavin, M.V. Avdeev (2020). Optimization of the initial interface configuration for in-situ neutron reflectometry experiments. *J. Surf. Investigation*. 14, 215–219.

[3] Ye.N. Kosiachkin, I.V. Gapon, A.A. Rulev, E.E. Ushakova, et al. (2021). Structural studies of electrochemical interfaces with liquid electrolytes using neutron reflectometry: experimental aspects. *J. Surf. Investigation*. 15, 787–792.

HIGH PRESSURE-ENHANCED MAGNETIC ORDERING AND MAGNETOSTRUCTURAL COUPLING IN GEOMETRICALLY FRUSTRATED SPINEL Mn_3O_4

D.P. Kozlenko¹, N.T. Dang^{2,3}, S.E. Kichanov¹, L.T.P. Thao^{4,5}, A.V. Rutkavkas¹, E.V. Lukin¹, B.N. Savenko¹, N. Tran^{2,3}, D.T. Khan⁵, L.H. Khiem^{6,7}, B.W. Lee⁸, T.L. Phan⁸, N.L. Phan⁹, N. Truong-Tho⁴, N.N. Hieu^{2,3}, T.A. Tran¹⁰, M.H. Phan¹¹

¹ Frank Laboratory of Neutron Physics, Joint Institute for Nuclear Research, 141980 Dubna, Russia

² Institute of Research and Development, Duy Tan University, 550000 Danang, Viet Nam

³ Faculty of Environmental and Natural Sciences, Duy Tan University, 550000 Danang, Viet Nam

⁴ Faculty of Electronics, Electrical Engineering and Material Technology, University of Sciences, Hue University, 530000 Hue, Vietnam

⁵ University of Science and Education, The University of Danang, 550000 Danang, Vietnam

⁶ Institute of Physics, Vietnam Academy of Science and Technology, 100000 Hanoi, Vietnam

⁷ Graduate University of Science and Technology, Vietnam Academy of Science and Technology, 100000 Hanoi, Vietnam

⁸ Department of Physics and Oxide Research Center, Hankuk University of Foreign Studies, Yongin 449-791, South Korea

⁹ Department of Physics, Ho Chi Minh City University of Education, 700000 Ho Chi Minh, Vietnam

¹⁰ Ho Chi Minh City University of Technology and Education, 700000 Ho Chi Minh, Vietnam

¹¹ Department of Physics, University of South Florida, Tampa, FL 33620, USA

E-mail: ltpthao@ued.udn.vn

High-pressure effects on the crystal and magnetic structures of Mn_3O_4 have been studied by X-ray and neutron powder diffraction techniques at high pressures up to 37 and 20 GPa and supplemented by the DFT calculations. Upon compression, the crystal structure transforms from the initial tetragonal hausmannite phase of $I4_1/amd$ symmetry into the orthorhombic $CaMn_2O_4$ -type ($Pbcm$ symmetry) phase via the intermediate orthorhombic $CaTi_2O_4$ -type ($Bbmm$ symmetry) phase. In the tetragonal phase, the application of pressure, $P > 2$ GPa leads to a suppression of low-temperature incommensurate and commensurate antiferromagnetic (AFM) orders with a propagation vector $k = (0, \sim 0.5, 0)$ and the expansion of the Yafet-Kittel-type ferrimagnetic phase, becoming the only ground state. The magnetic ordering temperature increases rapidly from 43(2) K at $P = 0$ GPa to 100(5) K at $P = 10$ GPa. In the orthorhombic $CaMn_2O_4$ -type phase, the AFM order on the sublattice of Mn^{3+} spins with a propagation vector $k = (1/2, 0, 0)$ is formed below $T_N = 275$ K. Considering the whole studied pressure range, the magnetic ordering temperature demonstrates a colossal rise in more than 6 times. The pressure behavior of the competing magnetic interactions has been established using density-functional-theory calculations and thereby the underlying mechanism of the observed magnetic phenomena has been discussed.

The work was supported by the RFBR and VAST grant No. 20-52-54002 and the Vietnam Ministry of Education and Training grant No. B2022-SPK-07. The work was also supported by National Research Foundation of Korea (NRF) grants funded by the Korea government's Ministry of Science and ICT (MSIT, 2020R1A2B5B01002184). Vietnamese researchers were supported by the RFBR–VAST cooperation program, grant number QTRU01.02/20-21. Le Thi Phuong Thao (L. T. P. Thao) was funded by Vingroup JSC and supported by the Master, PhD Scholarship Programme of Vingroup Innovation Foundation (VINIF), Institute of Big Data, code VINIF.2021.TS.043.

THE PRESSURE EFFECT ON THE CRYSTAL AND MAGNETIC STRUCTURE OF ScMnO₃

O.N. Lis^{1,2}, D.P. Kozlenko¹, V.P. Glazkov³ and P.A. Borisova³

¹*Frank Laboratory of Neutron Physics, Joint Institute for Nuclear Research, Dubna, Russia*

²*Kazan Federal University, Kazan, Russia*

³*National Research Center Kurchatov Institute, Moscow, Russia*

E-mail: olis@jinr.ru

It is well known that hexagonal RMnO₃ manganites (R = Ho-Lu, Y, In, and Sc) are the part of a class of promising multiferroic materials for spintronic application, where an antiferromagnetic transition of Mn³⁺ occurs between 70 K and 130 K, and a ferroelectric transition occurs between 570 K and 990 K due to a structural distortion. The strong coupling between the antiferromagnetic ordering and ferroelectric ordering allows the possibility of controlling magnetism with an electric field (and vice versa).

Hexagonal ScMnO₃ consists of stacked Mn-O and Sc layers, the Mn ions forming a nearly ideal two-dimensional triangular lattice [1], crystalizing in the P6₃cm space group. The Mn-Mn interactions between adjacent Mn planes are due to superexchange paths, via the apical oxygen ions of MnO₅ bipyramids, exhibiting AFM orderings below around 100 K. Interestingly, spin-reorientation phase transitions were reported at T_R < T_N for ScMnO₃ [2]. Furthermore, the observed rich variety of the magnetic properties of hexagonal manganites reflects a delicate balance between magnetic interactions, which can be easily modified by the changing in interatomic distances and angles by the application of high external pressure, that can lead to the discovery of new effects.

Neutron powder diffraction investigations of ScMnO₃ at pressures up to 2 GPa and low temperatures 10-300 K were performed at the DISC diffractometer at the neutron research reactor IR-8 (NRC “Kurchatov Institute”), using sapphire anvil high pressure cells. In the whole temperature and pressure ranges studied, the hexagonal crystal structure of P6₃cm symmetry remains unchanged. There is also a noticeable change in the relative intensity of the peaks associated with the reorientation of the magnetic moments Mn with respect to the hexagonal crystallographic axes (a,b). At temperatures below 130 K at ambient pressure, the appearance of magnetic peaks (100) and (101) was observed, indicating the formation of an antiferromagnetic state within a triangular lattice. The calculated magnetic moment is 3.33 μ_B at 10 K and decreases to 1.8 μ_B at 2 GPa. The baric evolution of the crystal structure parameters of ScMnO₃ as well as their temperature dependences were obtained.

[1] T. Katsufuji, M. Masaki, A. Machida, et al. (2002). Crystal structure and magnetic properties of hexagonal RMnO₃(R=Y, Lu, and Sc) and the effect of doping. *Phys. Rev. B.* 66. 134434

[2] A. Muñoz, J. A. Alonso, M. J. Martínez-Lope, et al. (2000). Magnetic structure of hexagonal RMnO₃(R=Y,Sc):Thermal evolution from neutron powder diffraction data. *Phys. Rev. B.* 62. 9498

PRELIMINARY STUDIES ON MAGNETIC AND NON-MAGNETIC CORE SILICA GELS BY SAXS, SANS, ESR, AND VSM METHODS

T. Nagorna^{1,2}, D. Chudoba^{1,3}, Z. Surowiec^{1,2}, I. Malinowska², M. Studziński², A. Woźniak-Braszak³, M. Baranowski³, A. Tomchuk^{1,4} and V. Ryukhtin⁵

¹*Joint Institute for Nuclear Research, Dubna, Russia*

²*Maria Curie-Skłodowska University, Lublin, Poland*

³*Adam Mickiewicz University, Poznan, Poland*

⁴*NASU Institute of Environment Geochemistry, Kyiv, Ukraine*

⁵*Nuclear Physics Institute of the CAS, Řež, Czech Republic*

E-mail: nagorna@jinr.ru

The work is dedicated to application of magnetic nanomaterials as biological active substances sorbents. It is a very important topic in medicinal and environmental protection of point of view [1-2]. Nanoparticle used for this purpose should consist from bioavailable components. Newly synthesized nanomaterials composed with: iron oxides magnetic core, silica or carbon nanotubes and bioavailable modifiers are investigated in accordance to sorption of biological active compounds.

Here were presented preliminary results on nanoparticles with the magnetic and non-magnetic core in silica shells modified with functional groups by small-angle X-ray and small-angle neutron scattering as well as electron spin resonance (ESR) and vibrating sample magnetometer (VSM) methods. The materials are potentially intended as drug carriers because of their unique magnetic and biological properties. The SAXS experiments were made at Frank Laboratory of Neutron Physics and the SANS experiments were conducted at the nuclear reactor LVR-15 operated by Research Centre Řež. The measurements were performed by Adani SPINSCAN X benchtop ESR spectrometer intended for spectra registration with continuous wave using the second modulation. Studies of magnetic-core particles with different functional groups using ESR methods are challenging due to the different responses under the influence of the silicone shell and its modification of the sample [3]. Research procedures applied to analyze magnetic-core particles take into account the impact of various functional groups on analyzed samples to achieve comparable results. We also presented results studies by vibrating the sample magnetometer at 100Hz at room temperature for each sample. In the research size distribution among magnetic nanoparticles and characterization of physical-chemical properties were provided.

[1] D.-P. Bai (2018). Teranostics Aspects of Various Nanoparticles in Veterinary Medicine. *International Journal of Molecular Sciences*. 19, 3299.

[2] M. Lewandowski (2017). Nitroxides as Antioxidants and Anticancer Drugs. *International Journal of Molecular Sciences*. 18, 2490.

[3] R. Krzyminiwski (2019). ESR as a monitoring method of the interactions between TEMPO-functionalized magnetic nanoparticles and yeast cells. *Scientific reports - Nature*. 9:18733

SPECTROSCOPIC AND NEUTRON DIFFRACTION INVESTIGATIONS ON GLASSES AND GLASS-CERAMICS IN THE $\text{Na}_2\text{O}/\text{BaO}/\text{TiO}_2/\text{B}_2\text{O}_3/\text{SiO}_2/\text{Al}_2\text{O}_3$ SYSTEM

M. Pernikov^{1*}, R. Harizanova¹, I. Gugov¹, I. Mihailova¹, N. D. Todorov², K. Krezhov^{3,4}, E. Popov³, G. Avdeev⁵, C. Rüssel⁶

¹ *Physics Department, University of Chemical technology and Metallurgy, 8 Kl. Ohridski Blvd, 1756 Sofia, Bulgaria*

² *Faculty of Physics, Sofia University "St Kliment Ohridski", 5 J. Bourchier Blvd., 1164, Sofia, Bulgaria*

³ *Joint Institute for Nuclear Research, Frank Laboratory of Neutron Physics, Joliot-Curie 6, Dubna, Russia*

⁴ *Institute for Nuclear Researches and Nuclear Energy, Bulgarian Academy of Sciences, 72 Tzarigradsko Shaussee, 1784 Sofia, Bulgaria*

⁵ *Institute of Physical Chemistry, Bulgarian Academy of Sciences, Acad. G.Bonchev Str. Bl. 11, 1113 Sofia, Bulgaria*

⁶ *Otto Schott Institute for Materials Research, Jena University, Fraunhoferstr. 6, 07743 Jena, Germany*

E-mail: martin.pernikov@abv.bg

Glasses were synthesized in the system $\text{Na}_2\text{O}/\text{BaO}/\text{TiO}_2/\text{B}_2\text{O}_3/\text{SiO}_2/\text{Al}_2\text{O}_3$ using a traditional melt-quenching technique and thereon based glass-ceramics were prepared by applying different time-temperature crystallization programs to the glasses.

The structures of the obtained glasses and selected glass-ceramics were investigated using Fourier-transformed infra-red and Raman spectroscopy and the presence of SiO_3 , SiO_4 , Si_2O_7 , BO_3 and BO_4 structural units was proposed. Additionally, the occurrence of multiple pre-nucleation clusters inhomogenously distributed in the glass matrix with compositions close to that of the barium titanate phase, BaTiO_3 could be suggested from the IR-data processing.

The phase composition of the prepared glass-ceramics was initially determined by conventional X-ray diffraction and further investigated by Raman spectroscopy. Thus, as main crystallizing phases BaTiO_3 and barium fresnoite, $\text{Ba}_2\text{TiSi}_2\text{O}_8$ were identified.

Additional information regarding the crystallization behaviour and phase formation for the glasses was gathered by using in situ crystallization combined with neutron diffraction analysis. The neutron diffraction data reveals crystallization of BaTiO_3 in all compositions. The authors express their gratitude to the Bulgarian National Science Fund, contract KII-06-H28/1 for the financial support.

CRYSTAL AND MAGNETIC STRUCTURES OF $\text{Sr}_2\text{FeMoO}_{6-\delta}$ AT HIGH PRESSURE

S.Demyanov,¹ A.Petrov¹, M.Yarmolich¹, I.Bobrikov², V.Sikolenko² and N.Kalanda¹

¹*Scientific-Practical Materials Research Centre of NAS of Belarus, Minsk, Belarus*

²*Joint Institute for Nuclear Research, Dubna, Russia*

E-mail: petrov@physics.by

The method of solid-phase reactions using ultrasonic dispersion was used to optimize the conditions for obtaining powders of the $\text{Sr}_2\text{FeMoO}_{6-\delta}$ compound with a high degree of superstructural ordering of iron and molybdenum cations, as well as with an average particle diameter of 200 nm. To investigate the crystal and magnetic structure of the compound under study, neutron diffraction studies were carried out in the temperature range 5–300 K using a high-resolution Fourier diffractometer (FDHR) installed at the IBR-2 pulsed reactor (JINR Dubna, Russia). High-resolution neutron diffraction patterns were obtained using detectors located at average neutron scattering angles of $\pm 152^\circ$ in the d-space range of 0.6–4.5 Å. The neutron diffraction patterns were analyzed using the FullProf software package [1].

According to the data of X-ray phase analysis, single-phase powders of strontium ferromolybdate were obtained with the value of superstructural ordering of Fe/Mo cations (86%). It has been established that the magnetic state of the samples correlates with their porosity, heterogeneity in size and shape of the $\text{Sr}_2\text{FeMoO}_{6-\delta}$ grains. The presence of antiferromagnetic chains in the compound reduces the probability of the formation of long-range ferrimagnetic ordering [2]. This leads to the splitting of large ferrimagnetic domains into smaller ones due to the tendency of the system to a minimum of the free energy, which consists of several components, such as magnetostatic, magnetoelastic, exchange interaction and magnetic anisotropy, which contributes to an increase in the coercive force.

The effect of pressure in a wide range of values (0.01 - 6 GPa) on the behavior of the crystalline and magnetic structures of the $\text{Sr}_2\text{FeMoO}_{6-\delta}$ double perovskite was studied by the neutron diffraction. It has been established that the $\text{Sr}_2\text{FeMoO}_{6-\delta}$ ceramic sample has a tetragonal structure with space group $I4/mmm$ and at $T_C \sim 420$ K it passes from the paramagnetic to the magnetically ordered state. It was found that an increase in the pressure does not lead to a change in the type of crystalline and magnetic structures, and with its increase, the average value of the magnetic moment of the iron sublattice increases monotonically. In this case, the average interionic distance between the metal and the ligand in the FeO_6 and MoO_6 octahedra does not change uniformly with increasing external pressure. The $\langle\text{Fe-O}\rangle$ bond lengths decrease, while the $\langle\text{Mo-O}\rangle$ bond lengths increase.

This work was supported by the Belarus-JINR project No. 29-2021.

[1] J.Rodríguez-Carvajal (2001) Recent developments of the program FULLPROF Commission on powder diffraction (IUCr). Newsletter. 26. 12–19.

[2] N.A.Kalanda, et al. (2019). Small-angle neutron scattering and magnetically heterogeneous state in $\text{Sr}_2\text{FeMoO}_{6-\delta}$. Physica Status Solidi (b). 256, 1800428-1-7.

INVESTIGATION OF PHASE TRANSITIONS IN SINTERED W-6wt.%B₄C - 2wt.%TiC -1wt.%C ALLOY IRRADIATED BY He IONS

A.I. Beskrovnyi¹, D. Neov^{1,2}, G. Nadjakov², L. Slavov^{1,3}, M.N. Mirzayev^{1,4},
E.P. Popov^{1,2,5}, E. Demir⁶, A.A. Donkov^{1,5}, Z. Slavkova⁵, V. Turcenko¹

¹Joint Institute for Nuclear Research, Dubna, Moscow distr., 141980, Russian Federation,

²Institute for Nuclear Research and Nuclear Energy, Bulgarian Academy of Sciences, Sofia, 1784, Bulgaria,

³Institute of Electronics, Bulgarian Academy of Sciences, Sofia, 1784, Bulgaria,

⁴Institute of Radiation Problems, Azerbaijan National Academy of Sciences, Baku, AZ1143, Azerbaijan,

⁵Institute of Solid State Physics, Bulgarian Academy of Sciences, 1784, Sofia, Bulgaria,

⁶Yeditepe University, Physics Department, Istanbul, 34755, Turkey

E-mail: epetropov@gmail.com

To achieve homogeneous sintering, the samples are subjected to a temperature gradient for 2 hours to 2550 °C, at a temperature step of 5 °C per minute. The weight ratio of the aforementioned materials determines also the ratio of the possible outcome, i.e. W2B, WB, W2B5, WB4 and WC phases. There is also a possibility for existence on non-stoichiometric W_xC compounds.

The Rietveld refinement analysis was carried out alongside the X-ray diffraction analysis. A comparison was made with neutron diffraction analysis. A basic W2B phase and a minimal amount of WB (~0.7%) phase were found on the surface. The following structural phases are observed inside: W, α-WB, β-WB, WB2. The W2B phase in the initial material inside is minimally available. After irradiation on the surface we see an increase in the WB phase by about 1%, at the expense of the W2B phase. Irradiation caused the disappearance of the W2B structural phase from the interior.

EP, AAD and LS acknowledge the support by the Grant of Plenipotentiary Representative of Republic of Bulgaria at JINR.

CRYSTAL AND MAGNETIC STRUCTURE OF HALF-HEUSLER COMPOUNDS $\text{MnNi}_{0.9}\text{M}_{0.1}\text{Sb}$ ($\text{M} = \text{Ti, V, Cr, Fe, Co}$) AT LOW TEMPERATURES

A.V. Rutkauskas¹, G.S. Rimsky², I.Yu. Zel¹, N.M. Belozeroval¹, D. P. Kozlenko and S.E. Kichanov¹

¹*Joint Institute for Nuclear Research, Dubna, Moscow Region, Russia*

²*SSPA «Scientific-Practical Materials Research Centre of NAS of Belarus», Minsk, Belarus*

E-mail: ranton@nf.jinr.ru

Half-Heusler magnetic intermetallic compounds of transition metals exhibit interesting physical properties such as magnetoresistance, ferromagnetic and antiferromagnetic magnetic states, and superconductivity. It is observed the shape memory effect and superelasticity with opportunity to control there phenomena by means magnetic field. It makes these compounds promising materials to apply for creation permanent magnets, elements of electronic devices and cooling technology.

To understand the formation of magnetic states in doped half-Heusler compounds based on MnNiSb it is necessary to correctly separate the contribution to the magnetic properties from the sublattices of nickel and manganese ions and to identify the relationship between the structural and magnetic properties of these materials.

In our work we present the results of investigation the crystal and magnetic structure of half-Heusler intemetallic compounds MnNiSb and $\text{MnNi}_{0.9}\text{M}_{0.1}\text{Sb}$ ($\text{M} = \text{Ti, V, Cr, Fe, Co}$) by means of neutron diffraction under normal conditions. Partial substitution of another transition element for nickel leads to a decrease in the magnetic moment of the Mn ions. Also MnNiSb , $\text{MnNi}_{0.99}\text{Sb}$, $\text{MnNi}_{0.9}\text{Cr}_{0.1}\text{Sb}$ and $\text{MnNi}_{0.9}\text{Fe}_{0.1}\text{Sb}$ compounds have been studied in the temperature range from 13 to 300 K. It has been found that the initial cubic structure $F\bar{4}3m$ and ferromagnetic phase remain in the investigated temperature range. New reflections corresponds to the antiferromagnetic phase have not been found. The unit cell volume increases in the MnNiSb and $\text{MnNi}_{0.9}\text{Fe}_{0.1}\text{Sb}$ compounds as the temperature decreases from 50 to 13 K. The $\text{MnNi}_{0.99}\text{Sb}$ alloy exhibits an isomorphic structural transition at low temperatures. This may be due to the metal-semimetal transition in these compounds.

This work have been supported by the Russian Foundation for Basic Research, project no. 20-52-04003 Bel_mol_a (Belarusian Foundation for Basic Research, project no. T21RM-029).

THERMOPHYSICAL PROPERTIES OF Y_2O_3 NANOPARTICLES UNDER THE INFLUENCE OF HIGH-INTENSITY FAST NEUTRONS

R.F. Rzayev and A.O. Dashdemirov

Azerbaijan State Pedagogical University, Baku, Azerbaijan

E-mail: rasilrzayev@mail.ru

Theoretical calculations show that the value of thermal conductivity in single crystal yttrium dioxide is 302 W/(m×K). However, experimental studies show that the value of the thermal conductivity of a sample of yttrium dioxide in the range of 25 °C -500 °C decreases from 150 W/(m×K) to 70 W/(m×K). Also, in the same type of experiments, the thermal conductivity of nitrogen (N₂) and high - entropy compounds of Y₂O₃ in the air from 1% Y₂O₃ + AlN to 10% Y₂O₃ + AlN varies in the range of 75-160 W/(m×K) and the maximum value is 160 W/(m×K) for 4% Y₂O₃ + AlN. It has been found that thermal conductivity of the compounds in the nitrogen (N₂) medium varies in the wider range. Studies on the electronic structure of Y₂O₃ compounds the basics of electronic configuration of O and Y atoms, changes in electron density, electron exchange during interaction with different compounds has been carried out, the participation and migration mechanisms of Y and O atoms in the thermal processes have been revealed [1,2]. On the other hand, in the study of the mechanisms of structural transitions under the influence of an aggressive chemical medium and ionizing radiation, it was found that the mechanism of degradation and amorphization in Y₂O₃ samples mainly occur by changing lattice parameters and interatomic distances.

It is known that structural changes and displacement of atomic coordinates affect the mechanical, electrical and thermal properties of the sample. From this point of view, the main purpose of the research was to study the thermophysical properties, values and patterns of change of heat capacity and required Wigner energy for recombination of structural defects after irradiation with fast neutrons having energy of 1 MeV at room temperature in nuclear reactors operating in pulse mode.

In the presented work Differential Scanning Calorimetric (DSC) analyses were performed in an Ar inert medium in the temperature range of 100-750 K for the Y₂O₃ compound with the purity rate of 99.99%, the density in powder form is 0.069 g/cm³, the specific surface area is 100-150 m²/g, the particle size is in the range of 8-10 nm irradiated with fast neutrons with different intensities ($E < 1$ MeV). Using mathematical approximation methods, the equations of dependence of the heat flux function on temperature and heat capacity after irradiation at different intensities for the Y₂O₃ compound over a wide temperature range were determined. It was found that in the temperature range of $150 \leq T \leq 750$ K, the value of the heat flux increases by 16.6%, up to 86 mW for the case of maximum radiation. At all radiation intensities, anomalies recorded with very small changes were observed in the spectra of the heat flux function related to the internal structural transitions.

[1] M.Dapiaggi, F.Magli, Il.Tredici, B.Maroni, G.Borghini, U.A. Tamburini (2010). Complex thermal evolution of size-stabilized tetragonal zirconia, *Journal of Physics and Chemistry of Solids*, 71, 1038-1041.

[2] E.Husson, C.Proust, P.Gillet, J.P.Itié (1999). Phase transitions in yttrium oxide at high pressure studied by Raman spectroscopy, *Materials Research Bulletin*, 34, 2085-2092.

NEUTRON DIFFRACTION STUDIES OF COMPOUNDS BASED ON MnGe UNDER HIGH PRESSURE AT LOW TEMPERATURES IN HIGH MAGNETIC FIELDS

D.O.Skanchenko¹, E.V.Altynbaev^{1,5}, N.Martin³, D.A.Salamatin², R.A.Sadykov^{2,4}, A.V.Tsvyaschenko² and S.V.Grigoriev^{1,5}

¹*Petersburg Nuclear Physics Institute National Research Center “Kurchatov Institute”, Gatchina, St. Petersburg, Russia*

²*Vereshchagin Institute for High Pressure Physics, Russian Academy of Sciences, Moscow, Russia*

³*Université Paris-Saclay, CNRS, CEA, Laboratoire Léon Brillouin, Gif-sur-Yvette, France*

⁴*Institute for Nuclear Research, Russian Academy of Sciences, Moscow, Russia*

⁵*Faculty of Physics, Saint-Petersburg State University, St. Petersburg, Russia*

E-mail: skanchenko_do@pnpi.nrcki.ru

We report on the study of $\text{Mn}_{1-x}\text{Fe}_x\text{Ge}$ compounds with $x = 0.1$ and 0.3 by small-angle neutron scattering (SANS) under the high pressure up to $P = 1$ GPa and a strong magnetic field up to 9 T. In order to fulfill the investigation, we have developed a non-magnetic high-pressure cell that fits the standard position of the sample and allows to apply the pressure up to 1.2 GPa. Slight modification of the cell opens the possibility of further pressure increase up to 2.5 GPa.

$\text{Mn}_{1-x}\text{Fe}_x\text{Ge}$ compounds crystallize into a non-centrosymmetric cubic structure of the B20 type. The appearance of the skyrmion lattice (SkX) in MnGe-based compounds with Fe-replacement of Mn atoms was observed under external magnetic field within the wide field range at temperatures far below T_C . With pressure increase all of the critical fields increases at low temperatures for both compounds, while the ordering temperature decreases. The temperature and field ranges of the existence of the SkX decreases with pressure increase. We believe that these facts are connected to the stabilization of the magnetic structure of MnGe-based compounds under pressure. This process is opposite to the Fe-replacement of Mn atoms despite the fact that the lattice constant continues to decrease.

Since the replacement of Mn atoms by Fe in the $\text{Mn}_{1-x}\text{Fe}_x\text{Ge}$ compound changes at least two parameters important for the stabilization of the magnetic structure, namely, the electron concentration and the cell constant, application of the high pressure allows to separate these two components. Thus, it is possible to estimate the influence of each process on the evolution of the field-temperature phase diagram.

STRUCTURAL ORGANIZATION OF NANODISPERSED ALUMINIC MATERIAL SYNTHESIZED IN A PLASMA REACTOR

O.V. Tomchuk^{1,2,3}, Yu.L. Zabulonov¹, V.M. Burtnyak¹, L.A. Odukalets¹, O.V. Puhach¹, O.M. Arkhipenko¹, O.S. Svechnikova², L.A. Bulavin², A.A. Nabiev³, O.Yu. Ivanshina³ and T.N. Vershinina³

¹*Institute of Environmental Geochemistry, NASU, Kyiv, Ukraine*

²*Taras Shevchenko National University of Kyiv, Kyiv, Ukraine*

³*Joint Institute for Nuclear Research, Dubna, Russia*

E-mail: tomchuk@jinr.ru

Microplasma generation technology is widely used for micro- and nanoparticles' synthesis from any material by a varying current, voltage and frequency [1]. In the course of a volumetric discharge in a liquid, cavitation and hydropercussion processes occur, as well as micro discharges, which lead to the formation of nanodispersed particles as a result of instantaneous evaporation of metals. This technology can also be effectively used for the purification of man-caused (chemically and radioactively) polluted waters [2,3]. Of great interest are studies of the effect of nanoparticles on the efficiency of polluted water treatment, when nanodispersed structures are synthesized directly in an impure liquid. Here, the structural features of plasma-generated aluminum powder on the nanoscale are considered. Small-angle neutron and X-ray scattering (Fig. 1) made it possible to conclude about 40-nm primary particles with a diffuse surface, which are assembled into fairly compact aggregates (fractal dimension 2.8). The relationship between the structural and thermodynamic properties of the studied material is analyzed.

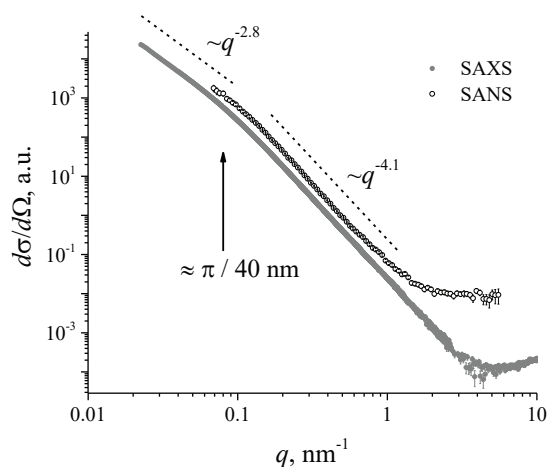


Fig. 1. Small-angle scattering data for nanodispersed aluminic powder. The characteristic power-law scattering regions are shown, as well as the crossover region between them, which is responsible for the nanoparticle size.

- [1] L. Lin, Q. Wang (2015). Microplasma: A new generation of technology for functional nanomaterial synthesis. *Plasma Chemistry and Plasma Processing*. 35, 925-962.
- [2] A. Zaporozhets (2022). *Systems, Decision and Control in Energy III*, Springer Nature.
- [3] Yu. Zabulonov *et al.* (2015). New approaches to cleaning of liquid radioactive waste. *Science and Innovation*. 11, 47-58.

STRUCTURAL FEATURES OF LIQUID CRYSTALLINE SUSPENSIONS OF DIAMOND NANOPARTICLES BY NEUTRON SCATTERING

O.V. Tomchuk^{1,2,3}

¹*Institute of Environmental Geochemistry, NASU, Kyiv, Ukraine*

²*Taras Shevchenko National University of Kyiv, Kyiv, Ukraine*

³*Joint Institute for Nuclear Research, Dubna, Russia*

E-mail: tomchuk@jinr.ru

In recent years, composite systems based on nanoparticles of inorganic materials dispersed in organic matrices have been actively studied, among which anisotropic liquids, liquid crystals are particularly noteworthy. The chemical and mechanical stability of carbon nanoparticles, including nanodiamonds, fullerenes, nanotubes and graphene, makes them suitable objects for filling liquid crystals to improve their characteristics. Various forms of nanocarbon have different geometries, which therefore significantly affects the local ordering of liquid crystal molecules in different ways.

The research was aimed at studying the structural features of liquid crystals filled with diamond nanoparticles both in bulk and at interfaces in model electro-optical cells (nodes of such important devices as solar batteries, touch screens, broadband optical polarizers, etc.). Until now, the structure of such systems has been studied mainly by optical methods, which made it possible to achieve a micron resolution. However, for the most part, the properties of the relevant nanosystems are determined by the structure at the submicron level down to the nanoscale. Moreover, near-surface layers on the electrode/liquid crystal interfaces play an important role in the functionalization of electro-optical cells. The goal was, firstly, to study the effect of the addition of diamond nanoparticles with various concentrations on the structural properties of liquid-crystal matrices, and secondly, to compare these properties of liquid-crystalline nanodiamond suspensions in the volume and at the interfaces using neutron scattering techniques (small-angle neutron scattering and neutron reflectometry). The use of the neutron scattering in structural research is primarily justified by a significant neutron contrast of the carbon particles concerning the dispersion medium, as well as the high penetration power of neutrons.

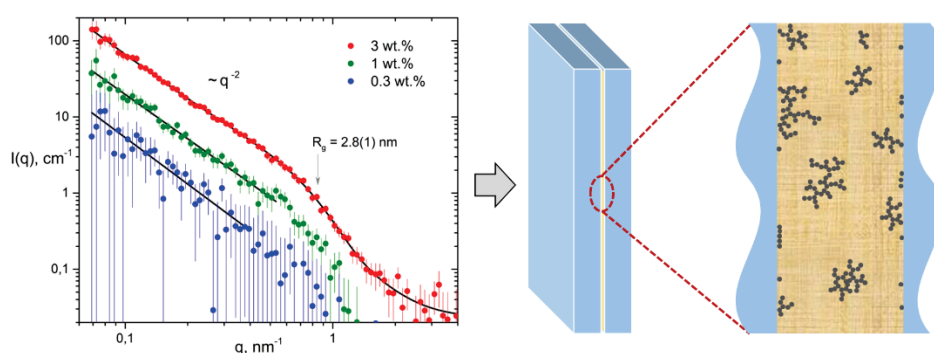


Fig. 1. Small-angle scattering data for liquid crystalline suspensions of diamond nanoparticles

ELECTRICAL PROPERTIES OF A HYDRATED CONTACT OF DIFFERENT-SIZED YSZ –PARTICLES

A.S. Zakharova^{1,2}, A.S. Doroshkevich^{1,3}, E.A. Gridina^{1,2}, A.I. Lyubchyk^{4,6}, B.L. Oksengendler⁷, N.N. Nikiforova⁷, M.A. Balasoui⁸, D. Lazar⁹, Chicea D¹⁰

¹ Joint Institute for Nuclear Research, Dubna, Russian Federation

² Dubna State University, Dubna, Russian Federation

³ Donetsk Institute for Physics and Engineering named after O.O. Galkin, Kiev, Ukraine

⁴REQUIMTE, Faculdade de Ciências e Tecnologia, Caparica, Portugal

⁵Research Centre in Industrial Engineering, Management and Sustainability, Lusófona University, Lisboa, Portugal,

⁶Nanotechcenter LLC, Kyiv, Ukraine

⁷U. A. Arifov Institute of ion-plasma and laser technologies of the Academy of Sciences of the Republic of Uzbekistan

⁸ Horia Hulubei National Institute for R&D in Physics and Nuclear Engineering (IFIN-HH), Bucharest, Romania

⁹ National Institute for Research and Development of Isotopic and Molecular Technologies Cluj-Napoca, Romania

¹⁰ University "LUCIAN BLAGA" of SIBIU (ULBS), Sibiu, Romania

E-mail: zakharova.anna.nano@gmail.com

Nanopowders based on dioxide of zirconium are of interest for practical application due to dimensional effects caused by the specific state of electronic subsystem of nanoscale objects. For example, the effect of electric charge accumulation by a compact of zirconium dioxide nanoparticles [1,2], the effects of adsorption-induced electrical conductivity [3], and many more, indicate interphase electronic exchange. It has been established that adsorption changes the electronic structure and physical properties of the nanoparticle material, in particular, imposes a spectrum of local levels of adsorbates on the energy spectrum of states with non-adsorption origin (surface states of the impurity type), which leads to interesting and extremely important effects.

The dimensional effects that occur at the contact of hydrated nanopowder of $ZrO_2 - Y_2O_3$ (YSZ) - systems are extremely interesting due to their possible application .

In this work, the contact of nanoparticles with the same chemical composition ($ZrO_2 - x$ mol % Y_2O_3 , $x=0; 3; 8$) but different sizes (7.5 and 10 nm) were studied by voltammetry at different relative humidity condition (85%, 75%, and 60% of humidity).

The nonlinear dependence of their electrical properties on direct current was established: (V-I characteristic, Fig.1).

As can be seen from Fig.1, for all humidity concentrations in the samples, there is a clear dependence of the current amplitude on the impurity concentration. The system without alloying component undergoes minimal changes in the electrical field (less than 5-10% of the equivalent value for systems with 3 and 8 mol % Y_2O_3). Impurity concentrations over 3%mol leads to a decrease in the amplitude of the current with an increase in the voltage modulus on the electrodes. It can be seen that the value of the limiting current (direct branch V-I reaches its maximum value at 85% of humidity (Fig.1a) at a concentration of 3 mol % Y_2O_3 and then decreases with increasing impurity concentration. At the hydration degree of the system is 75% the maximum current value is shown by the system with 8 mol% Y_2O_3 (Fig.1b). Thus, the concentration of humidity vapor corresponding to 85% and with 3 mol% of the impurity concentration (Fig.1a) ensures that the system reaches the maximum limit parameters both on the direct and reverse branches of the voltage curve.

As can be seen from Fig.1c, a decrease in the humidity concentration in the system leads to a decrease in the level of electrical characteristics of the contact, describing its rectifying properties. In particular, both the level of limiting characteristics and the nature of dependencies are reduced, for instance, the contact passes from the state of the rectifying contact with the most pronounced asymmetry to the state of the so-called "false connection".

A general pattern has been established for the studied systems, consisting in the dependence of the nature of the electrical properties on the humidity concentration in the samples. In particular, it was found that at a low humidity concentration (saturation in a humid atmosphere at 60% relative humidity (an insular layer of water molecules on the surface of nanoparticles), a "false connection" type of contact takes place. As the relative humidity of the atmosphere in which the system was saturated increases to 85% (free water in the pores), the nature of the contact changes to semiconductor, which indicates the significant role of the nature and dimension of electrical conductivity in the formation of semiconductor properties of the contact.

The study was performed in the scope of the H2020/MSCA/RISE/SSHARE number 871284 project and within the framework of the JINR-Romania cooperation program in 2022 (topic 03-4-1128-2017/2022).

- [1] Doroshkevich A. S., Shilo A.V and others (2019). Patent for invention of the Russian Federation "Solid-state capacitor ionistor with a dielectric layer which is made from a dielectric nanopowder, patent Owner: JINR.
 [2] Shilo A.V and others (2022) Hydrated zirconia nanoparticles as media for electrical charge accumulation // Journal of Nanoparticle Research J Nanopart Res

- [3] E.A. Gridina, and others (2019) The effect of percolation electrical properties in hydrated nanocomposite systems based on polymer sodium alginate with a filler in the form nanoparticles $ZrO_2 - 3mol\% Y_2O_3$. Advanced Physical Research. 1, №2, (pp.70-80).

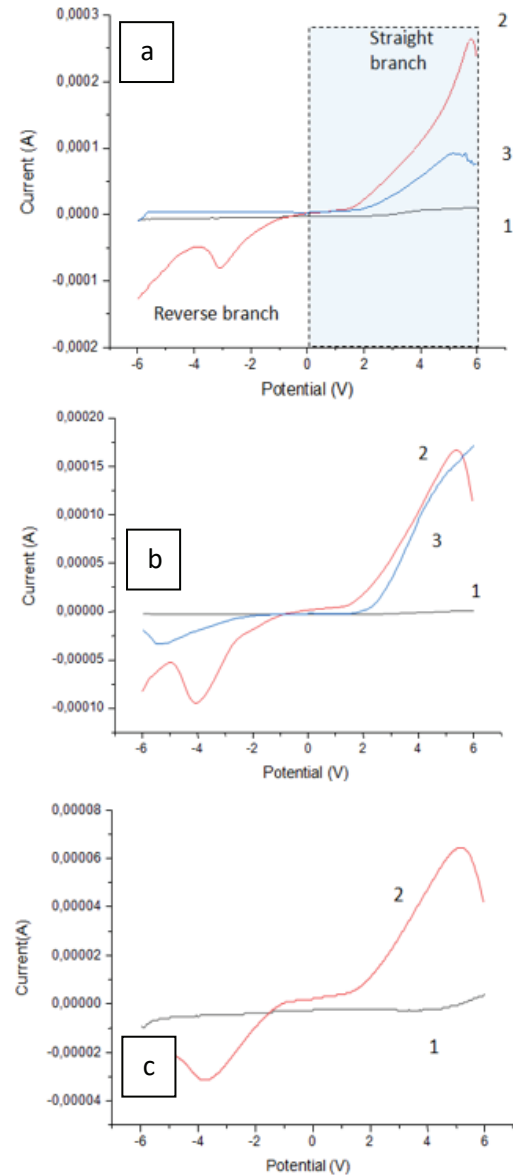


Fig.1. The group of VAC heterojunctions obtained at 85% (a), 75% (b) and 60% (c) humidity at the contacts of samples of the composition $ZrO_2 - 0 mol\% Y_2O_3$, (1), $ZrO_2 - 3 mol\% Y_2O_3$ (2) and ZrO_2

OBTAINING OF NANOSIZED POWDERS OF THE Sr-Ba-Fe-Mo-O SYSTEM BY SOL-GEL TECHNIQUE

M.Yarmolich¹, N.Kalanda¹, A.Petrov¹, S.Demyanov¹ and N.Sobolev²

¹ *Scientific-Practical Materials Research Centre of NAS of Belarus, Minsk, Belarus*

² *Universidade de Aveiro, Aveiro, Portugal*

E-mail: jarmolich@physics.by

Solid solutions of double perovskites of the Sr-Ba-Fe-Mo-O (SBFMO) system are promising materials for application in the field of spintronics. Their distinctive properties are high chemical stability in a reducing atmosphere, high (380–420 K) Curie temperatures, a high (~100%) degree of spin polarization of conduction electrons, and low values of the controlling magnetic fields ($B < 0.5$ T). At the same time, the values of the physical characteristics of these materials that are important for use in microelectronics, obtained by different authors, are quite different, which, apparently, is due to the peculiarities of the sample preparation methods. The main advantage of the sol-gel technique is the high degree of homogenization of the initial components. This method makes it possible to achieve a reduction in energy consumption and a high degree of purity of products at all stages of synthesis with a minimum cost to achieve it. In this regard, in order to obtain powders of the SBFMO system by the sol-gel technique, the composition of the solvent was determined and optimized, the conditions for obtaining a colloidal solution of the sol for the formation of a homogeneous gel, which made it possible to synthesize the nanodispersed powders of barium-strontium ferromolybdate. Also, this work was carried out in order to establish correlation dependences between the production modes (pH value of the initial solutions, temperature, annealing time) and phase composition during the synthesis of the SBFMO system powders.

As a result of the work carried out, the concentrations of the initial reagents ($\text{Sr}(\text{NO}_3)_2$, $\text{Ba}(\text{NO}_3)_2$, $\text{Fe}(\text{NO}_3)_3 \cdot 9\text{H}_2\text{O}$, $(\text{NH}_4)_6\text{Mo}_7\text{O}_{24}$), were selected and calculated, the solvent compositions were determined and optimized (aqueous solutions of nitrates were mixed with a solution of citric acid), as well as the conditions for obtaining a colloidal solution of the sol for the formation of a homogeneous gel, which will allow the synthesis of nanodispersed powders of barium-strontium ferromolybdate.

Investigations have been carried out to establish the influence of production modes (the value of the hydrogen index of the initial solutions, temperature and annealing time) on the phase composition during the synthesis of the Sr-Ba-Fe-Mo-O powders. It has been experimentally established that the most appropriate value of the hydrogen index of the initial solutions is $\text{pH}=4$. According to the data obtained, it was established that the powder of strontium-barium ferromolybdate during its synthesis in the temperature range of 743–1473 K is multiphase, containing the phases $\text{SrBaFeMoO}_{6-\delta}$, BaMoO_4 , $\text{Ba}_3\text{Mo}_{18}\text{O}_{28}$, $\text{SrFeO}_{7-\delta}$, SrCO_3 , BaCO_3 , Fe_3O_4 and MoO_3 . In this case, the percentage of the $\text{SrBaFeMoO}_{6-\delta}$ solid solution increases with increasing temperature, and at 1473 K, an almost single-phase compound of double perovskite is observed.

This work was supported by the European project H2020 –MSCA –RISE –2017 – 778308 – SPINMULTIFILM, and the project of the Belarusian Republican Foundation for Fundamental Research No. F21U-003.

DEVELOPMENT OF NEUTRON SCATTERING TECHNIQUES AND INSTRUMENTS

DEVELOPMENT OF LINEAR POSITION-SENSITIVE NEUTRON DETECTOR FOR MODERN NEUTRON SOURCES

Evgeniy Altylnbaev^{1,2}, Alexander Polyushkin¹, Bogdzel A.A.³, Kalyukanov A.I.⁴, Litvinenko E.I.³, Solovei Valeriy¹, Saveleva Tatiana¹, Churakov A.V.³

¹*Petersburg Nuclear Physics Institute National Research Center "Kurchatov Institute", Gatchina, 188300, Russia,*

²*Saint Petersburg State University, St.-Petersburg, 199034, Russia*

³*Joint Institute for Nuclear Research, Dubna, 141980, Russia*

⁴*National Research Centre «Kurchatov Institute», Moscow, 123098, Russia*

E-mail: altylnbaev_ev@pnpi.nrcki.ru

In the frame of creation of scientific instruments at the PIK research reactor complex, a new thermal neutron powder multi-detector diffractometer D3 is being developed for researches at the field of condensed matter under high pressures. An assembly of 96 (6x16) linear position-sensitive helium detectors with charge division is proposed to register the scattered neutrons at D3. Required parameters of the helium-filled tubes are: length 600 mm, diameter 8 mm, spatial resolution along the anode should be at least 3 mm.

Linear position-sensitive thermal neutron detectors (LPSD) operating on the principle of charge division are reliable, time-tested devices. However, high intensity of neutron beams at new modern sources can lead to overloads of existing models and dramatic reduction of spatial resolution. Degradation of the anode wire at high neutron fluxes can also lead to a drastic reduction in the service life of the detectors.

In order to solve this problem, the cooperation of the National Research Center "Kurchatov Institute" - PNPI and the Joint Institute for Nuclear Research initiated development of LPSDs and electronic systems capable of working on modern neutron sources. The first results of this work are presented in this report. The registration part was designed and manufactured in collaboration with the "SPF Consensus" firm (Russia). Two assemblies of the electronic system for these LPSDs were developed by JINR and NRC "Kurchatov Institute" - PNPI. Prototypes of the registration systems were made and their parameters were defined in cooperation with a neutron sources laboratory and with the neutron beam of the IR-8 research reactor at the NRC "Kurchatov Institute".

PROTOTYPES OF NEUTRON SCINTILLATION DETECTORS BASED ON ZnS(Ag)/LiF AND SiPM

Glushkova Tatyana¹, Trunov Dmitry^{1,2,3}, Marin Victor^{1,2}, Sadykov Ravil², Polyushkin Alexander¹

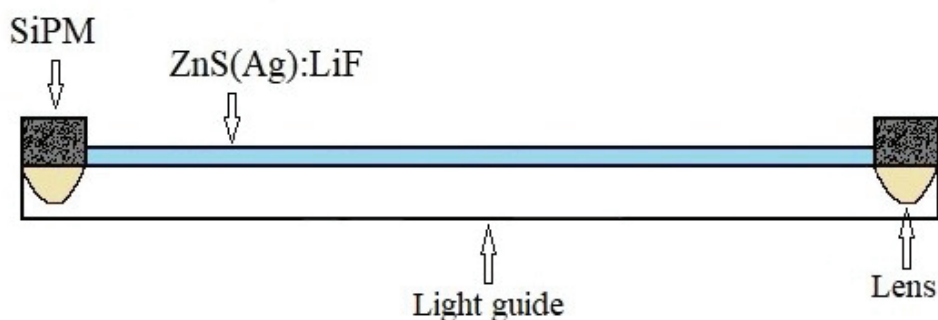
¹NRC "Kurchatov Institute" - PNPI, Gatchina, Russia

²INR RAS, Moscow, Russia

³NRC "Kurchatov Institute", Moscow, Russia

E-mail: dtrunov@inr.ru

Since 2012, a group of specialists has been developing neutron detectors based on the ZnS(Ag)/LiF scintillator and silicon photomultipliers (SiPM). A typical neutron scintillation counter consists of a scintillator glued to a Plexiglas light guide, with light-collecting lenses located at the ends of the light guide, and 2 SiPMs. (pic. 1). Scintillation counters of various sizes and modifications have been developed. A ring neutron detector has been created, which is successfully used on the neutron source IN-06 INR RAS.



Pic. 1. Typical neutron scintillation counter/

Simulation was carried out to analyze the propagation of light along the light guide, depending on the location of the light source relative to the detector. The simulation was carried out for scintillation counters with two types of absorbing surfaces: mirror anodized aluminum and fluoroplastic tape with diffusion reflection.

Two variants were simulated: the light source was located in the center of the detector and the light source was shifted from the center to the right and to the left by 20 mm. It has been established that when using a fluoroplastic tape, the total amount of light and the light separation coefficient (the value that determines how much the light is attenuated when the light source is displaced by 20 mm) increase. In the first case, when the light source is displaced, the separation factor is about 30%, and in the second, about 80%.

Taking into account the simulation results and the experience of previous developments, a test scintillation position-sensitive neutron detector was created with the possibility of extracting coordinates by two silicon photomultipliers.

In a one-dimensional scintillation counter, using a two-channel amplitude-to-digital spectrometric converter, the amplitude spectra corresponding to two positions of the neutron source relative to the SiPM counter were determined: at the extreme left and extreme right positions of the SiPM. The resulting differences in the spectra make it possible to determine the spatial coordinate of neutron detection along the counter.

The work was supported by the Ministry of Science of the Russian Federation, grant No. 075-10-2021-115 dated October 13, 2021.

INSTRUMENTS CONTROL SOFTWARE AT THE IBR-2 REACTOR: EXPERIENCE AND PROSPECTS

A.S. Kirilov, I.A. Morkovnikov, S.M. Murashkevich, T.B. Petukhova and L.A.Truntova

Frank Laboratory of Neutron Physics, Joint Institute for Nuclear Research, Dubna, Russia.

E-mail: akirilov@jinr.ru

The Sonix+ package [1] is the main instrument control software at the IBR-2 reactor. It was developed in the beginning of the 1990s for the NSHR texture diffractometer (beamline 6a of IBR-2). Later, the complex was transferred to other instruments, including those located outside FLNP. For all the time, about 20 package installations were performed. When developing the complex, we were guided both by the world trends [2] as well as by the specificity of our laboratory. Many important requirements were formulated by our users, therefore they can be considered as real co-authors of the project.

The modular organization of the software and use of the Python language for describing the experimental script make it relatively easy to adapt it to the specific features of various instruments.

The universal GUI based on the set of PyQt widgets can be used to control the experiment without further refinement. It provides all the necessary functions, including, preparation of a task for the experiment, its launch, monitoring of current values of parameters, and spectrum visualization. In addition, there are some instrument tuning programs and other useful tools.

Besides the instrument control itself, the complex also includes remote measurement supervising subsystem (WebSonix service) and the central repository for measurement results.

The Journal system provides automatic data logging of measurements.

The Microsoft Windows is used as the operating system on control computers.

Long-term experience in the complex operation without significant changes in its structure has proved the correctness of the basic principles underlying it. However, the complex is constantly developing in accordance with new requirements. The presentation is supposed to analyze the experience gained and to outline the main directions of the nearest changes.

[1] A.S.Kirilov et al (2020). Instrument control software at the IBR-2 reactor: features and prospects. *Journal of Surface Investigation*. 14, Suppl. 1, S93–S98.

[2] <https://www.nobugsconference.org/>

THIN-FILM CONVERTER BASED ON $^{10}\text{B}_4\text{C}$ FOR NEUTRON DETECTORS

Alexander Kolesnikov^{1,2}, Victor Bodnarchuk¹, Yuriy Kryukov²

¹ *Joint Institute for Nuclear Research, Dubna, Russia*

² *Dubna State University, Dubna, Russia*

E-mail: torgcentr2004@mail.ru

A promising material for use as a converter of slow neutrons in large-area detectors are thin-film coatings of boron carbide B_4C enriched with ^{10}B isotope deposited on large-area substrates. Thin-film coatings $^{10}\text{B}_4\text{C}$ on aluminum plates, on aluminum foil, on lavsan films (Mylar) and polyimide films (Kapton) are presented. The results of the study of adhesion, density and structure of $^{10}\text{B}_4\text{C}$ coatings, optical and electrical properties of coatings are presented.

RESULTS OF MODERNIZATION OF THE FSS NEUTRON FOURIER DIFFRACTOMETER AT THE IBR-2 REACTOR

A.A. Kruglov, I.V. Papushkin, V.V. Zhuravlev, T.B. Petukhova, S.M. Murashkevich, L.A. Truntova, N.D. Zernin and G.D. Bokuchava

Frank Laboratory of Neutron Physics, Joint Institute for Nuclear Research, Joliot-Curie str. 6, 141980 Dubna, Russia

E-mail: akruglov@nf.jinr.ru

Neutron Fourier diffractometer FSS (Fourier Strain Scanner) was used in 1990-2010 at the stationary reactor FRG-1 at the GKSS research center (Geesthacht, Germany) to study residual stresses in structural materials and industrial products. In 2010, the FRG-1 reactor was finally decommissioned. In this regard, in 2014 the FSS diffractometer was transported to FLNP JINR (Dubna, Russia) and located on channel No. 13 of the IBR-2 pulsed reactor.

Over the past few years, a large amount of work has been carried out to build beamline No. 13, develop its infrastructure, create biological shielding, as well as install and adapt the main FSS units to work on a pulsed source and perform the first test experiments. At the next stage, a new neutron guide with a supermirror coating ($m = 2$), radius of curvature $R = 1900$ m, and characteristic wavelength $\lambda_c = 0.95$ Å was installed at the FSS.

To improve the resolution of the FSS, a new Fourier chopper with a maximum rotation speed of $\Omega_{\max} = 6000$ rpm was installed. The new chopper is mounted on a movable platform, which allows the chopper to be remotely inserted and removed from the beam as needed, and thus quickly switch between TOF (high intensity) and RTOF (high resolution) modes. The results of test experiments showed that after the replacement of the chopper, the FSS resolution improved significantly (Fig. 1). In addition, old DAQ electronics was replaced with new MPD-32 RTOF analyzers for data accumulation in the list-mode, which allows one to set the necessary parameters of the TOF scale and ensure high accuracy of electronic focusing for individual detector elements.

Thus, the main work on the adaptation and modernization of the FSS diffractometer has been successfully completed. Further development of the FSS includes work on increasing the luminosity of the diffractometer, reducing the background level, improving the Fourier analysis parameters, and equipping the diffractometer with additional devices (loading machines, furnaces, etc.) to provide the external conditions on the sample.

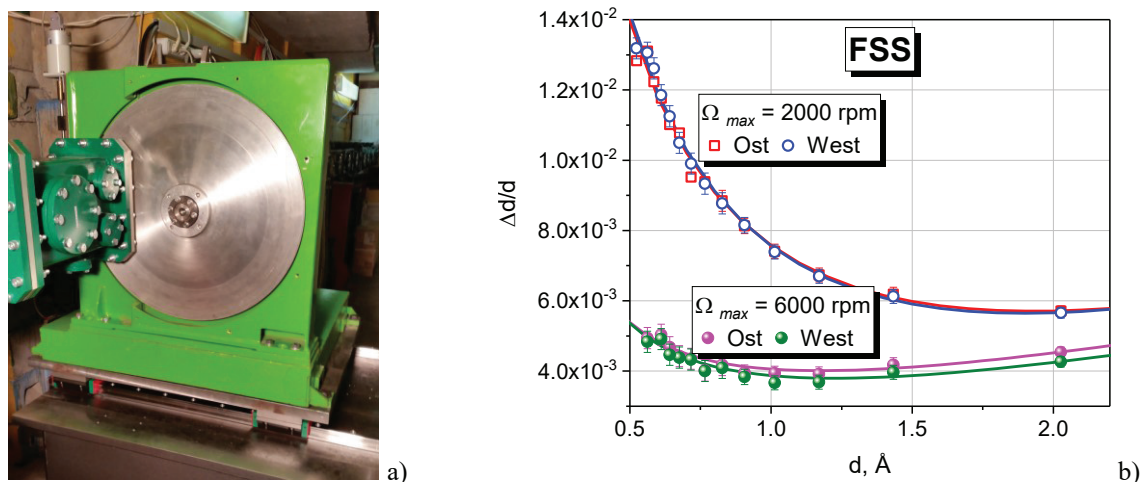


Fig. 1. a) The new Fourier chopper of the FSS diffractometer, mounted on a movable platform. b) Comparison of the resolution functions $\Delta d/d$, measured with a standard iron sample with old ($\Omega_{\max} = 2000$ rpm) and new ($\Omega_{\max} = 6000$ rpm) choppers.

GEANT4 SIMULATION OF A THERMAL NEUTRON DETECTOR WITH A BORON CONVERTER

A.K.Kurilkin¹, O.Daulbayev^{1,2}, A.A.Bogdzel¹, T.Enik¹, I.V.Gapon¹, A.G.Kolesnikov^{1,2} and V.Milkov¹

¹ *Joint Institute for Nuclear Research, Dubna, 141980, Russia*

² *Dubna State University, Dubna, 141980, Russia*

³ *The Institute of Nuclear Physics, Ministry of Energy of the Republic of Kazakhstan, 050032 Almaty, Kazakhstan*

E-mail: akurilkin@jinr.ru

This paper presents the results of evaluating the theoretical efficiency of a single-layer thermal neutron detector with a solid-state converter, depending on the B₄C deposition thickness. The software package Geant4 was used as a tool for numerical simulation by the Monte Carlo method. Various materials are considered as a substrate for deposition in order to reduce the influence of processes occurring in the detector in addition to the n+¹⁰B reactions. The simulation results are compared with experimental measurements.

SANS RESEARCH OF HEAT-RESISTANT NONMAGNETIC ALLOYS AT NEUTRON REFLECTOMETR - SANS INSTRUMENT «GORIZONT» IN INR RAS

V.S. Litvin¹, D.A. Buchnyi¹, A.V. Churakov², D.N. Trunov¹, S.N. Axenov, R.A. Sadykov¹, V.I. Bodnarchuk¹ and A.V. Belushkin¹

¹*Institute for Nuclear Research RAS, Moscow, Russia*

²*Joint Institute for Nuclear Research, Dubna, Russia*

E-mail: vlitvin@inr.ru

It is planned to carry out in situ measurements at high pressures at the neutron instruments at the Institute of Nuclear Research RAS. Using the SANS method, the structure of non-magnetic alloys based on Ni, Mo, and Cr was studied at the Gorizont setup. These alloys are of interest as a material for the manufacture of high-pressure cell for research in magnetic fields by neutron methods. The measurement of SANS spectra on samples of such alloys is necessary to select the optimal material for manufacturing cell. SANS spectra obtained on heat-resistant alloys 40HNU (Ni — base, Cr — 40% and Al — 3,5%), Be-bronze (Cu — base, Be — 2% , Ni — 0,2-0,5%) and MoTiC-alloy (Mo — base, Ti — 10%, C — 3%) presented at fig. 1. The Gorizont instrument at the IN-06 pulsed neutron source of the INR RAS [1] is designed to study two-dimensional nanostructures, such as multilayer nanofilms, by neutron reflectometry. Thanks to the vertical scattering plane, liquid samples, such as films on the surface of a liquid, can be examined. This device can also be used for studies of small-angle neutron scattering (SANS). The device consists of a 7-meter curved neutron guide, automatic collimator slits, a deflecting non-magnetic NiMo/Ti supermirror with $m = 2$ (which can be replaced by a polarizer), and a vibration-resistant sample. The facility is equipped with a two-coordinate monitor and a two-coordinate neutron detector manufactured by FLNP of JINR.

It can be concluded from the obtained spectra that the SANS cross section of the Be-bronze is one order of magnitude and MoTiC-alloy is two orders of magnitude smaller than that of 40HNU and, therefore, it is better for use in neutron diffraction measurements. The results were obtained with the financial support of the Russian Federation represented by the Ministry of Science and Higher Education, an agreement № 075-10-2021-115 from 13/10/2021 (№ 15.СИИ.21.0021).

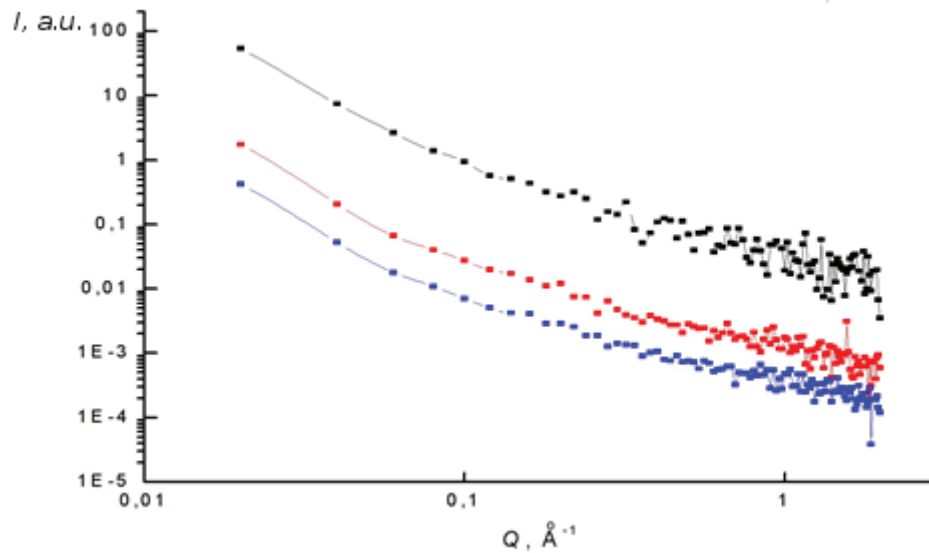


Fig. 1. SANS at 40HNU(black), Be-bronze (red), MoTiC-alloy(blue).

- [1] V.S. Litvin, V.A. Trounov, V.A. Ulyanov and others (2012). A new time-of-flight neutron reflectometer and SANS instrument GORIZONT at IN-06 spallation neutron source. *Journal of Physics: Conference Series*, 340, 012032.
- [2] V.S. Litvin, (2021). Simulation and Test Measurements Using Neutron Reflectometer and Small-Angle Spectrometer “Horizon” Operating at the IN-06 Pulsed Source. *Journal of Surface Investigation: X-ray, Synchrotron and Neutron Techniques*, 4, 645-651.

VARIATIONS OF PISTON-CYLINDER CELLS FOR NEUTRON SCATTERING UNDER HIGH PRESSURE

A.A. Paveleva¹, R.A. Sadykov² and E.V. Altynbaev²

^{1,2}*Petersburg Nuclear Physics Institute, Gatchina, Russia*

²*Institute for Nuclear Research of the Russian Academy of Sciences, Moscow, Russia*

E-mail: aleksandra-paveleva@mail.ru

The paper presents an overview of different types of piston-cylinder cells. Cells made of non-magnetic materials are used for neutron scattering and are capable of operating in the field of single-crystal and powder diffraction. These cells are capable of operating under high pressure and at low temperatures. The various non-magnetic materials used to make the cells are one of the main factors in determining the amount of pressure provided as an experimental parameter, in addition to the design of the cells. An additional determining factor is the hydrostatic limit of the working fluid, which affects the achieved working pressure and increases it when the fluid solidifies, which also makes its own adjustments to the experimental process.

PHYSICAL MODEL OF THE IN-BEAM SPECTROMETER ON PIK REACTOR

M.V. Remizov¹, D.I. Bogmut¹, Yu.V. Kulvelis¹, V.S. Kozlov¹, V.G. Semenov²,
V.T. Lebedev¹

¹ *B.P. Konstantinov Petersburg Nuclear Physics Institute, NRC Kurchatov Institute, 188300 Gatchina, Leningrad distr., Russia*

² *St. Petersburg State University, 198504 Petergof, St. Petersburg, Russia*

E-mail: m.remizov97@gmail.com

Among nuclear physics methods complementary to neutron diffraction, Mössbauer spectroscopy stands out. Especially it is related to in-beam spectrometers [1] at reactors for neutron pumping of gamma sources in these devices. This makes it possible to use the sources being neutron targets with nuclei (isotopes) that have too short lifetimes in an excited state to serve in standard type devices. Thus, the range of nuclei (sources) with the characteristics required for this method is expanded to four or more tens, which is relevant in many traditional and new problems of chemistry, geology, materials science, biology, physics and chemistry of nanostructures, technologies of catalysts, and many other areas [2-6]. There is a lot of studies in which gamma-resonance spectroscopy has become a precision tool, e.g. for the analysis of endofullerenes with 4f-metals (isotopes Gd-155, Dy-161) [2], new structures with 3d-metal, Fe@C60 and their fullerenols [3], for which the endohedral structure was confirmed. In connection with the prospects of biomedical applications, recent results of the analysis of the valence state and coordination of iron in composites with graphenes are in demand [4, 5]. In this regard, the authors are developing Mössbauer spectroscopy towards the creation of a full-scale instrument on the inclined channel of the PIK reactor (PNPI). For this purpose, PNPI together with the Institute of Chemistry of St. Petersburg State University has created a model as a prototype of the spectrometer (Fig. 1). It allows test new technical solutions and methods to be used in the main device, which will serve for the implementation in mineralogical, geochemical, biomedical scientific programs in Russia, and for the development of materials science in cooperation with the Central Research Institute for Structural Material "Promethey" in the developments of new steels and alloys for shipbuilding and nuclear energy technologies. Presently, this electrodynamic prototype-setup is involved in current research, including the study of surface and near-surface layers of metals and ceramics selectively in depth by using transmission and emission measurements in a fixed geometry, or when moving the sample under study and the source of resonant gamma quanta with the possibility of cooling the sample to liquid nitrogen temperature. The model spectrometer makes it possible to analyze the physicochemical properties of crystalline and amorphous materials, nanostructures, for example, endofullerenes with metal ions (Fe³⁺, Eu³⁺, Dy³⁺), nanotubes modified with iron atoms, and other objects. A choose of an appropriate gamma source used provides the experiments to determine the valence and coordination states of ions and the nature of their chemical bond; magnetic structure; coordination of atoms relative to the environment; features of the structure of the environment of the ion in the nearest coordination spheres (for example, relative to the fullerene cage around endohedral atom).

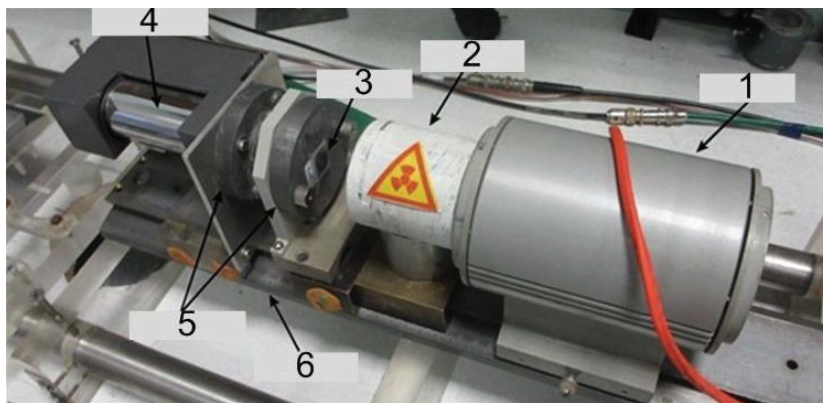


Fig.1. General view of the prototype installation: 1 - source of gamma radiation on a vibrating base, 2 - radiation shielding, 3 - sample, 4 - photomultiplier, 5 - collimators, 6 - optical bench.

The facility has been used to probe such nanostructures as detonation diamonds with grafted Eu ions [6], metal–carbon matrices (pyrolysates of Eu-diphthalocyanines), nanotubes, and graphenes intercalated with iron atoms [4,5]. Further development of a large-scale device at the PIK reactor with continuous activation of short-lived sources by reactor neutrons [1] is crucially important for the analysis of the electronic structure of various scientific objects and systems in combination with the study of their atomic (molecular) structure and dynamics by using the instrumental park available at the reactor for scientific, technological, and industrial researches.

- [1] I. Lázár, A. Szilágyi, G. Sáfrán, Á. Szegedi, S. Stichleutner, K. Lázár (2015) Iron oxyhydroxide aerogels and xerogels by controlled hydrolysis of $\text{FeCl}_3 \cdot 6\text{H}_2\text{O}$ in organic solvents: stages of formation. *RSC Advances*. 5, 72716–72727
- [2] Y.S.Grushko, E.G.Alekseev, V.S.Kozlov, L.I.Molkanov, G.Wortmann, H.Giefers, K.Rupprecht, M. A. Khodorkovskii (2000) ^{161}Dy Mössbauer study of the endohedral metallofullerenes $\text{Dy}@C_n$ ($n= 80, 82, 84$). *Hyperfine Interact.* 126, 1-4, 121-126.
- [3] V. M.Cherepanov, V. T.Lebedev, A. A.Borisenkova, E. V.Fomin, A. N.Artemiev, A. D. Belyaev, G.A.Knyazev, A.Y.Yurenya, M.A.Chuev (2020). Valence and Coordination of Iron with Carbon in Structures Based on Fullerene C_{60} According to NGR Spectroscopy and EXAFS. *Crystallography Reports*. 65, 3, 404–408. © Pleiades Publishing, Inc.
- [4] A.S.Kamzin, I.M.Obaidat, V.S.Kozlov, E.V.Voronina, E.B. V. Narayanaswamy, I.A. Al-Omari (2021) Graphene Oxide/Iron Oxide (GrO/FeOx) Nanocomposites for Biomedicine: Synthesis and Study. *Solid State Physics*. 63, 6, 807-816 (Rus.).
- [5] A.S.Kamzin, I.M.Obaidat, V.S.Kozlov, E.V.Voronina, E.B. V. Narayanaswamy, I.A. Al-Omari (2021) Magnetic nanocomposites graphene oxide/magnetite+cobalt ferrite (GRO/Fe 2O_4 +CoFe 2O_4) for magnetic hyperthermia. *Solid State Physics*. 63, 7, 900-910 (Rus.).
- [6] Yu. Kulvelis, V. Lebedev, E. Yudina, A. Shvidchenko, A. Aleksenskii, A. Vul, A. Kuklin (2020) Structural Studies of Detonation Nanodiamonds with Grafted Metal Ions by Small-Angle Neutron Scattering. *Journal of Surface Investigation: X-ray, Synchrotron and Neutron Techniques*. 14, Suppl. 1, S132–S133. © Pleiades Publishing, Ltd., 2020.

UPGRADE PLANS FOR EPSILON DIFFRACTOMETER

V.V. Sikolenko^{1,2}, B.I.R. Müller¹, A.Badmaarag¹, M.Klepacka³ and F.R. Schilling¹

¹*Karlsruhe Institute of Technology, Karlsruhe, Germany.*

²*Joint Institute for Nuclear Research, Dubna, Russia*

³*Adam Mickiewicz University, Poznan, Poland*

E-mail: vadim.sikolenko@kit.edu

The TOF diffractometer Epsilon at the beamline 7a of the IBR-2 reactor dedicated to the high resolution measurements of applied and residual strains of geological samples and functional materials.

In this report we present the current status of the instrument and upgrade plans till restart of the IBR-2 reactor in September, 2023

It includes an installation of focusing part of neutron guide, substitution of λ -choppers for vacuum tube, upgrade of uniaxial press and installation of new furnace.

STRUCTURAL STUDIES OF SURFACTANT-POLYMER ASSOCIATIONS IN
BULK AND AT INTERFACES

O.P. Artykulnyi^{1,2}, M.M. Avdeev^{1,3}, A.V. ShibeV³, V.I. Petrenko^{4,5}, O.I. Ivankov¹,
L.A. Bulavin²

¹Joint Institute for Nuclear Research, Dubna, Russian Federation

²Taras Shevchenko National University of Kyiv, Kyiv, Ukraine

³Lomonosov Moscow State University, Moscow, Russian Federation

⁴BCMaterials, Basque Center for Materials, Applications, and Nanostructures, 48940
Leioa, Spain

⁵Ikerbasque, Basque Foundation for Science, 48009 Bilbao, Spain

E-mail: artykulnyi@jinr.ru, artykulnyi@gmail.com

The surfactant-polymer association complexes of anionic surfactant dodecylbenzene sulfonate acid (DBSA) and neutral polymer polyethylene glycol (PEG) were studied in the bulk of solution by small-angle neutron scattering (SANS) [1,2] and at the surface of polymer brush system by neutron reflectometry [3]. The influence of polymer binding effect on the surfactant micelle structure clearly can be seen from SANS curves (Fig. a), scattering intensity of DBSA 3 vol. % micellar solution significantly changes after the addition of 3 vol. % PEG in solution, and cannot be represented by the sum of the scattering intensities of the polymer and micelles separately [1].

Polymer brush system of PEG ($M_w = 20$ kDa) was synthesized on a silica substrate using the “grafting to” method. Structural changes in the PEG polymer brush caused by the interaction with DBSA micelles were observed by neutron liquid cell reflectometry using a substrate with a titanium carrier layer for enhancing reflectivity signal (Fig. b) [3]. The effect is shown to be related to the formation of molecular polymer-micelle associates, which was previously studied by small-angle neutron scattering in a wide range of surfactant concentrations at various molecular weights of the polymer [1]. The structure of DBSA complexes in the dense medium of the PEG polymer brush under study remains unexplored and requires further investigations including the neutron reflectometry method.

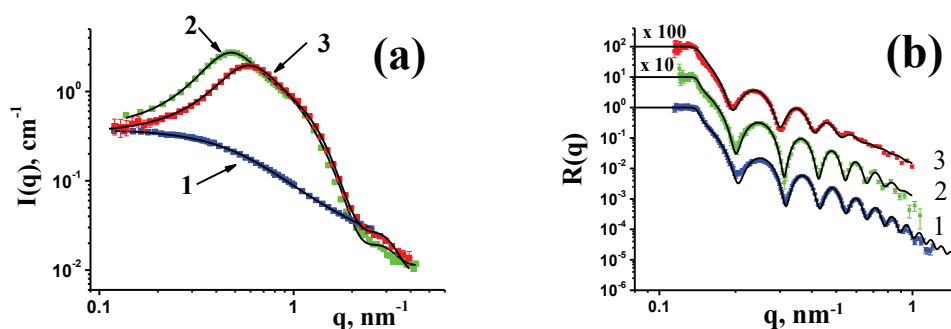


Fig. SANS data (a): scattering on PEG 20 kDa solution with 3 vol.% concentration (1), scattering on DBSA 3 vol. % solution (2), scattering on DBSA 3 vol. % + PEG 3 vol. % mixture solution (3); neutron reflectometry data (b): Si/Ti/SiO₂ substrate in the liquid cell (1), PEG polymer brush system at the substrate surface in the liquid cell (2), injection of 0.2 vol.% solution of DBSA in the liquid cell (3)

[1] O.P. Artykulnyi, A.V. Shibaev, M.M. Avdeev, et al. // *J. Mol. Liq.* (2020) 308, 113045

[2] O.P. Artykulnyi, V.I. Petrenko, L.A. Bulavin, et al. // *J. Mol. Liq.* (2019) 276, 806-811

[3] O.P. Artykulnyi, M.M. Avdeev, Ye.M. Kosiachkin, et al. // *Nucl. Phys. At. Energy* (2021) 22, 149-156.

SYNTHESIS OF POLYACRYLAMIDE GEL NANOLAYERS ON OXIDIZED SILICON SURFACE FOR USE AS SMART COATINGS WITH CONTROLLED RELEASE OF ANTISEPTICS

Avdeev M.M.¹, Kosiachkin Ye.N.², Artykulnyi O.P.², Gorshkova Yu.E.², Shibaev A.V.¹, Khokhlov A.R.,¹ Philippova O.E.¹

¹ Faculty of Physics, M.V.Lomonosov Moscow State University, Moscow, Russian Federation

² Frank Laboratory of Neutron Physics, Joint Institute for Nuclear Research, Dubna, Russian Federation

E-mail: avdeev@polly.phys.msu.ru

“Smart” polymeric layers on surfaces are promising for various applications, including the development of antiseptic coatings, low-friction surfaces, surface preparation for single-molecule studies (e.g. PALM[1], STORM[2], etc.) including the dynamics of biomolecules and complex clusters[3], etc. To create such layers, polymer passivation is used. Poly(ethylene glycol) (PEG) is traditionally used for such kind of procedures, when the coverslip is seeded with a linear polymer brush. In this work, we introduce an alternative method of surface preparation: copolymerization of acrylamide and TMSPPMA (3-(Trimethoxysilyl)propyl methacrylate, “anchor”) chemically bonded to the surface. It is supposed that two types of monomers equally involved in the radical polymerization, so, as a result, a nanolayer of an entangled the polymer network (CoPAM) is attached to silica surface. CoPAM is a sufficiently hydrophilic polymer, non-sensitive to salt additives. It is frequently employed in the synthesis and research of surfactant-polymer and copolymer systems. Via variation of concentration and ratio between compounds, one can control the structure of this passivated film. Here, we used fixed component concentration and varied temperature of polymer synthesis, because the polymer chain length depends on it.

The objective of our study is the analysis of the structure, quality of the polymer film and its chemical composition. Using the method of X-ray reflectometry, scattering length density profiles of dried polymer films were obtained for a number of samples prepared at different temperatures. Also, the surface of the samples was studied to find out any anomalies with the help of atomic force microscopy (AFM). With the help of dynamic light scattering technique (DLS) we have obtained hydrodynamic radii of macromolecules in bulk, which correspond to chains attached to silicon surface. Analysis of data from XRR and DLS gave us information about the dependence of polymer brush height over polymer length (scaling). Composition of polymer brush was proved with X-ray photoelectron spectroscopy (XPS). At the next stage, we plan to investigate the swollen polymer film in water by neutron reflectometry, because presence of polymer brush may cause the alteration of XRR curve [4].

The work is financially supported by the Russian Foundation for Basic Research (project № 20-04-60302). XPS measurements were provided by Research Center for Collective Use "Nanochemistry and Atmospheric Chemistry", operator S.V. Dvoryak (Faculty of Chemistry, MSU).

[1] Betzig E. et al (2006). Imaging Intracellular Fluorescent Proteins at Nanometer Resolution. Science 313, 1642–1645.

- [2] Linde S. et al (2011). Direct stochastic optical reconstruction microscopy with standard fluorescent probes. *Nature Protocols* 6, 991–1009.
- [3] Rusmini F., Zhong Z. and Feijen J. (2007). Protein Immobilization Strategies for Protein Biochips. *Biomacromolecules* 8, 1775–1789.
- [4] O.P. Artykulnyi, et al (2021). Neutron investigation of interaction between anionic surfactant micelles and poly (ethylene glycol) polymer brush system, *Nucl. Phys. At. Energy* 22, 149–156.

INVESTIGATION OF SEVERAL MOLLUSCK SHELLS FROM DANUBE DELTA AND CONSTANTA BLACK SEE SHORE BY MEANS OF SMALL-ANGLE NEUTRON SCATTERING AND ION BEAM ANALYSIS METHODS

Maria Bălăsoiu^{1,2}, Dmytro Soloviov^{2,3}, Dmitry Nikolayev², Tatiana Lychagina², Nikolai Lizunov², Ana Pantelică¹, Dan Pantelică¹, Diana Maria Mihai¹, Ibram Orhan⁴, Marius Belc⁵, Mirela Mihaela Bratu⁵, Liviu Miron⁶ and Alexandra-Maria Bălăsoiu-Găină^{2,7}

¹*Horia Hulubei National Institute of Physics and Nuclear Engineering, Magurele, Romania*

²*Joint Institute for Nuclear Research, Dubna, Russian Federation*

³*Institute for Safety Problems of Nuclear Power Plants, NAS of Ukraine, Kyiv, Ukraine*

⁴*“Danube Delta” National Institute for Research and Development, Tulcea, Romania*

⁵*University Ovidius of Constanta, Constanta, Romania*

⁶*Iasi University of Life Sciences, Iasi, Romania*

⁷*West University of Timisoara, Timisoara, Romania*

E-mail: masha.balasoiu@gmail.com

Humanity has consciously used biological materials such as bone, ivory and shells, since prehistoric times due to their special physical and chemical properties. The composite nature of biological materials at the nanolevel, in combination with a specific structural hierarchy up to the macroscopic level, provides them with exceptional properties [1].

Understanding the microstructure of the water mollusk shells is nowadays of great importance due to the fact that this structure may consist in a model for innovative nanostructured materials in various domains. The micro-structure of the shell is based on the “bricks and mortar” pattern, specific for the molluscan exoskeleton. “The bricks” consist in polygonal aragonite tablets in the case of the nacre or in calcite tablets, joined together by the matrix proteins synthesized by these organisms (“the mortar”). These proteins have special properties; the bio-activity studies performed on human fibroblasts, stroma cells and mouse pre-osteoblasts show the nacre soluble matrix ability to induce the cell differentiation to the osteoblast phenotype. Also the alkaline phosphatase activity rise and bone nodules are formed in the presence of the shell matrix proteins. The structure and functions of these proteins are poorly known till now. As consequence, the understanding of the microstructure and the synthesis process of the molluscan shell is of big importance in order to create new biomimetic materials with applications for example, in the medical domains [2]. Structural investigation of biogenic materials, can lead to the development of new synthetic strategies for controlling mineral morphologies [3].

Small-angle neutron scattering method is largely used in the studies of biominerals and biomineralization processes [4, 5]. In the present work, we explore the potential utility of small-angle neutron scattering (SANS) for investigating and ultimately differentiating the structure of mollusk shells based on species and locality of origin. The measurements have been accomplished at the YuMO instrument in function at the IBR-2 reactor.

For composition determination of the samples, the proton induced X-ray Emission (PIXE), proton induced gamma-ray emission (PIGE) and Rutherford backscattering spectrometry (RBS) measurements with alpha beam on thick samples have been performed at the 3MV Tandatron of IFIN-HH, Magurele [6].

Earlier at FLNP JINR have started investigations on the crystallographic texture of bivalve shells [7, 8, 9]. It was observed that the shells of mollusk species of the genus *Mytilus* consist of two phases, calcite and aragonite. It was concluded that the nature of the global textures of different phases in the same shells is different [8]. In addition, it was found that during the growth of the shell of some species (*Sinanodonta woodiana*), the crystallographic directions, a and b, of aragonite are reoriented and the strength of the texture increases [9].

Investigations of bivalve shells from the Gulf of Saldanha (South Africa) showed the existence of some correlation between the crystallographic texture and composition with respect to a number of chemical elements [10].

- [1] I. Reiche, A. Gourrier (2016). Informative Potential of Multiscale Observations in Archaeological Biominerals Down to Nanoscale (Chapter), in *Nanoscience and Cultural Heritage*, Eds. P. Dillmann, L. Bellot-Gurlet, I. Nenner, Springer, 75-122.
- [2] S.V. Popov (1992). Shell microstructure of some bivalve mollusk groups, *Proceedings of Paleontological Institute of the RAS*. 245, 46.
- [3] F. C. Meldrum and H. Cölfen (2008). Controlling Mineral Morphologies and Structures in Biological and Synthetic Systems, *Chem. Rev.* 108, 4332–4432.
- [4] Werner Götz, Edda Tobiasch, Steffen Witzleben and Margit Schulze (2019). Effects of Silicon Compounds on Biomineralization, Osteogenesis, and Hard Tissue Formation, *Pharmaceutics*. 11, 117 (1-27).
- [5] S. Kichanov, A. Pantelica, D. Pantelica, S. Stolyar, R. Iskhakov, D. Aranghel, P. Ionescu, R. Vladoiu, M. Balasoiu (2018). Structural and compositional specifications on biogenic ferrihydrite nanoparticles production by *Klebsiella Oxytoca*, *Romanian Reports in Physics* 70 (4), 511(1-10).
- [6] I. Burducea, M. Straticiuc, D.G. Ghita, D.V. Mosu, C.I. Calinescu, N.C. Podaru, D.J.W. Mous, I. Ursu, N.V. Zamfir (2015). A new ion beam facility based on a 3 MV Tandatron™ at IFIN-HH, Romania, *Nuclear Instruments and Methods in Physics Research B*. 359, 12–19.
- [7] Dmitry Nikolayev, Tatiana Lychagina, Alexey Pakhnevich, Maria Balasoiu, Liviu Miron (2017). Neutron quantitative texture analysis of the *Bivalvia* mollusks shells, *IBWAP 2017 Book of Abstracts*, S4 L1 (invited lecture), 127.
- [8] Dmitry Nikolayev, Tatiana Lychagina, Alexey Pakhnevich. (2019). Experimental neutron pole figures of minerals composing the bivalve mollusk shells, *SN Applied Sciences* 1, 344.
- [9] Monika Kučeráková, Jan Rohlíček, Stanislav Vratislav, Markéta Jarošová, Ladislav Kalvoda, Dmitry Nikolayev, Tatiana Lychagina and Karel Douda (2021). Texture of the Freshwater Shells from the Unionidae Family Collected in the Czech Republic Investigated by X-ray and Neutron Diffraction, *Crystals*. 11, 1483
- [10] Pavel Nekhoroshkov, Inga Zinicovscaia, Dmitry Nikolayev, Tatiana Lychagina, Alexey Pakhnevich, Nikita Yushin and Jacques Bezuidenhout (2021), Effect of the Elemental Content of Shells of the Bivalve Mollusks (*Mytilus galloprovincialis*) from Saldanha Bay (South Africa) on Their Crystallographic Texture, *Biology*, 10, 1093(1-18).

SMALL-ANGLE NEUTRON SCATTERING INVESTIGATION OF FERROFLUIDS WITH MAGNETITE NANOPARTICLES COATED WITH ASPARTIC-ACID, STARCH AND HYALURONIC ACID

Maria Bălăsoiu^{1,2}, Mihaela Răcuci³, Dorina Emilia Creangă⁴, Olexander Ivankov^{1,5}, Dmytro Soloviov^{1,5}, Florin Brinză⁴, Vadim Skoy^{1,6}, Alexandra-Maria Bălăsoiu-Găina^{1,7}

¹*Joint Institute for Nuclear Research, Dubna, Russian Federation*

²*Horia Hulubei National Institute of Physics and Nuclear Engineering, Magurele, Romania*

³*“Lucian Blaga” University of Sibiu, Sibiu, Romania*

⁴*“Alexandru Ioan Cuza” University of Iasi, Iasi, Romania*

⁵*Institute for Safety Problems of Nuclear Power Plants, NAS of Ukraine, Kyiv, Ukraine*

⁶*Moscow Institute of Physics and Technology, Dolgoprudniy, Russian Federation*

⁷*West University of Timisoara, Timisoara, Romania*

E-mail: masha.balasoiu@gmail.com

The development of water-based ferrofluids is important for applications such as cell separation, magnetocytolysis, drug delivery, treatment of tumors by hyperthermia, contrast enhancement in MRI screening, reduction of implant infection and enhancement of tissue growth, cell manipulation, DNA sequencing, etc. [1, 2]. To do this, different types of magnetic particles obtained using different protocols must be coated with molecules to ensure the stability of the systems, compatibility with biological fluids, and, ultimately, therapeutic effect [3,4,5,6].

In the present work, we focus on the structural analysis of ferrofluids with magnetite nanoparticles coated with aspartic acid, starch and hyaluronic acid and small-angle neutron scattering method is used for this purpose [7]. In addition, two aspartic acid coated samples, prepared by chemical precipitation but applying different protocols [8, 9] are discussed.

[1] O. Oehlsen, S.I. Cervantes-Ramírez, P. Cervantes-Avilés, I.A. Medina-Velo (2022). Approaches on Ferrofluid Synthesis and Applications: Current Status and Future Perspectives, ACS Omega 7, 4, 3134–3150.

[2] V.M. Socoliuc, M. Avdeev, V. Kuncser, R. Turcu, E. Tombacz, L. Vekas (2022). Ferrofluids and bio-ferrofluids: looking back and stepping forward, Nanoscale. (online).

[3] M. Racuciu (2009). Synthesis protocol influence on aqueous magnetic fluid properties, Current Applied Physics. 9, 1062–1066.

[4] M. Racuciu, D.E. Creanga, and A. Airinei (2006). Citric-acid coated magnetite nanoparticles for biological applications, Eur. Phys. J. E 21, 117-121.

[5] L. Popescu, D. Buzatu, M. Balasoiu, C. Stan, B. S. Vasile, L. Sacarescu, D. Creanga, O. Ivankov, D. Soloviov, A.-M. Balasoiu-Gaina (2019). Study on ageing of cobalt ferrite nanoparticles and their fate in the environment, Romanian Journal of Physics. 64, 818.

[6] A. Les, L. Popescu-Lipan, M. Grigoras, G. Ababei, I. Motrescu, G. Bulai, F. Branza, D. Creanga, M. Balasoiu (2022). Antioxidant molecule useful in the stabilization of nanoparticles in water suspension, Soft Materials. (online).

[7] D. Bica, L. Vekas, M.V. Avdeev, O. Marinica, V. Socoliuc, M. Balasoiu, V.M. Garamus (2007). Sterically stabilized water based magnetic fluids: Synthesis, structure and properties, Journal of Magnetism and Magnetic Materials. 311, 17–21.

[8] P. Berger, N.B. Adelman, K.J. Beckman, D. J. Campbell, A.B. Ellis, G.C. Lisensky (1999). Preparation and Properties of an Aqueous Ferrofluid, Journal of Chemical Education. 78(7), 943-948.

[9] A. Goodarzi, Y. Sahoo, M.T. Swihart, P.N. Prasad (2004). Aqueous Ferrofluid of Citric Acid Coated Magnetite Particles, Mat. Res. Soc. Symp. Proc. 789, N6.6(1-6).

STRUCTURAL INVESTIGATION OF MAGNETITE AND COBALT FERRITE MESOPOROUS NANOPARTICLES COATED WITH AMINO ACIDS AS STABILIZING AGENTS

Maria Bălăsoiu^{1,2}, Anton Ficai³, Denisa Ficai³, Dmytro Soloviov^{1,4}, Vitaliy Turchenko^{1,5,6}, Oleg Orelovich¹, Yu. Kovalev¹, Vadim Skoy^{1,7}, Alexandra-Maria Bălăsoiu-Găina^{1,8}, Alexander Doroshkevich^{1,6}

¹*Joint Institute for Nuclear Research, Dubna, Russian Federation*

²*Horia Hulubei National Institute of Physics and Nuclear Engineering, Magurele, Romania*

³*Faculty of Applied Chemistry and Materials Science, University "Politehnica" of Bucharest, Romania*

⁴*Institute for Safety Problems of Nuclear Power Plants, NAS of Ukraine, Kyiv, Ukraine*

⁵*South Ural State University, 76, Lenin Aven., Chelyabinsk, 454080, Russian Federation*

⁶*Donetsk Institute for Physics and Engineering named after O.O. Galkin, Kiev, Ukraine*

⁷*Moscow Institute of Physics and Technology, Dolgoprudniy, Russian Federation*

⁸*West University of Timisoara, Timisoara, Romania*

E-mail: masha.balasoIU@gmail.com

In this paper the magnetite and cobalt ferrite mesoporous nanoparticles synthesized by co-precipitation method using various stabilizing agents such as: L-aspartic acid, L-proline and L-asparagine are investigated by means of small-angle neutron and X-ray scattering methods.

For preparation of mesoporous magnetite, the following precursors have been used: sodium hydroxide – NaOH (Sikal Trading), iron (III) chloride – FeCl₃ (Sigma-Aldrich), ammonium iron (II) sulphate hexahydrate – Fe(NH₄)₂(SO₄)₂ · 6H₂O (Sikal Trading), L-proline C₅H₉NO₂ (Riedel-De Haën Ag Seelze-Hannover), L-aspartic acid C₄H₇NO₄ (Merck), L-asparagine C₄H₈N₂O₃ (Sigma). Earlier investigation [1] by using Fourier Transform InfraRed Spectroscopy (FTIR), powder X-ray diffraction (XRD), Brunauer–Emmett–Teller (BET) and scanning electron microscopy (SEM) of the use of L-asparagine, L-aspartic acid, L-proline as stabilizing agents of the magnetite core have shown important morphological changes which can be exploited in medical applications.

[1] I.L. Ardelean, D. Ficai, A. Ficai, G. Nechifor, D. Dragu, C. Bleotu (2018). Synthesis and characterization of new magnetite nanoparticles by using the different amino acids such as stabilizing agents, U.P.B. Sci. Bull., Series B, 80(1), 33-46.

CRYSTALLOGRAPHIC AND SMALL ANGLE SCATTERING STUDIES OF HEMOGLOBIN CRYSTAL NUCLEATION AND CLUSTER FORMATION

I. Baranova^{1,2}, A. Angelova³, Yu. E. Gorshkova⁴, J. Stransky⁵ and B. Angelov¹

¹*Institute of Physics, ELI Beamlines, Academy of Sciences of the Czech Republic, CZ-18221 Prague, Czech Republic*

²*MFF, Charles University, CZ-12116 Prague, Czech Republic*

³*Université Paris-Saclay, CNRS, Institut Galien Paris-Saclay, F-92296 Châtenay-Malabry, France*

⁴*Frank Laboratory of Neutron Physics, Joint Institute for Nuclear Research, Joliot-Curie Str. 6, 141980 Dubna, Russian Federation*

⁵*Institute of Biotechnology of the Czech Academy of Sciences, v.v.i., Prumyslová 595, Vestec, 252 50, Czech Republic*

E-mail: iuliia.baranova@eli-beams.eu

Hemoglobin is a key iron-containing oxygen-transport protein in the human red blood cells and in almost all vertebrates. The 3D structure of the hemoglobin molecule has been determined by X-ray crystallography since the early works of Max Perutz in 1959. In the context of COVID-19, it has been recently shown that lower hemoglobin levels increase the risk for severe respiratory failure [1]. We used X-ray diffraction (XRD) and small-angle neutron scattering (SANS) to investigate the cluster formation and the crystal nucleation of commercial protein hemoglobin in different crystallization media. The effects of pH variations and polyethylene glycol (PEG) concentrations in the nucleant solutions were examined in order to find suitable conditions for single protein crystal formation. The XRD results established the quality of the obtained hemoglobin crystals and the corresponding crystallographic resolution. The performed SANS and gel chromatography experiments revealed the existence of protein monomers and dimers as well as the formation of higher order clusters in the investigated nucleant media. The obtained crystals were either disk-like or wire-like, but never developed a complete 3D structure. Despite that this effect has been previously observed, it has not been systematically investigated and explained yet. Our results elucidate the structural diversity of the commercial hemoglobin nucleation and pave the road for obtaining higher resolution crystal structures of hemoglobin [2].

The performed research was funded by the projects “Advanced research using high-intensity laser produced photons and particles” (CZ.02.1.01/0.0/0.0/16_019/0000789) and “Structural Dynamics of Biomolecular Systems” (ELIBIO) (CZ.02.1.01/0.0/0.0/15_003/0000447) from the European Regional Development Fund. We acknowledge CMS-Biocev (“Biophysical techniques, Crystallization, Diffraction, Structural mass spectrometry”) of CIISB, Instruct-CZ Centre, supported by MEYS CR (LM2018127). B.A. obtained a financial support from the collaborative project with JINR, Dubna, Russia (3+3 program, No. 204, item 27 from 25.03.2020). AA acknowledges a membership in CNRS GDR2088 BIOMIM network.

[1] M. Anai, K. Akaike et al., (2021). Decrease in hemoglobin level predicts increased risk for severe respiratory failure in COVID-19 patients with pneumonia. *Respiratory Investigation*, 59, 187-193.

[2] I. Baranova, A. Angelova, W.E. Shepard, J. Andreasson, and B. Angelov, (2022) Cubic Ice Crystallization under Cryogenic Cooling in a Lipid Membrane Nanoconfined Geometry: Time-Resolved Structural Dynamics, *Communications Chemistry*, submitted.

CHROMATIN STRUCTURE IN THE TUMOR CELLS WITH RADIORESISTANT PHENOTYPE

Nikolay Verlov¹, Dmitry Lebedev¹, Vladimir Burdakov¹, Lyubov Ivanova¹, Gennady Kopitsa¹, Yulia Gorshkova², L. Almasy³

¹*Petersburg Nuclear Physics Institute NRC KI, Orlova Roscha, Gatchina, Russian Federation*

²*Frank Laboratory of Neutron Physics Joint Institute for Nuclear Research, Dubna, Russian Federation*

³*Budapest Neutron Centre, Hungary*

E-mail: burdakov_vs@pnpi.nrcki.ru

The use of radiation therapy in the treatment of malignant neoplasms has long faced the problem of the emergence of tumor cells with radioresistant phenotype [1]. The mechanisms of radioresistance are commonly associated with the activation of signaling pathways and molecular cascades, including repair factors and inhibition of apoptosis pathways [2]. However, such changes in the cell metabolism and transcriptional patterns appear unlikely to be induced on a pure genetic level, but rather seem to involve epigenetic mechanisms that may in turn rely on the changes in the chromatin arrangement in the cell nucleus [3]. Changes in the density of chromatin packing could have additional effects on radioresistance by increasing the availability of the damaged DNA for repair and decreasing the stacking density and therefore the likelihood of the formation of intra- and inter-strand cross-links. Using cytometry, confocal microscopy, and small angle scattering we have investigated the structural properties of chromatin isolated by the standard procedure [4] from cells exposed to γ -radiation. including radioresistant phenotype of the Ehrlich's adenocarcinoma cells (transplantable after irradiation of 40 Gy, compared to 20 Gy in the initial cell population) that was obtained in a series of tumor irradiations. The results of SANS and SAXS measurements show that in contrast with the normal rat lymphocytes, on the scales 10-100 nm the chromatin arrangement of Ehrlich's adenocarcinoma cells was only slightly affected by radiation doses up to 2 kGy, while most of the changes in chromatin in response to radiation were observed on the scales ~2-3 nm that corresponds to the size of the DNA double helix. A comparative analysis of the data obtained by various methods in conjunction with data on the radioresistant properties of the studied cell population indicate that chromatin structural organization exhibits different behavior in response to radiation damage in the cells with different radiosensitivity.

The study was supported by NRC "Kurchatov Institute" (№2757).

[1] F. Windholz (1947). Problems of Acquired Radioresistance of Cancer: Adaptation of Tumor Cells. *Radiology*. 48(4), 398–404.

[2] K. Sato, T. Shimokawa, T. Imai (2019). Difference in Acquired Radioresistance Induction Between Repeated Photon and Particle Irradiation. *Front. Oncol.* 9, 1213.

[3] D.V. Lebedev, Y.A. Zabrodskaya, V. Pipich (2019). Effect of alpha-lactalbumin and lactoferrin oleic acid complexes on chromatin structural organization. *Biochem Biophys Res Commun.* 520(1), 136-139.

[4] D.V. Lebedev, M.V. Filatov, A.I. Kuklin (2008). Structural hierarchy of chromatin in chicken erythrocyte nuclei based on small-angle neutron scattering: Fractal nature of the large-scale chromatin organization. *Crystallography Reports.* 53(1), 110-115.

CHARACTERIZATION OF CATION-ZWITTERIONIC LIPID INTERACTIONS: SMALL ANGLE NEUTRON/X-RAY SCATTERING AND DENSITOMETRY STUDY

S. Kurakin,^{1,2} O. Ivankov,^{1,3,4} V. Skoi,^{1,5} A. Kuklin,^{1,5} and N. Kučerka^{1,6}

¹*Frank Laboratory of Neutron Physics, Joint Institute for Nuclear Research, Dubna, Russian Federation*

²*Institute of Physics, Kazan Federal University, Kazan, Russian Federation*

³*Taras Shevchenko National University of Kyiv, Kyiv, Ukraine*

⁴*Institute for safety problems of nuclear power plants NAS of Ukraine, Kyiv, Ukraine*

⁵*Moscow Institute of Physics and Technology, Dolgoprudnyi, Russian Federation*

⁶*Department of Physical Chemistry of Drugs, Faculty of Pharmacy, Comenius University in Bratislava, Bratislava, Slovakia*

E-mail: ksa18@list.ru

The study of interactions between divalent cations and lipid membranes is one of the key goals of membrane biophysics, since it is supposed that ions affect structure of phospholipid bilayers and modulate the insertion and binding of proteins. Lipid-ion interactions are determined by a set of both external and internal factors associated with the membrane structure. One of the most significant structural parameters is the average lateral area of a phospholipid in the lipid bilayer, which characterizes the packing density of lipids and it is of decisive importance in assessing intermolecular interactions occurring in lipid membranes. In this regard, SANS, SAXS, and densitometry were used in this work to study the structural changes in model lipid bilayers composed of zwitterionic phospholipids of various lateral areas (DMPC, POPC, DOPC) upon the addition of biologically relevant Ca^{2+} and Mg^{2+} cations. Based on the obtained structural parameters of these lipid bilayers, various mechanisms of lipid-ion interactions were proposed, which are apparently governed by the lateral area, namely, lipid packing density related to the average interlipid distance [1], [2]. In the bilayers with a close packing of phospholipids (e.g., DMPC), the interlipid distance is small enough that it leads to the formation of lipid-ion-lipid bridges. This causes a membrane condensing in lateral direction. On the other hand, in a less densely packed lipid bilayer (e.g., DOPC), ions predominantly interact with lipids by forming separated lipid-ion pairs, which fluidizes the bilayer by enlarging its lateral area and reducing the thickness. In the case of POPC with a lateral area of $\sim 64 \text{ \AA}^2$, the average interlipid distance is approximately equal to the cutoff length of lipid-ion interactions, leading to a mixed type of interactions, where the two effects on the lipid bilayer structure are mutually compensated.

This work was supported by the Russian Science Foundation under grant № 19-72-20186 and JINR AYSS-2022 grant № 22-402-02.

[1] N. Kučerka, E. Ermakova, E. Dushanov, K.T. Kholmurodov, S. Kurakin, K. Želinská, D. Uhríková (2021). Cation-zwitterionic lipid interactions are affected by the lateral area per lipid. *Langmuir*. 37, 278-288.

[2] S.A. Kurakin, E.V. Ermakova, O.I. Ivankov, S.G. Smerdova, N. Kučerka (2021). The Effect of Divalent Ions on the Bilayer Structure of Dimyristoylphosphatidylcholine Vesicles. *Journal of Surface Investigation: X-ray, Synchrotron and Neutron Techniques*. 15, 211-220.

**METHODS OF FUNDAMENTAL PHYSICS AND APPLIED MATHEMATICS,
THERE IS NO SILVER LINING OR HOW TO TREAT CHRONIC DISEASES
WITH COVID**

N.V. Makhaldiani¹

¹*JINR, Dubna, Russian Federation*

E-mail: mnv@jinr.ru

Immunity interferes with the treatment of chronic diseases. Covid weakens the immune system, so it becomes possible and necessary to treat chronic diseases using modern methods of fundamental physics and applied mathematics.

DEVELOPMENT AND OPERATION TESTS OF THE TEMPERATURE/HUMIDITY SAMPLE CELL FOR NEUTRON REFLECTOMETRY

Ye.N. Kosiachkin^{1,2,3}, T.V. Tropin¹, M.V. Avdeev^{1,4} and L.A. Bulavin²

¹Frank Laboratory of Neutron Physics, Joint Institute for Nuclear Research, Dubna, Russian Federation

²Physics Department, Taras Shevchenko National University of Kyiv, Kyiv, Ukraine

³Institute for Scintillation Materials of NAS of Ukraine, Kharkiv, Ukraine

⁴Dubna State University, Moscow, Russian Federation

E-mail: kosiachkin@jinr.ru

Experimental investigations of materials structure and prototype devices performance at various conditions represent a growing field in science. Concerning neutrons and X-ray scattering investigations this is reflected by the increasing number of proposals in materials science submitted to the international research facilities. As a consequence, specific cells that provide various conditions at the sample are required.

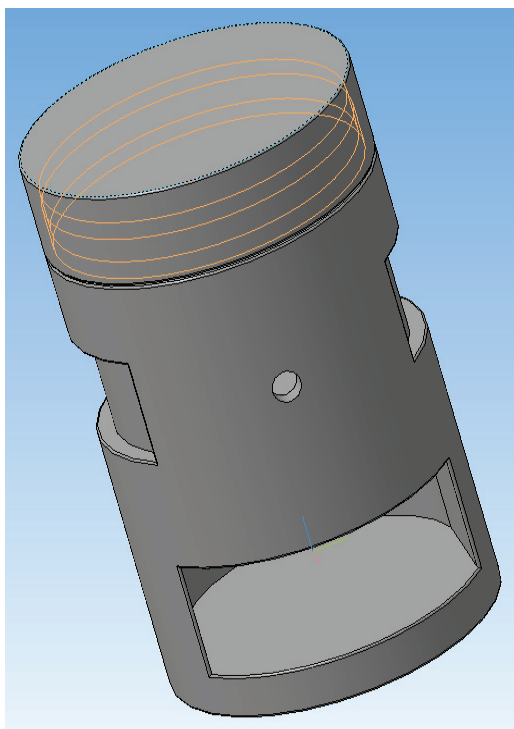


Figure. 1. Principal scheme of the temperature/humidity sample cell.

In this work, we report the development of a special cell with variable temperature and humidity for neutron scattering investigations of hybrid perovskite thin films by neutron reflectometry. The cell will be expected to provide a temperature range from room temperature up to 150°C and the relative humidity in the range of 40-100%. The principal scheme of the cell is presented in Figure 1 (cell dimensions ~20 × 30 cm). The thin (width < 1 mm) Al windows provide transparency for neutrons, within the heating elements enveloping the cell. The humidity will be controlled by the solutions of selected salts/alkali placed in a special bath located inside. Temperature and humidity are regulated through special entries in the cell case. The cell is planned to be used at the GRAINS time-of-flight neutron reflectometer (horizontal sample plane) at the IBR-2 pulsed reactor.

First tests of the cell regarding heating curves and humidity control will be presented. The measurements of test samples after temperature/humidity treatment are planned. The applications of the cell for studying hybrid perovskite thin film layers degradation at high temperatures/humidity for solar power sources will be discussed.

This study was supported by Russian Science Foundation, project 22-22-00281.

STRUCTURING OF TRISILOXANES-BASED SUPERSPREADERS AT INTERFACE AND IN BULK BY NEUTRON SCATTERING

N.A. Ivanova¹, M.O. Kuzmenko², I.V. Gapon^{2,4}, M.V. Avdeev², O.P. Artykulnyi^{2,3}, O.I. Ivankov³, L.A. Bulavin³

¹ *Photonics and Microfluidics Lab, Tyumen State University, Tyumen, Russian Federation*

² *Frank Laboratory of Neutron Physics, Joint Institute for Nuclear Research, Dubna, Moscow Region, Russian Federation*

³ *Physics Department, Kyiv Taras Shevchenko National University, Kyiv, Ukraine*

⁴ *Institute for Safety Problems of Nuclear Power Plants, NAS Ukraine, Chornobyl, Ukraine*

E-mail: kuzjaryna@gmail.com

Trisiloxanes-based surfactants, known as superspreaders, are widely used in agricultural industry [1]. However, some trisiloxane surfactants are toxic agents for honeybees and insect-pollinators, and pose a potential threat to human health. To develop biocompatible surfactants enabling the same effectiveness as trisiloxane surfactants, it is crucial to understand mechanism behind the superspreading effect. The mechanism is likely related to formation of multilayer aggregates of trisiloxane surfactant molecules in the bulk and at interfaces. Conditions at which trisiloxane surfactant solutions exhibit superspreading were proposed: (i) temperature of solutions is close to the phase transition temperature, T_{cp} , from transparent to turbid solution; and (ii) concentration of surfactants is above the critical wetting concentration (cwc) which is above the critical micelle concentration (cmc).

The aim of the current work was to investigate using neutron scattering how temperature variation influences structural conformation of molecular aggregates of trisiloxane surfactants during their adsorption at a solid interface (by specular neutron reflectometry) and self-organization in a bulk phase (by small-angle neutron scattering). The solutions of trisiloxane surfactant with 9 ethoxy units (TEO_9) and commercial trisiloxane surfactant Silwet L-77 with 7.5 EO units were studied at concentrations of 1.5 cmc , 1.5 cwc , 5 cwc in D_2O . For comparison, the solution of hydrocarbon surfactant $C_{12}EO_8$ at 5 cmc in D_2O was also investigated. Measurements were performed at different temperatures in the ranges below and above T_{cp} for each surfactant: Silwet L-77 ($T_{cp}=40^\circ C$), TEO_9 ($35^\circ C$), $C_{12}EO_8$ ($78^\circ C$). In the experiments on neutron reflectometry, silicon substrate was coated (magnetron deposition) by Ti film which then was oxidized to increase the wetting angle. Among three surfactants under study the adsorption layer of TEO_9 showed very low temperature sensitivity. For L-77 and $C_{12}EO_8$ the changes of the layer are observed at $T \geq T_{cp}$. For TEO_9 at $20^\circ C$ SANS data showed a transition from compact micelles (1.5 cwc) to anisotropic lamellar type micelles (5 cwc). The same transition takes place with the temperature increase (up to $T = 50^\circ C$) at 1.5 cwc . An increase in the temperature up to $75^\circ C$ results in the partial formation of a macrophase (with the Porod law in the scattering curve). The more the concentration the lower the temperature when this process starts.

[1] Ivanova, N.A., Kovalchuk, N.M., Sobolev, V.D., Starov, V.M., *Soft Matter*, 2015, 12(1), 26–30

MODEL OF LARGE-SCALE CHROMATIN ORGANISATION IN BIOLOGICAL CELL NUCLEI ON SANS

E. G. Iashina^{1,2}, E. Yu. Varfolomeeva¹, R. A. Pantina¹, V. Yu. Bairamukov¹,
R.A. Kovalev¹, N. D. Fedorova¹, V. Pipich³, A. Radulescu³, K.A. Pshenichnyi¹,
P.M. Pustovoit¹, O.D. Shnyrkov¹ and S. V. Grigoriev^{1,2}

¹*Petersburg Nuclear Physics Institute (PNPI), NRC Kurchatov Institute, Gatchina, Russian Federation*

²*Saint-Petersburg State University (SPSU), Saint-Petersburg, Russian Federation*

³*Jülich Centre for Neutron Science (JCNS) at Heinz Maier-Leibnitz Zentrum (MLZ), Garching, Germany*

E-mail: yashina_91@inbox.ru

One of the most exciting question in the cellular biology is how can meters of DNA be packed inside the 5 to 10 μm nucleus. The concept of the fractal organization of chromatin is the most productive hypotheses that, however, is not well established yet. The Small-Angle Neutron Scattering (SANS) experiments have shown bi-fractal organization of the chromatin in nuclei of three different types of cells: rat lymphocytes, chicken erythrocytes and HeLa cells [1-]. The large scale structure from hundreds nanometers some micrometers well described by the logarithmic fractal, while a smaller scale structure from tens to hundreds of nanometers appears to be a volume fractal with dimension slightly less than 2.5. The volume fractal units are self-similar and built of the DNA and architectural proteins. The maximal size fractal unit correspond to a crossover point in SANS curves between two fractal levels. These fractal units are densely packed and occupy rather homogeneously almost all of the nucleus space. The logarithmic fractal structure stand out from the background of chromatin and is attributed to a chromatin-free space shaped as a system of the diffusion channels those sizes are hierarchically changed upon scaling obeying the volume preserving principle. We believe that these channels provides fast diffusion for functional proteins. To demonstrate compliance of our model to real large scale chromatin structure we have simulated SANS experiment building the logarithmic fractal a structure obeying volume reserving principle. We show the equivalence in the power law of scattering intensity for the proposed model and for the real experiments.

[1] E. G. Iashina, E. Yu. Varfolomeeva, R. A. Pantina, V. Yu. Bairamukov, R. A. Kovalev, N. D. Fedorova, V. Pipich, A. Radulescu and S. V. Grigoriev, PRE 104, 064409 (2021).

[2] S. V. Grigoriev, E. G. Iashina, B. Wu, V. Pipich, Ch. Lang, A. Radulescu, V. Yu. Bairamukov, M. V. Filatov, R. A. Pantina, and E. Yu. Varfolomeeva, PRE 104, 044404 (2021).

[3] Grigoriev S. V., Iashina, E. G., Bairamukov, V. Y., Pipich, V., Radulescu, A., Filatov, M. V., ... Varfolomeeva, E. Y., PRE 102, 032415 (2020).

[4] Iashina E. G., Grigoriev S. V., JETP, 129, 3, 455-458 (2019).

[5] Iashina E. G., Filatov, M. V., Pantina, R. A., Varfolomeeva, E. Y., Bouwman, W. G., Duif, C. P., ... Grigoriev, S. V., Journal of Applied Crystallography, 52, 4, 844-853 (2019).

[6] Iashina E. G., Grigoriev S. V., Journal of Surface Investigation: X-ray, Synchrotron and Neutron Techniques, 11, 5, 897-907 (2017).

[7] Iashina E. G., Velichko, E. V., Filatov, M. V., Bouwman, W. G., Duif, C. P., Brulet, A., Grigoriev, S. V., PRE 96, 1, 012411 (2017).

[8] Iashina E. G., Bouwman, W. G., Duif, C. P., Filatov, M. V., Grigoriev, S. V., Journal of Physics: Conference Series, 862, 1 (2017).

STABILITY OF TRIMERS OF DIMERS OF *Np*SRII/*Np*HtrII COMPLEX AT LOW SALT CONCENTRATION

D. D. Kuklina¹, Yu.L. Ryzhykau^{1,2}, V. I. Gordeliy^{1,3,4,5} and A.I. Kuklin^{1,2}

¹Research Center for Mechanisms of Aging and Age-Related Diseases, Moscow Institute of Physics and Technology, 141700 Dolgoprudny, Russian Federation

²Frank Laboratory of Neutron Physics, Joint Institute for Nuclear Research, 141980 Dubna, Russian Federation

³Institute of Biological Information Processing (IBI-7: Structural Biochemistry), Forschungszentrum Jülich, 52425 Jülich, Germany

⁴JuStruct: Jülich Center for Structural Biology, Forschungszentrum Jülich, 52428 Jülich, Germany

⁵Institut de Biologie Structurale Jean-Pierre Ebel, Université Grenoble Alpes–Commissariat à l’Energie Atomique et aux Energies Alternatives–CNRS, F-38027 Grenoble, France

E-mail: kuklina.dd@phystech.edu

The subject of conducted research is a protein complex of sensory rhodopsin II (SRII) and its cognate transducer (HtrII) from archaea *Natronomonas pharaonis*. The complex represents a family of TCS (Two-Component Systems), which consist of a transmembrane receptor and adaptor proteins attached at their cytoplasmic tips. TCS are the most common signaling systems in all domains of life, however are absent in mammalian cells. This fact forms the interest in clarification of signal pathways through the bacterial membrane.

*Np*SRII/*Np*HtrII mediates negative phototaxis in halobacterial *N. pharaonis* and, similarly to chemoreceptors, the *Np*SRII/*Np*HtrII complex forms trimers of dimers in the *N. pharaonis* membrane [1]. *N. pharaonis* grows optimally at 3.5 M NaCl. It has been shown that structure and oligomerization state of the *Np*SRII/*Np*HtrII strongly depend on salt concentration [2]. In a previous research [3,4] small-angle neutron scattering (SANS) measurements were performed on the YuMO spectrometer (IBR-2, Dubna, Russia) with two-detector system [5,6]. It has shown that only at high salt concentrations the *Np*SRII/*Np*HtrII complex is able to form trimers of dimers, while at low salt concentrations the scattering curve is perfectly fit by dimers.

In this research, we present the result of chromatographic analysis, showing the stability of trimers of dimers. The fraction of trimers of dimers was transferred into low-salt buffer by gel-filtration. Further analysis by size exclusion chromatography shows that the protein is eluting at the same volume position as the trimers of dimer. It has proved the stability of trimers of dimers of the *Np*SRII/*Np*HtrII at low salt concentration even on time scales of several days.

The discovered stability of oligomeric state of trimers of dimers at low salt conditions can be used for the following studies in procedures that work better with low-salt buffers, such as reconstitution to nanodiscs or lipid vesicles, preparation of grids for cryo-EM studies, etc.

The reported study was funded by Russian Foundation for Basic Research (project no. 20-54-12027) and Deutsche Forschungsgemeinschaft (project no. 430170559).

[1] Orekhov, P. *et al.* Sensory Rhodopsin I and sensory Rhodopsin II form trimers of dimers in complex with their cognate transducers. *Photochem. Photobiol.* 93, 796–804 (2017)

[2] Budyak, I. L. *et al.* Shape and oligomerization state of the cytoplasmic domain of the phototaxis transducer II from *Natronobacterium pharaonis*. *Proc. Natl. Acad. Sci. USA* 103, 15428–15433 (2006)

[3] Ryzhykau, Y.L., Orekhov, P.S., Rulev, M.I. *et al.* Molecular model of a sensor of two-component signaling system. *Sci Rep* 11, 10774 (2021)

- [4] Ryzhykau, Y.L., *et al.* Ambiguities in and completeness of SAS data analysis of membrane proteins: the case of the sensory rhodopsin II–transducer complex. *Acta Cryst D* 77, 1386-1400 (2021)
- [5] Kuklin, A. I., Islamov, A. K. & Gordeliy, V. I. Scientific reviews: Two-detector system for small-angle neutron scattering instrument. *Neutron News* 16, 16–18 (2005)
- [6] Kuklin, A. I. *et al.* New opportunities provided by modernized small-angle neutron scattering two-detector system instrument (YuMO). *J. Phys. Conf. Ser.* 291, 012013 (2011)

MAGNETIC STRUCTURE OF Dy-Co NEAR THE COMPENSATION TEMPERATURE

M.V. Makarova^{1,2}, E.A. Kravtsov^{1,2}, Yu. Khaydukov³

¹*Institute of Metal Physics, Ural Branch of the Russian Academy of Sciences, Ekaterinburg, Russian Federation*

²*Ural Federal University, Ekaterinburg, Russian Federation*

³*Max Planck Institute for Solid State Physics, Stuttgart, Germany*

E-mail: makarova@imp.uran.ru

Rare-earth – transition metals (REM/TM) superlattices and alloys are a large class of magnetic materials allowing us to change their properties in a wide range through a change in the composition, temperatures or application magnetic field. Disordered ferrimagnetic (FI) materials demonstrate some very interesting properties, for example, magnetization compensation point, a point at which there is no magnetization below the Curie temperature [1]. Compared with their crystalline counterparts, the amorphous materials can have differing spin moments, a changed band structure, and strikingly different exchange values. Last years, interest in the Dy/Co system has increased, since it became possible to switch the magnetization of the system without applied magnetic field by means of a femtosecond laser pulses [2]. Important requirements for achieving switchable magnetic films are antiferromagnetic coupling between spins of REM and TM and perpendicular magnetic anisotropy (PMA) [3]. Therefore, it is crucial to find the correlation between the microstructure of thinner and thicker multilayers and their magnetic properties. The aim of this investigation was to define the influence of Dy thicknesses on the magnetic properties of Dy/Co multilayers.

The results investigation of the Dy/Co magnetic behavior, carried out by complementary methods: polarized neutron reflectometry and the magneto-optical Kerr effect (MOKE), are described. Using X-ray reflectometry, it was found that during the deposition of a layered structure, the Dy and Co layers are partially mixed with the formation of the DyCo₂ intermetallic compound [4]. To understand the mechanisms of effects observed in magnetic superlattices, we determined the magnetization profiles inside individual layers and found that a noncollinear magnetic state is observed near the compensation point. The triple hysteresis loops observed near the compensation temperature by MOKE can be explained by the inhomogeneity of the sample. PMA heterostructures containing FM (Co) in contact with a ferrimagnet (DyCo₂) can have potential applications in devices that require magnetization reversal by femtosecond laser pulses [5].

The results were obtained within the state assignment of Ministry of Education and Science of Russia (subject “Spin” no. AAAA-A18-118020290104-2) supported in part by RFBR (projects no. 20-42-660024).

[1] R.C. Taylor and A. Gangulee (1980). *Phys.Rev. B.* 22, 1320.

[2] T. Li, A. Patz, L. Mouchliadis, J. Yan, T.A. Lograsso, I.E. Perakis, J. Wang (2013). *Nature.* 496, 69–73.

[3] S. Mangin, T. Hauet, P. Fischer, D. H. Kim, J. B. Kortright, K. Chesnel, E. Arenholz, E. E. Fullerton (2008). *Phys. Rev. B* 78 024424.

[4] I.A. Subbotin, E.M. Pashaev, A.L. Vasiliev, Yu.M. Chesnokov, G.V. Prutskov, E.A. Kravtsov, M.V. Makarova, V.V. Proglyado, V.V. Ustinov (2019). *Physica B.* V. 573. 28.

[5] J. He, H. Liao, Z. Zhang, B. Ma, Q. Y. Jin (2011). *J. Appl. Phys.* 109, 023907.

STUDY OF THE EFFECT OF A WATER-SOLUBLE MONOMER ON MICELLES OF SURFACTANTS FOR MICELLAR POLYMERIZATION PROBLEMS

A.S. Ospennikov¹, A.A. Gavrilov¹, A.I. Kuklin^{2,3}, A. V. Shibaev¹, O.E. Philippova¹

¹ *Physics Department, Lomonosov Moscow State University, 119991 Moscow, Russian Federation*

² *Frank Laboratory of Neutron Physics, Joint Institute for Nuclear Research, 141980, Dubna, Russian Federation*

³ *Moscow Institute of Physics and Technology, 141701 Dolgoprudny, Russian Federation*

E-mail: aleks-16-1999@mail.ru

Recently, the study of wormlike micelles of surfactants has attracted much attention due to their remarkable rheological properties. Supramolecular surfactant chains are highly sensitive to external factors due to the nature of non-covalent interactions that bind molecules together within a micelle. However, the reaction of worm-like micelles to non-polar substances, for example, hydrophobic water-insoluble monomers, has been studied so far. The influence of water-soluble monomers has been studied in much less detail. At the same time, studying the interaction of vinyl monomers with worm-like micelles is an equally important issue for creating networks of hydrophobically modified polymers by emulsion copolymerization.

In this work, we studied the effect of a water-soluble monomer, acrylamide, on micelles of a worm-like surfactant for the purpose of further polymerization and the preparation of polyacrylamide/surfactant networks. It was found that acrylamide has a different effect on linear and branched micelles: for linear micelles (at low salt concentrations), the viscosity immediately decreases, and for branched micelles (at high salt concentrations), it first increases and then decreases. It has been shown by small-angle neutron scattering that linear cylindrical micelles are transformed into spherical micelles, and branched micelles are transformed into short cylindrical micelles. This difference in the behavior of linear and branched micelles is associated with different packing of surfactant molecules due to shielding of electrostatic interactions with changing salt concentration. It has been shown by fluorescence spectroscopy that some of the acrylamide molecules are incorporated into micelles, which causes changes in their structure. Using computer modeling, it was found that only a part of acrylamide molecules interact with micelles, while most of them are in aqueous solution and do not penetrate into micelles. The characteristic size of micelles at a high monomer concentration was determined.

Thus, it has been shown that acrylamide causes the destruction of the network of long micelles and their transformation into much smaller aggregates. This is caused by the interaction of acrylamide molecules with micelles, which is directly proven by various methods.

The work was financially supported by the Russian Science Foundation (project 21-73-10197).

STRUCTURE, SYNERGISTIC ENHANCEMENT OF VISCOELASTIC PROPERTIES AND RESPONSIVENESS TO HYDROCARBONS OF A NEW MIXED VISCOELASTIC SURFACTANT SYSTEM

A.S. Ospennikov¹, A.I. Kuklin^{2,3}, A. V. Shibaev¹, O.E. Philippova¹

¹ *Physics Department, Lomonosov Moscow State University, 119991, Moscow, Russian Federation*

² *Frank Laboratory of Neutron Physics, Joint Institute for Nuclear Research, 141980, Dubna, Russian Federation*

³ *Moscow Institute of Physics and Technology, 141701, Dolgoprudny, Russian Federation*

E-mail: aleks-16-1999@mail.ru

Surfactant molecules can self-assemble into long cylindrical or wormlike micelles (WLMs). WLMs can entangle and form a transient network with viscoelastic properties even at moderate surfactant concentrations. Also, micellar chains are highly responsive to external stimuli, e.g. to the addition of hydrocarbons, which can break the micelles. Viscoelasticity and responsiveness of the micellar networks is widely exploited in practical applications. For instance, these are the key properties for the application of surfactant solutions as hydraulic fracturing fluids in oil recovery. Therefore, a search for new surfactant systems with high viscoelasticity and responsiveness is of high demand. In the present work, we investigate a new viscoelastic surfactant system comprised by a mixture of an anionic (potassium oleate) and a cationic (1-dodecylpyridinium chloride) surfactants [1].

First, we investigated the influence of the molar ratio of cationic to anionic surfactant on the structure and rheological properties of the mixed system. A transition from spherical to cylindrical micelles was observed upon increasing content of cationic surfactant. By SANS it was discovered that the cylindrical micelles have an elliptical cross-section with a major radius close to the length of longer anionic surfactant tail and minor radius close to the length of shorter cationic surfactant tail. 1H NMR NOESY and SANS data suggest that both surfactants are segregated on the surface of the micelles. The viscosity goes through a maximum with increasing content of cationic surfactant, and at an optimal ratio of surfactants, the system shows high viscoelasticity. SANS data show that mixed surfactant system is responsive to hydrocarbons, which is a result of transformation of long cylindrical micelles into ellipsoidal microemulsion droplets.

The work was financially supported by the Russian Science Foundation (project 21-73-30013).

[1] A.V. Shibaev, A.S. Ospennikov, A.I. Kuklin, N.A. Arkharova, A.S. Orekhov, O.E. Philippova. Structure, rheological and responsive properties of a new mixed viscoelastic surfactant system. *Coll. Surf. A. Phys.-Chem. Eng. Asp.* 2020, 586, 124284

NOVEL RESORCINOL-FORMALDEHYDE AEROGELS: SYNTHESIS, STRUCTURE AND FRACTAL PROPERTIES

A.A. Pavlova^{1,2}, S.A. Lermontov³, A. N. Malkova³, Yu.E. Gorshkova⁴, V.V. Volkov⁵,
A.E. Baranchikov⁶, G.P. Kopitsa^{1,7}

¹ *Petersburg Nuclear Physics Institute NRC KI, Gatchina, Russian Federation*

² *Saint Petersburg State University, Saint-Petersburg, Russian Federation*

³ *Institute of Physiologically Active Compounds of the Russian Academy of Sciences, Chernogolovka, Russian Federation*

⁴ *Frank Laboratory of Neutron Physics, Joint Institute for Nuclear Research, Dubna, Moscow district, Russian Federation*

⁵ *FSRC "Crystallography and Photonics" of the Russian Academy of Sciences, Moscow, Russian Federation*

⁶ *Kurnakov Institute of General and Inorganic Chemistry of the Russian Academy of Sciences, Moscow, Russian Federation*

⁷ *Institute of Silicate Chemistry of the Russian Academy of Sciences, Saint-Petersburg, Russian Federation*

E-mail: alina.pavlova.htsc@gmail.com

Organic aerogels belong to a very attractive class of aerogel materials possessing both the properties inherent to traditional oxide aerogels (high specific surface and porosity, low apparent density), and unique flexible chemical composition (e.g. the presence of various functional groups). Organic aerogels can be synthesized by polycondensation of resorcinol and formaldehyde producing so-called resorcinol-formaldehyde (RF) aerogels. RF aerogels possess high porosity, specific surface area and pore volume, as well as low thermal conductivity (for instance, RF aerogels are better thermal insulators than commercial fiber glass). On the other hand, RF aerogels are stiffer and stronger than inorganic aerogels. During the synthesis of RF-aerogels, pH of a reaction mixture, concentration and resorcinol/formaldehyde ratio, the type of gelation catalyst (acid or base), and resorcinol/catalyst ratio govern the structural characteristics (density, specific surface area, particle size, pore size distribution).

In the present work, the small angle neutron scattering (SANS), the small angle X-ray scattering (SAXS) and low temperature nitrogen adsorption techniques have been used to study the mesostructure and fractal properties of resorcinol-formaldehyde aerogels prepared by the reaction between resorcinol and formaldehyde using different solvents (acetonitrile or perfluoroacetone). Additionally, RF-lyogels were aged at various temperatures from 20 to 70°C to achieve fine-tuning of the structure of aerogel materials.

The synthesis of the resorcinol-formaldehyde lyogels was conducted using acetonitrile and hexafluoroacetone hydrate as solvents. Hexafluoroacetone hydrate plays not only a role of a solvent, but also a gelling agent for the synthesis of RF-lyogels, this approach for the RF-lyogels synthesis was used for the first time. Supercritical drying in CO₂ allowed synthesizing monolithic (including flexible) RF aerogels possessing specific surface up to 400 m²/g, specific porosity up to 1.3 cm³/g. All the obtained RF-aerogels were hydrophilic.

Both the amount and type of the solvent used at the gelation stage allow varying the texture characteristics and the microstructure of the resultant RF-aerogels. In particular, the use of acetonitrile as a solvent resulted in aerogels with a highly developed surface; on the contrary, the use of hexafluoroacetone hydrate lead to the formation of macroporous aerogels consisting of submicron dense spherical particles with a virtually smooth surface. The rate of RF lyogel formation is governed by the type of the solvent used. In acetonitrile, the gel formed in several hours, in hexafluoroacetone hydrate – in a few seconds. The increase in the ageing temperature of RF-lyogels from 20 to 70°C resulted in

a significant decrease in the surface fractal dimension DS of aerogels (from ~ 2.5 to 2.0), which indicated a significant smoothing of the surface of the nanoparticle aggregates during the ageing process. On the contrary, the ageing temperature did not virtually affect the size of nanoparticle aggregates. A significant increase in the size of nanoparticle aggregates occurs when the gelling system is diluted (an increase in the amount of the solvent used).

The work was supported by Russian Science Foundation (grant 19-73-20125).

INTERACTION OF N,N'-DISUBSTITUTED BENZIMIDAZOLE-2-THIONE DERIVATIVES CONTAINING VANILLOID-LIKE FRAGMENTS WITH MODEL PHOSPHOLIPID MEMBRANES

D. Yancheva¹, Z. Slavkova² and M. Dimitrov¹, N. Hristova-Avakumova³, N. Anastassova¹

¹ *Institute of Organic Chemistry with Centre of Phytochemistry, Bulgarian Academy of Sciences, Sofia, Bulgaria*

² *Institute of Solid State Physics, Bulgarian Academy of Sciences, Sofia, Bulgaria*

³ *Department of Medical Physics and Biophysics, Faculty of Medicine, Medical University of Sofia, Sofia, Bulgaria*

E-mail: zslavkova@issp.bas.bg

Vanilloid compounds, such as apocynin (4-hydroxy-3-methoxy-acetophenone), capsaicin ((E)-N-(4-Hydroxy-3-methoxybenzyl)-8-methylnon-6-enamide) and syringaldehyde have shown antioxidant and promising neuroprotective effects. The N,N'-disubstituted benzimidazole-2-thione combining one benzimidazole core with two vanillin residues, linked through hydrazone side chains have also exhibited low toxicity, good radical-scavenging properties and neuroprotective activity on isolated rat brain synaptosomes in the model of 6-OHDA-induced oxidative stress [1].

The effects were attributed to the ROS scavenging activity and the preservation of the synaptosomal glutathione levels. Considering the fact that another N,N'-disubstituted benzimidazole-2-thione with vanilloid-like fragments – namely syringaldehyde residues, also had good radical-scavenging properties, but only the vanillin derivative protected effectively the synaptosomes from the 6-OHDA-induced oxidative stress, it was concluded that the neuroprotective effect of the latter is mediated through a more complex pathway. It was hypothesized that similar to vanillin, the underlying neuroprotective mechanism of the benzimidazolethione-vanillin hybrid could be due to mitochondrial protection via inhibiting lipid and protein peroxidation. Moreover, it was demonstrated that phenolic acids with hydroxy/methoxy moieties such as the ferulic, p-coumaric and caffeic acid interact with lipid membranes and can establish hydrogen bonding with the polar head groups of the membrane phospholipids at the water–lipid interface of the membranes. These interactions might contribute to the membrane stabilization. In this context, it is considered of interest to study the effect of the benzimidazolethione-vanillin hybrid on a model lipid membrane using calorimetry and infrared spectroscopy techniques and possibly contribute to the understanding of its underlying neuroprotective mechanism.

This work has been financially supported by the National Science Fund of Bulgaria, Contract KII-06-M49/3. Research equipment of Distributed Research Infrastructure INFRAMAT, part of Bulgarian National Roadmap for Research Infrastructures, supported by Bulgarian Ministry of Education and Science was used in a part of this investigation

[1] N. Anastassova, D. Yancheva, N. Hristova-Avakumova, et al. (2020). New benzimidazole-aldehyde hybrids as neuroprotectors with hypochlorite and superoxide radical-scavenging activity. *Pharmacol. Rep* 72, 846-856

ON THE TEMPERATURE DEPENDENCE OF THE THICKNESS AND STRUCTURE C₇₀/POLYSTYRENE THIN FILMS

T.V. Tropin¹, Ye.N. Kosiachkin^{1,2,3}, O.V. Tomchuk^{1,2,4}, I.V. Gapon^{1,3}, S. Woloszczuk⁵ and M.V. Avdeev^{1,6}

¹*Frank Laboratory of Neutron Physics, Joint Institute for Nuclear Research, Dubna, Russian Federation*

²*Physics Department, Taras Shevchenko National University of Kyiv, Kyiv, Ukraine*

³*Institute for Safety Problems of Nuclear Power Plants, NAS of Ukraine, Chornobyl, Ukraine*

⁴*Institute of Environmental Geochemistry, NASU, Kyiv, Ukraine*

⁵*Faculty of Physics, Adam Mickiewicz University of Poznan, Poznan, Poland*

⁶*Dubna State University, Moscow, Russian Federation*

E-mail: ttv@jinr.ru

The investigations and application of polymer nanocomposites, consisting of different nanoparticles presented into polymer matrix, are on the rise since 1990s following a number of interesting discoveries. The researchers are interested in studying the physics that lead to the enhanced properties of these materials [1].

In this work, we are investigating the nanocomposite thin films, taking one of the most common polymers, atactic polystyrene (aPS), and the calibrated highly symmetric carbon nanoparticles, fullerenes. The system of aPS with fullerene C₆₀ has been a subject of interest for the last several years. Taking account of the recent results, we continue research in this field. Here we report the results of our investigations of the polystyrene-fullerene thin films prepared by spin-coating from toluene solutions on silicon substrates by neutron, X-ray reflectometry, and molecular dynamics simulations. A review of recently obtained results is given [2], as well as new measurements of thin films at different temperatures passing through the glass-transition range. The comparison of novel data with the data for fullerene C₆₀ (and other nanoparticles) may be important for discussion on future applications and enhancement of dispersion of nanoparticles in polymer matrix.

[1] M.A. Yaklin, P.M. Duxbury, M.E. Mackay (2008). Control of Nanoparticle Dispersion in Thin Polymer Films. *Soft Matter*. 4, 2441.

[2] T.V. Tropin, M.L. Karpets, Ye. Kosiachkin, I.V. Gapon, Yu.E. Gorshkova, V.L. Aksenov (2021). Evaluation of fullerenes C₆₀/C₇₀ layers in polystyrene thin films by neutron and X-ray reflectometry. *Fullerenes, Nanotubes and Carbon Nanostructures*. 15(4), 768-772.

TUNABLE SPIN-FLOP TRANSITION IN ARTIFICIAL FERRIMAGNETS

N. O. Antropov,^{1,2} E. A. Kravtsov,^{1,2} M. V. Makarova,^{1,2} V. V. Proglyado,¹ T. Keller,^{3,4} I. A. Subbotin,⁵ E. M. Pashaev,⁵ G. V. Prutskov,⁵ A. L. Vasiliev,^{5,6} Yu. M. Chesnokov,⁵ N. G. Bebenin,¹ M. A. Milyaev,¹ V. V. Ustinov,¹ B. Keimer,³ and Yu. N. Khaydukov^{3,4,7}

¹*Institute of Metal Physics, Ekaterinburg, Russian Federation*

²*Ural Federal University, Ekaterinburg, Russian Federation*

³*Max-Planck-Institute for Solid State Research, Stuttgart, Germany*

⁴*Max Planck Society Outstation at the Heinz Maier-Leibnitz Zentrum (MLZ), Garching, Germany*

⁵*National Research Center "Kurchatov Institute", Moscow, Russian Federation*

⁶*Moscow Institute of Physics and Technology, Dolgoprudniy, Russian Federation*

⁷*Skobeltsyn Institute of Nuclear Physics, Moscow State University, Moscow, Russian Federation*

E-mail: nikolayantropovekb@gmail.com

In this work we propose to use artificial ferrimagnets (FEMs) in which the spin-flop transition (SFT) occurs without anisotropy and the transition field can be lowered by adjusting exchange coupling in the structure. This is proved by experiment on artificial Fe-Gd FEMs where usage of Pd spacers allowed us to suppress the transition field by two orders of magnitude.

Spin-flop transition (SFT) consists in a jump-like reversal of antiferromagnetic (AF) lattice into a noncollinear state when the magnetic field increases above the critical value. Potentially the SFT can be utilized in many applications of a rapidly developing AF spintronics. However, the difficulty of using them in conventional antiferromagnets lies in (a) too large switching magnetic fields (b) the need for presence of a magnetic anisotropy, and (c) requirement to apply magnetic field along the correspondent anisotropy axis. artificial FEMs based on magnetic heterostructures give a possibility to tune the SFT field by varying parameters of ferromagnetic layers and by introducing nonmagnetic spacers.

In case of artificial FEMs magnetic signal from thin films is heavily polluted by dia- or paramagnetic signal of thick substrates. This makes it difficult, if not impossible at all, to use integral magnetometric methods to study the SFTs. Neutron scattering, being a depth-selective magnetometric technique is a widely used method for studying AFs and FEMs. Using PNR at N-rex instrument and complementary techniques, we performed a systematic study of magnetic configuration of [Fe(3.5 nm)/Pd(t)/Gd(5.0 nm)/Pd(t)]_{x12} heterostructures with $t = 8-28$ Å. By measuring neutron spin-flip scattering we have detected the presence of a magnetically noncollinear state at temperatures $T < 50$ K in magnetic fields of above $H > 500$ Oe for the samples with 10 Å $< t < 14$ Å. By using an extended Stoner-Wohlfarth model we were able to describe the observed transition as a competition of Zeeman energy, bilinear interaction of order of 1 erg/cm², and biquadratic addition of the order of 0.5 erg/cm². The coupling energies can be tuned by varying the thickness of the spacer between 1 and 1.4 nm leading to the shift of the transition field below kilo-Oersted range.

[1] N. O. Antropov et al., Tunable spin-flop transition in artificial ferrimagnets, *Physical Review B*. V. 104, 54414 (2021)

EFFECT OF HIGH TEMPERATURES ON THE MAGNETIC PROPERTIES OF Fe₃O₄ NANOPARTICLES

T.A. Darziyeva

Baku State University, Baku, Azerbaijan

E-mail: tamaradarziyeva@gmail.com

Among nanomaterials, metal nanoparticles are the most studied. It has been established that the addition of metal nanoparticles changes not only the mechanical properties of polymeric materials, but also other physical properties. Therefore, more and more new nanocomposite materials are being synthesized and their physical properties are being studied. To explain the various properties observed in composite materials, it is necessary to carefully study the properties of the components of these materials. Composite materials containing Fe₃O₄ nanoparticles also have magnetic properties, which expands the possibilities of their application [1-3]. Therefore, it is very important to study the magnetic properties of iron oxide nanoparticles, the influence of pressure and temperature on them.

In the present work, the magnetic properties of Fe₃O₄ nanoparticles with a size of $d = 20\text{--}30$ nm were studied. Fe₃O₄ nanoparticles were synthesized by Skyspring Nanopowder and Nanoparticles (SkySpring Nanomaterials, Inc. 2935 Westhollow Drive, Houston, TX, 77082, USA, <https://www.ssnano.com/>). The density of nanoparticles with a size of $d = 20\text{--}30$ nm was determined: $\rho = 4.8\text{--}5.1$ g/cm³. The sample was taken with a purity of 99%. The crystal structure of the samples was studied by the X-ray diffraction method, and the thermophysical properties were studied by the DSC method.

The magnetic properties of Fe₃O₄ nanoparticles were studied by vibrational magnetometry. This method is a unique method for studying the magnetic properties of solids under external influences (external magnetic field, temperature, etc.). The study of magnetic properties was carried out in the temperature range $T = 300\text{--}800$ K. It was found that Fe₃O₄ nanoparticles have ferromagnetic properties under normal conditions and at room temperature. The value of the specific magnetic moment was determined: $M = 33.4$ emu/g. It has been established that under the influence of temperature, a decrease in the value of the specific magnetic moment in Fe₃O₄ nanoparticles is observed. This is explained by an increase in the amplitude of vibrations of atoms in the crystal lattice under the influence of temperature. It is determined that at a temperature of $T_C = 655$ K, a ferromagnet-paramagnetic phase transition occurs and the value $M = 0$ is obtained.

[1] L.Shen, B.Li, Y.Qiao (2018). Fe₃O₄ nanoparticles in targeted drug/gene delivery systems, *Materials (Basel)*, 11, 2, 324.

[2] A.G.Magdalená, I.M.B.Silva, R.F.C.Marques, A.R.F.Pipi, P.N.Lisboa-Filho, M.Jafelicci (2018). EDTA-functionalized Fe₃O₄ nanoparticles, *Journal of Physics and Chemistry of Solids*, 113, P.5-10.

[3] A.Hasanpour, M.Mozaffari, J.Amighian (2007). Preparation of Bi-Fe₃O₄ nanocomposite through reduction of Bi₂O₃ with Fe via high-energy ball milling, *Physica B: Condensed Matter*, 387, 1-2, P.298-301.

SELF-ASSEMBLED PARTICLE LAYERING INDUCED BY ELECTRIC FIELD IN TRANSFORMER OIL-BASED FERROFLUID BY NEUTRON REFLECTOMETRY

M.L. Karpets^{1,2}, M. Rajnak^{1,2}, V.I. Petrenko^{3,4}, I.V. Gapon^{5,6}, M.V. Avdeev⁶, B. Izdikowski⁷, L.A. Bulavin⁵, M. Timko¹ and P. Kopcansky¹

¹ *Institute of Experimental Physics SAS, Košice, Slovakia*

² *Technical University of Kosice, Kosice, Slovakia*

³ *BCMaterials. Basque Centre for Materials, Applications and Nanostructures, Leioa, Spain*

⁴ *IKERBASQUE, Basque Foundation for Science, Bilbao, Spain*

⁵ *Taras Shevchenko National University of Kyiv, Kyiv, Ukraine*

⁶ *Joint Institute for Nuclear Research, Dubna, Russian Federation*

⁷ *Institute of Molecular Physics, Polish Academy of Sciences, Poznan, Poland*

E-mail: karpets@saske.sk

Understanding the physical-chemical processes during magnetic nanoparticles (MNPs) assembly and manipulation of the assembly process is highly important for synthesis of well-defined architectures from a nanometer scale and thus fabrication of such novel functional nanostructures will open horizon for new materials and devices. Assembly could lead to controllable NPs arrangement in bulk or at interfaces and it can be achieved just by using some template or external stimuli such as magnetic or electric fields. At interfaces, a uniform magnetic field amplifies the dipole-dipole interaction between MNPs in ferrofluids (due to one-direction alignment of particle magnetic moments) which enhances the layering of MNPs on a planar surface. The regulating properties by external electric fields for dielectric ferrofluids was recently reported based on the small-angle neutron scattering studies of a transformer oil-based ferrofluid (TOFF) showing bulk structuring and phase separation under electric fields [1]. The nanofluids are of practical importance - especially they have been used in several thermal management systems, as they contribute to the augmentation of the heat dissipation rates in many applications. The theoretical consideration [2] shows that sufficiently strong applied electric fields cause non-uniform distributions of particles between electrodes. The macroscopic structural changes in a simple ferrofluid consisting of iron oxide nanoparticles coated with oleic acid and dispersed in transformer oil under electric field have been proved [3]. Effects of magnetic field on ferrofluids at planar interface were revealed by neutron reflectometry (NR) based on the analysis of the evolution of specular reflectivity [4, 5].

The aim of this work is to investigate the interface structural changes in TOFF with magnetite nanoparticles as well as the magnetic fluid-solid interfaces under electric fields. An important question is whether electric fields, similar to magnetic fields, could be a driven force to induce the assembly of magnetic nanoparticles at the interface and whether formation of additional layers in ferrofluids at the inner surface of transformer could increase dielectric breakdown voltage. Specular reflectivity of non-polarized neutrons was measured at the neutron reflectometer GRAINS with a horizontal sample plane configuration installed at the IBR-2 pulsed reactor of JINR (Dubna, Russia). Assembling of superparamagnetic NPs of a dilute classical ferrofluid - magnetite coated with oleic acid in transformer oil – on a planar surface of the metal electrode (copper) was observed when an out-of-plane electric field is applied to the interface. The obtained NR curves were processed in a standard way in terms of the Parratt formalism using the Motofit package for the IGOR Pro software.

For the initial state (no electric field) the best fits are obtained when assuming one ‘wetting’ layer of MNPs on the surface. The corresponding SLD profile is presented in Fig. 1a. The reflectivity curves for the interface under electric field were fitted with all

fixed values of the solid components parameters and all vary parameters of FF components. The electric field induced evolution of the ‘liquid part’ of the interface in terms of the changes in the SLD profile is followed in Fig. 5b. As expected, the increase in the electric field slightly affects the structure of 1-st layer determined by the surfactant shell; one can see small reduction in thickness, roughness and SLD of this layer. More significant changes are observed for the 2-nd layer. It becomes thicker and more concentrated thus evidencing the enhanced adsorption of MNPs. The layer thickness grows with the electric field increase together with the SLD. Starting from 300 kV/m, the fits of the reflectivity curves are better if an additional layer #3 is introduced. At maximum field (700 kV/m) it becomes even higher. On the one hand, there is a tendency towards a saturation (regarding the content of MNP) of the two adsorption layers with the electric field increase. At the same time, some redistribution of MNP in the two layers takes place at maximum field intensity, reflecting a decrease of the MNPs content in the first layer. NR curves were also measured in different moments during 9 hours after the field of 700 kV/m was reduced to zero. It is interesting that the adsorbed layers evolve to some extent after the external field is switched off.

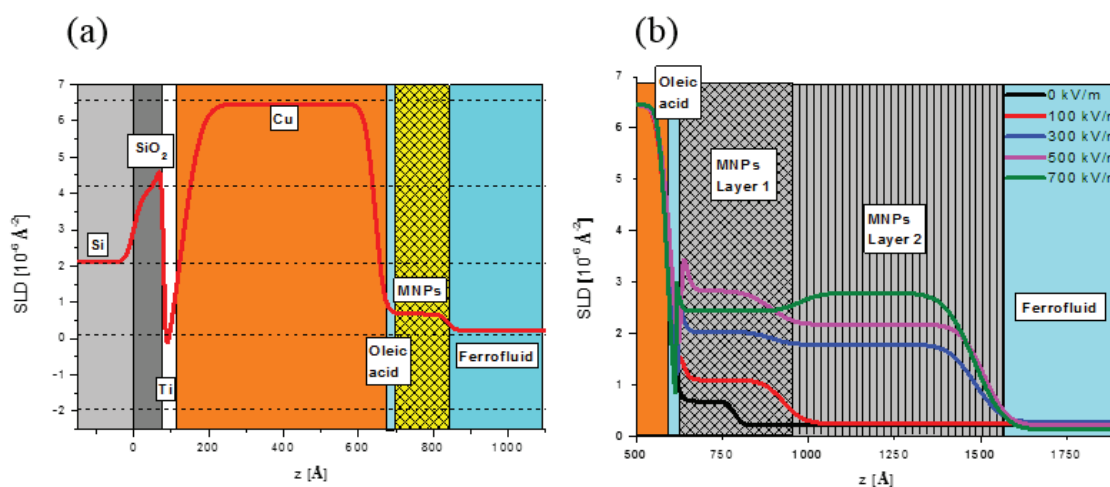


Figure 1. SLD depth profiles (plotted as a function of the distance z from the substrate surface) determined from the fits to the NR data (a) SLD profile in full z -range for zero field (initial configuration). For comparison, theoretical SLD values for the interface components are shown by dashed lines. (b) SLD profiles at the electrode-ferrofluid interface at different intensities of the external electric field.

The reason of the observed effects is related to the polarization of the particles in the electric field and their inter-action as dipoles. The observed self-assembled layering could be used as an additional barrier at the inner surface of transformer to increase dielectric breakdown voltage of working fluids.

- [1] M.Rajnak et al. (2015). Direct Observation of Electric Field Induced Pattern Formation and Particle Aggregation in Ferrofluids, *Appl. Phys. Lett.* 107, 073108.
- [2] P.A.Selyshchev et al. (2019). Non-Uniform Distribution of Ferrofluids Spherical Particles under External Electric Field: Theoretical Description, *J. Mol. Liq.* 278, 491–495.
- [3] M.Rajnak et al. (2017). Structure and Viscosity of a Transformer Oil-Based Ferrofluid Under an External Electric Field, *J. Magn. Magn. Mater.* 431, 99–102.
- [4] A. Nagorny et al. (2019). Particle Assembling Induced by Non-Homogeneous Magnetic Field at Transformer Oil-Based Ferrofluid/Silicon Crystal Interface by Neutron Reflectometry, *Appl. Surf. Sci.* 473, 912–917.
- [5] K.Theis-Bröhl et al. (2020). Self-Assembly of Magnetic Nanoparticles in Ferrofluids on Different Templates Investigated by Neutron Reflectometry, *Nanomaterials.* 10.

NEUTRON ABSORPTION AND SCATTERING IN A RESONATOR STRUCTURE

E. D. Kolupaev^{1,2}, Yu.V. Nikitenko¹ and V.D. Zhaketov¹

¹*JINR, Dubna, Russian Federation*

²*MSU, Moscow, Russian Federation*

E-mail: kolupaev.ed15@physics.msu.ru

A cold neutron storage project is being considered for the projected NEPTUNE reactor. The neutron density in the storage is determined by the absorption and scattering (leakage) of neutrons on the walls of the storage. To determine the probability of neutron leakage, it is proposed to use a neutron wave resonator in which the probabilities of the studied processes are increased. The resonator is made in the form of a three-layer Cu/Al/Cu structure. Experimental studies were carried out for two structures manufactured in NRC “Kurchatov Institute” - PNPI (Gatchina) and IMP UB RAS (Ekaterinburg). It is shown that the main contribution to neutron leakage is associated with scattering on roughness and non-flatness of the interface.

[1] S.K. Sinha, E.B. Sirota, and S. Garoff (1988). X-Ray and neutron scattering from rough surfaces. *Physical Review B*, volume 38, number 4

[2] V. L. Aksenov, Yu. V. Nikitenko (2006). Scientific Reviews: Polarized Neutron Reflectometry at IBR-2. *Neutron News*, 16:3, 19-23

ANGULAR DIVERGENCE OF NEUTRON MICROBEAMS FROM PLANAR WAVEGUIDES

S.V. Kozhevnikov¹, V.D. Zhaketov¹, A.V. Petrenko¹, T. Keller^{2,3} and F. Radu⁴

¹*Frank Laboratory of Neutron Physics, JINR, Dubna, Russia*

²*Max Planck Institut für Festkörperforschung, Stuttgart, Germany*

³*Max Planck Society Outstation at the Heinz Maier-Leibnitz Zentrum, Garching, Germany*

⁴*Helmholtz-Zentrum Berlin für Materialien und Energie, Berlin, Germany*

E-mail: kozhevn@nf.jinr.ru

Planar waveguides are resonant tri-layer structures transforming a conventional collimated neutron beam into a slightly divergent neutron microbeam [1] with the width about 1 – 10 μm . Such extremely narrow microbeam can be used for the investigations of quasi one-dimensional local microstructures (wires, magnetic domains, lithographic gratings, magnetic vortices) with high spatial resolution [2,3]. The neutron microbeam width depends on its angular divergence and the distance from the waveguide exit to the investigated sample. Therefore, the investigation of the neutron microbeam angular divergence is an actual task. The angular divergence of the neutron microbeam is mainly defined by Fraunhofer diffraction on a narrow slit as $\delta\alpha_f \propto \lambda/d$ where λ is the neutron wavelength and d is the width of the middle guiding layer (or channel) of the planar waveguide [4,5].

We investigated the neutron microbeam divergence $\delta\alpha_f$ as a function of the incident neutron beam divergence $\delta\alpha_i$. The experiments were done on the time-of-flight polarized neutron reflectometer REMUR at the pulsed reactor IBR-2 (FLNP JINR, Dubna, Russia). Experimental details can be found in [6]. The waveguide structure $\text{Ni}_{67}\text{Cu}_{33}(20\text{ nm})/\text{Cu}(150)/\text{Ni}_{67}\text{Cu}_{33}(50)/\text{Si}(\text{substrate})$ was investigated. The substrate sizes are $1 \times 1 \times 25\text{ mm}^3$. The alloy $\text{Ni}(67\text{ at. \%})\text{Cu}(33\text{ at. \%})$ is nonmagnetic at room temperature and has high neutron scattering length density. The grazing angle of the incident beam is equal to $\alpha_i = 0.211^\circ$. The corresponding neutron wavelength for the resonance order $n = 0$ is 2.5 \AA . In the experiment, we registered the neutron microbeam intensity in dependence on the final scattering angle α_f for various values of the incident neutron beam divergence. It is obtained that the angular width of the neutron microbeam peak (FWHM) of the resonance order $n = 0$ is linearly depends on the incident neutron beam divergence as $\delta\alpha_f = 0.096 + 4.4 \cdot \delta\alpha_i$. The reason is broadening of the spectral width of the neutron resonances with increasing of the incident neutron beam divergence [6].

This work was supported by JINR-Romania scientific project № 366/11.05.2021, item 40.

[1] F. Pfeiffer et al., Phys. Rev. Lett. 88 (2002) 055507.

[2] S.V. Kozhevnikov et al., Physics of the Solid State 56 (2014) 57.

[3] F. Ott, et al., NIM A 788 (2015) 29.

[4] S.V. Kozhevnikov et al., JETP 127 (2018) 593.

[5] S.V. Kozhevnikov et al., NIM A 915 (2019) 54.

[6] S.V. Kozhevnikov et al, JETP 123 (2016) 950.

VISCOELASTIC PROPERTIES AND STRUCTURE OF DUAL NETWORKS OF POLYMER AND MICELLAR CHAINS.

A.L. Makarova¹, A.V. Shibaev¹, A.I. Kuklin^{2,3}, O.E. Philippova¹

¹*Physics Department, M.V.Lomonosov Moscow State University, Moscow, Russian Federation*

²*Joint Institute for Nuclear Research, Dubna, Russian Federation*

³*Moscow Institute of Physics and Technology, Dolgoprudniy, Russian Federation*

E-mail: aleshina@polly.phys.msu.ru

Viscoelastic properties of wormlike micelles (WLMs) can be enhanced by mixing them with polymeric chains. Nowadays, the study of double networks based on polymers and surfactants are widely studied in order to increase the mechanical properties of the system compared to the mechanical properties of the components separately. Therefore, different ways of increasing the mechanical properties of wormlike micellar solutions are proposed. One approach is based on mixing wormlike micelles with polymer molecules [1]. In order to increase viscoelasticity, the addition of polymer should not result in the disruption of wormlike micelles, which may happen, for instance, in the case of weakly hydrophobic polymers.

In this work, we studied systems prepared by mixing WLMs of surfactants with polysaccharide chains of hydroxypropyl guar with molar mass 1,600,000 g/mol. The WLMs were composed of two surfactants with opposite charge. It was shown that this system is homogeneous over a wide range of concentrations of both components. It also was shown that the system is reached microphase separation with the formation of two parts: the first is polymer rich and the second surfactant rich. Also it was found that at a wide range of surfactants concentrations and constant HPG concentration scattering curves can be well fitted by a form-factor of cylinder, that means that HPG does not affect wormlike micelles structure.

At this work the rheological properties of mixed structures were observed. It was found that the rheological properties of individual components were lower than the same properties of dual networks. The viscosity of mixed structure is 180 times higher in comparison with the separate components. This synergetic effect of properties can be described by formation polymer-rich and surfactant-rich areas and lack of electrostatic interactions between components, which leads to an increase in the number of the increase of intermicellar and interpolymer entanglements. This synergetic effect of rheological properties can be widely used at different applications: for example, commercial hydraulic fracturing fluids.

The work is financially supported by the Russian Science Foundation (project 19-73-20133).

[1] Roland, S., Miquelard-Garnier, G., Shibaev, A. V., Aleshina, A. L., Chennevière, A., Matsarskaia, O., Sollogoub C., Philippova O.E., Iliopoulos, I. Dual transient networks of polymer and micellar chains: Structure and viscoelastic synergy. // *Polymers*. – 2021. – Vol. 13. - № 23 (4225). – P. 4255.

INTERACTION OF AGGREGATES IN FERROFLUIDS ACCORDING TO SMALL-ANGLE SCATTERING DATA

A.V. Nagorny^{1,2,3}, O.I. Ivankov^{1,2,4}, A.V. Shulenina^{5,6}, Yu.L. Zabulonov³, L.A. Bulavin², V. Socoliuc⁷, L. Vekas⁷, and M.V. Avdeev¹

¹*Joint Institute for Nuclear Research, Dubna, Moscow Region, Russian Federation*

²*Taras Shevchenko National University of Kyiv, Kyiv, Ukraine*

³*Institute of Environmental Geochemistry, NAS of Ukraine, Kyiv, Ukraine*

⁴*Institute for Safety Problems of Nuclear Power Plants, National Academy of Sciences of Ukraine, Chernobyl, Ukraine*

⁵*Faculty of Physics, Lomonosov Moscow State University, Moscow, Russian Federation*

⁶*National Research Centre 'Kurchatov Institute', Moscow, Russian Federation*

⁷*Center for Fundamental and Advanced Technical Research, Timisoara Branch of Romanian Academy of Sciences, Romania*

E-mail: avnagorny@jinr.ru

Problems of studying various interaction effects between aggregates in real ferrofluids with a stable aggregation phase are considered. Small-angle scattering of X-rays and neutrons is the most direct experimental method for evaluating correlations on a scale from ~1 nm to ~100 nm. Even in highly stable ferrofluids (e.g. magnetic particles with single coating by surfactants in organic solvents); the aggregation phase can exist in thermodynamic equilibrium with monomeric particles because of competing interactions: magnetic attraction and Brownian repulsion between particles. In some cases, despite the presence of colloidal (non-equilibrium) aggregation in ferrofluids based on highly polar media (e.g. water), the systems remain stable in time. Compact colloidal clusters consisting of comparatively small number of particles in them are of current interest regarding some applications (e.g. magnetic hyperthermia) due to a specific behavior of magnetization different from that for purely superparamagnetic systems. In concentrated (but still stable) systems, a significant fraction of magnetic particles are in the aggregate state, which means that the clusters, interacting with each other in solution, start to contribute to the correlation effects reflected in small-angle scattering. This report is devoted to the analysis of these effects for concentrated water-based ferrofluids with double-layered surfactant (fatty acids) coating of magnetic nanoparticles [1].

[1] Nagorny A.V., Socoliuc V., Petrenko V.I., Almasy L., Ivankov O.I., Avdeev M.V., Bulavin L.A., Vekas L., *J. Magn. Magn. Mater.* 501 (2020) 166445

INVESTIGATION OF THE FE-CR SUPERLATTICE WITH NON-COLLINEAR MAGNETIC ORDERING

E. S. Nikova^{1,2}, Yu. A. Salamatov¹, E. A. Kravtsov^{1,2}

¹*M.N. Miheev Institute of Metal Physics UB RAS, Ekaterinburg, Russian Federation.*

²*Ural Federal University, Ekaterinburg, Russian Federation.*

E-mail: e.nikova@mail.ru

The moments of all iron layers will line up strictly ferromagnetically in a sufficiently strong external field – the saturation field. However, at intermediate fields, nontrivial magnetic configurations can arise. This is due to the action of the competing mechanisms: an external field, interlayer exchange coupling of the antiferromagnetic type, crystal anisotropy, the influence of the surface, etc. Magnetic behavior of layer systems was theoretically described in [1]. Experimental evidence for the existence of the inhomogeneous configurations was obtained by polarization neutron reflectometry [2]. In a superlattice of the ⁵⁷Fe/Cr type in an external field of 195 Oe a fan-type ordering with a variable angle between moments was observed. In addition, there are two types of vertical magnetic domains.

In this work, the results of a study of the metallic superlattice Al₂O₃//Cr(100 Å)/[Fe(90 Å)/Cr(11 Å)]₁₂/Gd(50 Å)/Cr(50 Å) are presented. The reflectivity experiments were carried out with full polarization analysis at time-of-flight reflectometer REMUR at the pulsed reactor IBR-2 (JINR, Dubna) in an external field of 24 Oe. An external magnetic field was applied along the sample surface (in the layer plane). Before the start of measurements, the sample was magnetized to saturation in a field of ~5 kOe, then the field was reduced to a value of 24 Oe. Significant diffuse scattering was found in the neutron reflection for different scattering channels.

Processing of experimental data was carried out by two methods: with phase-amplitude functions [3] and with reference layer [4]. As a result of the processing of experimental data by the method of phase-amplitude functions and the method of the reference layer, the structures of the studied sample were obtained: Al₂O₃//Cr(133 Å)/[Fe(94 Å)/Cr(10 Å)]₁₂/Gd(53 Å)/Cr(25 Å)/Cr₂O₃(24 Å) and Al₂O₃//Cr(86 Å)/[Fe(94 Å)/Cr(13 Å)]₁₂/Gd(50 Å)/Cr(25 Å)/Cr₂O₃(25 Å), respectively. The agreement between the thicknesses for the two methods is quite good. There is a discrepancy for the Cr buffer layer, which can be explained by different results on the substrate roughness in the two methods.

The angles of deviation of the magnetic moments from the direction of the external magnetic field for the system under study are shown in Figure 1.

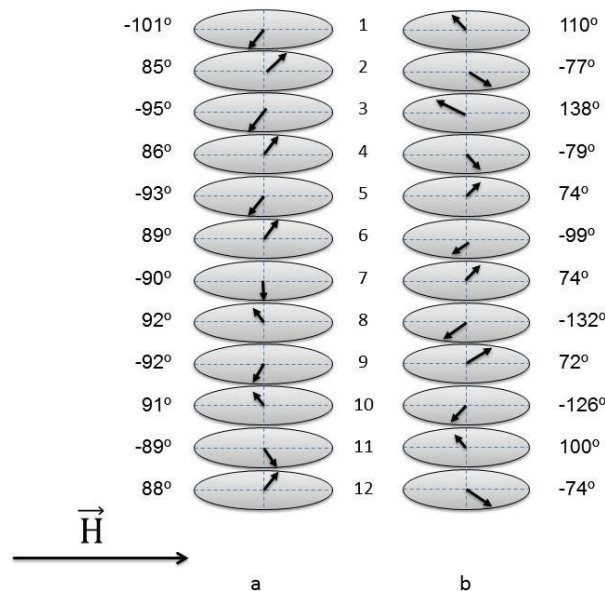


Figure 1. Angles of deviation of the magnetic moment in each layer of iron from the direction of the external magnetic field: a - calculated by the reference layer method; b - calculated by the method of phase-amplitude functions.

An analysis of the parameters obtained by two methods shows that a weak external field slightly disturbs the antiferromagnetic ordering of the magnetic moments of the Fe layers. The angles between the moments of neighboring layers are not the same and lie in the range from 140° to 180° . This ordering can be conditionally considered as helicoidal with an irregular step. The total magnetic moment of the superlattice is close to zero.

Two different methods of processing experimental data showed two sets of angles for magnetic moments differing from each other by about 180° , which indicates indirectly the presence of a domain structure. This is also evidenced by the presence of diffuse scattering. It can be assumed that these sets correspond to two types of magnetic domains.

With an increase in the external field, the antiferromagnetic exchange interaction will be overcome and the moments of the layers will begin to deviate more strongly in the direction of the external field, and a nonzero total moment will arise. The helicoidal ordering will turn into a fan ordering with variable angles between the moments.

The work was carried out with the support of the Ministry of Science and Higher Education of the Russian Federation, agreement № 075-10-2021-115 of October 13, 2021 (internal number 15.SIN.21.0021).

[1] V.V.Ustinov (2007) Spin-flop transition scenario in finite layered antiferromagnets. Journal of magnetism and magnetic materials. 310, 2219-2221.

[2] V.Lauter-Pasyuk, H.J.Lauter, B.P.Toperverg, L.Romashev, V.Ustinov (2002) Transverse and lateral structure of the spin-flop phase in Fe/Cr antiferromagnetic superlattices. Physical review letters. 89, № 16, 167203.

[3] Ю.А.Саламатов, Е.А.Кравцов (2021) Применение метода фазово-амплитудных функций в рентгеновской и нейтронной рефлектометрии. Поверхность. Рентгеновские, синхротронные и нейтронные исследования. 5, 3-12.

[4] E.S.Nikova, Yu.A.Salamatov, E.A.Kravtsov, M.V.Makarova, V.V.Proglyado, V.V.Ustinov, V.I.Bodnarchuk, A.V.Nagorny (2019) Experimental approbation of reference layer method in resonant neutron reflectometry. Physics of metals and metallography. 120, 838-844.

STRUCTURAL AND MAGNETIC CHARACTERIZATION OF Fe/MgO/Gd NANOSYSTEMS

E.M. Yakunina¹, E.A. Kravtsov^{1,2}, D.I. Devyaterikov¹ and V.V. Proglyado¹

¹ *Institute of Metal Physics UB RAS, Yekaterinburg, Russian Federation*

² *Ural Federal University, Yekaterinburg, Russian Federation*

E-mail: eyakuninaart@gmail.com

With the development of spintronics, the study of the magnetic behavior formed in metal multilayer nanostructures as a result of the addition of MgO layers becomes especially important, since their interaction with metal atoms creates complex effects that affect the formation of the magnetic properties of the entire structure [1, 2]. As shown by our recent studies [3, 4], magnetization reversal processes in ferromagnetic layers can be controlled by placing MgO layers between metal layers [5, 6] and by changing their thickness. It can be expected that the location of MgO relative to different types of metallic layers, as well as their thickness, will determine complex magnetic configurations in such nanostructures. Gadolinium (Gd) is one of the most attractive materials for various kinds of research due to its unique magnetic and electrical properties. Several studies have mentioned that the magnetization on the Gd surface is antiferromagnetically related to the bulk magnetization. In addition, Gd is known as a material that exhibits a large Rashba spin-orbit splitting on the surface. Since the contributions of the interface to the tunnel magnetoresistance (TMR) are much stronger than the contributions in the volume, the determination of the TMR characteristics is one of the most effective methods for studying the interface of magnetic materials.

Nanostructures Fe/MgO/Gd is a new material in which the interlayer coupling of the magnetic moments of Fe is provided by alternating thin layers of dielectrics, metals and rare earth metals. At present, materials of this type are poorly studied. There are only a few publications on the study of systems based on Gd/MgO/Fe [7, 8]. At the moment, it is not known how the magnetic moments of Fe will interact through a thin layer of MgO and layers of the rare earth metal Gd, and also what effects can be formed as a result. The present research is aimed at creating and step by step analysis of the structural and magnetic properties of Fe/MgO/Gd systems. The results of this work are an important part of the future, a more detailed understanding of the formation of the microscopic pattern of magnetization reversal in Fe/MgO/Gd systems depending on the properties of the separating MgO and Gd layers.

In this work, we studied the complex structural and magnetic properties of a series of Nb(20 nm)/Fe(1 nm)/MgO(t nm)/Gd(1 nm)/Nb(3 nm) nanosystems with different thicknesses of MgO dielectric layers ($t=0, 0.4, 0.8$ and 1.2 nm). High-resolution X-ray reflectometry data confirmed the formation of a layered structure of nanosystems with layer thicknesses close to nominal and an RMS interface roughness value of 10% of the total layer thickness. Vibrational magnetometry revealed a difference in the hysteresis loops of a sample without a MgO layer and samples with MgO layers of different thicknesses.

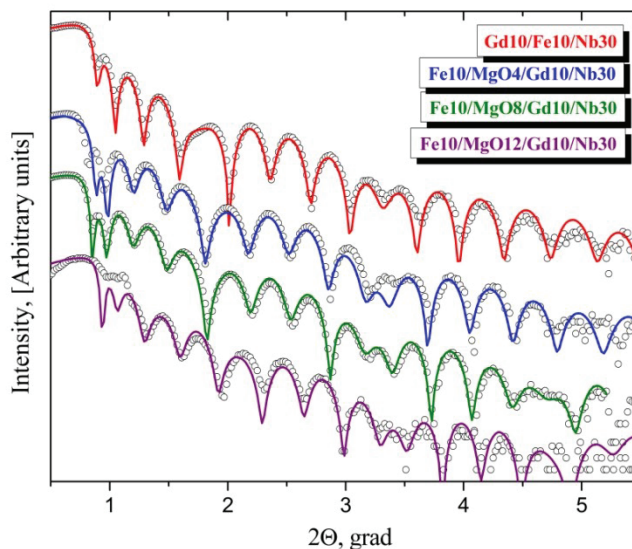


Figure 1. Experimental X-ray reflectogram of samples with different MgO layer thicknesses (symbolo line) and model curve (strate line).

The results were obtained with the financial support of the Russian Federation represented by the Ministry of Science and Higher Education, agreement No. 075-10-2021-115 dated October 13, 2021 (internal number 15.SIN.21.0021)

- [1] F. Hellman, A. Hoffmann, Ya.Tserkovnyak et al. (2017) Interface-Induced Phenomena in Magnetism. *Reviews of Modern Physics*. 89, 025006
- [2] G.-H. Yu, W.-L. Peng, J.-Ya. Zhang (2017) *Rare Metals*. 36, 155–167
- [3] Е. М. Якунина, Е. А. Кравцов, Ю. Н. Хайдуков и др. (2021) Структура и магнетизм в многослойных наносистемах Fe/MgO/Cr/MgO/Fe. *Поверхность. Рентгеновские, синхронные и нейтронные исследования*. 8, 16-22
- [4] Е. М. Якунина, Е. А. Кравцов, Ю. Н. Хайдуков и др. (2021) Синтез, структура и магнитные свойства многослойных наногетероструктур Fe/MgO/Cr/MgO/Fe. *Физика твердого тела*. 9, 1306
- [5] G. Yanga, J.-Y. Zhang, S.-L. Jiang *et al.* (2017) *Applied Surface Science*. 396, 705–710
- [6] A. Koziół-Rachwał, W. Janus, M. Szpytmaet al. (2019) Interface engineering towards enhanced exchange interaction between Fe and FeO in Fe/MgO/FeO epitaxial heterostructures. *Applied Physics Letters*, 115, 141603
- [7] Y. T. Takahashi, Y. Shiota, S. Miwa et al. (2013) Fabrication of Fe/MgO/Gd Magnetic Tunnel Junctions. *IEEE Transactions on Magnetics*. 49, 4417 - 4420
- [8] N. Funabashia, R. Higashida, K. Aoshima and K. Machida (2019). Magneto-optical light modulation using the VCMA effect in MgO/Co–Fe/Gd/Gd–Fe layers. *AIP Advances*. 9, 035336

SIMPLE METHOD FOR CORRECTION OF CENTER OF ROTATION IN NEUTRON TOMOGRAPHY

I.Yu. Zel¹

¹*Joint Institute for Nuclear Research, FLNP, Dubna, Russian Federation*

E-mail: zel@jinr.ru

Neutron tomography has been recently become one of the widely used non-destructive techniques along with synchrotron and X-ray imaging. The routine usage of neutron imaging requires careful pre-processing of projection or sinogram data to avoid the artifact occurrence in the reconstructed data due to misalignment in sample-detector system and degradation of detector system itself. In this work strong artifacts appeared due to misalignment of center of rotation with respect to center of the projection image are considered. I propose a simple method to calculate the shift by which the projections should be translated to align the center of rotation with the center of the projection image. As in already existed methods in the proposed one two projections taken at 0° and 180° are utilized in calculations. But further calculations are performed on binary images using basic morphological operations. Computation algorithm can be easily implemented in ImageJ software.

STUDY OF CULTURAL HERITAGE OBJECTS FROM THE ANCIENT TURKIC CULT-MEMORIAL COMPLEX OF EAST KAZAKHSTAN WITH NON – DESTRUCTIVE NEUTRON METHODS

A.Zh. Zhomartova^{1,2,3}, K.M. Nazarov^{1,2,3}, S.E. Kichanov¹, M. Kenessarin³, R.S. Zhumatayev⁴, B. Mukhametuly^{1,3,4}, A.T. Toleubayev⁴,

¹*Joint Institute for Nuclear Research, Dubna, Russian Federation*

²*L.N. Gumilyov Eurasian National University, Nur-Sultan, Kazakhstan*

³*Institute of Nuclear Physics, Almaty, Kazakhstan*

⁴*Al-Farabi Kazakh National University, Almaty, Kazakhstan*

E-mail: zhomartova@jinr.ru

The peculiarities of studying historical artifacts due to their existence in a single copy require non-destructive research methods. Modern methods of non-destructive testing allow us to obtain unique scientific information about the elementary, chemical and phase composition of the object under study, allow us to identify hidden defects in various types of structures, study and visualize internal (volumetric) properties, as well as determine the internal structure of the object under study. Of particular note are such methods of structural non-destructive diagnostics as neutron diffraction and tomography. The nature of the interaction of neutrons with matter determines the high penetrating power of these methods and sensitivity to hydrogen-containing phases or components of the object under study.

This work reports on the results of the study of metal and ceramic objects of cultural heritage (weapons and household items) found in the cult-memorial complex of Eleke Sazy, located on the territory of Tarbagatay district of East Kazakhstan region. The Eleke Sazy cult-memorial complex appeared on the site of the burning of the body of one of the khagans of the Western Turkic Khaganate. The emergence of the cult-memorial complex on Tarbagatay reflects the cultural processes in the center of Asia associated with the entry into the historical arena of the ancient Turks, their spiritual, ideological, religious and philosophical orientations.

To determine the mineral phase composition of the studied ceramics, the neutron diffraction method was used on the DN-6 [1] neutron diffractometer of the IBR-2 pulse reactor (JINR, Dubna, Russia). The features and spatial distribution of phases and the internal structure of metal objects were studied by neutron radiography and tomography [2] at the experimental station TITAN on the 1st channel of the stationary research reactor WWR-K. The obtained data on the mineral composition of the studied ceramic fragments indicate the production of tableware mainly from clay with a natural admixture of feldspar, quartz and mica. The structural features and spatial distribution of various components within the volume of ceramics are also investigated. Neutron tomography made it possible to obtain three-dimensional data on the spatial distribution of chemical elements in the bronze alloy of the samples under study, as well as on internal voids and features of the casting process.

[1] D.P. Kozlenko (2018). The DN-6 Neutron Diffractometer for High-Pressure Research at Half a Megabar Scale Crystals 8, 331.

[2] K.M. Nazarov (2021). Non-destructive analysis of materials by neutron imaging at the TITAN facility. Eurasian Journal of Physics and Functional Materials. 5(1), 6-14.

PHOTOCONDUCTIVITY OF $\text{Ge}_{1-x}\text{Nd}_x\text{S}$ AT HIGH TEMPERATURES

A.O. Dashdemirov and A.S. Alekperov

Azerbaijan State Pedagogical University, Baku, Azerbaijan

E-mail: dashdamirovarzu@gmail.com

Studies of semiconductor materials with REE impurities revealed that these metals "purify" materials from slags and impurities and annihilate vacancies. The electronic structure of REEs differs significantly from that of other impurities, and REE-based centers yield temperature-independent lines in the luminescence spectrum; therefore, doping with REEs is of great practical importance. REE atoms form complexes with impurity atoms, such as oxygen and other sixth-group elements. At the same time, Coulomb or chemical interaction of some REE atoms with participation of host atoms and intrinsic point defects may lead to the formation of various atomic complexes in a crystal [1].

In contrast to GeS single crystals, the growth of $\text{Ge}_{1-x}\text{Nd}_x\text{S}$ single crystals ($x = 0.005$ and 0.01) is accompanied by the formation of Nd_2O_3 complexes. Gamma irradiation to low doses decomposes atomic complexes and forms an ordered state in the crystals, while a sharp increase in temperature prevents the formation of excitons. The purpose of this study was to analyze the possibility of applying these REE properties to increase the exciton photoconductivity (EPC), which is observed at low temperatures in layered GeS single crystals [2,3]. The investigations showed that γ irradiation to low doses (30 kRad) improves the physical parameters of both the GeS host and impurity compounds. However, it was also found that γ irradiation not only improves the GeS parameters but, in contrast, eliminates EPC.

In this work the spectral dependences of photoconductivity in a wide temperature range ($T = 80\text{--}300$ K) of layered GeS single crystals, both intentionally undoped and Nd-doped, have been experimentally investigated and analyzed. In contrast to GeS single crystals, elementary exciton-type excitation has been found in the photoconductivity spectrum of $\text{Ge}_{1-x}\text{Nd}_x\text{S}$ single crystals ($x = 0.005$ and 0.01) in the temperature range of $200 < T < 350$ K. Upon heating, exciton–impurity complexes are decomposed, thus resulting in the excitonic photoelectric effect. After γ irradiation to a dose of 30 kRad, no exciton states are observed in the photoconductivity spectrum. The intensity of X-ray diffraction reflections increases by a factor of ~ 35 , which can be explained by decomposition of complex atomic aggregates and formation of an ordered state in layered $\text{Ge}_{1-x}\text{Nd}_x\text{S}$ single crystals ($x = 0.005$ and 0.01).

[1] A.O.Dashdemirov, S.G.Asadullayeva, A.S.Alekperov, N.A.Ismayilova, S.H.Jabarov (2021). Electronic and optical properties of GeS and GeS:Gd, *International Journal of Modern Physics B*, 35, 30, 2150305.

[2] A.S.Alekperov, A.O.Dashdemirov, N.A.Ismayilova, S.H.Jabarov (2020). Fabrication of a Ge-GeS:Nd heterojunction and investigation of the spectral characteristics, *Semiconductors*, 54, 11, 1406-1409.

[3] A.S.Alakbarov, A.O.Dashdemirov, R.B.Bayramli, K.S.Imanova (2021). Effect of the gamma irradiation on the structure and exciton photoconductivity of layered GeS:Sm single crystal, *Advanced Physical Research*, 3, 1, 39-45.

RESEARCH OF ELECTRIC PROPERTIES OF HYDRATABLE CRYSTAL MnSe-CuInSe_2 PROMISING FOR USING IN RENEWABLE ENERGY

Didenko E.A.^{1,2}, Doroshkevich A.S.^{2,3}, Samedovaa^{2,9} U. F., Kirillov A.K.², Vasilenko T.A.⁴, Oksengendler B.L.⁵, Nikiforova N.N.⁵, Balasoui M.^{2,6}, Stanculescu A.^{7,8}, Mardare D.⁹, Mita C.⁹

¹*Dubna State University, Dubna, Russian Federation, 19 Universitetskaya street, Dubna, Moscow region, 141982;*

²*Joint Institute for Nuclear Research, Dubna, Russian Federation;*

³*Donetsk Institute for Physics and Engineering named after O.O. Galkin, Kiev, Ukraine,*

⁴*Saint-Petersburg Mining University, St.-Petersburg, Russian Federation;*

⁵*Ion-plasma and laser technologies Institute after U.Arifov, Uzbekistan, Tashkent;*

⁶*Horia Hulubei National Institute for R&D in Physics and Nuclear Engineering (IFIN-HH), Bucharest Romania;*

⁷*Alexandru Ioan Cuza" University of Iasi, Faculty of Physics, Bld. Carol I, No. 11, Iasi 700506, Romania;*

⁸*National Institute for Materials Physics (NIMP) Strada Atomistilor 405, Măgurele 077125, Romania;*

⁹*Institute of Physics, National Academy of Sciences of Azerbaijan, pr. Dzhavida 33, Baku, AZ1143 Republic of Azerbaijan.*

E-mail: dea.21@uni-dubna.ru

At present time problem of renewable energy sources is actual due to depletion of traditional energy sources [1, 2]. In this respect put attention on development of converter of solar energy in electro form [3, 4]. New technologies based on the new physical mechanisms are made. Unique results were received in the area of adsorptive electrical energy industry [5, 6].

Projects of mechanisms converting chemical energy of adsorption of atmosphere moisture into electric form by electrostatic charge capture of microscopic water droplet [7] with help electrostriction caused by water adsorption [8] etc. [9, 10, 11].

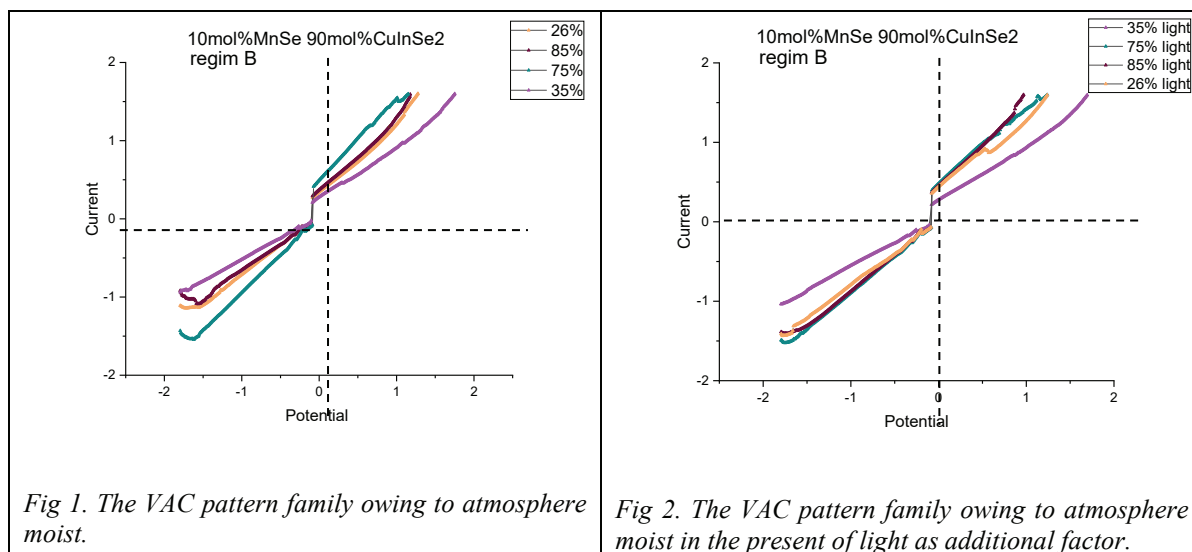
In this respect materials of system MnSe-CuInSe_2 are interesting due to their high adsorptive ability to moisture and photovoltaic conversion. It's a possible to practical realization of hybrid energy sources converting photon energy and energy of adsorption of atmosphere moisture into electric form based on the new materials.

Purpose of the work is research of electric properties of system MnSe-CuInSe_2 .

Researched object is crystals 10mol% $\text{MnSe-90mol\%CuInSe}_2$, what have 9 mm length, 3 mm highness, 5 mm width. System MnSe-CuInSe_2 were obtained with help the chemical technology [12]. Voltamperograms were obtained in the lineal evolute regime (from -2000 mV to +2000 mV, stereotype amount – 1800 mV, final amount 1800 mV, maximum potential 2000 mV, minimum potential -2000 mV) by device R-20 ("Elinns") in moisture saturation regime in four point (85, 75, 35 и 26% $\pm 5\%$). Research was carried out in closeted container with 350 ml volume, also this container owns controlled moisture by salts KCl (85%), NaCl (35%) and NaCl (75%) [13].

VAC, what were obtained in conditions of different moisture of atmospheric air, were showed on the figure 1. VAC, what were obtained in conditions of different moisture of atmospheric air and light as additional factor, were showed on the figure 2. All VAC have close to linear form what testifies about carrying-out of Ohm's law in researched object. Straight and reverse traces site in first and fourth quadrant respectively. Both traces are almost symmetrical relatively of coordinates starting. Righting qualities weren't observed. Leap of current is at the null voltage value. This leap testifies to availability of barrier potential about 0,3 V at low moisture and about 0,4-0,5 V at high moisture. It means that barrier potential value is proportionally of quantity of moisture in crystal pores. On the

figure 2 illumination results in lowering of barrier potential (about 1 mV) and more sharp than in «dark» regime lowering resistance of material (curve lean to X-axis). Lowering resistance in the first and second variant was caused generation of charge free-carrier. Moisture and illumination are additive. Conclusion: making of hybrid energy sources based on the researched materials is possible.



The study was performed in the framework of the JINR-Romania cooperation program in 2022 (topic 03-4-1128-2017/2022).

[1] Lyubarskaya M. A. Review of trends in innovative development of renewable energy technologies //Russian Economic online magazine. – 2019. – №. 3. – p. 54-54.

[2] Chernyshev A. S., Mordvinov S. E. Review of renewable energy sources //Youth and knowledge-a guarantee of success-2019. – 2019. – p. 146-149.

[3] Strebkov D. S. Et al . Solar energy: state and prospects of development //Machinery and equipment for the village. – 2019. – №. 3. – p. 43-47.

[4] Tychkov A. Yu. Et al. Alternative energy at military facilities: a literary review //Bulletin of the Penza State University. – 2020. – №. 4 (32). – p. 101-106.

[5] S. Doroshkevich, A. I. Lyubchyk, A. V. Shilo, T. Yu. Zelenyak, V. A. Glazunovae, V. V. Burhovetskiy, A. V. Saprykina, Kh. T. Holmurodov, I. K. Nosolev, V. S. Doroshkevich, G. K. Volkova, T. E. Konstantinova, V. I. Bodnarchuk, P. P. Gladyshev, V. A. Turchenko, S. A. Sinyakina Chemical-Electric Energy Conversion Effect in Zirconia Nanopowder Systems. Journal of Surface Investigation: X-ray, Synchrotron and Neutron Techniques, 2017, Vol. 11, No. 3, pp. 523–529. DOI: 10.1134/S1027451017030053

[6] S. Doroshkevich, A. I. Lyubchyk, A. V. Shilo, T. Yu. Zelenyak, V. A. Glazunovae, V. V. Burhovetskiy, A. V. Saprykina, Kh. T. Holmurodov, I. K. Nosolev, V. S. Doroshkevich, G. K. Volkova, T. E. Konstantinova, V. I. Bodnarchuk, P. P. Gladyshev, V. A. Turchenko, S. A. Sinyakina Chemical-Electric Energy Conversion Effect in Zirconia Nanopowder Systems. Journal of Surface Investigation: X-ray, Synchrotron and Neutron Techniques, 2017, Vol. 11, No. 3, pp. 523–529. DOI: 10.1134/S1027451017030053

[7] N.Miljkovic, D. Preston, R. Enright, and E. Wang. Jumping-droplet electrostatic energy harvesting // APPLIED PHYSICS LETTERS. 2014. V. 105, P.013111.

[8] Georgen B., Nienhaus H., Weinberg W. H., Mc Farland E. Chemically induced electronic excitations at metal surfaces // Science. 2001. V.294. P. 2521–2523.

[9] Leandra P. Santos, Telma R. D. Ducati, Lia B. S. Balestrin, and Fernando Galembeck* Water with Excess Electric Charge // J. Phys. Chem. C 2011, 115, 11226 –11232. Dx. Doi.org/10.1021/jp202652q.

- [10] Rubia F. Gouveia and Fernando Galembeck Electrostatic Charging of Hydrophilic Particles Due to Water Adsorption // J. AM. CHEM. SOC. 2009 , 131 , 11381–11386 9 11381.
- [11] Rubia F. Gouveia, Carlos A. R. Costa, and Fernando Galembeck* Water Vapor Adsorption Effect on Silica Surface Electrostatic Patterning // J. Phys. Chem. C 2008, 112, 17193–17199.
- [12] Sh. M. Gasanly , A. A. Abdurragimovb, and U. F. Samedovaa The Electric and Thermoelectric Properties of CuInSe₂-based Chalcopyrite // Surface Engineering and Applied Electrochemistry, 2012, Vol. 48, No. 5, pp. 439–443, 1068-3755, DOI 10.3103/S106837551205004.
- [13] Relative humidity of air above saturated solutions / A.G.Tereshchenko – Tomsk, 2010. – p. 22.

RADIATION RESISTANCE OF THERMOREGULATING COATINGS IRRADIATED USING IBR-2

V.V. Harutyunyan¹, A.P. Aprahamian, E.M. Aleksanyan, V.V. Arzumanyan, A.H. Badalyan, A.H. Hovhannisyan, V.V. Baghramyan², A. A. Sargsyan, O.A. Culicov³, I.A. Bobrikov

¹*A.Alikhanyan National Science Laboratory, Yerevan, Armenia*

²*Institute of General and Inorganic Chemistry of NAS RA, Yerevan, Armenia*

³*FLNP JINR, Dubna, Russian Federation*

E-mail: vharut@mail.yerphi.am

The main trends of modern instrumentation are the use of physical modeling methods for a comprehensive study of the behavior of thermoregulating coatings under conditions of ground-based forced action of the main factors of outer space: deep vacuum, flows of high-energy charged particles (electrons, protons, and neutrons), electromagnetic solar radiation, thermal cycling, etc. [1]. Ideal thermoregulating coatings should have high melting point, low thermal conductivity, excellent chemical stability, and no phase transitions at operating temperatures, high adhesion to the substrate, and their thermal expansion coefficient should be similar to that of the substrate. The absorption coefficient of solar radiation (α_s) and the light reflectance of coatings are important characteristics of absorption and heat transfer for the spacecraft surface.

Coatings with α_s of about 0–30% and reflectance of about 0.8–0.9 can effectively remove excess heat from the spacecraft surface [1, 2]. To a greater extent, this applies to the thermoregulating coatings of the “solar reflector” class that includes enamel and ceramic coatings based on pigments with organic and inorganic binding agent. Among the pigments for coatings of this class, powders of silicate solutions of silica-containing rocks, such as zinc silicates, zirconium, etc., have found the greatest application as the most stable to the action of charged particles.

To study radiation-structural properties (crystallinity and phase composition) by X-ray diffraction analysis (XRD), zinc silicates obtained by hydrothermal microwave synthesis, modified by rare earth elements (Ce, Y), and subjected to neutron flux irradiation at doses of 10^{12} and 10^{15} n/cm² using at the FLNP JINR IBR-2 reactor were used. Phase constitution Zn_2SiO_4 silicate in of zinc crystalline form is rarely found in nature, however its optical, anticorrosive properties, high chemical stability, radiation resistance, and other properties determine its high demand, which determines its wide application in various fields. Zn_2SiO_4 exists in α - and β -crystalline phases. β - Zn_2SiO_4 is metastable and transforms into the α -phase at high temperatures. α - Zn_2SiO_4 does not exhibit solid phase transitions below its melting point (1550°C) and is a suitable phosphor matrix due to its excellent luminescence properties in the blue, green and red spectral regions. Ceramics based on Zn_2SiO_4 is traditionally produced by the solid-phase reaction of well-mixed ZnO and SiO₂ powders at 1100–1500°C. To completely remove bound water, the zinc orthosilicate samples Ce/Y- Zn_2SiO_4 were thermally treated at 1050°C [2]. It has been established that the mechanism of action of neutron flux on zinc silicates is completely different and determined by the atomic and molecular structure of the substance. When thermoregulating powders are irradiated with neutron flux, radiation color centers can form, namely, the following two types of defects: a) on the defects formed before the irradiation due to the crystal structure nonstoichiometry and on surface intrinsic point defects, b) on the defects formed in the crystal lattice during the irradiation. The concentration of the first type defects largely depends on the specific surface area and grain size of the powders. With increase in the specific surface area, the concentration of defects, as a rule, increases and then decreases. Doping with cerium or yttrium up to 5% helps to obtain a highly crystalline nanoscale structure. These elements also stabilize the

crystal structure due to the difference between the electric fields of the cations, e.g. Ce_3^+/Ce_4^+ and Zn_2^+ . Such difference can lead to a decrease in the total energy of the lattice, which will make it more stable when irradiated with neutrons of different energy and dose densities. It can be seen from the results of X-ray phase analysis that Ce- Zn_2SiO_4 , Y- Zn_2SiO_4 samples reveal sharp and wide diffraction peaks of α - Zn_2SiO_4 rhombohedral structure with space group R-3 and cell constant $a=b=1.395$ nm, $c=0.9312$ nm. The average grain size is no more than 20.2 nm. XRD diffraction patterns show that after irradiation there is a deformation of the structure of the thermoregulating samples due to the process of radiation defect formation, but the crystallinity of the phases is preserved. Thus, the modification of thermoregulating coatings with nanopowders is a fairly effective method for increasing radiation resistance, due to the fact that nanoparticles have a large specific surface area and are "drains" for electron excitations arising during irradiation.

[1] M. Hołyńska, A. Tighe, C. Semprinoschnig, (2018). Coatings and thin films for spacecraft thermo-optical and related functional applications, *Adv. Mater. Interfaces* 5 1–20. [2] V.V. Baghranyan, A.A. Sargsyan, N.B. Knyzyan, V.V. Harutyunyan, A.H. Badalyan, N.E. Grigoryan A. Aprahamian, K.V. Manukyan (2020). Pure and cerium-doped zinc orthosilicate as a pigment for thermoregulating coating, *Ceramics International*, Volume 46, Issue 4, 2020, pp. 4992-4997.

THERMAL ANALYSIS AND SYNTHESIS OF NEW MATERIALS IN FLNP JINR

O.Yu. Ivanshina¹, I. Zuba^{1,2}, T.N. Vershinina¹, S.V. Sumnikov¹, V.D Zhaketov¹,
A. Pawlukoć^{1,2}, Yu.V. Nikitenko¹

¹*Joint Institute for Nuclear Research, Dubna, Russian Federation*

²*Institute of Nuclear Chemistry and Technology, Warsaw, Poland*

E-mail: ioyu@nf.jinr.ru

Thermogravimetric analysis (TGA) and differential scanning calorimetry (DSC) are developing along with neutron methods for condensed matter research in FLNP JINR. Netzsch TGA 209 F1 Libra gravimeter gives the opportunity to determine the content of volatile components in the samples, to determine the limit of thermal stability of compounds, and to precise the composition of the samples. For example, TGA allowed to confirm the presence of amorphous manganese oxide MnO₂ in the adsorbent based on iron oxide Fe₃O₄ [1].

Differential thermal analysis is useful addition to the study of phase transformations in materials. Netzsch 204 F1 Phoenix differential scanning calorimeter allows to do the research not only during heating, but also at low temperatures (to 93K). We carry out thermal analysis both in an inert atmosphere (argon, nitrogen) and in an air, which allows to investigate oxidation processes.

Along with the study of the physicochemical properties of materials, sometimes tasks of the synthesis of new materials arises. The synthesis of the studied materials directly in FLNP can significantly expand the area of our research. And we have this possibility to synthesize materials. Our equipment (furnaces and autoclaves) allows to conduct annealing in an inert or oxidative atmosphere, as well as to carry out hydrothermal (solvothetical) synthesis in solutions at elevated pressure. The main objects of synthesis are inorganic materials, including cathode materials for sodium-ion batteries (SIBs) and metal-organic frameworks (MOFs). SIBs are interesting as an alternative to lithium-ion batteries due to higher sodium content in nature compared with lithium. The synthesis of cathode materials with high capacity and good stability is an important task for wide use of SIBs.

MOFs are crystalline materials consisting of an infinite network of metal-ions, or metal-ion clusters, bridged by organic ligands through coordination bonds into porous two- or three- dimensional extended structures. They are attracting increasing interest due to their unique adsorption properties. In the last time, the problem of water purification from dangerous substances is becoming more and more acute. A large number of studies are devoted to the extraction of heavy metals from aqueous solutions [2]. The creation of solid adsorbents with high capacity and stability in the aquatic medium is a very important task. MOFs are one of the promising types of adsorbents. But very few MOFs are used as adsorbents from aqueous solutions because most MOFs are unstable in aqueous medium [2]. We synthesized Ni-MOF {[Ni(*L*-trp)(bpe)(H₂O)]·H₂O·NO₃}_n (*L*-trp = *L*-tryptophan, bpe = 1,2-bis(4-pyridyl)ethylene) and Zr-MOF MIP-202(Zr), based on *L*-aspartic acid. They are stable in an aquatic environment. With UV-Vis spectrometry, we investigated the properties of Ni-MOF and Zr-MOF in the process of ruthenium sorption from aqueous solutions of ruthenium chloride.

Another attribute of MOFs is magnetism. Most magnetic frameworks are those containing paramagnetic metal centers. Research of the magnetic properties of MOFs with Ni and Co synthesized in FLNP was carried out on the spectrometer of polarized neutrons REMUR (IBR-2). It was shown that samples are capable to magnetization. The biggest effect was observed on the compound bis(*L*-histidinato)nickel(II) monohydrate. Magnetic domains formation is possible at low magnetic field. We plan to continue this research.

- [1] I. Zuba, A. Pawlukojć, J. Waliszewski and O. Ivanshina (2021). Fe₃O₄@MnO₂ inorganic magnetic sorbent: Preparation, characterization and application for Ru(III) ions sorption. *Separation Science and Technology*.
- [2] N. Manousi, D.A. Giannakoudakis, E. Rosenberg and G.A. Zachariadis (2019). Extraction of Metal Ions with Metal–Organic Frameworks. *Molecules*. 24, 4605.

THERMAL PROPERTIES OF THE $\text{La}_{0.73}\text{Ba}_{0.27}\text{MnO}_3$ AT HIGH TEMPERATURE

A.X. Nabiyeva

Institute of Physics ANAS, Baku, Azerbaijan

E-mail: aynurnabiyeva@inbox.ru

It is known that the physical properties of crystals change under external influences. The most widely studied of these effects is temperature. As the influence of temperature increases, the amplitude of oscillations of the atoms that make up the crystal lattice increases, and the physical properties change accordingly. Therefore, the study of the thermo physical properties of crystals plays an important role in determining the working area of these materials. In this work, $\text{La}_{0.73}\text{Ba}_{0.27}\text{MnO}_3$ was synthesized and thermo gravimetric analysis was carried out at high temperatures.

The compound $\text{La}_{0.73}\text{Ba}_{0.27}\text{MnO}_3$ was synthesized by the standard method, which is typical for complex oxides. The thermal properties of the polycrystalline sample were studied by thermo gravimetric analysis (TGA) at high temperatures. The experiments were carried out on an STA 449 F3 Jupiter® instrument in the temperature range $T = 300\text{--}900$ K. In order to minimize the cost of oxidation, the studies were carried out in an argon inert gas environment [1,2].

The temperature dependence of the mass of the $\text{La}_{0.73}\text{Ba}_{0.27}\text{MnO}_3$ compound shows that there are no sharp changes in this compound, which is due to the fact that it has a stable crystal structure at high temperatures. A sample weighing $m = 77.62$ mg was taken as the object of study. It has been established that with an increase in temperature in the range $T = 300\text{--}337$ K, a rapid increase in the mass value is observed, which is due to oxidation. At $T = 337$ K, the mass of the sample was $m = 77.75$ mg. Stabilization occurred in the temperature range $T = 337\text{--}435$ K and a slow rapid increase in body weight was observed. The exoeffect with a central peak $T = 482$ K was observed in the range $T = 435\text{--}530$ K. This effect is explained by the evaporation of water molecules from crystals. This is due to the fact that at the end of the effect, a sharp decrease in mass was observed, which corresponds to the rejection of the molecular composition.

The TGA spectrum of the $\text{La}_{0.73}\text{Ba}_{0.27}\text{MnO}_3$ compound shows that after the completion of the exoeffect, stabilization occurs again, and at a temperature $T \leq 900$ K, a slow increase in mass is observed. It is known from thermodynamics that the thermo gravimetric method of analysis is very sensitive to temperature in crystals. As can be seen, even in very small quantities of objects of study, it is possible to determine the effect of temperature. In the course of these studies, it was found that the compound $\text{La}_{0.73}\text{Ba}_{0.27}\text{MnO}_3$ has a stable crystal structure over a wide temperature range, and these properties correspond to crystals with high symmetry. This is because crystals with low symmetry undergo structural changes under the influence of high temperatures, and it is impossible to observe a stable phase in them.

[1] M.N. Mirzayev, E. Popov, E. Demir, B.A. Abdurakhimov, D.M. Mirzayeva, V.A. Sukratov, A.K. Mutali, V.N. Tjep, S. Biira, M.Yu. Tashmetov, K. Olejniczak, O. Kristavchuk (2020). Thermophysical behavior of boron nitride and boron trioxide ceramics compounds with high energy electron fluence and swift heavy ion irradiated, *Journal of Alloys and Compounds*, 834, P.155119.

[2] S.R. Azimova, Y.I. Aliyev, D.M. Mirzayeva (2020). The behavior of thermodynamic kinetic on Bi_2Se_3 compound by ion implantation, *Modern Physics Letters B*, 34, 36, P.2050417.

NEW PROGRAM IN WOLFRAM MATHEMATICA: CALCULATE PEAKS EASILY

A.S. Kazantsev¹, Yu.L. Ryzhykau¹, A.V. Vlasov¹, A.I. Kuklin^{1,2}

¹Moscow Institute of Physics and Technology, Dolgoprudny, Russian Federation

²Joint Institute of Nuclear Research, Dubna, Russian Federation

E-mail: kazantsev@phystech.edu

Experimental data obtained by small-angle scattering may contain diffraction peaks. Simple and fast calculation of its parameters is an important task for structure-obtaining workflow. We developed a program in Wolfram Mathematica. The program provides an interface for loading and processing sets of points with errors using predefined but mutable parameters (Figure 1).

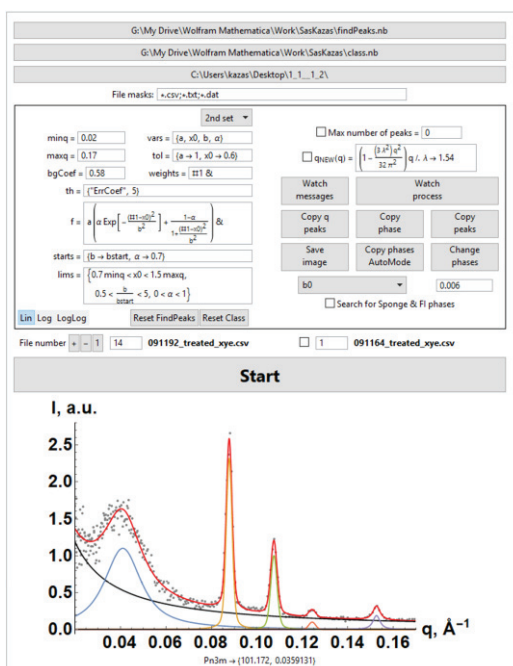


Figure 1. The interface of the program. The upper part contains parameters of loading and processing, the lower one – a processed picture. Legend of the picture: gray dots are experimental data, black line is a background signal, calculated by the program, multicolor curves are peaks, calculated by the program too, and the red line is the final approximation.

The program was initially developed for faster defining of lipidic cubic phase types. Therefore, it does two main things: calculation of peaks and definition of exact phase set by proportions of peaks' parameters.

Calculation of peaks is conducted by approximation of experimental data by Goal fit function:

$$(A \cdot x^b) + \sum_i PeakFunc(x)$$

“PeakFunc” is a peak function; its form may be defined by user. Number of peak functions in the sum equals to number of peaks, found by the program. $A \cdot x^b$ – background, which parameters are calculated by the program too, as described below.

The pipeline of approximation of experimental data consists of the following.

- Make approximation of experimental data by background.
- Subtract $k \cdot$ background ($k \leq 1$ and user-defined) from data.
- Search for groups of experimental points, which intensities are higher than user-defined threshold.
- Repeat until there are no such groups:

- For each group:
 - select a point of maximal intensity;
 - make parabolic approximation of nearest to it points;
 - approximate nearest points by user-defined “PeakFunc”, using parabolic approximation params as start values.
- Nonlinear Model Fit of the Goal fit function; start values are obtained from the last approximation for all peaks.

Approximation of experimental data has calculation parameters. They are presented in Wolfram Language style. The description of the most important of the parameters is presented below.

A peak function is customizable. A user can change the predefined function (gaussian) to his own one. A function should contain parameter “a” as height, “b” as width, and “x0” as a peak center. A function may contain any other parameters. All function parameters should be presented in “vars” parameter.

A user is able to define custom constraints for peak function variables in “lims” parameter.

The default value is $\{0.7\text{minq} < x0 < 1.5\text{maxq}, 0.5 < \frac{b}{b\text{start}} < 5\}$. In this parameter several special symbols may be used: “minq” and “maxq” are the abscissa limits for loaded data, and “bstart”, which is a first (parabolic) approximation for peak width.

The “starts” parameter defines which values the main approximation starts from for all parameters except “a” and “x0”.

The second part of the program is definition of lipidic mesophase set. The main characteristic for phases’ definition is proportions between coordinates of peak centers (q-ratio) and between their heights [1-3]. These proportions reveal the crystallographic group of lipidic cubic phases (LCP) or type of non-crystal structure, and their lattice parameters. The program is able to define a set of different types of mesophases in a sample. In addition, search for Sponge and Fluid Isotropic phases (wide peaks) and for $L\alpha$ (laminar) phase with only 1 peak is also provided by the program.

To understand the significance of the program, it was compared to known analogs. In the part of peak centers calculation, OriginPro 2016 was chosen. Test on a standard experimental data, obtained from Pn3m LCP, failed: we were not able to tune approximation process correctly. In general, all attempts to approximate at least five-peaks-data with OriginPro were not successful. In the part of lipidic mesophase set definition, comparison was conducted with [3]. The crucial difference is that comparator cannot distinguish multiple mesophases.

The program is not limited by small-angle diffraction experimental data. Fill free to use it for any data containing peaks no more than 20.

Thus, our novel program fills empty space in data processing necessities.

[1] Hahn T. International tables for crystallography Volume A: Space Group Symmetry. 2002.911 p.

[2] Cherezov V. The Cherezov Lab - LCP Resources: Useful Equations [Electronic resource]. URL: http://cherezov.usc.edu/lcp_equations.htm (accessed: 26.04.2017).

[3] Joseph J.S. et al. Characterization of lipid matrices for membrane protein crystallization by high-throughput small angle X-ray scattering // Methods. Elsevier Inc., 2011. Vol. 55, № 4. P. 342–349.

EVALUATION OF COPPER SALTS CONSEQUENCE ON *TRITICUM AESTIVUM*

M.L. Soran¹, O. Culicov^{2,3}, I. Lung¹, A. Ciorîță¹, O. Opriș¹, A Stegarescu¹, I. Zinicovscaia², N. Yushin² and K. Vergel²

¹ National Institute for Research and Development of Isotopic and Molecular Technologies, 67-103 Donat, Cluj-Napoca 400293, Romania

² Joint Institute for Nuclear Research 141980 Dubna, Moscow Region, Russian Federation

³ National Institute for R&D in Electrical Engineering ICPE-CA Bucharest, Romania

E-mail: loredana.soran@itim-cluj.ro

Copper is an essential micronutrient required for healthy growth of plants and its deficiency can decrease phenolics in the plants [1]. In excessive amounts, it is toxic to plant growth, the toxicity of copper depending on the metal concentration, exposure duration and the developmental stage of plants [2].

In this study was evaluated the influence of the copper (II) sulfate and cupric nitrate on the wheat (*Triticum aestivum*) plants. In this regard, the effect of the two salts on the content of assimilative pigments, polyphenolic compounds and elemental content of wheat was followed. The possible ultrastructural changes in the leaves of the plants were also followed. It was observed that, the amount of chlorophyll a, chlorophyll b and total carotenoids were lower in the control plants than in the treated ones (Fig. 1), while the amount of polyphenols in the treated plants is lower than in the control ones.

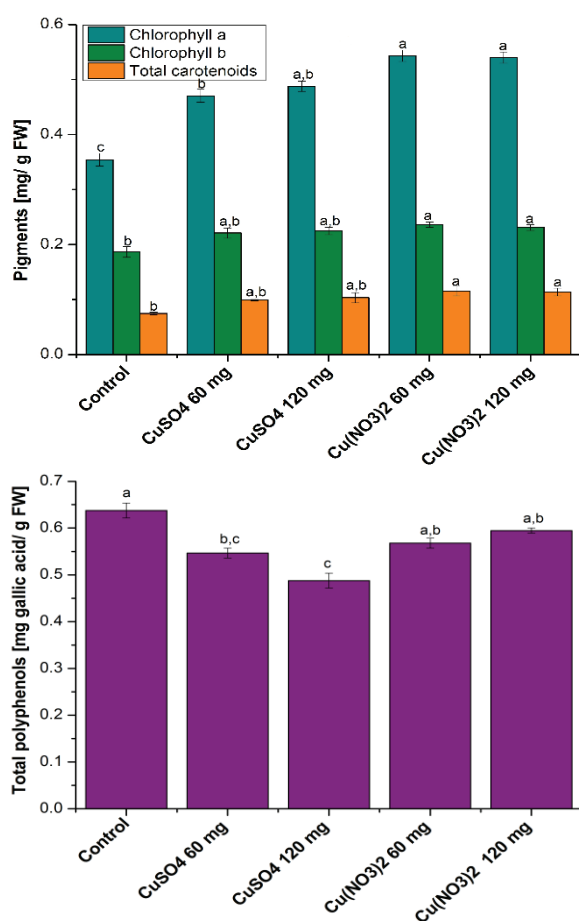


Fig. 1. Comparative diagram of the pigment and polyphenols content.

Comparing the plants treated with the two copper salts, it was observed that the amount of pigments was lower in the case of plants treated with CuSO₄ than in those treated with Cu(NO₃)₂, with no significant differences in the amount of salt added in soil.

Regarding on the polyphenols content, the type of salt, plants treated with $\text{Cu}(\text{NO}_3)_2$ have higher amounts of polyphenols compared to those treated with CuSO_4 . In plants treated with the same salt, with increasing of the CuSO_4 amount, the quantity of polyphenols decreases, while in the case of $\text{Cu}(\text{NO}_3)_2$ increases.

The wheat leaves were analyzed through transmission electron microscopy (TEM), in order to determine if the salts affect the ultrastructure of the cells or chloroplasts. It was found that the leaves start to develop starch granules [3] and the chloroplasts will slowly transform into amyloplasts [4]. The plants treated with both solutions at 120 mg had electron dense accumulations near the tonoplasts, which could indicate the formation of nanoparticles.

Element content in roots of wheat grown on soil with CuSO_4 and $\text{Cu}(\text{NO}_3)_2$ is mostly positive correlated. Fourteen of 31 elements (Na, Cl, K, Mn, Co, Cu, As, Br, Rb, Ag, Sb, Cs, Ba, Au) have correlation coefficient higher than 0.75. Only a few elements (Mg, Mo, Ta, U) have a negative correlation coefficient but for none of them it is not lower than -0.55. Cluster analysis was applied to experimental data to give a better insight into uptake of elements by plants and to assess the contribution of specific factors that may have an effect on plant behavior (Fig 2).

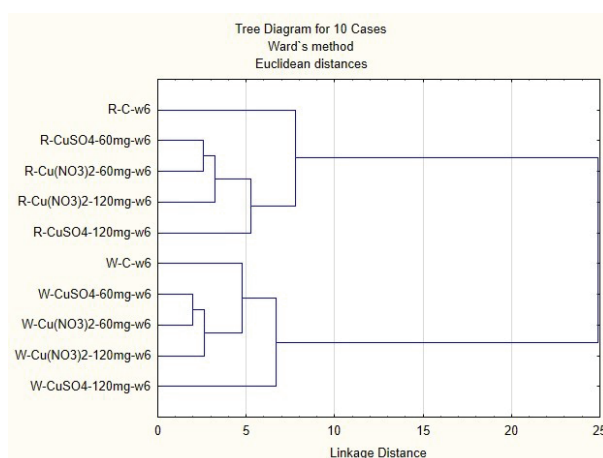


Fig. 2. Hierarchical clustering dendrograms for the analysis of the chemical elements that are present both in the roots and wheat.

It can be concluded that the differences between the roots and the green part of the plants are more significant than other parameters, and the exposure time becomes significant within the green part of wheat.

This work was carried out in the framework of Romanian-JINR cooperation (Order 395-30/27.05.2019; 396-55/27.05.2019 and Order 397-57/27.05.2019).

[1] R. Munene, E. Changamu, N. Korir, J.O. Gweyi (2017). Effects of different nitrogen forms on growth, phenolics, flavonoids and antioxidant activity in amaranth species. *Trop. Plant Res.* 4, 81-89.

[2] T.P.A. Merlin, G.P.P. Lima, S. Leonel, F. Vianello (2012). Peroxidase activity and total phenol content in citrus cuttings treated with different copper sources. *S. Afr. J. Bot.* 83, 159-164.

[3] Y.A. Yin, J.C. Qi, W.H. Li, L.P. Cao, Z.B. Wang (2012). Formation and developmental characteristics of A- and B-type starch granules in wheat endosperm. *J. Integr. Agric.* 11, 73-81.

[4] M.S. Buttrose (1960). Submicroscopic development and structure of starch granules in cereal endosperms 1. *J. Ultrastruct. Res.* 4, 231-257.

Научное издание

Condensed Matter Research at the IBR-2

Programme and Abstracts of the International Conference

Исследования конденсированных сред на реакторе ИБР-2

Программа и аннотации докладов международной конференции

E3-2022-17

Сборник отпечатан методом прямого репродуцирования
с оригиналов, предоставленных оргкомитетом.

Ответственная за подготовку сборника к печати *В. С. Смирнова*.

Подписано в печать 19.04.2022.

Формат 60 × 90/16. Бумага офсетная. Печать цифровая.
Усл. печ. л. 11,88. Уч.-изд. л. 19,28. Тираж 70. Заказ 60400.

Издательский отдел Объединенного института ядерных исследований
141980, г. Дубна, Московская обл., ул. Жолио-Кюри, 6.
E-mail: publish@jinr.ru
www.jinr.ru/publish/

